

Advancing human thermo-physiological modeling

Citation for published version (APA):

Veselá, S. (2021). *Advancing human thermo-physiological modeling: Challenges of predicting local skin temperatures during moderate activities*. [Phd Thesis 1 (Research TU/e / Graduation TU/e), Mechanical Engineering]. Technische Universiteit Eindhoven.

Document status and date:

Published: 15/04/2021

Document Version:

Publisher's PDF, also known as Version of Record (includes final page, issue and volume numbers)

Please check the document version of this publication:

- A submitted manuscript is the version of the article upon submission and before peer-review. There can be important differences between the submitted version and the official published version of record. People interested in the research are advised to contact the author for the final version of the publication, or visit the DOI to the publisher's website.
- The final author version and the galley proof are versions of the publication after peer review.
- The final published version features the final layout of the paper including the volume, issue and page numbers.

[Link to publication](#)

General rights

Copyright and moral rights for the publications made accessible in the public portal are retained by the authors and/or other copyright owners and it is a condition of accessing publications that users recognise and abide by the legal requirements associated with these rights.

- Users may download and print one copy of any publication from the public portal for the purpose of private study or research.
- You may not further distribute the material or use it for any profit-making activity or commercial gain
- You may freely distribute the URL identifying the publication in the public portal.

If the publication is distributed under the terms of Article 25fa of the Dutch Copyright Act, indicated by the "Taverne" license above, please follow below link for the End User Agreement:

www.tue.nl/taverne

Take down policy

If you believe that this document breaches copyright please contact us at:

openaccess@tue.nl

providing details and we will investigate your claim.

Advancing human thermo-physiological modeling

Challenges of predicting local skin temperatures
during moderate activities

PROEFSCHRIFT

ter verkrijging van de graad van doctor aan de Technische
Universiteit Eindhoven, op gezag van de rector magnificus
prof.dr.ir. F.P.T. Baaijens, voor een commissie aangewezen door
het College voor Promoties, in het openbaar te verdedigen op
donderdag 15 april 2021 om 11:00 uur

door

Stephanie Veselá

geboren te Potsdam, Duitsland

Dit proefschrift is goedgekeurd door de promotoren en de samenstelling van de promotiecommissie is als volgt:

voorzitter: prof.dr. L.P.H. de Goey
1e promotor: prof.dr.ir. D.M.J. Smeulders
co-promotor: dr.ir. A.J.H. Frijns
leden: prof.dr.ir. A.A. van Steenhoven
prof.dr. H.A.M. Daanen (Vrije Universiteit Amsterdam)
prof.dr.ir. J.L.M. Hensen
prof.dr. W.D. van Marken Lichtenbelt (Universiteit Maastricht)
adviseur(s): dr. B.R.M. Kingma (TNO)

Het onderzoek of ontwerp dat in dit proefschrift wordt beschreven is uitgevoerd in overeenstemming met de TU/e Gedragscode Wetenschapsbeoefening.

*We judge ourselves by what we feel capable of doing,
while others judge us by what we have already done.*

Henry Wadsworth Longfellow



Copyright © 2021 by Stephanie Veselá.

All rights reserved. No part of this publication may be reproduced, stored in a retrieval system, or transmitted, in any form, or by any means, electronic, mechanical, photocopying, recording, or otherwise, without the prior permission of the author.

Cover design by Stephanie Veselá

Cover picture by Ivan Smuk/Shutterstock.com (Standard licence)

Typeset with L^AT_EX

Printed by Ipskamp Printing

A catalogue record is available from the Library Eindhoven University of Technology
ISBN: 978-90-386-5243-6

Societal summary

The building sector is currently responsible for about 40% of the total energy consumption in the European Union. Thus, energy efficient technology for heating, ventilating and air conditioning (HVAC) in buildings can contribute largely to the European targets to significantly reduce CO₂ emissions. However, the occupants of a building still need to feel thermally comfortable to ensure health and productivity. Hence, a balance between energy efficient technology and human thermal comfort is needed.

The HVAC systems in buildings generally condition the whole occupied space according to a set temperature. In larger offices, this method might be inefficient. Hence, researchers developed personalized HVAC systems, where the overall air temperature is moderately reduced (17 to 20 °C) in case of heating or moderately increased (26 to 28 °C) in case of cooling. To ensure the occupants' thermal comfort, local heating or cooling devices are installed at the working desk or space. Examples include heated chairs, heated mats under or on the table, or local ventilation systems.

To test the personalized HVAC systems, large studies using human subjects are performed. These studies are often timely and expensive. Simulation models of the human thermal response to the indoor thermal environment, namely thermo-physiological models, can help testing personalized HVAC systems to limit the human subject experiments to the most promising designs. To estimate human thermal comfort, thermo-physiological models predict skin temperatures based on a simplified geometry of the human, and use mathematical models for the heat transfer within the body, the heat exchange with the thermal environment and for the main human thermoregulatory responses such as sweating and shivering. The calculated skin temperatures are then processed in thermal sensation and comfort models to estimate

the human thermal comfort in a given thermal environment. Mostly, these models have been developed to predict the average skin temperature and consequently, the overall thermal comfort. Additionally, their validation was often done under laboratory conditions with low clothing and low activity levels of the human subjects. However, for the design optimization of personalized HVAC systems, the accurate prediction of the skin temperature is also required for specific (local) body parts for clothed and moderately active people.

The aim of this thesis was to investigate shortcomings of thermo-physiological models when calculating local skin temperatures, and to enhance their prediction quality. Hereby, our focus was set on typical office environments and activities. Firstly, we tested the current performance of a thermo-physiological model in predicting local skin temperatures using a case study with 5 subjects wearing typical office clothing ensembles and performing moderate activities. Our results showed discrepancies between the measured and simulated skin temperatures, especially on the extremities, e.g., the feet. The detected reasons included the uncertainty of the provided local clothing data and the need for re-evaluating local physiological effects, e.g., skin blood flow (SBF).

Secondly, we addressed both issues in separate experimental studies. 1) We obtained a large variety of local clothing data using a movable sweating thermal manikin, on which temperatures and heat fluxes could be measured. Also, we determined equations to adjust the local clothing properties to different clothing fits (tight versus loose fit). 2) We developed an improved SBF model for the feet on the basis of human subject experiments, where the subjects performed moderate activities while their physiological data (e.g., skin temperature, energy expenditure, and skin perfusion) was recorded.

Thirdly, we applied the newly measured clothing properties and the improved foot SBF model to the simulations of the original case study. Our results show that the new foot SBF model has the largest impact on the local skin temperature outcome. In most cases, the skin temperature prediction is improved in the finalized thermo-physiological model.

Contents

Societal summary	i
1. General introduction	1
1.1. Energy efficiency in the built environment and human thermal comfort	1
1.1.1. Human thermal sensation and comfort	2
1.1.2. Personalized heating and cooling systems	3
1.2. Human thermal physiological modeling	3
1.2.1. Overview	3
1.2.2. ThermoSEM	4
1.2.3. Areas of application	5
1.3. Thesis outline	6
2. Performance of ThermoSEM in realistic environments - a case study	9
2.1. Introduction	9
2.2. Methods	10
2.2.1. Measurements	11
2.2.2. Input parameters for the model	11
2.2.3. Analysis	11
2.3. Results and Discussion	13
2.3.1. Sitting in an office	13
2.3.2. Walking indoors	15
2.3.3. Walking outdoors	18
2.3.4. Effects of local parameter variation on foot skin temperature .	18
2.3.5. Analysis of local skin perfusion	20

2.4. Conclusions	21
3. Local thermal sensation modeling	
- a review on the necessity and availability of local clothing properties and local metabolic heat production	23
3.1. Introduction	23
3.2. Representation of clothing in thermo-physiological models	24
3.2.1. Clothing in thermo-physiological models	26
3.2.2. Local clothing insulation and evaporative resistance values	27
3.2.3. Effect of air penetration on clothing properties	29
3.2.4. Summary and discussion of necessity and availability of local clothing values	31
3.3. Metabolic rate and its distribution over the body	31
3.3.1. Local metabolic heat production in multi-segment thermo-physiological models	33
3.3.2. Discussion on local metabolic heat distribution coefficients	35
3.4. Effect of local personal factors on local skin temperature and its implication on local thermal sensation	36
3.4.1. Differences in local skin temperature for different sets of local clothing values	38
3.4.2. Differences in local skin temperature for different distribution coefficients of local metabolic heat	40
3.4.3. Implication of differences in local skin temperature on local thermal sensation	42
3.4.4. Limitations of the analysis	44
3.5. Conclusions	44
4. Local clothing thermal properties of typical office ensembles under realistic static and dynamic conditions	47
4.1. Introduction	47
4.2. Methods	49
4.2.1. Measuring equipment	49
4.2.2. Garments and ensembles	50
4.2.3. Local clothing area factor	50
4.2.4. Local dry thermal resistance	56
4.2.5. Local evaporative thermal resistance	57

4.3. Results and Discussion	59
4.3.1. Local clothing area factors	59
4.3.2. Local dry thermal resistance	63
4.3.3. Local evaporative thermal resistance	72
4.3.4. Future research	75
4.4. Conclusions	77
5. Effect of local skin blood flow during light and medium activities on local skin temperature predictions	79
5.1. Introduction	79
5.2. Methods	81
5.2.1. Human subject experiments	81
5.2.2. ThermoSEM and input parameters	84
5.2.3. Data analysis	89
5.3. Results	90
5.3.1. Comparison of measured and simulated local skin temperatures	90
5.3.2. Measured versus simulated SBF	92
5.3.3. Changes in skin temperature prediction for prescribed measured skin blood flow	95
5.3.4. Improvement of the model	96
5.4. Discussion	99
5.5. Conclusions	104
6. Performance improvements of ThermoSEM in realistic environments – case study revisited	105
6.1. Introduction	105
6.2. Methods	106
6.2.1. Adjusted clothing properties	106
6.2.2. Individualization	107
6.2.3. Improved SBF neurophysiological model	107
6.3. Results and Discussion	109
6.3.1. Adjusted clothing properties	109
6.3.2. Individualization	111
6.3.3. Improved foot SBF neurophysiological model	112
6.3.4. Combined effect	114
6.4. Conclusions	115

7. General conclusions and future work	117
7.1. Conclusions	117
7.2. Recommendation for future research	119
7.2.1. Application to personalized heating and cooling	119
7.2.2. Muscle Activity level of specific body parts	119
7.2.3. Advancing the SBF model for further body parts	120
A. Supplementary figures and tables	123
A.1. Introduction	123
A.2. Case study - Performance of ThermoSEM	126
A.3. Local thermal sensation modeling – a review	129
A.4. Local clothing properties	132
A.5. Effect of local SBF on local skin temperature	141
A.6. Case study - revisited	149
B. The thermo-physiological model ThermoSEM	153
Bibliography	159
Summary	175
Acknowledgments	177
List of Publications	179
Curriculum Vitae	181

CHAPTER 1

General introduction

1.1. Energy efficiency in the built environment and human thermal comfort

The international energy agency (IEA) reports that space heating and cooling as well as water heating are responsible for almost 55% of the global buildings energy use. Moreover, the report states that the energy consumption of these sectors needs to be reduced by at least 25% by 2050 to meet the 2°C target for climate global warming (IEA, 2013). Hence, heating, ventilation and air conditioning (HVAC) systems need to be increasingly energy efficient. However, these systems should also provide a healthy and comfortable thermal indoor environment for the occupants of the building. A large number of adults work in office buildings, where they need to daily perform at their best and stay healthy. This objective can be achieved, when the indoor environment meets their individual needs (Seppänen et al., 2006; Urlaub et al., 2013). Hence, researchers and building engineers aim to design the HVAC systems of the buildings to be energy efficient, while also providing a thermally comfortable environment to all occupants.

1.1.1. Human thermal sensation and comfort

The design of energy efficient and thermally comfortable buildings requires the prediction of the future occupants' thermal comfort. In current standards, e.g. EN-ISO 7730:2005, the predicted mean vote (PMV) and percentage of people dissatisfied (PPD) are used to evaluate the environmental condition with regard to the overall thermal comfort of an average person. The PMV predicts the average thermal sensation of a large group in a given thermal environment based on regression equations developed by Fanger (1970). Thermal sensation is a subjective measure to assess the environmental conditions, and it is usually marked on a continuous scale with the categories cold, cool, slightly cool, neutral, slightly warm, warm and hot (ASHRAE, 2004). Further on, this method was reviewed in several papers and adaptive thermal comfort models were developed (de Dear and Brager, 1998; Nicol and Humphreys, 2002).

With the development of human thermo-physiological (TP) models (see section 1.2), thermal sensation (TS) and thermal comfort (TC) models were introduced that predict overall thermal sensation based on the predicted mean skin temperature, core temperature and their time derivatives. These models are based on regression analysis, which maps these physiological parameters to the thermal sensation of a group of human subjects. Examples of these models were developed by Fiala (2012, 2003) and Zhang (2003). A different approach is given in Kingma et al. (2012; 2014b), where neurophysiological responses of cold and warm receptors are included. Hence, the overall TS modeling is based also on real physiological processes rather than exclusively on regression analysis.

Local thermal sensation for office building applications is only computed in the model by Zhang (2003). This model can be applied in steady state and transient conditions. It calculates the local thermal sensation as a function of local and mean skin temperatures as well as both their set points, the time derivatives of the local skin and the core temperature, and four coefficients that depend on the specific body part. The set points for local and mean skin temperature have to be measured in neutral conditions for every individual or a group of subjects under specific conditions. Hence, it is not possible to predict local thermal sensation entirely based on computational models.

1.1.2. Personalized heating and cooling systems

Among other solutions, personalized heating and cooling systems show a high potential for saving energy in office buildings as compared to conventional systems while providing a comfortable indoor thermal environment (Arens et al., 1991; Foda and Sirén, 2012; Melikov et al., 1994; Parkinson et al., 2015; Verhaart et al., 2015; Veselý and Zeiler, 2014). Personalized heating and cooling systems influence the climate around specific body parts (here referred to as local) of the occupants, while the overall environmental temperature of a room or building is reduced in case of heating or raised in case of cooling in order to save energy consumption and costs. Examples for personalized heating systems include heated chairs, supply of warm air at desk level, or heated mats under or on top of the desk (Foda and Sirén, 2012; Melikov and Knudsen, 2007; Watanabe et al., 2010; H. Zhang et al., 2010b; Y. F. Zhang et al., 2007). Personalized cooling is mainly achieved by cooling fans at different locations at the desk (Veselý and Zeiler, 2014). Currently, these systems have to be tested with extensive human subject experiments. An alternative would be the use of a computer model, which predicts local skin temperatures and a coupled TS model for the prediction of overall and local thermal sensation.

1.2. Human thermal physiological modeling

1.2.1. Overview

Individual thermal comfort might be assessed using modern human TP and coupled TS models. Thermal models have been developed since the 1960s and continuously improved. Detailed summaries of these models and their development are given, for example, by Cheng et al. (2012), Miimu et al. (2013), de Dear et al. (2013), Fabbri (2015) and Katic and Zeiler (2014). Accordingly, human thermal models can be clustered into two main categories: 1) TP models and 2) TS models, which are also referred to as psychological models, e.g. by Cheng et al. (2012). These two categories are connected in a general concept of human thermal modeling (Figure 1.1). This concept also includes that TP models require input of environmental variables (e.g. operative temperature, humidity, wind speed), two personal factors, namely clothing and metabolic rate, and, optionally, individual characteristics (e.g. weight, height, age).

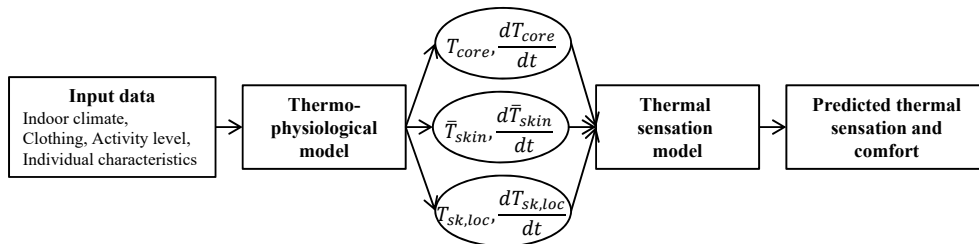


Figure 1.1.: General concept of human thermal modeling.

Using this information, TP models calculate core, mean and local skin temperatures (T_{core} , T_{skin} and $T_{sk,loc}$) as well as their time derivatives (dT/dt) with the use of heat transfer and bio-heat equations. Core and skin temperatures as well as the change in skin temperature are consecutively used to predict thermal sensation and comfort via a TS model.

TP models can also be divided into single-segment and multi-segment TP models. Segments are representations of the body or body parts, consisting of one or multiple layers around a cylindrical or spherical core. In single-segment models the exact geometry of body representation is less important and is used to define balances and characteristics. Multi-segment models divide the human body into several body parts, and the geometry (radius, length, layer thickness, etc.) becomes more important. Every segment is usually assigned its own heat and mass balance, which is then combined in a whole-body balance. Tables A.1 to A.3 on pages 123–125 summarize the most important attributes of selected thermal models in each of the defined categories. This thesis addresses specifically multi-segment TP and coupled TS models.

1.2.2. ThermoSEM

All simulations in this thesis are done with the TP model ThermoSEM as described by Kingma (2012) and Severens (2008). The model originates from Fiala’s thermoregulation model (Fiala et al., 1999, 2001). Major difference to Fiala’s model is the neurophysiological model for skin blood flow (Kingma et al., 2014b). To represent the human body, the model consists of 18 concentric cylinders and one concentric semi-sphere connected to a central blood pool (Figure 1.2). Every part has multiple tissue layers with defined attributes, e.g. basal metabolic heat, specific density and

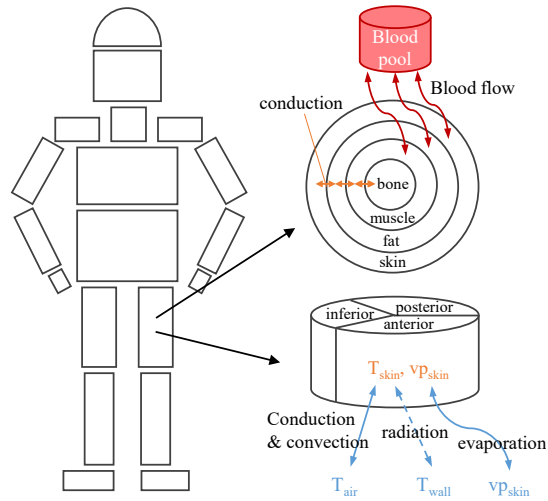


Figure 1.2.: Representation of the human body by ThermoSEM based on Kingma (2012)

conductivity. Moreover, the elements are divided into anterior, posterior and inferior sectors, to account for differences due to the orientation. Also, thermoregulatory control mechanisms, like shivering, sweating and (skin) blood flow are modeled. The detailed attributes of the model are provided in Appendix B on page 153. In this default configuration, these specifications represent an adult man with a weight of 73.5 kg, a height of 1.73 m, a body surface area of 1.86 m² and a body fat percentage of 14%. The resulting basal metabolic heat production is 87.1 W.

1.2.3. Areas of application

Built environment

Multi-segment TP and coupled TS models are mainly applied to predict human whole-body thermal comfort in a built environment and, therefore, are focused on the prediction of global values such as mean skin temperature and core temperature. As mentioned above, heating and cooling systems influencing also the climate of specific body parts were developed to improve the thermal comfort and energy balance in office buildings (Arens et al., 1991; Foda and Sirén, 2012; Melikov et al., 1994; Parkinson et al., 2015; Veselý and Zeiler, 2014). An accurate prediction of local and overall thermal sensation and comfort for these systems could help to preselect promising

designs and improve the efficiency of human subject experiments. Therefore, the ability of thermal models to also predict local thermal comfort and sensation has to be re-evaluated.

Medical application

TP models can also be applied in medicine to predict and observe a patient's temperature during medical treatments. For instance, Severens et al. (2007) use a TP model to predict the afterdrop in core temperature following cardiac surgeries. Moreover, the model is used to investigate the effectiveness of different heating measures to reduce the core temperature drop after surgery and therefore, to improve the patient's recovery time. Another example is the prediction of thermal and circulatory effects during hemodialysis including ultrafiltration as described by Droog et al. (2012). In this study, the thermo-physiological model was coupled with an advanced cardio-vascular model by Cavalcanti and Di Marco (1999). The combination showed a good prediction quality of the patient's core temperature and cardiac output. Also, the simulation of local effects of vasoconstriction and the resulting local skin blood flow was important to investigate potential cardiac vascular complications for the patient.

Sport science

In sport science, TP models might be applied to predict and manage the heat stress of athletes before a training unit or competition (Havenith, 2001; Havenith and Fiala, 2016). The athletes' performance can be improved by pre- or percooling the whole body or specific body parts to reduce the heat stress (Bongers et al., 2015; Eijsvogels et al., 2014; Luomala et al., 2012). Finding a suitable cooling strategy using human subject experiments is costly and time consuming. Hence, a preselection of promising cooling designs using a TP model can reduce the time and cost of such an endeavor.

1.3. Thesis outline

Present TP models are generally capable of simulating the local skin temperature to be processed in TS and TC models. However, most models were validated for the mean skin temperature prediction of an average person under low clothing as well as low activity conditions. For local skin temperature prediction, deviations can be found especially at the extremities (Martínez et al., 2016; Psikuta et al., 2012; van

Marken Lichtenbelt et al., 2007; Veselá et al., 2015b). The aim of this thesis is to further develop the TP model ThermoSEM such that the prediction quality of local skin temperatures is improved for moderate clothing and activity levels.

To identify the most critical aspects of local skin temperature prediction for higher activity and clothing levels, we performed a case study in a real office environment (Chapter 2). For this test, 5 individuals (3 male, 2 female) underwent six 1-hour trials combining typical office activities and clothing insulation values. During the experiments, we measured the local skin temperatures as well as the temperature and humidity of the environment, and then compared them to the simulation results in ThermoSEM.

Next, we investigated two main aspects in a broad literature review (Chapter 3): 1. the necessity and availability of local clothing properties and local metabolic heat production (above 1 met), and 2. influences on the local skin temperature predictions. In a sensitivity analysis included in the review, we analyzed the contribution of both aspects to the prediction accuracy of distal skin temperatures.

The missing data on local clothing properties was addressed by measuring local clothing parameters on a thermal sweating manikin in cooperation with Empa, St. Gallen, Switzerland (Chapter 4). For the dry thermal insulation values and local area factors, 23 typical office outfits were measured at three air speeds and body movement. The evaporative resistance was measured for two representative outfits at all air speeds and body movement. Additionally, we determined the local dry and local evaporative clothing resistance as well as the clothing area factors of three typical office shoes. For the dry thermal insulation, a correlation to the fit of the clothing (ease allowance) was investigated for one level clothing outfits.

To quantify the influence of different physiological factors on the local heat balances, we conducted human subject experiments at Maastricht University, where the participants performed light to medium activities while skin and core temperature, skin blood perfusion at the foot and their energy expenditure were measured (Chapter 5). With the help of these experiments, we re-analyzed the foot skin blood flow model.

At last, the case study was revisited to see if applying the measured local clothing properties and the foot skin blood flow model would improve the skin temperature prediction (Chapter 6).

CHAPTER 2

Performance of ThermoSEM in realistic environments - a case study*

2.1. Introduction

Current thermoregulation and coupled thermal sensation models are mostly based on and validated for laboratory settings as has been done, for example, by Fanger (1970), Huizenga et al. (2001) and Fiala (1998). However, their intention is to predict the human response in real office or outdoor conditions to provide a healthy and comfortable built environment through building design. Like any model, the predictive quality is highly dependent on the quality of the input. Thermal sensation models, therefore, require an accurate prediction of skin temperatures (Kingma, 2012). The

*This chapter is an extended version of the following conference papers:

- Veselá, Stephanie; Kingma, Boris R. M., and Frijns, Arjan J. H. (2015a). “Effects of sweating on distal skin temperature prediction during walking”. In: *Extreme Physiology and Medicine* 4.Suppl 1, A31
- Veselá, Stephanie; Kingma, Boris R. M., and Frijns, Arjan J. H. (2015b). “Taking Thermal Regulation Models From the Lab To the World: Are Current Views Ready for the Challenge?” In: *Healthy Buildings Europe 2015*. Ed. by Loomans, M.G.L.C. and Kulve, Marije te. Vol. 2015-May. Eindhoven

objective of the study is to conduct experiments with human subjects in a real office as well as outdoor environment, and compare the findings with the simulation results of the mathematical thermoregulation model ThermoSEM (Kingma et al., 2014b). Short sensitivity analyses indicate potential areas of improvement for future studies.

2.2. Methods

The experiments were done from October to December 2014. In this study, two activities were included: sedentary work (1.0 met) and walking (indoors and outdoors) at a moderate speed (2.8 to 2.9 met) (Ainsworth et al., 2011; Parsons, 2014). All scenarios were performed for one hour. To limit the effect of radiation through sunshine and the effect of moisture, the experiments were done on cloudy, but dry days. Additionally, the effect of clothing insulation on the skin temperatures was investigated. To obtain comparable results, the components of clothing insulation were set for three typical office combinations (Table 2.1). An overview of the chosen scenarios in this study is also given in Table 2.1. Five young to middle-aged adults (3 males and 2 females) were included in the study. The characteristics are provided in Table 2.2. The subjects were asked not to drink hot or caffeine beverages or eat shortly before and during the experiments.

Table 2.1.: Scenario overview

	Sitting in office	Walking indoors	Walking outdoors
Clothing combination 1: underwear, jeans, short sleeved t-shirt, socks and shoes	X	X	
Clothing combination 2: combination 1 + long-sleeved shirt	X	X	
Clothing combination 3: combination 2 + winter jacket		X	X

Table 2.2.: Subject characteristics

	Male 1	Male 2	Male 3	Female 1	Female 2
Body mass [kg]	80	90	76	62	63
Height [m]	1.92	1.82	1.86	1.68	1.70
Age [years]	42	32	32	27	26

2.2.1. Measurements

During the experiments, the skin temperature of the subjects was measured at the 14 sites (see EN-ISO 9886:2004) plus the fingertip of an index finger using iButtons (Thermochrom iButton DS1922L, Maxim Integrated, USA) (van Marken Lichtenbelt et al., 2006). The environmental parameters (RH and air temperature) were also registered during the experiments with iButtons (Hygrochron iButton DS1923, Maxim Integrated, USA). This RH/T sensor was attached to the outer layer of the clothing at the thorax and was kept at a distance of about 10 cm in front of the person using a wooden clip. The temperatures and relative humidity were recorded every 60 seconds.

2.2.2. Input parameters for the model

For the environmental conditions, ThermoSEM requires the air and radiation temperature, relative humidity and the effective air speed. The first three are taken from the measurements of the environmental conditions as described above. The effective indoor air speed is assumed to be mainly due to walking at 4 to 5 km/h. The walking speed of the subjects was measured while walking outside using GPS tracking. Outdoor experiments were done on windless days. Hence, we assume that the effective air speed is equal to the walking speed.

The local clothing insulation and clothing area factors are based on the study by Lee et. al (2013). The values are shown in Tables 2.3 to 2.5. The required moisture permeability index is set to 0.38 for all clothed body parts, except for upper body parts covered by a jacket, where it is 0.34 (ISO 9920: 2009).

Basal metabolic rate is set to 87 W for males and 72 W for females (Harris and Benedict, 1918). The activity level for sedentary work is set to 1 met (Ainsworth et al., 2011). The activity level for walking is calculated with the equation by Morrissey and Liou (1984). For a walking speed of 5 km/h the value varies around 2.8 to 2.9 met.

2.2.3. Analysis

For the analysis of the skin temperature, the results are grouped into mean, proximal, upper and lower arm, upper and lower leg, hand and foot skin temperature. The

Table 2.3.: Thermal insulation [clo] of the upper body for the different clothing ensembles.

	Head, Face	Neck	Shoulder	Thorax/ Abdomen, Anterior	Thorax/ Abdomen, Posterior
Clothing 1		0	1.05	1.22	0.89 (1.03)
Clothing 2	0	0.25	3.08	3.88	2.28 (2.42)
Clothing 3		0.36	3.50	4.46	2.54

(): insulation with chair, when sitting

Table 2.4.: Thermal insulation [clo] of the extremities for the different clothing ensembles.

	Upper Arm	Forearm	Hand	Upper Leg	Lower Leg	Foot
Clothing 1	0.55	0	0	0.73		
Clothing 2	1.89	1.41	0.16	(0.83)	0.58	0.83
Clothing 3	2.62	1.89	0.17			

(): insulation with chair, when sitting

mean skin temperature is the average of all measured points except fingertip. In the simulation, the points are chosen accordingly. For the proximal skin temperature, the measured and simulated points of the thorax and abdomen are averaged. For direct comparison, the last 45 minutes of each experiment are considered to take into account the time for dynamic thermal responses of the subjects' bodies, since their thermal history is unknown.

A limited sensitivity analysis of foot skin temperature is applied to the simulation of subject male 1 for the walking indoors scenario with clothing combination 2. For the investigation in the numerical model, the dry local clothing insulation at the foot is varied from 0.8 to 1.6 clo, the (overall) metabolic rate is increased from 2.8 to 3.3 met and the moisture vapor resistance is decreased to 0.1 and 0.01. Also, the combination of 1.6 clo and a moisture permeability of 0.1 is included in the analysis.

Additionally, the local skin perfusion of the feet during the experiments was calculated for the measured local skin temperature. To obtain these values, the simulated skin perfusion in ThermoSEM was iteratively adjusted in a way that the measured and simulated local skin temperatures were the same in a small window of error.

Table 2.5.: Clothing area factors

	Head, Face, Neck	Shoulder, Thorax, Abdomen, Upper Arm	Fore- arm	Hand	Upper Leg	Lower Leg	Foot
Clothing 1		1.1	1				
Clothing 2	1	1.13	1.13	1	1.09	1.2	1.03
Clothing 3		1.25	1.25				

2.3. Results and Discussion

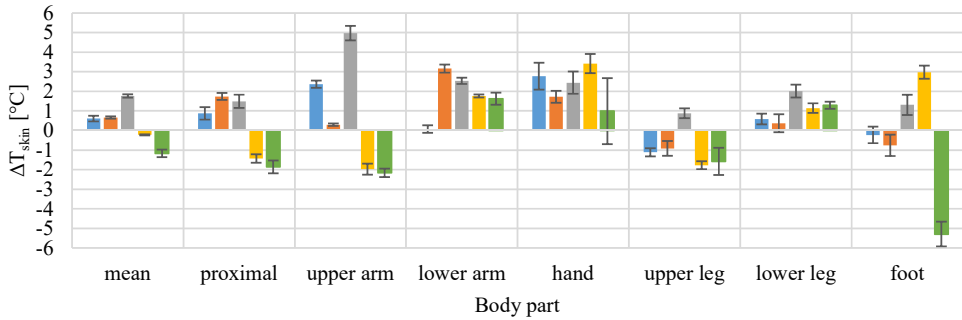
2.3.1. Sitting in an office

The average temperature difference and standard deviation between simulated and measured values of the scenarios “sitting in an office” are summarized in Figure 2.1 and Table A.4 on page 126. Additionally, the absolute temperatures over the course of the last 45 minutes are shown exemplary for the mean, proximal, hand and foot skin temperature for “sitting in an office” with clothing combination 1 in Figure 2.2 and with clothing combination 2 in Figure A.1 on page 127. The environmental temperatures during these office experiments were 21 to 24 °C.

For both scenarios, the difference between simulated and measured results for mean, proximal, and arm temperatures are relatively constant, which is represented by the low standard deviations of the individual subjects of mostly under 0.4 °C in Table A.4 on page 126. Higher standard deviations are found for temperature difference at the hand, legs and foot. This observation can also be seen in Figure 2.2, where the measured skin temperature of the hand and foot show higher changes than the ones for the mean and proximal temperature.

The average mean, proximal, upper arm, upper leg and foot skin temperatures deviations of all subjects are less than 1 °C (Table A.4 on page 126). This deviation might be considered acceptable, since it is within the measurement error of the iButtons (van Marken Lichtenbelt et al., 2006). For the lower arm, hand and lower leg, the skin temperatures are mostly overestimated by the simulation with values of up to 2.9 °C. However, the individual results for all body parts are very divers, which is

(a) Sitting in office, clothing combination 1



(b) Sitting in office, clothing combination 2

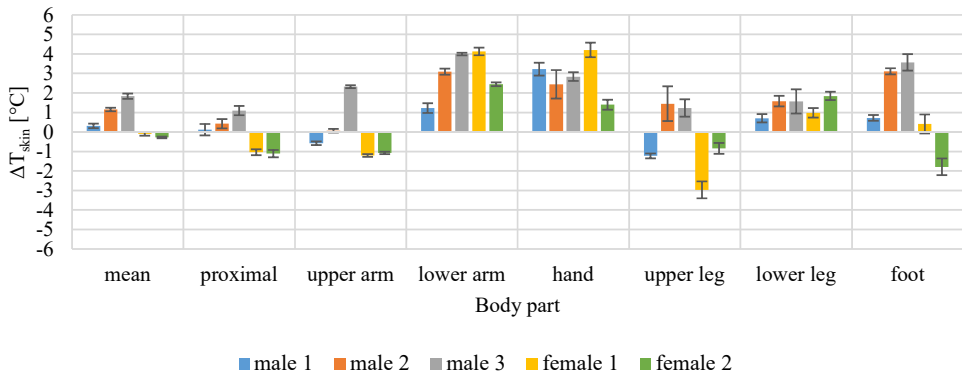


Figure 2.1.: Skin temperature difference (simulated – measured) and standard deviation for all subjects and representative body parts while sitting in an office wearing clothing combination 1 or 2

represented by the large standard deviation of the average. The highest spread between the subjects of 8.3 °C and 4.4 °C can be found for the foot skin site for the “sitting in an office” scenario with clothing combination 1 and 2, respectively.

A possible systematic difference between genders can be seen for the proximal, upper arm and resulting mean skin temperature difference. For all male subjects, the simulation overestimates the measured skin temperatures at these locations, whereas the measured skin temperatures of the female subjects are underestimated.

The main issue for the “sitting in an office” experiments is the large temperature differences in distal skin temperature occurring in both scenarios and most subjects. The overestimation of distal skin temperature indicates that 1) the amount of heat delivered to the skin via blood flow is higher than it should be in reality or 2) not

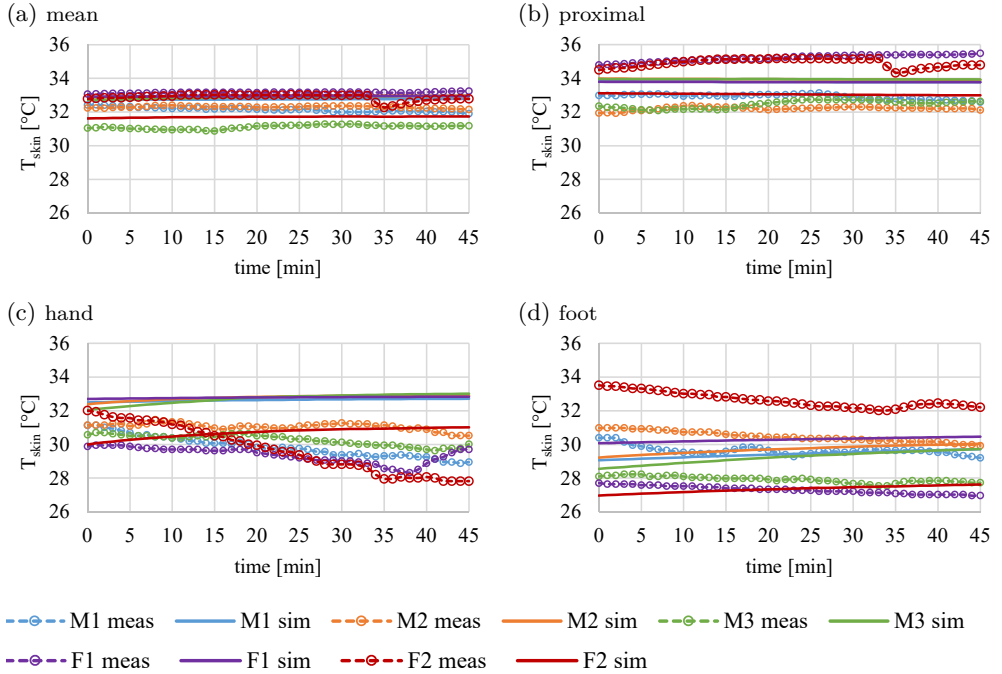


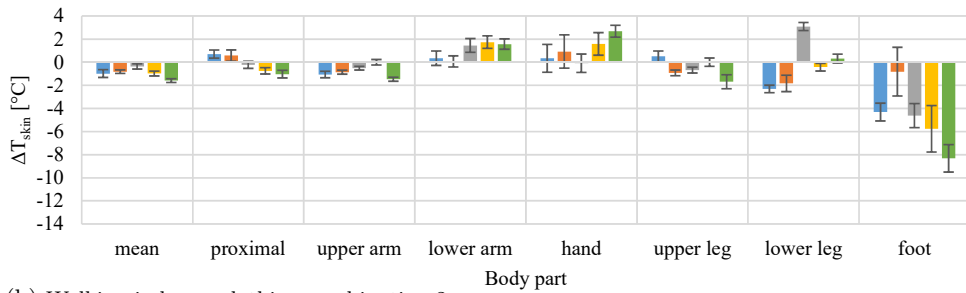
Figure 2.2.: Sitting in office, clothing combination 1: Measured and simulated skin temperatures of last 45 min

enough heat is dispersed to the environment. Since the second option is hard to measure, it is of interest to study the skin blood flow profile during office activities e.g. by laser Doppler flowmetry. Then, the measured skin blood flow and its content of heat can be compared to detailed results of the simulation.

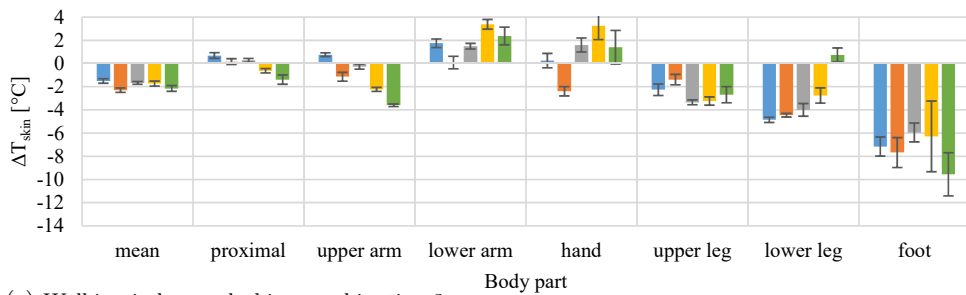
2.3.2. Walking indoors

For walking indoors, the environmental conditions vary the most due to temperature differences on indoor bridges, open spaces and office areas (14 to 22 °C). Since these measured ambient temperatures and relative humidity serve as input data for the model, the variation is also present in the simulation and varies throughout the walking activity. To summarize the results, the mean difference between simulated and measured skin temperatures for the last 45 minutes is shown in Figure 2.3 for all indoor walking scenarios. Also, the absolute measured and simulated temperatures are given in Figures A.2 to A.4 on pages 127–128.

(a) Walking indoors, clothing combination 1



(b) Walking indoors, clothing combination 2



(c) Walking indoors, clothing combination 3

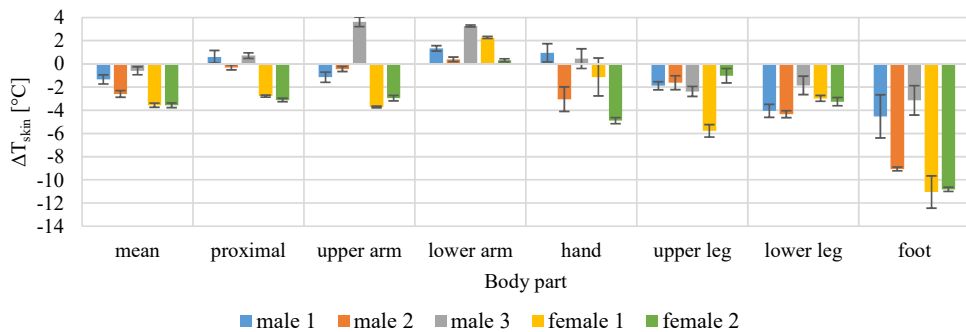


Figure 2.3.: Skin temperature difference (simulated – measured) and standard deviation for all subjects and representative body parts while walking indoors wearing clothing combination 1, 2 or 3

The computed results for the mean and proximal skin temperature at clothing combination 1 and 2 in Figure 2.3 are in good agreement with the measurements. It is seen that the computed values tend to underestimate the measured ones. The underestimation increases with higher upper body insulation and reaches values up to -4°C for clothing combination 3. This effect can also be seen for upper arm skin temperature differences when adding the winter jacket to clothing combination 2. In

conclusion, the added insulation value in the model seems to be too low at these body parts. In contradiction to this finding, the skin temperature difference of the lower arm, is mostly overestimated by up to 4 °C and does not follow the discussed pattern. For local insulation values, the available input data is limited to one recent study (Lee et al., 2013). The values have been determined for a thermal manikin in sitting position in an indoor environment. The influence of walking and air penetration is not included and leads to an uncertainty in the used values.

The proximal skin temperature tends to be different for female and male subjects. For example, the proximal temperature difference of males is overestimated by 2 K for clothing combination 1, whereas it is underestimated for females. For higher upper body insulation, the measured proximal temperature of females is underestimated up to -3 °C, showing a large difference to the male results (-1 °C). This indicates that the body composition in the model, which is based on a male subject, should take into account the gender and stature of the subject.

For the mean hand skin temperature differences, a large variation can be seen between subjects and scenarios. The values vary from 4 to -5.5 °C. Also, the standard deviation is comparatively high. Since no clothing insulation is applied to the hands, the hands are sensitive to the quick changes in environmental temperature during the walk indoors, which are not entirely represented in the minutely data for the simulation. Moreover, the movement of the hands was not prescribed. Hence, it is unclear if subjects moved their hands, held them still or even put their hands into pockets. For the first two options, the heat production in the hands (and arms) would slightly differ. Further issues with the heat distribution to the limbs are discussed below.

For the skin temperatures of lower body parts, the temperature difference is the highest for nearly all subjects as well as all scenarios and, as a general trend, is increasingly underestimated with higher upper body insulation. The difference reaches values of -2 to -5 °C for the legs and up to -12 °C for the foot skin temperature. This underestimation in lower body skin temperature can either be caused by lower heat input in the model than it is in reality or by overestimated heat losses. In present thermoregulation models, heat work due to activity is distributed to the body parts by default values based on the study by Stolwijk (1971). Any effect of local increase in heat production due to muscle activities during walking is not taken into account, and therefore, the heat production can be underestimated in a cold environment.

Additionally, the activity level of 2.8 met is estimated for a typical walking speed of 5 km/h (section 2.2). However, this value was not controlled, and therefore, could be different during the measurements. As mentioned for the “sitting in an office” scenarios, knowledge of skin blood flow could give further insights for the heat transported to the skin and indicate local differences in metabolism. Additionally, heat losses due to sweating could be overestimated in current models. Since the feet are covered in socks and shoes, the heat losses are expected to be low. However, the moisture permeability index is only estimated in the model due to the lack of verifying studies on local values.

2.3.3. Walking outdoors

The temperature differences of simulated and measured values for the outdoors scenario are shown in Figure 2.4. The environmental temperature ranged from about 5 to 11 °C for the different subjects. The results of the scenario when walking outdoors with clothing combination 3 are similar to the results of the scenario when walking indoors. For the mean skin temperature, the temperature difference is low for most subjects (maximum 2 °C), and also, the variation between subjects is low. The proximal temperature varies for individual subjects, and it is underestimated by the simulation for females by up to 4 °C. The highest temperature differences can be found for distal skin temperatures: The hand skin temperature is overestimated by up to 6 °C and the foot skin temperature is underestimated by up to -14 °C. Hence, the local heat balance is not accurately represented in the simulation. For the hand, there seems to be too high heat input or too low heat loss to the environment. Since the subjects wore winter jackets, one possibility would be that the sleeves of the jacket covered part of the hand, causing lower heat losses than predicted in the simulation. For the foot, the simulated heat input is too low or heat losses to the environment are too high as discussed in the previous section. Also, the results have to be interpreted very carefully, since the influence of the wind is uncertain. Even though days with low wind velocities were selected, it is not known whether the wind increased at some point.

2.3.4. Effects of local parameter variation on foot skin temperature

The previous section reveals a large error in the prediction of distal and especially, foot skin temperature. To investigate the sources of the error, a limited parameter

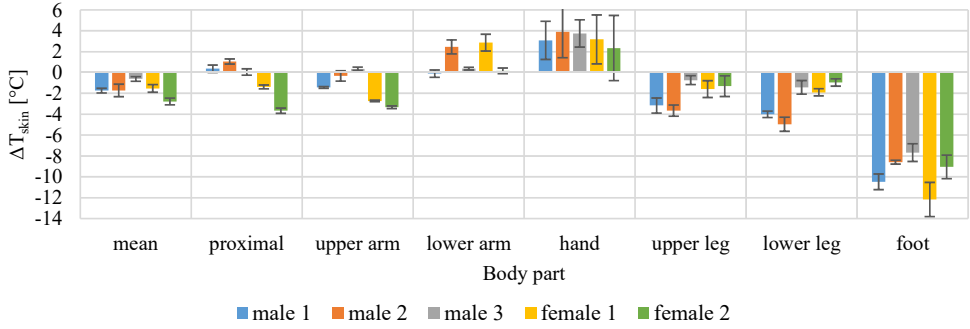


Figure 2.4.: Skin temperature difference (simulated – measured) and standard deviation for all subjects and representative body parts while walking outdoors wearing clothing combination 3

study was applied to the results of subject male 1 for the walking indoors scenario with clothing combination 2 (see section 2.2). For this sensitivity analysis, the overall activity level, the dry clothing insulation at the foot $I_{cl,foot}$ and the permeability index at the foot $i_{cl,foot}$ were varied. The default values were 2.8 met, $I_{cl,foot} = 0.83$ clo and $i_{cl,foot} = 0.38$. The results of this sensitivity analysis are shown in Figure 2.5. The following variations were implemented, while keeping the other values unchanged:

1. higher activity level of 3.3 met, accounting for a possible larger walking speed,
2. larger dry clothing insulation at the foot, where $I_{cl,foot} = 1.6$ clo, in case of higher insulating shoe wear,
3. lower permeability index of the shoes, where $i_{cl,foot} = 0.1$ and $i_{cl,foot} = 0.01$, assuming a higher evaporative resistance of (closed) shoes compared to other clothing items
4. a combination of larger dry clothing insulation, where $I_{cl,foot} = 1.6$ clo, and lower permeability index, where $i_{cl,foot} = 0.1$

Compared to the default foot skin temperature difference of -8°C , all measures reduce the underestimation of the simulation. The increased overall activity level, the increased shoe dry clothing insulation and the reduced shoe moisture permeability of 0.1 lead to foot skin temperature differences of about -6°C , -4.5°C and -3.6°C , respectively. The lowest underestimation of about 1°C is reached by the reduced shoe moisture permeability of 0.01 and the increased shoe dry insulation combined with reduced shoe moisture permeability of 0.1.

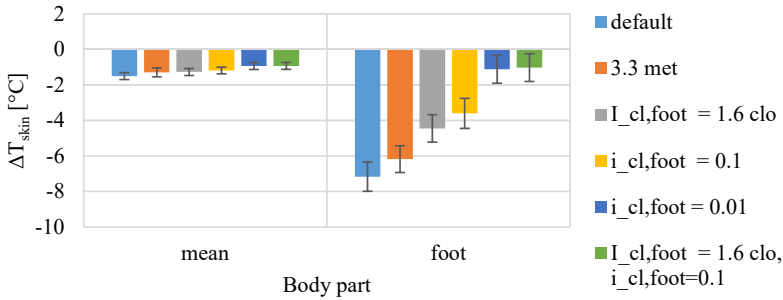


Figure 2.5.: Skin temperature difference (simulated – measured) and their standard deviation for subject M1 while walking indoors wearing clothing combination 2 for the default simulation (2.8 met, $I_{cl,foot} = 0.83 \text{ clo}$ and $i_{cl,foot} = 0.38$) and the changes of the sensitivity analysis (while keeping the other values at default)

This short sensitivity analysis shows that the simulated foot skin temperature is sensitive to local clothing properties and changes in local heat input due to activity through local skin blood flow or local muscular activity. However, there is limited data available on local metabolic rate, local clothing insulation and local moisture permeability indices. This uncertainty of input values for the numerical model leads to a large uncertainty in local skin temperatures prediction. Hence, there is a need for experimental investigation of local clothing properties and local heat balances.

2.3.5. Analysis of local skin perfusion

Figure 2.6 compares the last 45 minutes of the simulated foot skin blood flow (foot SBF) of the default simulation and the simulation with the changed foot clothing properties ($I_{cl,foot} = 1.6 \text{ clo}$ and $i_{cl,foot} = 0.1$) to the foot SBF of the simulation with the implemented measured foot skin temperatures. For the default simulation, the foot SBF is almost zero with an average of 0.001l/min. Adjusting the foot clothing properties leads to a slightly raised foot SBF of 0.0021l/min. If the clothing properties are not adjusted, a foot SBF of up to 0.05l/min is needed to reach the measured foot skin temperatures.

Both, the adjusted foot clothing properties and recalculated foot SBF result in an acceptable foot skin temperature prediction. This means that the “true” values are unknown at the current stage. Hence, local clothing properties and local skin perfusion need to be investigated to improve local skin temperature prediction quality.

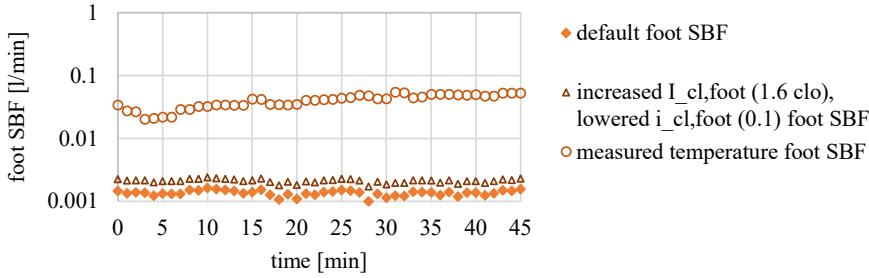


Figure 2.6.: Comparison of foot skin blood flow of the default simulation, with adjusted local clothing properties and with input of measured foot skin temperature

2.4. Conclusions

The ThermoSEM model predicts the mean skin temperature for the chosen scenarios within 2 K. Compared to former studies under laboratory conditions (Kingma et al., 2014b) and low clothing insulation the maximum error for mean skin temperature increased by 1 K. The main reason for this finding is the large underestimation of distal, especially foot, skin temperature during walking activity due to underestimated heat gain by skin blood flow and/or overestimation of heat loss. Two possible issues are identified, which may cause the low distal skin temperature: 1) uncertainty of local clothing values and 2) uncertainty of local skin perfusion and local metabolic rates. Additionally, the specific geometry of the subjects (i. e. height, body mass, body fat percentage) may add to the skin temperature deviations.

To specify the impact of the local heat gain through skin blood flow and heat losses through clothing layers, direct measurements of the skin blood flow and local clothing properties should be added to future experiments. Additionally, the general input data for local clothing insulation values is based only on one study and does not include the effect of air penetration or different local moisture permeability indices. The clothing model input data, therefore, needs revision with regard to higher effective air speeds and air penetration as well as local evaporative heat losses.

All in all, the described measures would improve the skin temperature prediction quality of ThermoSEM and other thermo-physiological models. These accurate skin temperatures can then be used in thermal sensation and comfort models to optimize the built environment, especially using personal heating and cooling systems.

CHAPTER 3

Local thermal sensation modeling - a review on the necessity and availability of local clothing properties and local metabolic heat production*

3.1. Introduction

Accurate prediction of local thermal sensation (LTS) depends on accurate local skin temperatures from thermo-physiological (TP) models, which in turn need accurate local input values. The difficulty of obtaining precise input is different for environmental and personal parameters. Environmental conditions can mostly be easily obtained, since they are set or measured. However, personal factors such as local clothing values,

*The contents of this chapter have been published in:

- Veselá, Stephanie; Kingma, Boris R. M., and Frijns, Arjan J. H. (2017b). “Local thermal sensation modeling - a review on the necessity and availability of local clothing properties and local metabolic heat production”. In: *Indoor Air* 27.2, pp. 216–272

metabolic heat production and its local distribution over the body, as well as local tissue insulation have to be estimated. The latter factor is, for example, discussed by Wijers et al. (2010) and Veicsteinas et al. (1982), but is not part of this chapter. The whole-body clothing and metabolic data as described in the standards were reviewed in a paper by Havenith et al. (2002), and suggestions were made for improvements. For instance, Havenith et al. (2002) proposed to include clothing vapor resistance into thermal comfort calculations and to account for the effect of air and body movement on all clothing properties. Moreover, they question the precision of the measurements for metabolic rates and suggest enlarging the database for low level activities. However, for local personal input data (clothing and metabolic heat production) the availability, the accuracy and the limits have not been reviewed and discussed so far. To fill in this gap, this chapter gives an overview of present models and addresses the following three main topics:

1. the necessity and availability of input data for local clothing properties and the options to account for changes in them due to air speed and body movement,
2. the necessity and availability of metabolic heat production and its local distribution,
3. the effects of uncertainties of local personal factors on LTS modeling.

3.2. Representation of clothing in thermo-physiological models

TP models account for sensible and evaporative heat loss from the clothed body to the environment. Sensible heat exchange consists of a conductive, radiative and convective part. Conduction from the clothing surface to the environment is usually neglected, due to its small contribution to the overall heat losses. The radiation and convection heat are defined by:

$$R = h_r f_{cl} (T_{cl} - T_r) \quad (3.1)$$

$$C = h_c f_{cl} (T_{cl} - T_a) \quad (3.2)$$

where R and C are the radiative and convective heat loss (W m^{-2}), h_r and h_c are the linearized radiant and convective heat transfer coefficients ($\text{W m}^{-2} \text{ }^\circ\text{C}^{-1}$), f_{cl} is the

3.2. Representation of clothing in thermo-physiological models

clothing area factor (ratio of the skin surface area of a nude person A_{Du} (D. Du Bois and E. F. Du Bois, 1916) and the surface area of the clothed body A_{cl} (ISO 9920: 2009)), T_{cl} is the clothing surface temperature, T_r is the mean radiant temperature, and T_a is the ambient temperature (all temperatures in °C). The linearized radiant heat transfer coefficient is hereby dependent on the temperature in the following way (ASHRAE, 2001):

$$h_r = 4\sigma\varepsilon \cdot \left(\frac{T_{cl} - T_r}{2} + 273.2 \right)^3 \cdot \frac{A_r}{A_{Du}} \quad (3.3)$$

where σ is the Stefan-Boltzman constant ($5.67 \cdot 10^{-8} \text{ W m}^{-2} \text{ K}^{-4}$), ε is the emissivity of the clothed body surface and A_r is the effective radiation area of the body (m^2). Mostly, convective and radiative heat losses ($C+R$) from the skin to the environment are considered together in:

$$C + R = \frac{T_{sk} - T_{cl}}{R_{cl}} = \frac{T_{sk} - T_{a,o}}{R_{cl} + \frac{1}{f_{cl}(h_r + h_c)}} \quad (3.4)$$

where T_{sk} is the skin temperature (°C), R_{cl} is the thermal resistance of clothing ($\text{m}^2 \text{ K W}^{-1}$), and $T_{a,o}$ is the ambient operative temperature (°C).

The evaporative heat loss E_{sk} can be written as:

$$E_{sk} = \frac{w(P_{sk} - P_a)}{R_{e,cl} + \frac{1}{f_{cl}h_e}} \quad (3.5)$$

where w is the total skin wettedness, P_{sk} is the saturated water vapor pressure at the skin surface (kPa), P_a is the water vapor pressures of the ambient air (kPa) and h_e is the evaporative heat transfer coefficient ($\text{W m}^{-2} \text{ °C}^{-1}$).

The clothing properties, thermal resistance R_{cl} , evaporative resistance $R_{e,cl}$ and clothing area factor f_{cl} have to be known to account for heat losses through clothing. The thermal resistance R_{cl} is also often called clothing insulation I_{cl} , which is then given in the clo unit ($1 \text{ clo} = 0.155 \text{ m}^2 \text{ K W}^{-1}$). The clothing insulation is part of the total insulation I_T provided by the clothing and the adjacent air layer. The total insulation can be calculated from the clothing insulation, the insulation of the air layer I_a and the clothing area factor:

$$I_T = I_{cl} + \frac{I_a}{f_{cl}} \quad (3.6)$$

Evaporative heat losses are often calculated using the clothing permeability index i_{cl} , which is calculated from the thermal and evaporative resistance, R_{cl} and $R_{e,cl}$, respectively, as well as the Lewis relation LR (0.0165 K Pa^{-1}):

$$i_{cl}LR = \frac{R_{cl}}{R_{e,cl}} \quad (3.7)$$

All clothing properties are generally given as whole-body coefficients and values are provided in current standard, e.g. ISO 9920:2009 or ASHRAE/55 (2004).

3.2.1. Clothing in thermo-physiological models

Multi-segment TP models assign clothing separately to every simulated body part. However, the modeling of the local clothing is approached differently in the models and the required input data may vary as well (Tables A.5 and A.6). In summary, the modeling of local clothing can be divided into three approaches:

1. detailed differential equations for heat and mass transfer,
2. integration of thermal and evaporative resistances for heat losses from the skin to the environment and
3. calculation of convective and radiative heat losses using the clothing temperature.

The first concept is used in the TP models by Stolwijk (1971), Wissler (1985) as well as Fu and Jones (1996). The main disadvantage of these models is the difficulty to measure or estimate the required input data, e.g. air gap width. The second method for local clothing modeling is established in the more recent TP models. Even though their concepts are similar, they are implemented differently. Lotens and Havenith (1992), for instance, uses a detailed resistance scheme for a skin-clothing-air-clothing-air system, where radiation, diffusion and ventilation are integrated (Figure A.5). In contrast, models by and based on Fiala (1998) and Tanabe (2002) define a local effective heat transfer coefficient U_{cl}^* (3.8) and a local effective evaporative coefficient $U_{e,cl}^*$ (3.9) to account for heat and moisture exchange between the skin and the environment:

$$U_{cl}^* = \frac{1}{\sum_{j=1}^n (I_{cl}^*)_j + \frac{1}{f_{cl}^*(h_c+h_r)}} \quad (3.8)$$

3.2. Representation of clothing in thermo-physiological models

$$U_{e,cl}^* = \frac{LR}{\sum_{j=1}^n \left(\frac{I_{cl}^*}{i_{cl}^*} \right)_j + \frac{1}{f_{cl}^* \cdot h_c}} \quad (3.9)$$

where I_{cl}^* is the local heat resistance of the j -th clothing layer ($\text{W m}^{-2} \text{K}^{-1}$), f_{cl}^* is the local clothing area factor and i_{cl}^* is the local moisture permeability index. Lastly, for the improved UCB clothing model, a distinction is made between clothed and not-clothed pathway from core to environment (Figure A.6). The third approach to local clothing modeling is only found in the Multi-segment Pierce model (Foda and Sirén, 2011). To calculate the convective and radiative heat losses with equations (3.1) and (3.2), an iterative procedure is performed to choose the correct clothing temperature.

3.2.2. Local clothing insulation and evaporative resistance values

In current data bases, e.g. ISO 9920:2009 and McCullough (1985, 1989), clothing insulation and evaporative resistance is given for whole-body approaches. Therefore, these values cannot be directly applied at local segments. Most TP models described in section 3.2.1 use their own local data, which is either measured for specific cases or taken from an in-house database, which is not publicly accessible. Only a few papers were published on local clothing properties, which will be presented here.

In the available literature, four studies were found which published sufficient data on local clothing insulation values: Curlee (2004) and Nelson et al. (2005), Havenith et al. (2012), Lee et al. (2013) and Lu et al. (2015). In Table 3.1, local clothing insulation values for different body parts are given for the four published studies using an example of a clothing ensemble consisting of underwear, t-shirt, trousers, socks and shoes. The table shows that local clothing insulation values vary across these studies. For instance, the local clothing insulation on the chest ranges from 0.116 to $1.14 \text{ m}^2 \text{K W}^{-1}$ and on the feet even from 0.079 to $0.287 \text{ m}^2 \text{K W}^{-1}$. Thus, it is difficult to choose an adequate value to be used in a TP model.

The reasons for the differences in the clothing thermal resistances can be found in the different approaches taken and different clothing specifications used in the four papers. The data of Curlee (2004) is based on a computational method, where the whole-body thermal clothing insulation values, evaporative resistances and area factors by McCullough (1989) were recalculated into local values. In contrast, Lee et al. (2013) and Lu et al. (2015) report measured values, which were obtained in

Table 3.1.: Comparison of local clothing thermal resistance for a light clothing ensemble

Body part	Clothing items	Local clothing area factor ^b	Local clothing insulation (m ² K/W)			
			Lee (No. 8)	Lu (EN 9)	Nelson & Curlee	Havenith (22°C)
Whole-body	–	–	0.081	/	0.088 ^a	0.081
Head/ Hand	None	–	0.00	/	0.00	0.00
Chest	Bra, t-shirt	1.22	0.177	0.169	0.174	0.116
Back	Bra, t-shirt	1.22	0.130	0.122	0.174	0.116
Abdomen	T-shirt	1.23	/	0.169	0.116	0.116
Pelvis	Panty + t-shirt + trousers	1.17	0.161	0.223	0.321	0.116
Upper arm	T-shirt	1.23	0.065	0.068	0.116	0.116
Forearm	None	(1.23)	0.00	0.023	0.000	0.104
Thigh	Trousers (fitted)	1.20	0.090	0.085	0.144	0.126
Lower leg	Trousers (loose)	1.44	0.096	0.076	0.197	0.126
Foot	Socks + shoes	1.25	0.127	/ ^c	0.287	0.079

^a Men's Summer Casual from McCullough et al. (1989)

^b taken from Nelson et al. (2005)

^c for the simulations in chapter 4, a value of 0.127 m² K W⁻¹ is assumed

experimental conditions following the standards ISO 9920:2009, but with different thermal manikins and postures. A third approach was taken by Havenith et al. (2012), who collected local thermal insulation values depending on the ambient temperature and then transferred the findings into empirical equations for 7 body parts. Apart from the different methods, the actual material, drape of the clothing or air gaps between clothing and manikin might be different as well. Limited material information can only be found for Curlee (2004) and Lu et al. (2015). For example, the t-shirt is described in Curlee (2004) as “broadcloth” and in Lu et al. (2015) as “cotton”. In Lee et al. (2013) and Havenith et al. (2012), no specifications of the materials are given. In all cases, the drape of the clothing or occurring air gaps are hardly described. All in all, these variations in methods and clothing specifications lead to a high uncertainty for the usage of these values in TP modeling.

Further values for clothing insulation and evaporative resistances can be found in studies investigating the effect of air speed and body movement on these values (see section 3.2.3 on the next page). However, these studies mostly feature only one or two clothing ensembles.

3.2.3. Effect of air penetration on clothing properties

Air penetration in clothing due to air or body movement reduces the clothing thermal insulation and evaporative resistance. This was shown in several studies for overall thermal insulation (Havenith et al., 1990b; Havenith and Nilsson, 2004; Holmér et al., 1999; Nielsen et al., 1985; Parsons et al., 1999) and total evaporative resistance (Havenith et al., 1990a). The standard ISO 9920:2009 provides equations to correct the whole-body values for air velocity and walking speed. The same correction factor is applied for thermal insulation and evaporative resistance.

In the revised UC Berkeley clothing model by Fu et al. (2014), different approaches to clothing insulation correction factors were compared to the values given in standard ISO 9920:2009. The authors concluded that the equations in standard ISO 9920 might be used as a first approach. However, for wind speed it was said that the correction for the trunk might be overestimated and for the extremities it might be underestimated. Furthermore, it was assumed that the equation for the evaporative resistance is also valid on segment level, but no investigation was done yet.

Wang et al. (2012) investigated the effect of air and body movement on the local clothing evaporative resistance for three light clothing ensembles (0.132 clo, 0.225 clo and 0.237 clo) at 14 body elements. The experiments were conducted at three research facilities all using a Newton sweating manikin and in standard conditions (ISO 9920: 2009). Local clothing evaporative resistances were measured at three air speeds (0.13 m s^{-1} , 0.48 m s^{-1} and 0.70 m s^{-1}) and three walking speeds (0 m s^{-1} , 0.96 m s^{-1} and 1.17 m s^{-1}). The results show that air speed reduced the local evaporative resistance at all body parts, and the reduction ranges from about 50% up to 86% depending on the site. Walking speed reduced the local evaporative resistance, especially at distal body parts such as hands and calves. Additionally, the article provides correction equations for combined air and body movement. It was concluded that the measurements need to be conducted for more clothing ensembles and a larger variety of wind and walking speeds to facilitate proper use for human thermal modeling. Moreover, the results are compared to the equations provided by ISO 9920:2009. In contrast to Fu et al. (2014), the authors concluded that the equations in the standard are not accurate enough for calculating the correction of local evaporative resistance.

As mentioned in section 3.2.2, Lu et al. (2015) conducted measurements on local

thermal insulation and the effect of body movement and air speed. Moreover, the interaction of body movement and air speed was analyzed using multiple nonlinear regression. The authors came up with correction equations for 11 body parts and the whole body as functions of air and walking speed. The results are based on three clothing combinations representing light, medium and protective clothing insulation. Hence, the results are very specific to the clothing ensembles and cannot directly be used for other outfits. However, the results give a good estimation of the reduction to be expected on local thermal insulation by air speed and body movement. Similar studies were done by Anttonen and Hiltunen (2009) for a military clothing ensemble and by Oguro et al. (2001, 2002) for a clothing combination of panties, bra, long sleeved shirt, trousers, socks and shoes.

Based on Tanabe's model (Tanabe et al., 2002), Wan and Fan (2008) described a transient model including heat loss from the microclimate between skin and clothing due to clothing ventilation and air penetration. Clothing ventilation and air penetration are included in energy and mass balances at every segment with the terms Q_{vent} and \dot{m}_{vent} , respectively. Both terms can be expressed using the formulas by Qian (2005):

$$Q_{vent,i} = KVI(V_{wind} + 2V_{walk} - v_0)(T_{mc,i} + T_a) \quad (3.10)$$

$$\dot{m}_{vent,i} = \frac{KVR}{\lambda} (V_{wind} + 2V_{walk} - v_0)(P_{mc,i} - P_a) \quad (3.11)$$

where KVI and KVR are empirical parameters for calculating the heat and moisture transfer caused by ventilation, V_{wind} is the wind speed of the environment, V_{walk} is the walking speed, v_0 is a reference air velocity, $T_{mc,i}$ is the temperature of the micro-climate, T_a is the temperature of the environment, λ is the latent heat of evaporation of water, $P_{mc,i}$ is the water vapor pressure of the micro-climate, and P_a is the water vapor pressure of the environment. Moreover, the authors apply an electric circuit analogy including clothing ventilation and air penetration in a skin-clothing-environment system to calculate convective coefficients for heat and moisture transfer (Figure A.7). In Qian (2005), the constants KVI and KVR were derived based on measurements and regression analysis of whole-body thermal properties. Hence, the application at segment level might be questionable. Wan and Fan compared simulation and experimental results for mean skin temperature, but due to the whole-body nature of KVI and KVR , outcomes for local skin temperature might differ.

3.2.4. Summary and discussion of necessity and availability of local clothing values

There is a variety of clothing models used for thermal modeling which can consider clothing on a body segment level (Tables A.5 and A.6 on page 130 and on page 131). The main input parameters for the models are the local clothing insulation I_{cl}^* or resistance R_{cl}^* , the local clothing evaporative resistance $R_{e,cl}^*$ or moisture permeability index i_{cl}^* , and the local clothing area factor f_{cl}^* . Values of these input parameters were measured or computed by the authors of the TP models for validation or research purposes. However, the used values were generally not published. Consequently, this fact limits the usability of TP models by other researchers, who have to rely on other published data, general data bases, e.g. standards, or require the appropriate measurement equipment, e.g. a sweating thermal manikin.

For local thermal insulation, there are limited publications on measured data. Additionally, standards, e.g. ISO 9920:2009, only provide global values. In one study, the effort was made to recalculate global clothing insulation into local values for a large number of clothing items which then can be combined to clothing ensembles. However, the comparison of clothing insulation values of the found studies shows discrepancies. In case of evaporative resistances even fewer values are available. Both outcomes emphasize the uncertainty attached to these values as input in TP models.

Local clothing properties are also influenced by air speed and body movement. Studies have investigated the reduction rates for clothing insulation and evaporative resistance for a small number of clothing ensembles. However, the results cannot be generalized, because of the limited number of tested clothing outfits.

All in all, research for local clothing properties seems to lack dependable and consistent data to be used in TP modeling.

3.3. Metabolic rate and its distribution over the body

The human body needs energy for maintaining the core temperature at approximately 37°C and for executing mechanical work. The energy is provided in a biochemical process at cell level, where food and oxygen is transformed to heat H and also

external work W as well as carbon dioxide and water as released byproducts. The detailed process can be found in standard literature for human biology or physiology, e.g. Guyton and Hall (2006). The total amount of energy converted ($H + W$) is referred to as (total) metabolic rate M . The metabolic rate is often provided in the met unit, which is based on the amount of energy used by a resting, seated person: $1 \text{ met} = 50 \text{ kcal/m}^2/\text{h} = 58.15 \text{ W m}^{-2}$ (ASHRAE, 2001; Parsons, 2014). The metabolic rate for maintaining basic body functions and temperature in supine position is defined as basal metabolic rate and is usually set to 0.8 met.

Individual total metabolic rates can be measured by direct or indirect calorimetry. For direct calorimetry, the subject is placed in a whole-body calorimeter and the energy balance of this person is carefully considered. Indirect calorimetry measures the oxygen consumption and carbon dioxide production of a subject. Further details of the measurement methods can be found in Parsons (2014), Havenith, Holmér et al. (2002) or in the standard EN-ISO 8996:2004. Based on these measurements, empirical equations and generalized tables for a variety of activities are available. Empirical models calculate metabolic rates using for example the human's weight, height or heart rate as input parameters. One example is the revised Harris and Benedict equations (Roza and Shizgal, 1984) which calculated the basic metabolic rate (BMR) in kcal/d for males and females:

$$BMR_{male} = 88.362 + (13.397 \cdot w) + (4.799 \cdot h) - (5.677 \cdot a) \quad (3.12)$$

$$BMR_{female} = 447.593 + (9.247 \cdot w) + (3.098 \cdot h) - (4.330 \cdot a) \quad (3.13)$$

where w is the weight (kg), h is the height (cm), and a is the age (years). Further equations are also summarized in Parsons (2014). Additionally, tables for metabolic rates of basic activities are provided in standard EN-ISO 8996:2004 or ASHRAE/55 (ASHRAE, 2004). Tabularized values give an approximation for metabolic rates, but their error can be significant (up to $\pm 50\%$) especially for activity levels over 3 met (ASHRAE, 2001). This uncertainty is mainly due to the differences in body composition of a specific subject and the average person in the model.

For temperature calculation in TP models, the metabolic heat production (H) has to be distinguished from the total metabolic rate (M) and the mechanical work (W). Thus, a mechanical efficiency factor η is introduced (equation (3.14)), which then is

3.3. Metabolic rate and its distribution over the body

used to calculate the metabolic heat production (equation (3.15)):

$$\eta = \frac{W}{M} \quad (3.14)$$

$$H = M(1 - \eta) \quad (3.15)$$

According to Parsons (2014) and Wyistdham et al. (1966), η ranges from zero for activities below 1.6 met and linearly increases up to 0.2 for activities from 1.6 to 5 met, i.e. at least 80% of the metabolic rate is used for heat production.

3.3.1. Local metabolic heat production in multi-segment thermo-physiological models

In multi-segment TP models, the total metabolic heat production is the sum of the heat production in all tissue layers at all segments. In Stolwijk's model (Stolwijk, 1971), the heat production is split up into three parts: 1) local basal heat production in all tissue layers (total of 0.8 met), 2) extra metabolic heat production in the muscle layers due to activity > 0.8 met (muscular heat production) and 3) heat production due to shivering (not discussed here). The principle was adopted by the consecutive models of Fiala et al. (1999), Huizenga et al. (2001) and Tanabe et al. (2002). A different approach is taken by Wissler (1985), who calculated metabolic heat production based on chemical reactions using O_2 and glucose intake in the body. For the multi-segment TP models by Smith (1991), Fu (1995) and Foda and Siren (2011), the approach to local metabolic heat production is not clear from the published papers.

Basal local metabolic heat production in Stolwijk's TP model (Stolwijk, 1971) is based on Aschoff and Wever (1958). The values of the six body parts add up to 74.4 kcal/h or 86.5 W, which is the total basal metabolic heat production for an average man.

In the model by Fiala (1998), the values for the basal metabolic heat production of each body part are taken from Werner and Buse (1988), who also refer to Stolwijk (1971). These values are obtained in thermo-neutral conditions, i.e. the human body does not need any regulation mechanism to maintain its core temperature. If the tissue temperature T differs from the temperature of thermal neutrality T_0 , local basal metabolic heat production changes. This change is described with the Q_{10} -effect with

a rate change of 2 (Werner and Buse, 1988):

$$\Delta q_{m,bas} = q_{m,0,bas} \cdot \left[2^{\frac{(T-T_0)}{10}} - 1 \right] \quad (3.16)$$

where $\Delta q_{m,bas}$ is the change in metabolic heat production, $q_{m,0,bas}$ is the basal metabolic heat production, and T and T_0 are the actual and thermo-neutral temperature of a tissue layer, respectively.

The metabolic heat production in the UC Berkley model by Huizenga et al. (2001) is calculated using the formulas by Harris and Benedict (1918):

$$BMR_{male} = 66.5 + (13.75 \cdot w) + (5.003 \cdot h) - (6.755 \cdot a) \quad (3.17)$$

$$BMR_{female} = 655.1 + (9.563 \cdot w) + (1.850 \cdot h) - (4.676 \cdot a) \quad (3.18)$$

where BMR is the basal metabolic rate (kcal/d), w is the weight (kg), h is the height (cm), and a is the age (years). In contrast to the other models based on Stolwijk, it is not mentioned how the heat is distributed over the body parts and their layers. However, since the model “is based on the Stolwijk model as well as on work by Tanabe in Japan” (Huizenga et al., 2001), it can be assumed that the values for local basal metabolic heat production are similar to either of these models. In Tanabe et al. (2002), values for local basal metabolic rates are published without a primary source.

Additional total muscular heat production H (see also equation (3.15)) is added to the local basal metabolic heat of the muscle layers $q_{m,bas,muscle}$ with the means of distribution coefficients $a_{m,w}$:

$$\begin{aligned} q_{m,muscle} &= q_{m,bas,muscle} + q_{m,w,muscle,Stolwijk} \\ &= q_{m,bas,muscle} + a_{m,w,Stolwijk} \cdot H \end{aligned} \quad (3.19)$$

The first set of coefficients was published by Stolwijk and were based on bicycle exercises (see Table 3.2). However, these coefficients were kept constant for all activities including sitting and standing. Fiala’s model (Fiala, 1998) adopted this basic principle, but the additional metabolic heat production in a muscle layer $q_{m,w,muscle,Fiala}$ depends also on the volume of the muscle V_{mus} :

$$q_{m,w,muscle,Fiala} = \frac{\delta(a_{m,w,i}H)}{\delta V_{mus,i}} \quad (3.20)$$

3.3. Metabolic rate and its distribution over the body

Table 3.2.: Comparison of distribution coefficients for heat production in muscles due to exercise for different body-parts in different TP models namely Stolwijk, Fiala and Tanabe

Body part	Distribution coefficients for external work			
	Stolwijk	Fiala (standing)	Fiala (seated)	Tanabe
Head	/	/	/	/
Shoulders and Neck		0.03	0.08	0.052
Chest/ Thorax		0.07	0.12	0.091
Back	0.30 ^a	/	/	0.080
Abdomen/ Pelvis		0.20	0.46	0.129
Upper arm/ Forearm	0.08	0.08	0.19	0.028
Hand	0.01	0.01	0.02	0.01
Thigh				0.402
Lower leg	0.60 ^b	0.60 ^c	0.11 ^c	0.198
Foot	0.01	0.01	0.02	0.01

^a In Stolwijk's model, the shoulders, neck, chest and back are combined in one body part.

^b In Stolwijk's model, the thigh and lower leg are combined in one body part.

^c In Fiala's model, the thigh and lower leg are combined in one body part.

The distribution coefficients $a_{m,w,i}$ for standing activities are the same as in Stolwijk (1971), but for the upper body the value is divided between neck, shoulders, thorax and abdomen. In the case of sedentary work, Fiala (1999) adjusted $a_{m,w,i}$ to higher values in the upper body (Table 3.2). Lastly, Tanabe et al. (2002) calculated the heat production in the muscle layers using equation (3.21):

$$q_{m,w,muscle,Tanabe} = 58.2 (M - q_{m,bas,muscle}) A_{Du} Metf_{muscle} \quad (3.21)$$

where M is total metabolic rate and $Metf_{muscle}$ is the muscular metabolic heat distribution coefficient in Tanabe's model (Table 3.2). Similar to Stolwijk, the coefficients are not changed for different activities.

3.3.2. Discussion on local metabolic heat distribution coefficients

The heat production in muscle layers is determined by local metabolic heat distribution coefficients (LDCs). The amount of heat produced in a specific muscle layer depends on the intensity of the activity, but also on the type of and posture during the activity. For example, walking at moderate speed and sorting books into a shelf can have similar activity levels. However, the muscles performing the work and therefore, producing heat might be different. Hence, the LDCs should be adjusted to different types of

activity. In contrast to this reasoning, most current TP models adopted the LDCs based on bicycle exercise by Stolwijk (1971) for all activities, even though, the activity level for riding a bicycle is higher than for other activities like sitting or standing and the muscular activity is also different. Some adjustments to these LDCs were made empirically by Fiala (2001) for seated conditions and by Tanabe (2002) for the distribution of muscle activity at the upper body (Table 3.2). The papers by Munir et al. (2009) and Psikuta et al. (2012) show that the change by Fiala (2001) improved the prediction of the local skin temperatures. However, adjusting the LDCs empirically carries the risk that the values are only valid for the specific case. For a sufficient empirical determination of the LDCs, the environmental conditions, the clothing and the individual characteristics have to be varied while performing the same activity. Moreover, other sources for error have to be excluded. In the case of the adjusted values by Fiala (2001), the reasoning behind the modification is not published and therefore, the certainty of these values is unknown. One reason for the empirical approach to LDCs is that a practical measurement method for the values does not exist. All in all, the reliability of the currently used LDCs might be questioned. To fill this gap, methods are needed to determine reliable LDCs for different activities.

3.4. Effect of local personal factors on local skin temperature and its implication on local thermal sensation

The previous sections showed that the literature provides different sets of clothing insulation values for a similar clothing ensemble, and also, varying LDCs. To assess the significance of the discrepancies in these input data, their effect on local skin temperature and ultimately, on local thermal sensation (LTS) needs to be discussed. For this purpose, we computed the local skin temperatures in two cases: 1) for the four sets of clothing properties listed in Table 3.1 and 2) for three sets of LDCs in Table 3.2, two by Fiala (2001) and one by Tanabe (2002). The basic values by Stolwijk (1971) were excluded, because no details were given on how the coefficient for the upper body is distributed over the single body parts. All scenarios in each case were named according to the main authors: “Nelson & Curlee”, “Havenith”, “Lee” and “Lu” for the comparison of clothing (case 1), and “Fiala seated”, “Fiala standing” and

“Tanabe” for the comparison of muscular metabolic heat distribution coefficients (case 2). For all simulations, the TP model ThermoSEM was used as defined by Kingma (2012), which is a multi-segment model consisting of 19 body parts. Further details of this TP model are given in Appendix B on page 153. The default geometry of the model is not changed for the simulations in this study. Additionally, ThermoSEM requires input data for the activity level, the environmental conditions, and worn clothing ensemble. These values are set differently for the comparison of local skin temperatures based on different clothing insulation values or various LDCs.

In case 1, the activity level was set to a value of 1 met to reduce the influence of heat production due to activity on the local skin temperatures. Furthermore, ThermoSEM uses the muscular heat distribution coefficients by Fiala (1999) for a seated position as default values (Table 3.2). The environmental conditions were assumed to be uniform and steady state. The effect of different environmental temperatures on the results was investigated by choosing an operative temperature of 22 °C and 26 °C. Other environmental parameters were not changed (air speed of 0.05 m s⁻¹, 40 % relative humidity).

In case 2, we investigated two activities namely standing and walking at 4.3 km h⁻¹ resulting in activity levels of 1.2 met and 2.6 met, respectively (ASHRAE, 2001). No clothing insulation was applied to eliminate its influence. To reduce the influence of vasomotion in the body, the operative temperature was calculated to represent thermal balance of the body with the environment (Kingma et al., 2014a). This calculation resulted in an operative temperature of 26 °C for standing, and 20 °C for walking at 4.3 km h⁻¹.

For all computations, the simulation time was set to 60 minutes and all skin temperatures were averaged over the last 45 minutes in each scenario. Since the main interest was in the maximal possible deviation in skin temperature, this maximum difference for any body part x in case 1 and case 2 were calculated as follows:

$$\begin{aligned} \Delta T_{sk,max,case1,x} = \max(& |(\bar{T}_{sk,Curlee,x} - \bar{T}_{sk,Havenith,x})|, |(\bar{T}_{sk,Curlee,x} - \bar{T}_{sk,Lee,x})|, \\ & |(\bar{T}_{sk,Curlee,x} - \bar{T}_{sk,Lu,x})|, |(\bar{T}_{sk,Havenith,x} - \bar{T}_{sk,Lee,x})|, \\ & |(\bar{T}_{sk,Havenith,x} - \bar{T}_{sk,Lu,x})|, |(\bar{T}_{sk,Lee,x} - \bar{T}_{sk,Lu,x})|) \end{aligned} \quad (3.22)$$

$$\Delta T_{sk,max,case2,x} = \max(|(\bar{T}_{sk,FialaSeated,x} - \bar{T}_{sk,FialaStand,x})|, |(\bar{T}_{sk,FialaSeated,x} - \bar{T}_{sk,Tanabe,x})|, |(\bar{T}_{sk,FialaStand,x} - \bar{T}_{sk,Tanabe,x})|) \quad (3.23)$$

where $\Delta T_{sk,max,case1/2,x}$ is the maximum difference in skin temperature for any body part x in case 1 or 2 and $\bar{T}_{sk, "Scenario", x}$ is the 45-minute average of the skin temperature of any body part x in any scenario. For comparison, also the averages are calculated analog to equations (3.22) and (3.23) by dividing the sum of all the differences by the number of scenarios in each case.

Finally, in section 3.4.3, the impact of the temperature differences on LTS is discussed using the LTS model by Zhang (2003).

3.4.1. Differences in local skin temperature for different sets of local clothing values

Figure 3.1 shows the maximum and average skin temperature differences of all four clothing data sets for the mean and six local body sites in two operative temperatures (T_o). It can be seen that the maximum and average difference in skin temperature depends on the body site and also on the operative temperature. For most body parts, the variation in skin temperatures ranges from about 0.4 to 1.4 °C with lower values for the higher operative temperature. In contrast to the other body parts, the foot skin temperature shows the highest maximum and average temperature discrepancy of up to 4.4 °C and 2.4 °C for $T_o = 22$ °C and 26 °C, respectively. Furthermore, the difference in skin temperature does not necessarily relate to the difference in clothing insulation (see Table 3.3). For example, the difference in clothing insulation for the abdomen and foot are the same, but the skin temperature difference of the foot is much higher than the one of the abdomen. Additionally, also temperature deviations can be found at body parts without clothing for instance the forehead and hand.

The temperature deviations at non-clothed body parts and the lacking correlation between differences in clothing and skin temperatures may be explained by looking at the local heat balances in the TP models. At every body part, heat is gained through metabolic processes, lost to the environment due to the temperature difference between skin and environment, stored in the tissue layers, and exchanged internally via blood perfusion. When adding clothing insulation to the heat balances, this reduces the heat

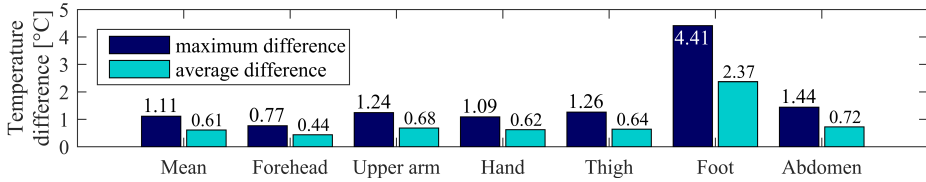
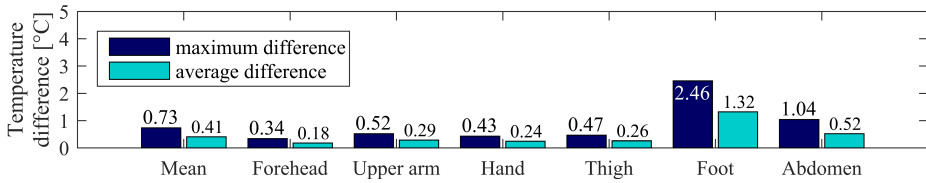
(a) $T_o = 22\text{ }^\circ\text{C}$ (b) $T_o = 26\text{ }^\circ\text{C}$ 

Figure 3.1.: Maximum and average local skin temperature differences for all four clothing data sets

Table 3.3.: Comparison of maximum difference in clothing insulation and skin temperature at $T_o = 22\text{ }^\circ\text{C}$

	Fore-head	Upper arm	Hand	Thigh	Foot	Abdomen
Max. difference in skin temp. [°C]	0.8	1.2	1.1	1.3	4.4	1.4
Max. difference in clo. insulation [m ² W ⁻¹ · 10 ⁻²]	0	4.65	0.16	6.2	20.8	20.8

losses to the environment at the clothed body part. To restore a thermal balance (heat production equals heat losses), more heat should be removed via the uncovered body parts by increasing local skin temperatures. Since heat is also exchanged internally via the blood perfusion, the clothing also indirectly influences other local heat balances. In detail, the heat fluxes of the blood flows from each body part are mixed in the central blood pool. From this step, the temperatures for the returning blood flows are calculated for the next simulation step. Some of these temperatures are corrected for counter current heat exchange that takes place due to closely located arteries and veins in some body parts. All in all, this physiological mechanism requires that the local clothing data is precise at all body parts.

The influence of operative temperature on the variation in the skin temperature differences is also due to its effect on the heat balances of the model. Firstly, higher operative temperatures lead initially to reduce heat losses to the environment, because

of the decreased temperature difference between the skin and the environment. Because of the smaller effective temperature difference, the influence of clothing is reduced as well. Secondly, the operative temperature can also affect the thermoregulatory processes in the body and their implications for the local heat balances. On one hand, in cold environments vasoconstriction may occur in some body parts. This response decreases the blood flow and hence, the heat exchange with other body parts. In this case, the impact of clothing might be kept more locally. On the other hand, warm environments lead to vasodilation, i.e. the blood flow to the body parts is increased. This process may lead to a larger influence of the calculated returning heat flux from the blood pool which depends on all other body parts. However, in the moderate conditions presented here, both processes are absent.

3.4.2. Differences in local skin temperature for different distribution coefficients of local metabolic heat

The impact of different sets of LDCs was calculated for two activities for an average man without clothing. The maximum and average temperature difference in-between scenarios for these simulations are shown in Figure 3 for the body average and for 6 separate body parts. In all cases, the temperature differences are equal to or lower than 1.3 °C. When comparing the activity levels, the temperature difference is higher for upper arm, hand and thigh, and much lower for mean, forehead and abdomen. Additionally, the temperature differences do not entirely relate to the differences in the LDCs (Table 3.4), which is similar to the results for the local clothing. For example, the difference in LDCs for the hand is very low, but still a maximum skin temperature difference of 0.8 °C can be seen. For the abdomen, the effect is reversed. Here, the variation in LDCs is larger, but the skin temperature difference is low. Also, differences in skin temperature for body parts without allocated muscular heat, e.g. the forehead, are found, but they are below 0.3 °C.

In the simulations of this section, the heat gain at the local balances is influenced by the sets of LDCs which determine how the overall metabolic heat production is redistributed to the local energy balances. Since these heat balances directly relate to the skin temperatures, uncertainties in the LDCs may increase the error in predicting local skin temperatures. As discussed in the previous subsection on the effect of local clothing properties, the skin temperature of one body site is also affected by all other

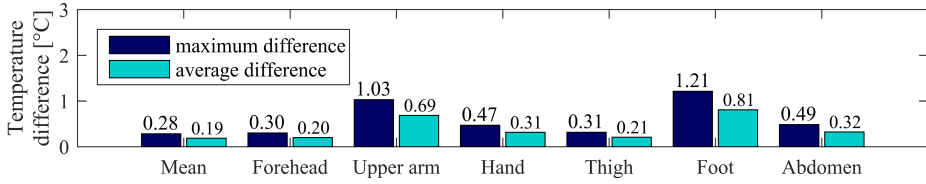
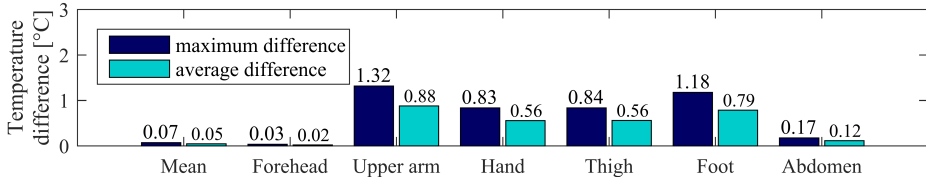
(a) Activity level of 1.2 met, $T_o = 26^\circ\text{C}$ (b) Activity level of 12.6 met, $T_o = 20^\circ\text{C}$ 

Figure 3.2.: Maximum and average temperature differences for all three sets of muscular metabolic heat distribution coefficients

Table 3.4.: Comparison of maximum difference in local heat distribution coefficients and skin temperature at operative temperature $T_{a,o} = 20^\circ\text{C}$ and an activity level of 2.6 met.

	Fore-head	Upper arm	Hand	Thigh	Foot	Abdomen
Max. difference in skin temp. [°C]	0.03	1.3	0.8	0.8	1.2	0.2
Max. difference in metabolic heat distribution[]	0	0.04	0.005	0.17	0.005	0.33

body parts through the internal heat exchange of blood flows via the central blood pool. Furthermore, the heat exchange might be influenced by vasomotion. Again, this physiological effect is not present in the presented simulations.

As discussed in section 3.3.2, the actual heat production in specific muscles also depends on the type of activity. The simulations for Figure 3.2 are based on different LDCs which represent different types of activity. For example, the scenario “Fiala standing” was originally based on bicycle experiments by Stolwijk and the scenario “Fiala seated” was fitted for a sitting position. Therefore, the comparison of the simulation results for the different sets of LDCs may lead by itself to some deviation in local skin temperature. However, in most TP models one set of LDCs is set as default or the specific type of activity for which they were defined is not traceable, e.g. Tanabe (2002). Hence, the comparison in this paper shows the consequence when LDCs are not adjusted to the type of activity simulated.

The graphs in Figure 3.2 also emphasize that the results for mean and local skin temperatures can be very different. Most of the current TP and coupled TS models (Tables A.2 and A.3) are validated for mean skin temperature and overall thermal sensation (OTS), respectively. For expanding these models to local skin temperature and LTS, the impacts on the local heat balances, as discussed above, have to be carefully considered.

3.4.3. Implication of differences in local skin temperature on local thermal sensation

The previous sections showed that uncertainties in local clothing properties and LDCs lead potentially to deviations in local skin temperature. To estimate the need for accurate input data, the impact of these findings on LTS was investigated. This evaluation was done using the functions for LTS provided by Zhang (2003) for static conditions:

$$LTS_{stat} = 4 \left(\frac{2}{1 + e^{-C1(T_{sk,loc} - T_{sk,loc,set}) - K1[(T_{sk,loc} - T_{sk,loc,set}) - (\bar{T}_{sk} - \bar{T}_{sk,set})]}} - 1 \right) \quad (3.24)$$

where $T_{sk,loc}$ is the local skin temperature, $T_{sk,loc,set}$ is the local skin temperature in neutral conditions (set point), \bar{T}_{sk} is the mean skin temperature, $\bar{T}_{sk,set}$ is the mean skin temperature in neutral conditions (set point), and $C1$ as well as $K1$ are regression coefficients for a specific body part. As examples, the body sites upper arm and foot were chosen (Figure 3.3), since these locations showed the highest temperature differences in the simulations of the previous sections. Additionally, they have an important influence on the OTS and thermal comfort, as was discussed by Zhang et al. (2010a).

Figure 3.3 displays the functions of LTS for the two body parts. LTS is displayed according to the 9-point ASHRAE scale from “very cold” to “neutral” to “hot”. The graphs depend on the deviation of the local and mean skin temperature from their set points. Assuming that the set points are fixed, an estimation of the influence of local skin temperature on LTS can be made. For example, the maximum temperature difference for the upper arm was 1.3°C. This result translates into a change in thermal sensation from neutral ($T_{sk,loc} - T_{sk,loc,set} = 0^\circ\text{C}$) to slightly warm/warm or neutral to slightly cool/cool for $T_{sk,loc} - T_{sk,loc,set}$ equals 1.3°C and -1.3°C , respectively. More

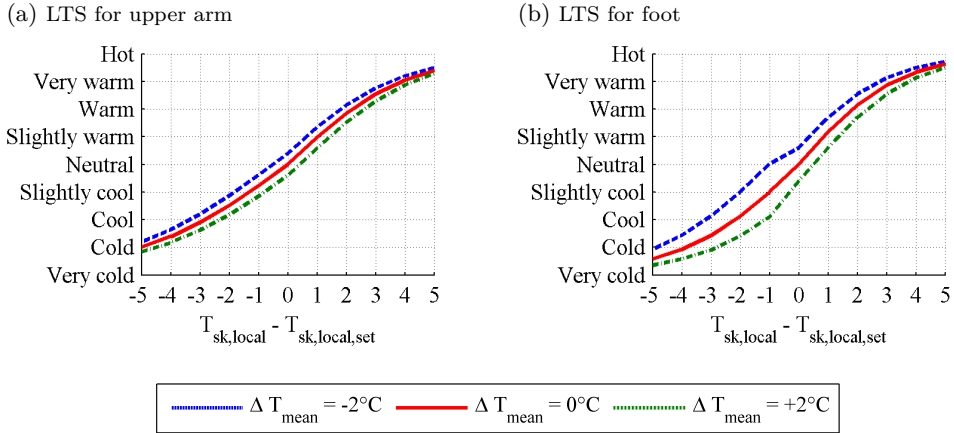


Figure 3.3.: Functions of LTS for a) upper arm and b) foot. The deviation from mean skin temperature to its set point is varied from -2 to 2°C as shown in the legend.

extreme changes are found for the foot, where the temperature deviation ranged from 2.2°C up to 4°C . Starting from neutral, these discrepancies change the LTS starting from neutral to warm/very warm or cool/cold. However, in general the reported skin temperature differences are around 1°C or lower. Thus, for these body parts, the change in LTS is around one step on the sensation scale.

The impact of these findings on local heating and cooling research can be seen from two perspectives: 1) considering the normal fluctuations in LTS votes and 2) considering the statistical significance between two sensation votes. For the first point of view, studies show that LTS votes within a group of subjects vary between 2 steps on the sensation scale (Dalewski et al., 2014; Melikov and Knudsen, 2007). This finding would be in line with the presented variation of thermal sensation for most body parts, excluding upper arm and foot. For the second perspective, researchers found significant differences in thermal comfort in scenarios, where the LTS was changed with environmental measures one step on the sensation scale (Kaczmarczyk et al., 2010; Li et al., 2010). This implies that the input data of all body parts is critical for local thermal modeling.

All in all, this analysis shows that variations in local skin temperatures can result in large difference in LTS. Hence, the data for clothing properties and LDCs should be chosen carefully, to avoid false results.

3.4.4. Limitations of the analysis

The analysis in section 3.4.1 to 3.4.3 gives an example of how the deviations in local clothing properties or in LDCs can affect LTS. The results are dependent on the reliability of the used TP and TS model. However, the impact of their inaccuracy on the conclusions is limited, because the same models were used in all cases. Furthermore, the simulations were simplified by implementing only uniform conditions, a single clothing outfit and an average man. In contrast, studies on local heating and cooling deal with non-uniform conditions, a variety of clothing sets and divers human subjects. These variations may lead to even more uncertainties in the input parameters resulting in large variations in local skin temperatures. Therefore, additional data is required and it should be measured as accurate as possible.

3.5. Conclusions

To help develop efficient local heating and cooling concepts as well as to test the comfort boundaries for non-uniform environments in modern buildings, local thermal modeling is required. Thermal sensation can be modeled with multi-segment thermo-physiological and coupled sensation models. These models calculate local skin temperatures and, furthermore, can account for local clothing properties as well as for changes in local metabolic heat. This study gives an overview of available local data, investigated their consistency throughout literature and examined their effect on local thermal sensation modeling. The following conclusions can be drawn:

- Full and consistent data sets for local clothing properties including insulation, evaporative resistance and their change due to air penetration are not fully available in published literature for a typical variety of office clothing sets.
- Distribution coefficients for muscular heat production are not verified for office activities, namely sitting, standing and walking, but were adapted empirically.
- Variations in local clothing properties and in coefficients for muscular heat distribution affect the accuracy of the local sensation output (about one step on a 9-point thermal sensation scale per 1 °C change in local skin temperature).

These conclusions lead to possible future research which could include:

- a systematic study on local clothing properties and their change due to air speed and body movement,
- development of feasible methods for measuring and validating local heat production.

Finally, since thermo-physiological models aim to be applied in design phases of modern buildings and therefore, might be used by building and civil engineers, an effort might be needed to include local clothing and local metabolic heat data in available standards.

CHAPTER 4

Local clothing thermal properties of typical office ensembles under realistic static and dynamic conditions*

4.1. Introduction

Most adults spend their major part of their day at work, typically in an office building. To enable workers at office buildings to perform at their best and stay healthy, it is necessary that the indoor environment meets their individual needs (Seppänen et al., 2006; Urlaub et al., 2013). However, office buildings also have to be energy efficient to adhere to modern standards. Hence, researchers and building engineers aim to

*The contents of this chapter have been published in:

- Veselá, Stephanie; Psikuta, Agnes, and Frijns, Arjan J. H. (2018c). “Local clothing thermal properties of typical office ensembles under realistic static and dynamic conditions”. In: *International Journal of Biometeorology* 62.12, pp. 2215–2229
- Veselá, Stephanie; Psikuta, Agnes, and Frijns, Arjan J. H. (2018b). “Determination of the local evaporative resistances of two typical office clothing ensembles and the effect of air speed and body movement”. In: *12th International Manikin and Modelling Meeting 29-31 August 2018, St. Gallen, Switzerland*

design the heating, ventilation and air conditioning (HVAC) systems of the building to be energy efficient, while also providing a thermally comfortable environment to all occupants. To achieve this goal, personalized heating and cooling systems are being developed (Arens et al., 1991; Foda and Sirén, 2012; Melikov et al., 1994; Parkinson et al., 2015; Veselý and Zeiler, 2014). To test the thermal comfort provided by these systems, a large number of human subjects are usually required, which increases the cost and length of the studies. This situation could be improved by using local thermal sensation and coupled thermal comfort models for preselecting promising designs. To achieve a high predictability of local skin temperatures, thermo-physiological models require reliable input data of the local dry clothing resistance, local evaporative clothing resistance and clothing area factor. However, Veselá et al. (2017b)/ Chapter 3 show that the available data is limited for typical office clothing ensembles. Additionally, few studies were performed on the local effect of increased air speeds and body movement.

Studies published on local clothing insulation values are, for example, Lee et al. (2013), Lu et al. (2015), Nelson et al. (2005) and Havenith et al. (2012). In Lee et al. (2013), measurements were carried out on a thermal manikin seated on a chair with different clothing sets. Their study contained a large variety of ensembles, but the effect of air speed, and body movement, were not included. Lu et al. (2015) studied the effect of air speed and body movement for dry local clothing insulation, but only two clothing ensembles are usable for office settings. A different approach is found in Nelson et al. (2005), where local insulation values were recalculated from the global values published by McCullough et al. (1985, 1989). Their study includes a large variety of single garments that can be combined to whole-body ensembles as needed. However, local effects of overlaying clothing items were not considered in this approach. Havenith et al. (2012) presented empirical equations based on the seasonal dressing customs of Europeans according to the outdoor air temperature to determine the local clothing insulation for seven body parts. This approach gives a rough estimation on the clothing insulation worn in a specific season of the year, but does not include the properties of the worn garments, such as the clothing material or fit, and neglects the parameters of the indoor environment. Further details on the different studies are described in detail in section 3.2.1 on page 26.

In conclusion, current literature does not provide enough local clothing properties for a variety of typical office clothing ensembles under different air speeds and with body movement. To close this gap, we measured the local dry thermal resistance of

eight body parts at three different air speeds and including body movement of a large variety of office clothing ensembles using a sweating agile manikin and a sweating foot manikin at Empa, Switzerland. For a selection of clothing ensembles, also the local evaporative resistance was measured for different air speeds and body movement. In addition, the local clothing area factors were estimated based on 3D scans of the clothing items. Here, the results of the measurements are presented and the effect of air speed, body movement and garment fit on the local clothing thermal properties is discussed.

4.2. Methods

4.2.1. Measuring equipment

The local dry thermal resistance ($R_{T,i}$) and local evaporative resistance ($R_{eT,i}$) of the office clothing ensembles was measured using the sweating agile manikin (SAM) (Richards and Mattle, 2001) at Empa, Switzerland as shown in Figure 4.1a. The manikin consists of 22 shell elements, which are made from thin-walled aluminum-polyethylene composite. Moreover, nine guards (hands, feet, elbows, knees and the face block) are installed to minimize the heat exchange between elements and the environment. All elements are uniformly and separately heated. The mean temperature of each shell part is measured at its outer surface with evenly distributed nickel resistance wires. Additionally, a water system with 125 outlets on the manikin's skin surface is installed to simulate sweating. The "sweat rate" of each segment can be controlled between 20 ml h^{-1} and 41 h^{-1} . To spread the water more evenly, SAM is dressed in a 0.7 mm thick polyester "skin" as shown in Figure 4.1b (Koelblen et al., 2017). Furthermore, SAM can be connected with a movement simulator, which enables the manikin to perform realistic movements of up to 2.5 km h^{-1} walking speed.

Because SAM has no foot segments, $R_{T,i}$ and $R_{eT,i}$ of representative shoe and sock combinations were measured with the foot simulator as described by Babic et al. (2008) and Bogerd et al. (2012). The foot manikin (Figure 4.2) represents a right foot of size EU 43 and consists of 13 separately heated metal elements. Furthermore, walking can be simulated with a net force of up to 25 kg and with a maximum of 25 steps per minute.

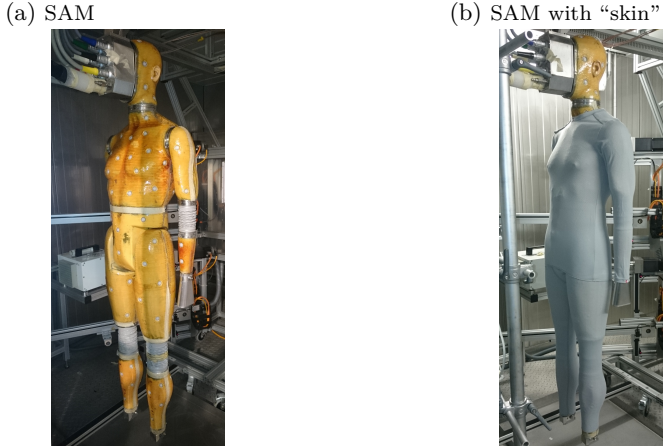


Figure 4.1.: Sweating agile manikin (SAM) a) without clothing and b) with “skin”

Both manikins are placed in separate climate chambers. The temperature and relative humidity of the chambers can be controlled within ± 1 °C and ± 5 %, respectively.

4.2.2. Garments and ensembles
















In this study, garments and their combinations typically worn in an office environment are considered. Since SAM has an average male stature, mainly male clothing items were chosen. The detailed properties of all clothing items are summarized Table A.7. To account for different preferences in clothing fit, the t-shirt, long-sleeved shirt (abbreviation: shirt), long-sleeved smart shirt (abbreviation: smart shirt) and jeans were included in different sizes, representing tight (T), regular (R) and loose (L) fits. The clothing items were combined to 23 whole-body and three foot combinations, which are summarized in Tables 4.1 and 4.2 as well as Figure 4.2.

4.2.3. Local clothing area factor

The total clothing area factor f_{cl} accounts for the increase of the total body surface area by the addition of clothing and is defined as follows:









$$f_{cl} = \frac{A_{dressed}}{A_{nude}} \quad (4.1)$$

Table 4.1.: Whole-body clothing ensembles (all outfits include briefs) - Ensembles 1-15

1	2	3	4	5
				
t-shirt (R), jeans (R)	shirt (R), jeans (R)	smart shirt (R), jeans (R)	t-shirt (L), jeans (R)	shirt (T), jeans (R)
6	7	8	9	10
				
smart shirt (T), jeans (R)	shirt (L), jeans (R)	smart shirt (L), jeans (R)	smart shirt (R), jeans (L)	smart shirt (R), jeans (T)
11	12	13	14	15
				
smart shirt (T), jeans (T)	smart shirt (L), jeans (L)	smart shirt (R), dress pants	smart shirt (R,in), dress pants	undershirt, t-shirt (R), jeans (R)

T=tight fit, R=regular fit, L=loose fit, in=tucked in pants

Table 4.2.: Whole-body clothing ensembles (all outfits include briefs) - Ensembles 16-23

16	17	18	19	20
				
t-shirt (R,in), smart shirt(L), jeans (R)	undershirt, smart shirt (R,in), pants	t-shirt (R,in), smart shirt (L,in), pants	t-shirt (R, in), sweater, jeans (R)	undershirt, smart shirt (R), sweater, jeans (R)
21	22	23		
				
undershirt, smart shirt (R,in), jacket, pants	smart shirt (R, in), skirt (with tights)	smart shirt (R, in), jacket, skirt (with tights)		

T=tight fit, R=regular fit, L=loose fit, in=tucked in pants



Figure 4.2.: Shoe/ sock combinations

where $A_{dressed}$ is the outer surface area of the dressed body and A_{nude} is the surface area of a nude body (ISO 9920: 2009). For the local clothing area factor $f_{cl,i}$, this definition is applied to all body parts separately.

For obtaining $f_{cl,i}$ of all used garments, a 3D scanner was used to scan the nude and dressed shop window manikin James to obtain the respective surface areas (Psikuta et al., 2012, 2015). In a 3D surface inspection software (Geomagic Control 2014, 3D Systems®, USA), the scans of the nude and dressed manikin were cut according to the defined body parts (Figure 4.3a) before $f_{cl,i}$ of the single sections were calculated. In all cases, uncovered areas, e.g. opening of the jacket on the chest, were not considered.

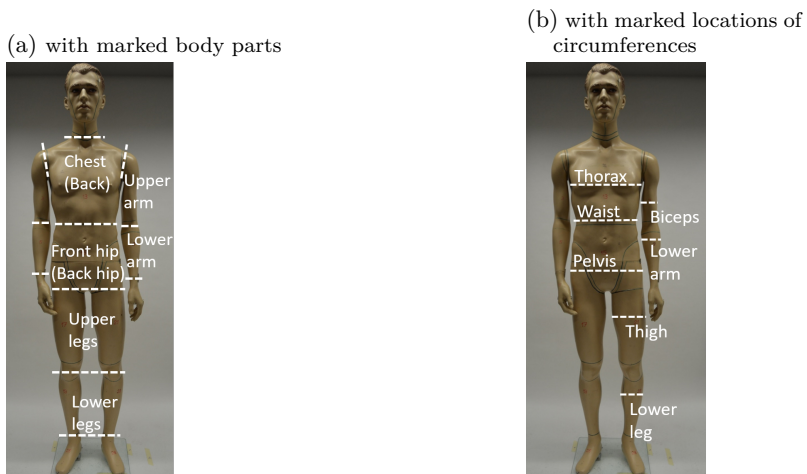


Figure 4.3.: Manikin James used to obtain local clothing area factors

A special case is $f_{cl,i}$ of the skirt since the inner thighs are not covered by a fabric. In this study, we decided to reduce the nude area of the thighs for the upright, stationary posture of the manikin, since the thighs are close to each other and therefore, the heat loss is reduced in this area. The nude area of the thighs, in the described case, was determined by drawing a line from the middle front and back of the skirt to the center of the thigh (Figure 4.4). Only the skin surface at the outer sides of the thighs (bold lines in Figure 4.4) are used for calculating the nude skin area A_{nude} which is needed for computing $f_{cl,i}$ (equation (4.1)). Hence, the inner parts of the thighs were left out. For the measurement with the moving manikin, the whole nude area of the thighs was considered.

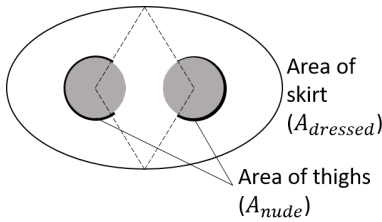


Figure 4.4.: Schematic for obtaining the thigh area factor for a person wearing a skirt

For most garments, the surface areas were obtained for three scans. Between the scans, the manikin was redressed to account for differences in draping. All results of $f_{cl,i}$ measured on James can be found in Tables A.8 and A.9 on page 133 and on page 134.

When considered strictly, $f_{cl,i}$ depends on the garment fit at a specific body part. Hence, $f_{cl,i}$ should be adjusted, when using other manikins, human subjects or garment fit. A measure of clothing fit is the ease allowance EA which is the difference between the circumferences of a clothing item ($CF_{cloth,i}$) and the manikin (or person) ($CF_{man,i}$) at a specific body landmark (Figure 4.3b) (ISO 8559: 1989).

$$EA_i = CF_{cloth,i} - CF_{man,i} \quad (4.2)$$

The garments were marked and measured at the same positions. All EA were then calculated for all items at the relevant positions. For the skirt, only the EA of the hip was measured. The EA of the clothing items on James are summarized in Table 4.3. Negative values indicate that the clothing is locally stretched while wearing it. Since the geometry of other manikins and real persons is slightly different, a correction is

Table 4.3.: Ease allowances of clothing items - James manikin

	Bi- ceps	Lower arm	Tho- rax	Waist	Pelvis	Thigh	Lower leg
t-shirt – regular	2	/	7	22	8	/	/
t-shirt – loose	10	/	12	39	19	/	/
shirt – tight	1	-1	-8	10	-9	/	/
shirt – regular	3	0.5	0	20	1	/	/
shirt – loose	9	3	8	28	9	/	/
smart shirt - tight	9	7.5	1	12	1	/	/
smart shirt – regular	11	8.5	10	24	11	/	/
smart shirt - loose	14	11	18	39	21	/	/
sweater	6	7	13	42	22/ -10*	/	/
business jacket	12.5	11	14	34	23	/	/
jeans – tight	/	/	/	/	6	3	3.5
jeans – regular	/	/	/	/	6	6	7.5
jeans – loose	/	/	/	/	9	10	12.5
dress pants	/	/	/	/	14	12	15.5
skirt	/	/	/	/	20	/	/

* EA of sweater at pelvis includes loosely falling main body of sweater (EA = 22cm) and tight ribbed band (EA = -10cm).

needed. The $f_{cl,i}$ for thermal manikin SAM are adjusted by measuring the respective circumferences and correcting the EA accordingly (see Table 4.4).

The $f_{cl,i}$ of the shoe/ sock combinations were estimated using the more classical method of calculating the nude and dressed areas using photographs and post-processing them in suitable software, e.g. Photoshop Elements (Adobe Systems Software, Ireland) (Havenith et al., 2015; McCullough et al., 1985).

Table 4.4.: Circumferences of manikin James and SAM as well as correction for EA

Location	Circumference on James [cm]	Circumference on SAM [cm]	Correction of ease allowance [cm]
Biceps	30	31	-1
Lower arm	27.5	24	3.5
Thorax	101	102	-1
Waist	74	78	-4
Pelvis	94	93	1
Upper leg	53	58	-5
Lower leg	35.5	39.5	-4

4.2.4. Local dry thermal resistance

The local dry thermal resistance ($R_{T,i}$) was measured according to standard ISO 15831:2004. For the measurements of the whole-body clothing ensembles on SAM, the surface temperature T_{skin} was set to 34 °C, the operative temperature of the environment T_{op} to 21 °C and the relative humidity to 40 %. The environmental conditions were monitored using a measurement tree with the sensors placed in front of the manikin (ThermCondSys5500 and AirDistSys 5000, Sensor electronic, Poland). The operative temperature and relative humidity was obtained at the height of the waist and their standard deviation was typically around 0.1 °C and 1 %, respectively. The air speed was measured at three heights, namely ankles, waist and head. The standard deviation for the air speed varied from about 0.02 m s⁻¹ for lowest air speed to 0.1 m s⁻¹ for largest air speed. In the reference case (test case 1), the air speed was set to 0.2 m s⁻¹ and SAM was in standing position. In these conditions, $R_{T,i}$ of all clothing ensembles (Tables 4.1 and 4.2) were measured. To analyze the influence of varying air speed and the addition of body movement, $R_{T,i}$ of six outfits (no. 1, 3, 14, 19, 21, 22) was determined in four additional test cases (TC 2-5). In test case 2 and 3, SAM was in standing position and the air speed was set to 0.4 m s⁻¹ and to 1.0 m s⁻¹, respectively. For the fourth and fifth test case, SAM was connected to the moving simulator and air speeds of 0.2 m s⁻¹ and 1.0 m s⁻¹ were used, respectively. The walking speed of the movement simulator was controlled to 2.5 km h⁻¹. In all cases, the air was directed from the front of the manikin. The local thermal resistance of the air layer $R_{a,i}$ was defined as the thermal insulation of the nude manikin. For each condition, three independent measurements were done for $R_{a,i}$.

Each clothing ensemble was measured in the relevant test cases at least twice for 45 minutes. If the difference between the two measurements exceeded 4 % for the total dry thermal resistance or 10 % for the local dry thermal resistances, an additional repetition was conducted (ISO 15831: 2004). In between the experiments, the manikin was redressed to account for differences in the draping of the garments. During the experiments, the dry heat loss $\dot{Q}_{loss,i}$, the skin temperature $T_{skin,i}$ of all body parts i and the environmental parameters were recorded. Then, $R_{T,i}$ and the local intrinsic clothing insulation $R_{cl,i}$ of a specific body part i were computed as an average of the last 20 minutes (steady state) using the measured $f_{cl,i}$ as described in sections 4.2.3

and 4.3.1 and equations (4.3) and (4.4), respectively.

$$R_{T,i} = \frac{T_{skin,i} - T_{op}}{\dot{Q}_{loss,i}} \quad (\text{m}^2 \text{K W}^{-1}) \quad (4.3)$$

$$R_{cl,i} = R_{T,i} - \frac{R_{a,i}}{f_{cl,i}} \quad (\text{m}^2 \text{K W}^{-1}) \quad (4.4)$$

In the case of the foot manikin, the skin temperature set point was set to 35 °C. The air speed in this climate chamber could not be altered. Measurements during the experiments showed that the air speed varied between 0.15 m s⁻¹ and 0.2 m s⁻¹. The standard deviation of the operative temperature and relative humidity during the experiments in this chamber were 0.1 °C and 1 %, respectively. To investigate the effect of movement, measurements were performed on the static foot and on the moving foot with a speed of 25 steps per minute (about 1.2 km h⁻¹) and a pressure of 25 kg. A larger number of steps per minute would be closer to the walking speed of SAM, but is not supported by the current system (Babic et al., 2008; Bogerd et al., 2012). Each shoe/ sock combination was then measured three times for 60 minutes in each scenario with changing shoes in between measurements. The resulting total clothing insulation $R_{T,foot}$ was determined for the sectors of the foot manikin, which represent the actual foot (below ankle) and are mostly covered by the shoes and socks.

4.2.5. Local evaporative thermal resistance

Measurements for the local evaporative resistance $R_{eT,i}$ in isothermal conditions were performed according to standards ISO 9920:2009 and ASTM F2370-10 (2010) using SAM with the polyester skin (Figure 4.1b). With respect to the standards, T_{op} was set to same temperature as the skin, i.e. 34 °C. The relative humidity was kept at approximately 40 %. The environmental conditions were monitored as described in section 4.2.4. Because of the skin, some outfits were too tight to be fitted on SAM, hence outfits 5, 7, 10, 20, 21 and 23 had to be excluded from these experiments. For all remaining clothing ensembles, $R_{T,i}$ were measured on the non-moving manikin with an air speed of 0.2 m s⁻¹ (TC 1). The representative office clothing ensembles 1 and 14 were selected to investigate the effect of two additional air speeds (0.4 m s⁻¹ and 1.0 m s⁻¹) and body movement. The set-up of the test cases 2-5 were the same as for the measurement of $R_{T,i}$ (section 4.2.4). The evaporative air layer resistance $R_{ea,i}$

was measured on the SAM wearing only the polyester skin for each environmental condition. For each clothing ensemble in a specific condition, three repetitions of 70 minutes were performed. Again, additional repetitions were done, if the deviation of the measurements were larger than 10% for $R_{eT,i}$. After one completed measurement, the clothes were completely dried, before the manikin was redressed. Again, the dry heat loss $\dot{Q}_{loss,i}$, the skin temperature $T_{skin,i}$ of all body parts i and the environmental parameters were documented during each experiment. The local total and clothing evaporative resistances, $R_{eT,i}$ and $R_{ecl,i}$, were then calculated as an average of the last 30 minutes for all body parts i using the results of $R_{T,i}$ and $f_{cl,i}$ (sections 4.3.1 and 4.3.2):

$$R_{eT,i} = \frac{(P_{sk,s,i} - P_a) A_i}{\dot{Q}_{loss,i} - \frac{(T_{sk,s,i} - T_{op}) A_i}{R_{T,i}}} \quad (\text{m}^2 \text{ kPa W}^{-1}) \quad (4.5)$$

$$R_{ecl,i} = R_{eT,i} - \frac{R_{ea,i}}{f_{cl,i}} \quad (\text{m}^2 \text{ kPa W}^{-1}) \quad (4.6)$$

where $P_{sk,s,i}$ is the partial vapour pressure at the skin's surface at a body part i and P_a is the partial vapor pressure in the air. The partial vapor pressure at the temperature t ($^{\circ}\text{C}$) can be calculated by Antoine's equation for the saturated vapor pressure P_{sa} multiplied by the relative humidity Φ at the skin's surface and in the air, respectively (Parsons, 2014). For the skin's surface, it is assumed that Φ is 1.

$$P_{sa} = 0.1 \cdot \exp\left(18.956 - \frac{4030.18}{t + 235}\right) \cdot \Phi \quad (\text{kPa}) \quad (4.7)$$

To calculate $R_{eT,i}$ and $R_{ecl,i}$ according to ASTM F2370-10 (2010) correctly, the surface temperature of the manikin's skin is needed instead of the manikin's surface temperature $T_{manikin}$ as provided by the system of SAM. The skin surface temperatures can be approximated according to Wang et al. (2017):

$$T_{sk,s,i} = T_{manikin} - a \cdot \dot{Q}_{loss,i} \quad (4.8)$$

where a is the "wet" conductive thermal resistance ($\text{m}^2 \text{ }^{\circ}\text{C W}^{-1}$) calculated using the regression equation for polyester and the skin thickness of 0.7 mm:

$$\begin{aligned} a &= 0.0055 \cdot d_{skin} + 0.0047 = 0.0055 \cdot 0.7 \text{ mm} + 0.0047 \\ &= 0.00855 \text{ m}^2 \text{ }^{\circ}\text{C W}^{-1} \end{aligned} \quad (4.9)$$

The literature often does not give $R_{eT,i}$ and $R_{ecl,i}$ directly, but mostly provides the total and clothing permeability indices $i_{m,T,i}$ and $i_{m,cl,i}$, respectively. These values can be derived from the local dry and evaporative resistances divided by the Lewis relation ($LR = 16.5 \text{ K kPa}^{-1}$) (ISO 9920: 2009):

$$i_{m,t/cl,i} = \frac{R_{T/cl,i}}{LR \cdot R_{eT/ecl,i}} \quad (4.10)$$

A particular issue arises when measuring and calculating the local evaporative resistances as compared to the total values. Due to gravity and absorption of the polyester skin, the (warm) water of one body part can travel to another site. This error might cause slight changes in the power that needs to be supplied to a body part, and hence, can lead to errors in the results. We tried to avoid this issue, by limiting the sweat rate in a way that the skin is just fully wetted.

4.3. Results and Discussion

4.3.1. Local clothing area factors

To obtain $f_{cl,i}$ for the used garments on manikin SAM, the correlation between $f_{cl,i}$ and the EA were investigated. In Figures 4.5 and 4.6, the linear fitting and R^2 -values are shown for all body parts. High linear correlations (R^2 -value > 0.8) between $f_{cl,i}$ and EA are seen for the upper and lower arm, back, back hip for lower body items as well as the lower and upper leg. For the chest, the R^2 -value is higher, when the sweater and jacket are excluded from the graph. This observation might be due to the design differences between the sweater, the jacket and the other shirts. For the EA pelvis - $f_{cl,i}$ front hip correlation in Figure 4.5e, two linear trend lines are shown, because the EA of the sweater includes the loosely falling main body of the sweater ($EA = 22 \text{ cm}$, solid line) and the tight ribbed band ($EA = -10 \text{ cm}$, dashed line). The squared Pearson coefficient is low for the linear correlation including the negative EA of the sweater ($R^2 = 0.33$) and higher when the larger EA is taken into account ($R^2 = 0.84$). Another option to predict $f_{cl,i}$ of the front and back hip of the upper body is to use the correlation to the EA of the waist (Figures 4.5f and 4.5h). Furthermore, the slope of the linear correlations varies for the different body parts. At the chest, for example, $f_{cl,i}$ for different EA varies only from 1.05 to 1.20. In contrast, $f_{cl,i}$ at the lower arm

covers a range from 1.15 to 1.7. Hence, the importance to adjust $f_{cl,i}$ with regards to EA depends on the body part. It can also be noted that $f_{cl,i}$ of some body parts at the same body landmark is very similar. For example, this observation can be seen for $f_{cl,i}$ of the chest and back at the thorax and for the front hip and back at the waist.

To estimate $f_{cl,i}$ of the whole-body ensembles in relation to SAM (Table 4.5), the following procedure was applied:

- The linear correlations, as shown in Figures 4.5a to 4.5d and 4.5f as well as Figures 4.5h and 4.6a to 4.6d were applied.
- It is assumed that the outermost garment defines $f_{cl,i}$ of a specific body part.
- In case of SAM, the hip is defined from the waist downwards (Figure 4.3), and hence, it is mainly covered by the upper body garment. Therefore, $f_{cl,hip}$ is taken mostly from the upper body garment. Only when the long-sleeved smart shirt is worn inside the dress pants, is $f_{cl,i}$ of the hips defined by these trousers.
- Skirt: No equation can be used to calculate the reduction of $f_{cl,i}$ because of the larger upper legs on SAM. For the jeans and pants, $f_{cl,i}$ of the upper legs was reduced by 0.10 to 0.15. Therefore, $f_{cl,i}$ of the upper leg of the skirt is also reduced from 2.29 to 2.15 for the stationary and from 1.5 to 1.35 for the moving manikin as an estimation.

For the shoe/ sock combinations, $f_{cl,i}$ were are as follows:

- ballerina/ nylon socks: 1.2
- sneakers/ athletic socks: 1.4
- business shoes/ athletic socks: 1.3

For tight clothing items, the described method can lead to calculated $f_{cl,i}$ below 1. This situation happens when the circumference of a specific body part on a manikin or human subject is larger than the one of the original manikin (James), so that the EA for the larger body becomes negative. For example, the calculated $f_{cl,i}$ of the tight jeans on the upper leg (outfit 10 and 11) and the tight long-sleeved shirt on the front hip (outfit 5) were 0.94 and 0.99, respectively. However, in reality the garment will stretch and the minimum value can only be the circumference of the specific body part with added thickness of the fabric. For the tight jeans on the upper leg the calculation reads $f_{cl,i,min} = \frac{(58 \text{ cm} + 2 \cdot \pi \cdot 0.067 \text{ cm})}{58 \text{ cm}} = 1.007$ and for the tight long-sleeved shirt on the hip it is $f_{cl,i,min} = \frac{(93 \text{ cm} + 2 \cdot \pi \cdot 0.087 \text{ cm})}{93 \text{ cm}} = 1.006$. Hence, these minimal values were used for further calculations.

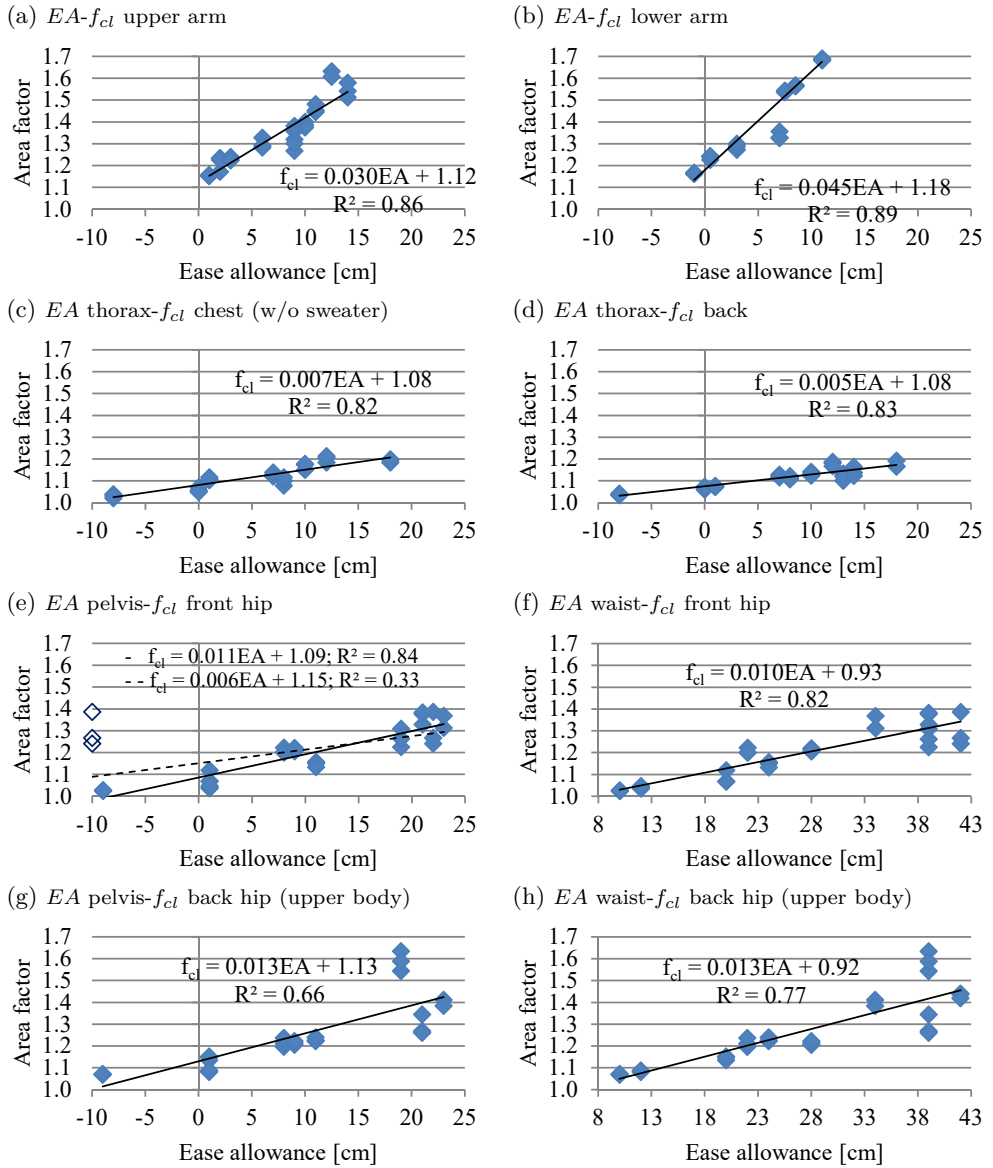


Figure 4.5.: Correlation of local clothing area factors $f_{cl,i}$ and ease allowances EA - Part 1

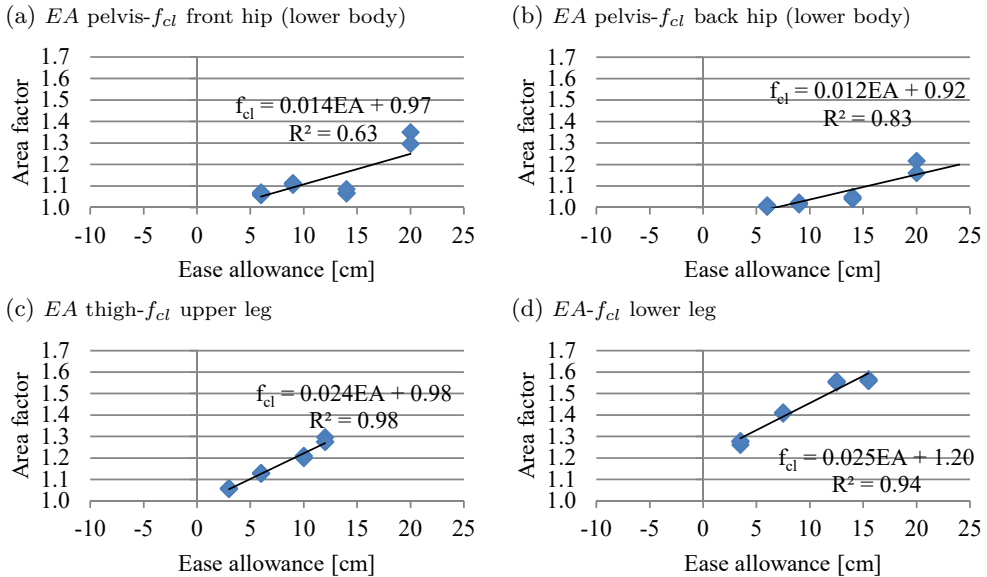


Figure 4.6.: Correlation of local clothing area factors $f_{cl,i}$ and ease allowances EA - Part 2

Comparison to values found in the literature

As mentioned in the introduction, there are very few values for $f_{cl,i}$ in the literature. In fact, the ones found in Nelson et al. (2005) are attributed to entire clothing items, and not to single body parts. Since the air gaps between the clothing item and the body surface can vary for different body parts, this may lead to false values for some body parts covered by the clothing item, especially if its area is small compared to the area of the whole garment. For example, $f_{cl,i}$ of the long-sleeved shirt with shirt collar in Nelson et al. (2005) is 1.24. This value is slightly higher but comparable to $f_{cl,i}$ of the chest, back, front and back hip of the regular long-sleeved smart shirt in this paper (1.12 – 1.17). However, it is much lower than $f_{cl,i}$ of the upper and lower arm (1.43 and 1.71, respectively). Another issue is that the fit of the clothing items are described very briefly with general terms such as “fitted” or “loose”. The straight, long trousers in Nelson et al. (2005), for instance, have a $f_{cl,i}$ of 1.20 in the “fitted” case. However, this value is by 0.1 to 0.2 larger than the values obtained for the measured tight jeans (outfits 10-11) and also the regular fitting jeans (outfits 1-8) of this study on the hip and upper leg. A larger $f_{cl,i}$ would mean that a smaller adjacent air insulation value is subtracted from the measured total thermal insulation of garment to calculate the intrinsic clothing insulation of a specific body part (see equation (4.4)). For example,

Table 4.5.: Estimated $f_{cl,i}$ for different clothing ensembles for SAM

Outfit	Local clothing area factor							
	Upper arm	Lower arm	Chest	Back	Front hip	Back hip	Upper leg	Lower leg
1	1.15	/	1.13	1.11	1.11	1.15	1.01	1.29
2	1.18	1.36	1.07	1.07	1.09	1.13	1.01	1.29
3	1.42	1.72	1.16	1.12	1.13	1.18	1.01	1.29
4	1.39	/	1.17	1.13	1.28	1.37	1.01	1.29
5	1.12	1.29	1.01	1.03	1.01	1.01	1.01	1.29
6	1.36	1.68	1.08	1.08	1.01	1.02	1.01	1.29
7	1.37	1.47	1.14	1.11	1.17	1.23	1.01	1.29
8	1.51	1.83	1.22	1.17	1.28	1.37	1.01	1.29
9	1.42	1.72	1.16	1.12	1.13	1.18	1.10	1.42
10	1.42	1.72	1.16	1.12	1.13	1.18	1.01	1.19
11	1.37	1.67	1.09	1.08	1.00	1.03	1.01	1.19
12	1.51	1.83	1.22	1.17	1.28	1.37	1.10	1.42
13	1.42	1.72	1.16	1.12	1.13	1.18	1.15	1.49
14	1.42	1.72	1.16	1.12	1.18	1.09	1.15	1.49
15	1.42	1.72	1.16	1.12	1.13	1.18	1.01	1.29
16	1.51	1.83	1.22	1.17	1.28	1.37	1.01	1.29
17	1.42	1.72	1.16	1.12	1.18	1.09	1.15	1.49
18	1.51	1.83	1.22	1.17	1.18	1.09	1.15	1.49
19	1.27	1.65	1.18	1.14	1.31	1.41	1.01	1.29
20	1.27	1.65	1.18	1.14	1.31	1.41	1.01	1.29
21	1.46	1.83	1.19	1.15	1.23	1.30	1.15	1.49
22	1.42	1.72	1.16	1.12	1.13	1.18	2.15*	1.00
23	1.46	1.83	1.19	1.15	1.23	1.30	2.15	1.00

* local clothing area factor of the skirt in case of movement (1.35)

the upper leg has an air layer insulation of $0.08 \text{ m}^2 \text{ W}^{-1}$. $f_{cl,i}$ of 1.0 and 1.2 would lead to the subtraction of $0.08 \text{ m}^2 \text{ W}^{-1}$ or $0.067 \text{ m}^2 \text{ W}^{-1}$ of air insulation, respectively, which is a difference of 16% in the intrinsic clothing insulation. Hence, a more exact measurement for the fit of clothing items, such as the ease allowance may help to avoid the mentioned inaccuracies.

4.3.2. Local dry thermal resistance

The detailed results for $R_{cl,i}$ of the whole-body clothing ensembles and $R_{a,i}$ of all test cases are shown in Tables A.10 and A.11 on page 135 and on page 137. For the sock/shoe combinations, $R_{T,i}$ in the non-moving case is $0.11 \text{ m}^2 \text{ K W}^{-1}$ for the ballerinas

with nylon socks and $0.13 \text{ m}^2 \text{ K W}^{-1}$ for both the sneakers and business shoes combined with the athletic socks. These values are reduced by movement to $0.09 \text{ m}^2 \text{ K W}^{-1}$ and $0.12 \text{ m}^2 \text{ K W}^{-1}$, respectively. The air layer insulation could only be determined for the non-moving foot and is $0.09 \text{ m}^2 \text{ K W}^{-1}$. Hence, $R_{cl,i}$ of the sneakers, business shoes and ballerinas for the non-moving foot manikin can be computed by equation (4). Their values are $0.07 \text{ m}^2 \text{ K W}^{-1}$, $0.06 \text{ m}^2 \text{ K W}^{-1}$ and $0.04 \text{ m}^2 \text{ K W}^{-1}$, respectively.

Comparison to values found in the literature

For a clothing ensemble consisting of a t-shirt and jeans, the measured $R_{cl,i}$ of this study, namely outfit 1 and 4 (with regular and loose t-shirt, respectively), can be compared to four other studies (Havenith et al., 2012; Lee et al., 2013; Lu et al., 2015; Nelson et al., 2005) as shown in Table 4.6. For the empirical equations by Havenith et al. (2012) an air temperature of 22°C is assumed. The comparison in Table 4.6 reveals that the differences in $R_{cl,i}$ vary depending on the body part. For example, $R_{cl,i}$ of the upper arm found in the literature are comparable to ones measured in this study. For the back, the values from the literature are generally smaller than from outfit 1 or 4. The most variance between the studies and our values is seen at the front and back hip. These observed variations might be caused by the distinct material and fit of the garments. Garments made of thicker material and with a looser fit, i.e. larger air gap, would result in increased clothing insulation values. Moreover, the differences in the construction, set-up, and posture of the used manikins can affect the result. For example, SAM has pronounced anatomical shoulder blades, unlike most of the other thermal manikins with simplified or smoothed body shapes, which creates a higher clothing insulation through a larger air gap when the clothing is on. Moreover, the manikin in Lee et al. (2013) was in sitting position, which causes smaller air gaps at the back, pelvis, thigh, and calf. Also, in a sitting position, the draping of the clothing is different than in upright position (Mert et al., 2017). Another issue comparing different studies is that the body parts are defined differently. This difference especially occurs for the torso. In Lee et al. (2013), for instance, the torso is divided in the chest, back and pelvis, whereas in Lu et al. (2015) it consists of the chest, back, abdomen and pelvis. In these regions, the clothing draping pattern can differ as discussed by Frackiewicz-Kaczmarek et al. (2015). Another factor that can cause different $R_{cl,i}$ is slight variations in the environmental conditions. For example, the air speed in the studies by Lee et al. (2013) and Lu et al. (2015) is 0.1 m s^{-1} and 0.15 m s^{-1} , respectively, whereas the air speed in this study was set to 0.2 m s^{-1} . However, the

Table 4.6.: Comparison of local intrinsic clothing thermal resistance for a light clothing ensemble (Havenith et al., 2012; Lee et al., 2013; Lu et al., 2015; Nelson et al., 2005)

Body part	Local clothing resistance [m ² K/W]					
	Lee (No. 8)	Lu (EN 9)	Nelson & Curlee	Havenith (22°C)	Measured Outfit 1	Measured Outfit 4
Chest	0.18	0.17	0.10	0.12	0.09	0.10
Back	0.13	0.12	0.10	0.12	0.17	0.18
Upper arm	0.07	0.07	0.10	0.12	0.08	0.12
Front hip		0.17	0.24	0.12	0.13	0.16
Back hip	0.16	0.22	0.24	0.12	0.15	0.19
Thigh	0.09	0.09	0.08	0.13	0.06	0.05
Lower leg	0.10	0.08	0.13	0.13	0.09	0.08
					Business shoes/ Sneakers	
Feet	0.13	/	0.22	0.08	0.06/ 0.07	

compared papers do not contain all of this information. Hence, it is difficult for users of thermo-physiological or thermal sensation models to extract the most suitable set of $R_{cl,i}$ for a specific simulation case.

The intrinsic clothing insulation of the business shoes and sneakers are also included in Table 4.6 and compared to the values found in the mentioned studies. In general, the variation of the values for the foot dry insulation is high with the values of this study being the lowest. The range of the measured values (excluding the value by Nelson et al. (2005)) is 0.6 to 0.13 m² K W⁻¹. In an inter-laboratory test on thermal foot manikins by Kuklane et al. (2005), the effective insulation values also varied by ± 0.3 to 0.6 m² K W⁻¹ depending on the tested shoe/sock combination. When compared to the measurements on army boots on the same foot manikin by Bogerd et al. (2012), $R_{T,i}$ of the business shoes and sneakers are in line with $R_{T,i}$ of army boots which was around 0.18 m² K W⁻¹.

For the ballerinas, no comparable values were found. In Lee et al. (2013), the sandals have a local intrinsic insulation value of around 0.4 clo (0.06 m² K W⁻¹), and in Kuklane et al. (2009), the described sandal has an effective insulation ($R_{T,i} - R_{a,i}$) of 0.06 m² K W⁻¹. In both cases, the values are higher than for the ballerinas, even though a similar range would be expected. Three issues can be raised on these shoe insulation measurements. Firstly, the two sandals touched the ground during measurements, whereas the non-moving foot was hanging free. Hence, there was no convection on the sole of the sandals, which can result in overall higher $R_{T,i}$.

Secondly, the sandals of the study by Kuklane et al. (2009) have the highest effective sole insulation ($0.261 \text{ m}^2 \text{ K W}^{-1}$) in the study, which also results in relatively high $R_{T,i}$ for the whole sandals. Lastly, the shoe insulation depends on the included sectors of the foot manikin in the calculation. For this study, the sectors of the foot manikin below the ankle were used. However, the ballerinas, for instance, do not cover the dorsal foot, which means that $R_{T,i}$ of the whole foot will be less than $R_{T,i}$ of the covered areas. In our case the values are $0.11 \text{ m}^2 \text{ K W}^{-1}$ and $0.13 \text{ m}^2 \text{ K W}^{-1}$, respectively. Conclusively, these issues should be considered and reported in studies on shoe insulation measurements to be able to do a fair comparison. This information will also help to choose the best values to use in thermo-physiological models.

Effect of air speed and body movement

For six outfits (1, 3, 14, 19, 21, 22), $R_{cl,i}$ was obtained for two additional air speeds and body movement (Table A.10 on page 135 and Figure 4.7). Also, the correction factors were calculated using test case 1 as the reference and can be found in Tables A.13 to A.16 on page 139. Additionally, the graphs showing the influence of increased air speed and the addition of body movement on $R_{T,i}$ are given in Figure A.8 on page 140. In general, the effect of increased air speed and body movement are more pronounced, but comparable, in $R_{T,i}$, because the air layer is excluded for $R_{cl,i}$. For the upper and lower arm, chest, front hip, upper and lower leg the increase in air speed and addition of body movement mostly reduced $R_{cl,i}$. At an air speed of 0.4 m s^{-1} , the reduction is minor and mostly within the standard deviation of $R_{cl,i}$. For an air speed of 1.0 m s^{-1} , low influence can be found for the upper and lower leg (except when a skirt is worn), whereas the reduction can reach up to 30 to 40% at the arms and chest. The effect of body movement is generally larger than for the increase in air speed for these body parts. This observation is more pronounced for upper legs with pants than with jeans. For the chest and front hip, the increase to an air speed of 1.0 m s^{-1} or the addition of body movement yielded similar results. The differences of the effect of body movement on the reduction in $R_{cl,i}$ might be caused by differences in the pumping effect, which is more pronounced for looser fitting clothing and on moving body parts. Hence, the pumping effect will be smaller for the relatively small movement of the torso when the manikin is in motion mode, and larger at the arms and legs, especially for looser fitting garments such as the pants. For the back and back hip, the results are more diverse. Surprisingly, the increase of air speed and body movement leads to an increase in $R_{cl,i}$ in a large number of cases. This outcome might

be caused by two possible issues: 1) as mentioned above, the anatomy of SAM results is an unnaturally hollow back and 2) the direction of the wind from the front to the back results in the displacement of the garments towards the back. In both cases, the air gap between the skin of the manikin and garment(s) will increase for higher air speeds until a critical speed is reached, where the air will leave through the lower opening of the shirt. Due to the hollow back, this critical wind speed value might be relatively high compared to other manikins, causing the rise in $R_{cl,i}$ for at least a wind speed of 0.4 m s^{-1} . The addition of body movement might emphasize this effect for low wind speeds, since the upper garment might to be push upwards creating a larger air gap due to the attachment of the legs to the moving simulator.

In the published literature for overall clothing insulation, general equations are given for the reduction of R_T due increased air speeds and body movement (Havenith and Nilsson, 2004; ISO 9920: 2009; Nilsson, 1997; Nilsson et al., 2000). However, the effect of increased air speed and the addition of body movement cannot be generalized for our measurements, i.e. the local total and intrinsic clothing insulation. For the thermo-physiological modeling, this finding means that the effect of increased air speed and body movement should be considered separately for each body part rather than using a general reduction factor for the whole body as suggested in ISO 9920: 2009.

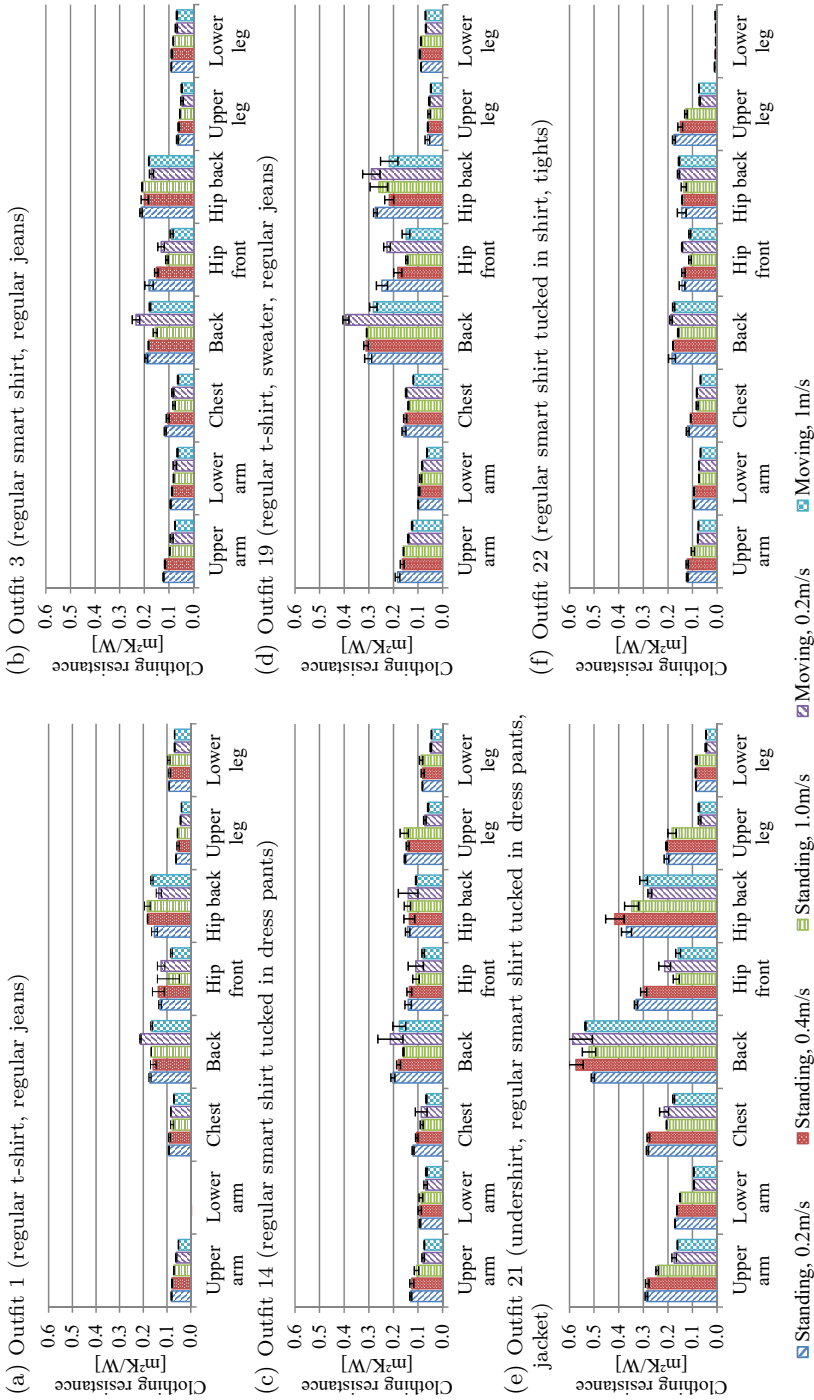


Figure 4.7.: Influence of air speed and body movement on local intrinsic clothing insulation

Effect of clothing fit

For this study, the four clothing items t-shirt, long-sleeved shirt, long-sleeved smart shirt, and jeans were available in different fits. In Figures 4.8 and 4.9, their $R_{cl,i}$ are shown in relation to their EA at the respective body landmarks for outfits with one clothing layer. In most cases, $R_{cl,i}$ increases for larger EA . These differences are relatively small for the lower arm, lower leg and back hip, but larger for the upper arm, chest, back, front hip and upper leg. The $R_{cl,i}$ of the smart shirt at the hips have more variation because it is combined with a larger variety of lower body garments, which overlap at the hips. Therefore, it is concluded that the knowledge of the exact fit, i.e. measurement of EA , is important when $R_{cl,i}$ values are published.

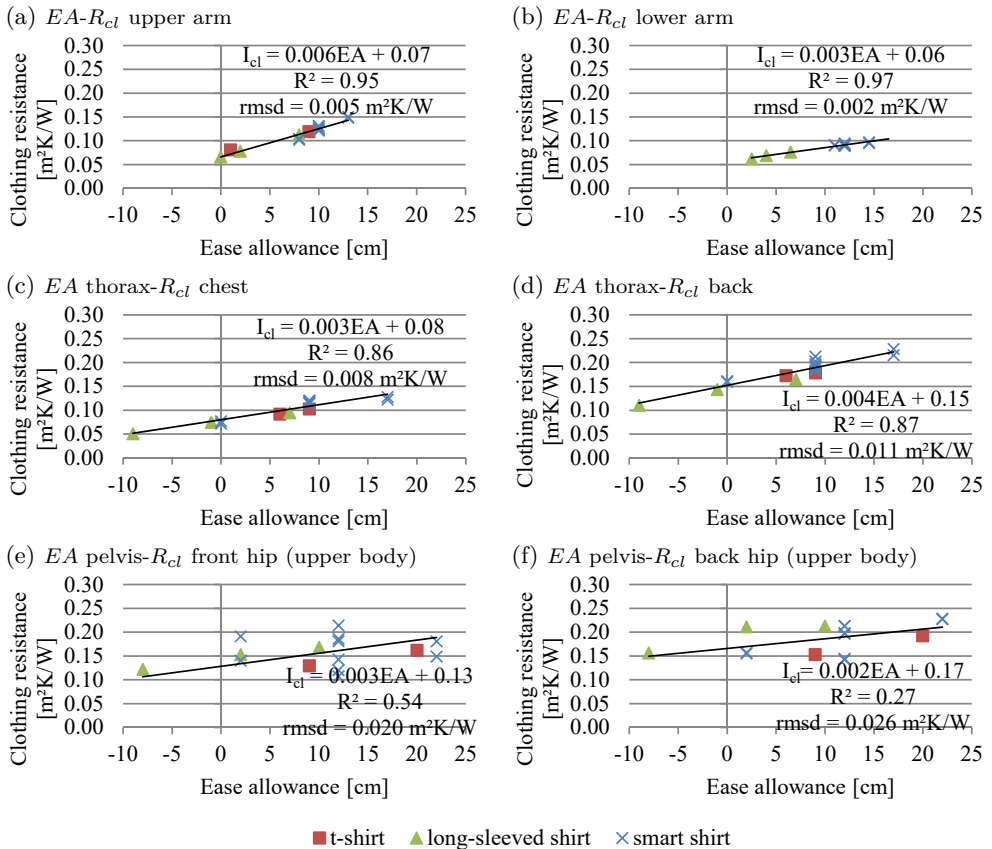


Figure 4.8.: Correlation of local dry clothing insulation and ease allowances - upper body

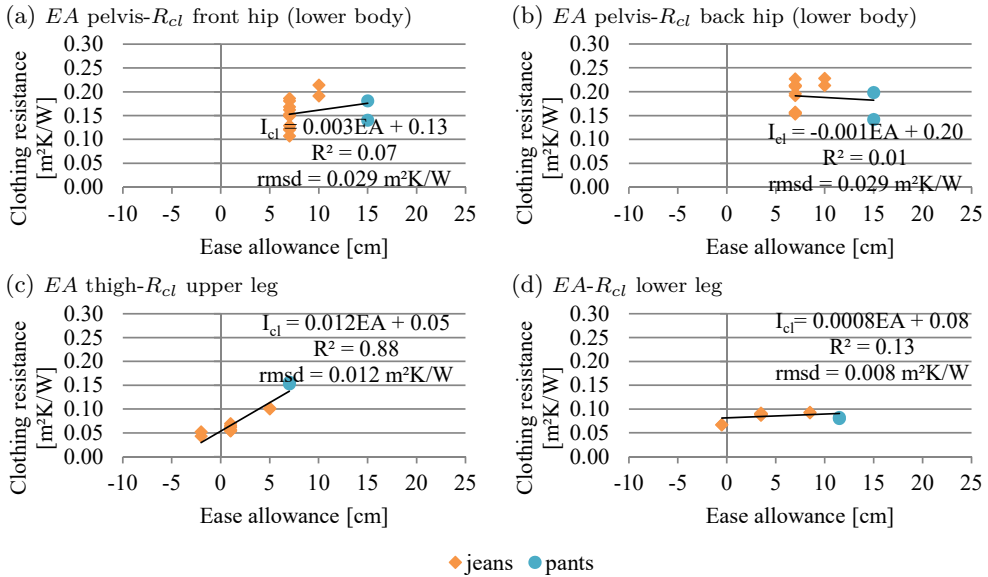


Figure 4.9.: Correlation of local dry clothing insulation and ease allowances - lower body

Correlation of local ease allowance and local dry clothing resistance

In this study, $R_{cl,i}$ of specific garments were measured. To apply these results to other research projects with similar outfits, the correlation between the local EA and $R_{cl,i}$ values for single layer outfits was investigated. In our range of EA the trend might be approximated as linear, because EA is linearly correlated to air gap thickness (Frackiewicz-Kaczmarek et al., 2015; Mert et al., 2017) and air gap thickness, in turn, is close-to-linearly correlated to the heat transfer coefficient for the air gap range of 4 to 32 mm as investigated by Mert et al. (2017). The range of air gap thickness investigated in this paper is well covered by this study, and Figures 4.8 and 4.9 provide the linear correlation, R^2 -values and root-mean-square deviation (rmsd) for all body parts.

High linear correlations ($R^2 > 0.85$) and low rmsd values can be found for the upper and lower arm, chest, back, and upper leg. Hence, $R_{cl,i}$ could be estimated using the provided linear correlations for other garments, manikins or human subjects. In contrast, the linear correlation at the front and back hip is weak ($R^2 < 0.6$) and the results are more diverse. The main reason is that the clothing items of the upper and lower body overlap at this body part. Hence, a second air gap influences the

result, which is not represented by EA measurement. The effect of this air gap can, for example, be seen in the difference of the regular smart shirt being tucked in the dress pants or not ($0.14 \text{ m}^2 \text{ K W}^{-1}$ vs $0.18 \text{ m}^2 \text{ K W}^{-1}$, respectively; Table A.10 on page 135). However, the R^2 -value does not increase much if EA of the waist is used or only the upper body garments worn with the regular jeans are considered. Hence, for estimating $R_{cl,i}$ at the hip for other garments, further factors, e.g. width of second air gap, should be considered. In the case of the lower leg, $R_{cl,i}$ is very similar for all clothing items regardless of their fit (low R^2 and low $rsmd$). Hence, $R_{cl,i}$ for the lower leg cannot be predicted by a correlation equation, but might be assumed to be approximately $0.08 \text{ m}^2 \text{ K W}^{-1}$. One reason for this result might be that the shape of the lower leg is very versatile ranging from 23 to 39 cm. The EA was measured at the widest place and, according to Table 4.3, there was a large selection of different EA . This is also shown by the steeper slope of $f_{cl,i}$ vs EA in Figure 4.6d. However, thermally, it seems that even for small EA the air gap at the lower part of the lower leg were relatively large. According to the dry heat transfer theory, the change in heat loss is minimal for further increase in air gap (Mert et al., 2016, 2017). Hence, the heat loss for all trousers is comparable.

The found correlations provide only an estimation of $R_{cl,i}$ values for single layer outfits. For clothing ensembles with multiple layers, a correlation to EA cannot be expected, because this measurement does not include information about the number of layers and their air gaps. In future research, it could be investigated if an additional clothing layer would result in a similar increase in $R_{cl,i}$ for a variety of single layer clothing ensembles.

In a recent study by Fojtlín et al. (2019), the dry thermal clothing resistance using the regression equations in Figures 4.8 and 4.9 and local clothing area factors were compared to values of other studies and a reference model. The measured values of this thesis are in good agreement with the reference model. Hence, the case study by Fojtlín et al. (2019) demonstrates the applicability of the measured local clothing properties and the regression equations.

4.3.3. Local evaporative thermal resistance

Tables A.11 and A.12 on page 137 and on page 138 give the detailed results for $R_{ecl,i}$ and $R_{ea,i}$ for all clothing ensembles and test cases. The results for the shoe/sock combinations are summarized in Table 4.7. Unfortunately, only the results for the non-moving case can be reported, due to some malfunctioning of the foot manikin during the moving scenarios.

Comparison to values found in the literature

As mentioned in section 3.2.2 on page 27, only a few measured $R_{ecl,i}$ for office clothing ensembles have been published. In fact, for the clothing ensembles of this thesis, no measured values were found for direct comparison. In ISO 9920:2009, a generalized clothing permeability index of 0.38 is given. Figure 4.10 compares the local clothing permeability indices of selected clothing ensembles and the shoe/sock combinations to the standard value. The local clothing permeability indices ranges from about 0.1 to 0.8. Hence, the value of 0.38 might be an agreeable estimation for average skin temperature and thermal sensation calculations. However, considering the separate body parts, the suggested value of 0.38 would only be a good estimation for the upper arm and lower leg in most cases. The permeability index of the feet $i_{cl,feet}$ is very low in comparison to the other values. However, it is in-line with values published by Bogerd et al. (2012). The sensitivity analysis in section 2.3.4 on page 18 shows that the foot skin temperature is sensitive to a change in the permeability index. Here, the change from 0.38 to 0.10 results in skin temperature change of approximately 3 °C. For the other body parts, the effect might be lower, since they seem to be generally less sensitive to changes in clothing properties (section 3.4.1 on page 38). The effect of the newly measured clothing properties in comparison to the ones found in the literature

Table 4.7.: Results for evaporative resistances and permeability indices of shoe/sock combinations (non-moving case)

	Ballerina/ nylon socks	Sneaker/ athletic socks	Business shoe/ athletic socks
Total evaporative resistance $[\text{m}^2 \text{kPa W}^{-1}]$	0.060	0.080	0.088
Clothing evaporative resistance $[\text{m}^2 \text{kPa W}^{-1}]$	0.020	0.052	0.057
Total permeability index	0.120	0.097	0.090
Clothing permeability index	0.100	0.076	0.066

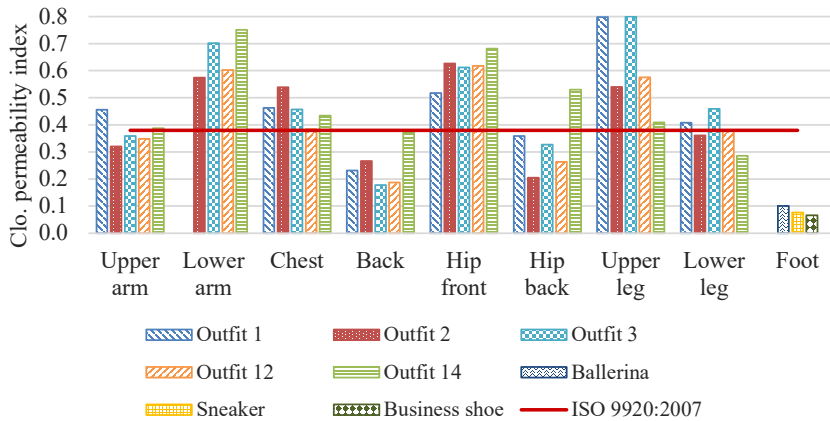


Figure 4.10.: Comparison of local clothing permeability indices to value in ISO 9920:2009

is discussed in detail in section 6.3.1 on page 109. All in all, it is suggested to use the local values, for local application of clothing properties, e.g. thermo-physiological simulations.

Effect of air speed and body movement

The effect of air speed and body movement on $R_{et,i}$ and $R_{ecl,i}$ are presented in Figure 4.11 for the eight body parts and the two outfits. In most cases, the increase in air speed and the addition of body movements reduced $R_{et,i}$ and $R_{ecl,i}$. These results are to be expected because the higher convection at the garments outer surface reduced the water vapor concentration at that surface. The effects are larger for $R_{et,i}$ and $R_{ecl,i}$, since the adjacent air layer is excluded from $R_{ecl,i}$ calculation. However, $R_{ecl,i}$ is still mostly reduced by increased air speed and body movement. Hence, it can be assumed that in both cases the air movement in the enclosed air layer between the surface of the manikin and the garment is increased or the thickness of the air layer is reduced, which leads to a reduction of $R_{ecl,i}$. Increasing the air speed to 0.4 m s^{-1} , has much lower effect than the other test cases, and, considering the standard deviation, the results are often very similar to the values at an air speed of 0.2 m s^{-1} .

The magnitude of the reduction by increased air speed and body movement is different for the eight body parts. The largest effects for increased air speed can be seen for $R_{et,i}$ and $R_{ecl,i}$ at the back. However, there is hardly any change for the addition of

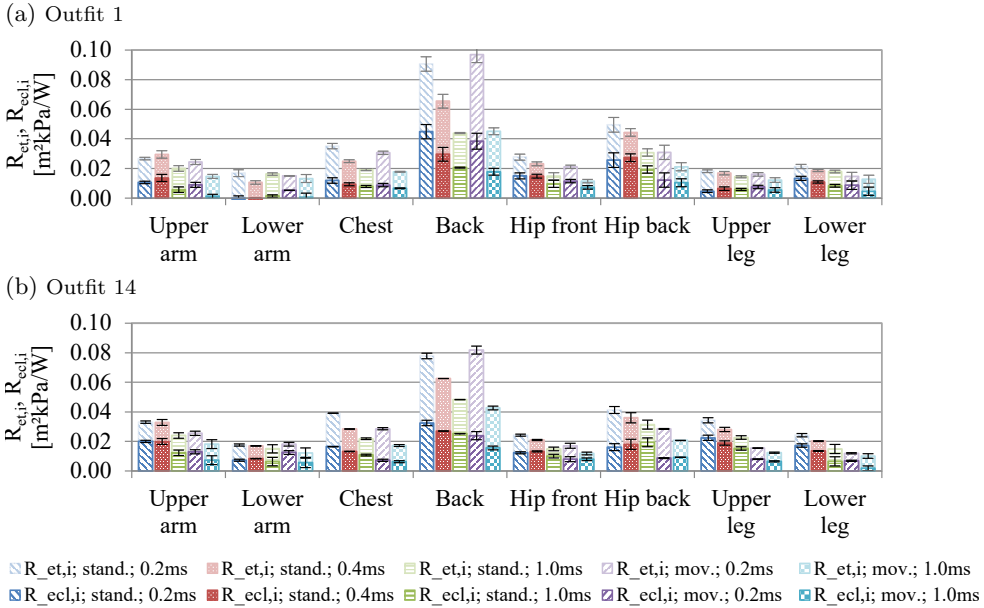


Figure 4.11.: Local total and intrinsic evaporative resistances ($R_{et,i}$ and $R_{ecl,i}$) for outfit 1 and outfit 14

body movement (same air speed). Relatively, low effects can also be seen for $R_{ecl,i}$, for example, for the upper leg of outfit 1 and the lower arm of outfit 14. These small effects might be caused by different draping of the garments due to the attachment to the moving simulator. It seems that the air layer between the surface of the manikin and the garment might be increased, which would lead to an increase in $R_{et,i}$ and $R_{ecl,i}$, counteracting any possible pumping effect, which reduces $R_{et,i}$ and $R_{ecl,i}$.

Correlation of local ease allowance and local evaporative clothing resistance

Similar to section 4.3.2 on page 70, the relationship of $R_{ecl,i}$ and the local EA is investigated as shown in Figure 4.12. The figures also provide the regression equations, the R^2 -value and the residual mean squared deviation (rmsd). In most cases, the slope of the regression equations is very small (<0.003). Also, the R^2 -value is mostly low. However, in combination with the low rmsd-values, it means that $R_{ecl,i}$ does mostly not depend on EA and therefore, $R_{ecl,i}$ does not need to be adjusted for different clothing fits. A slightly deeper slope can be seen for $R_{ecl,i}$ of the back (Figure 4.12d), which might be worth do consider when adjusting $R_{ecl,i}$ to different clothing fits.

The main reason for the low dependency of $R_{ecl,i}$ on EA might be found in the measurement procedure. Because of the water distributed on the skin surface, the clothing items get wet and are more likely to stick to the surface. Hence, the air gap between the clothing items and the skin surface is reduced. Especially for one layer outfits, this observation will result in a low change in $R_{ecl,i}$ for different EA .

4.3.4. Future research

In this thesis, the local clothing thermal resistance, local clothing evaporative resistance and local clothing area factors of a number of typical office clothing ensembles are calculated and analyzed for an upright position of the manikin SAM. However, a typical office situation also includes the sitting position. The measurements on SAM for this posture could not be conducted due to technical reasons. The largest influence of a sitting position can be expected for the contact areas with the chair, namely back hip and upper legs, and minor changes might be expected due to variations in draping of the clothing on the other body parts (Mert et al., 2016, 2017). Two effects are to be expected at these body parts: (1) The air layer between the skin and the clothing is reduced and (2) The clothing insulation is influenced by the insulation of the chair. The first point was investigated by Mert et al. (2017). The second point raises the question regarding the kind of chair to be used and if measurements should be done for several chairs. Also, it might be inquired if the effect of the chair can be generalized.

This study also discusses the effect of the wind directed from the front to the back of the manikin on the resulting, relatively large, clothing insulation values of the back. Hence, future research may consider to vary the direction of the air to investigate the effect on the results. Then, the most appropriate value for a certain situation or the average might be considered depending on the application.

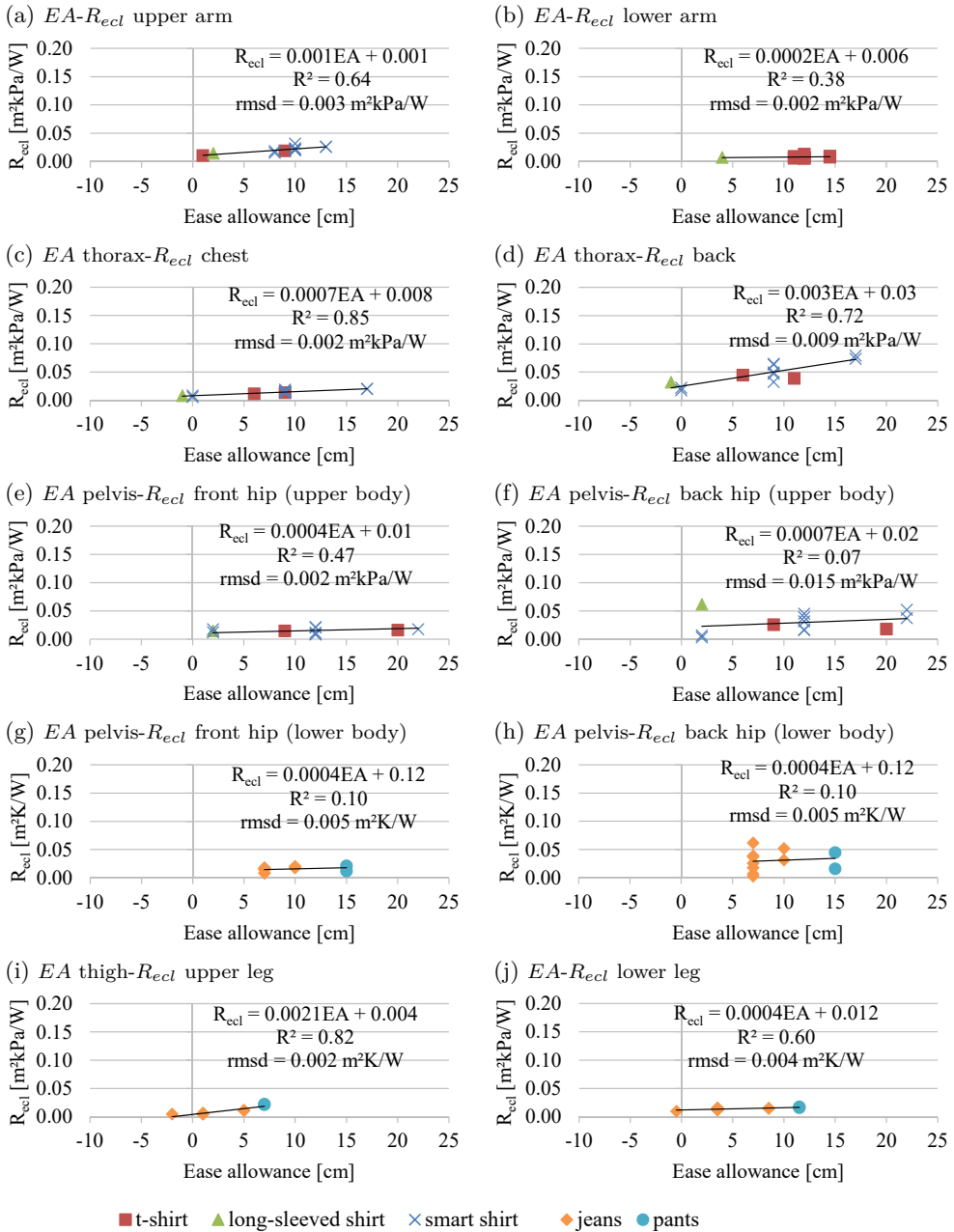


Figure 4.12.: Correlation of local evaporative clothing resistance and local ease allowance

4.4. Conclusions

This study extends the database of local clothing insulation and local clothing area factors of typical office clothing ensembles. For the local clothing area factors, empirical equations are provided to adjust the value for different garments, manikins or human subjects using the ease allowance as a reference. The local clothing insulation of most body parts are decreased by increased air speed and added body movement. However, the reduction is different for all body parts and therefore, cannot be generalized. Moreover, the fit of the garments also influences the local clothing insulation value. It is suggested to use the ease allowance for specifying the exact fit, rather than using general terms such as “fitted” or “loose”. In the case of single layer clothing combinations, the local clothing insulation correlates linearly to the ease allowance for most body parts covered with a single layer. In general, this study emphasizes the need for well documented measurements to get reproducible results and to choose accurate clothing parameters for thermo-physiological and thermal sensation modeling.

CHAPTER 5

Effect of local skin blood flow during light and medium activities on local skin temperature predictions*

5.1. Introduction

To predict the overall and local thermal sensation and comfort of the users of these systems efficiently, human thermo-physiological models and coupled thermal sensation models can be used. Therefore, thermo-physiological models such as UTCI-Fiala (Fiala et al., 2012, 1999, 2001), ThermoSEM (Kingma, 2012; Kingma et al., 2014b; Severens, 2008; Severens et al., 2007), Berkeley Comfort Model (Huizenga et al., 2001; H. Zhang et al., 2001) or Tanabe's model (Tanabe et al., 2002) predict the mean and local skin temperatures, which are then processed in thermal sensation and comfort

*The contents of this chapter have been published in:

- Veselá, Stephanie; Kingma, Boris R.M.; Frijns, Arjan J.H., and van Marken Lichtenbelt, Wouter D. (2019b). "Effect of local skin blood flow during light and medium activities on local skin temperature predictions". In: *Journal of Thermal Biology* 84, pp. 439–450

models. Because of their main application in the built environment, these models are designed and validated for mild cold to mild warm environmental conditions (approximately 15 to 35 °C, depending on clothing). Within this environmental temperature range, the prediction of mean and local skin temperatures need to be as accurate as possible. Validations of thermo-physiological models show high accuracies for mean skin temperatures, but deviations can be found in local skin temperatures, especially at the extremities (Martínez et al., 2016; Psikuta et al., 2012; van Marken Lichtenbelt et al., 2007; Veselá et al., 2015b). To improve the prediction of local skin temperatures, influencing factors of the local heat balances in these models need to be re-evaluated.

One important component of these balances is the local skin blood flow (SBF), which is a large thermoregulatory factor (Kellogg, 2006). Local SBF is mainly controlled via the nervous system of warm and cold sensitive neurons at the skin sites and in the hypothalamus (Boulant, 2005). Depending on the fire rate of these thermosensitive neurons, SBF will be reduced or elevated through vasoconstriction or vasodilation to avoid or increase heat loss, respectively (I. Mekjavič and J. B. Morrison, 1985; Nakamura and S. F. Morrison, 2008a,b). The modeling of local SBF can be done using different approaches, for example Wissler's or Fiala's empirical SBF models (Fiala et al., 2001; Wissler, 2008), the SBF model by Tanabe where the SBF is a function of the external work and shivering heat production (Tanabe et al., 2002), Pennes' empirical blood flow perfusion term in the Berkley Comfort model (Huizenga et al., 2001; Pennes, 1948) and the neurophysiological approach by Kingma et al. (2014b). The validation of the neurophysiological approach by Kingma et al. (2014b), which was implemented in the thermo-physiological model ThermoSEM, showed improved forearm and abdomen SBF and mean skin temperature prediction.

ThermoSEM including the neurophysiological approach for SBF was developed and validated for several environmental conditions. However, the activity levels were low at 0.8 to 1 met for most scenarios and in sitting or supine position with low clothing insulation (Kingma et al., 2014b). Higher activity levels such as standing (about 1.5 met) or walking (2 to 4 met) were not included in the validation of the model. In the most recent thermo-physiological models, the overall activity level is used to take different activities into account (Fiala et al., 2001; Huizenga et al., 2001; Tanabe et al., 2002). However, during activities, like walking, a local increase in muscle activity/metabolism takes place, but also a large increase in local blood perfusion is observed

(Hinds et al., 2004; Joyner et al., 2001; Savard et al., 1988; Snell et al., 1987). Yet, data on local (increased) metabolic rates and local increase in blood perfusion during activities is lacking or incomplete (Veselá et al., 2017b). Moreover, most models use an average, usually male, person for simulation purposes. Havenith (2001) and Van Marken Lichtenbelt et al. (2004) show that the individual body characteristics of human subjects, such as height, body mass, body fat percentage and metabolism, improve the models quality in predicting individual skin temperatures. Our final aim is to extend the thermo-physiological model ThermoSEM such that it includes both localized increase in tissue perfusion and local increase in metabolic rates that depend on the type of activity. In this chapter, our focus was on the local increase in blood perfusion and its effect on the increase in local skin temperatures. The main focus was hereby on the foot, since the largest deviations of up to 10 °C in skin temperature between simulation and measurements were found here (Veselá et al., 2015b).

To verify and improve the foot skin temperature prediction of ThermoSEM for light and medium activity levels as usually found in the built environment (sitting, standing, walking at about 2 to 3 km h⁻¹), the influence of the SBF at the ankle is investigated. Therefore, local skin temperatures and ankle SBF of twenty human subjects were measured for activities reaching from 1 to 3 met for this study. The main objective was to investigate the effect of the measured SBF on local skin temperature prediction based on individual characteristics in the thermo-physiological simulation model ThermoSEM. Moreover, the influence of walking activity level and gender was included in the neurophysiological approach.

5.2. Methods

5.2.1. Human subject experiments

The experiments were conducted at the Metabolic Research Unit of Maastricht University (MRUM) and took place from February to August 2016. The experiments described in this paper were part of a larger study investigating the thermal challenges of modern day humans. The medical ethical committee of Maastricht University Medical Centre+ authorized the experimental protocol. All participants in this study signed a letter of consent prior to the experiments.

Table 5.1.: Participants characteristics (10 males, 9 females)

Characteristics	Mean (\pm SD) - all	Mean (\pm SD) - male	Mean (\pm SD) - female	P-values male vs. female
Age [yr]	28.7 \pm 10.6	30.2 \pm 11.0	26.1 \pm 9.7	0.44
Body mass [kg]	69.4 \pm 9.4	75.2 \pm 8.7	63.1 \pm 4.9	<0.01
Height [m]	1.76 \pm 0.08	1.81 \pm 0.06	1.71 \pm 0.06	<0.01
BMI [kg m ⁻²]	22.3 \pm 2.4	22.9 \pm 2.7	21.7 \pm 1.7	0.28
Body fat [%] ^a	24.7 \pm 7.0	21.9 \pm 8.1	27.9 \pm 3.3	0.06
Surface area [m ²] ^b	1.85 \pm 0.15	1.95 \pm 0.12	1.74 \pm 0.08	<0.01

^a measured via Bod Pod©

^b method by Du Bois and Du Bois (1916)

Subjects

The subjects had to meet the following inclusion criteria: Caucasian, generally healthy, age between 18 to 60 years, BMI of 20 to 25 kg m⁻² and sharing an office with another participant of different gender. The last criterion was required for the wider study. Hence, ten pairs of male-female volunteers were recruited for this study (Table 5.1). One female subject was excluded from the analysis, because no skin perfusion of the ankle was recorded due to a malfunction of the LDF probe. As shown in Table 5.1, there is a significant difference in body mass, height and body surface area between the male and female test persons.

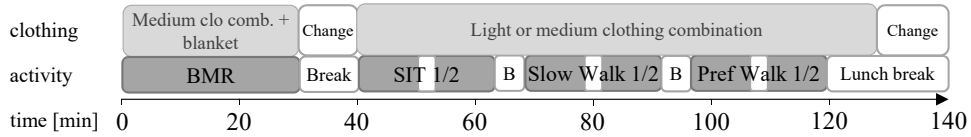
Measurement protocol

The recruited volunteers visited MRUM for one day. The air temperature of the climate chamber was set to 22 °C and was recorded using hygrochron iButton® dataloggers (DS1923, Maxim Integrated, USA) at four heights (0.1 m, 0.6 m, 1.1 m, 1.7 m above ground) along with the relative humidity (RH in %). The participants were asked to refrain from caffeine or alcoholic beverages and food up to twelve hours before the start of the experiments. After arriving at 8:30 am, the subjects swallowed a small telemetric temperature pill (CorTemp™, USA), before they changed into the standardized medium warm clothing combination consisting of underwear, a t-shirt, a sweater, sweatpants, socks and sneakers (total insulation about 0.8 clo, see section 5.2.2 on page 87 and Table A.17 on page 141). While dressing, thermochron iButton® dataloggers (DS1922L, Maxim Integrated, USA) were attached on the test persons with medical tape on 14 positions plus the fingertip in accordance to EN-ISO 9886:2004

as shown in Figure A.9 on page 142. Furthermore, skin perfusion was measured using Laser Doppler Flowmetry (LDF) (PF4000 & PF5000, Perimed AB, Sweden). For practical reasons, the participants wore regular footwear, and to avoid distortion of the regular walking patterns, the SBF was measured at the ankles instead of the feet or toes.

With the sensors attached, the volunteers then performed the measurement protocol as shown in Figure 5.1. Firstly, they laid in supine position on a stretcher for 30 minutes to measure baseline metabolic rate (BMR). To ensure that the participants' thermal state was close to neutrality, they were covered with a thin cotton blanket. Energy expenditure (EE) was measured during all parts of the experiments by indirect calorimetry using a mask connected to an automated respiratory gas analyser. After the BMR measurement, the subjects were given a light breakfast and changed into either the light clothing combination consisting of underwear, a t-shirt, shorts, socks and sneakers (total insulation about 0.5 clo) or left on the medium clothing combination (0.8 clo, see section 5.2.2 on page 87 and Table A.17 on page 141). The starting clothing combination (light or medium) was randomized for all pairs of subjects. Then, they switched to a treadmill where three activities took place for a total 23 minutes each (Figure 5.1a). After the first ten minutes of each activity, there was a small break (approximately 3 minutes) to perform additional measurements, e.g. blood pressure, and thermal comfort questionnaires (not evaluated in this thesis). Because of this small break, all activities were split into two subsections, which are separated by the small white line in Figure 5.1 and are numbered for further analysis 1/2 for the morning and 3/4 for the afternoon session. The activities were sitting on a chair, walking at a speed of 1 km h^{-1} (Slow Walk) and walking at preferred speed (Pref Walk). The slow walking period replaced a period of standing, which was found to be too hard on the participants in pretests. Hence, the walking speed was set to the lowest possible setting of the treadmills. In between the activities, the test persons could take off the EE mask for a couple of minutes and get a drink of water. The third activity was followed by a lunch break of 45 minutes. A light, standardized lunch of cheese and crackers was provided to the subjects. Also, the participants were asked to change into the second clothing combination. After the lunch break, the subjects performed the same three activities as before (Figure 5.1b). However, due to technical reasons the seated period had to be performed as the final session. After the experiments, all sensors were detached and the volunteers' anthropometric data was

(a) Morning session



(b) Afternoon session

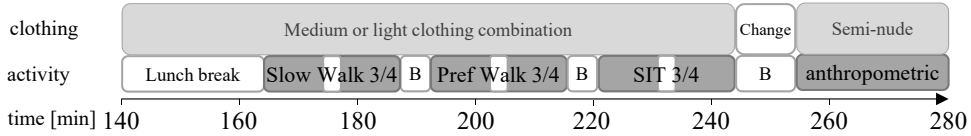


Figure 5.1.: Time line of measurement protocol. Light gray areas represent times of defined clothing, dark gray areas represent times of defined activities, white areas represent any kind of break (B) for taking measurements, changing clothing or eating and drinking. (The notation 1/2 and 3/4 refer to the two parts of each experimental session divided by a small break for taking measurements in the morning and afternoon, respectively.)

measured. These data included the height, body mass, and body composition via Bod Pod® (Life Measurement Inc., Concord CA, USA).

5.2.2. ThermoSEM and input parameters

The thermo-physiological model ThermoSEM was evolved from Fiala’s thermoregulation model (Fiala, 1998; Fiala et al., 1999) with modifications implemented by Severens et al. (2007) and Kingma et al. (2014b). In ThermoSEM, the human body is divided into 19 body parts which are represented by 18 concentric cylinders and one concentric semi-sphere. Each part consists of multiple tissue layers, e.g. bone, muscle, fat or skin, with a specific geometry and characteristics. The biggest difference between Fiala’s model and the current version of ThermoSEM is the implementation of a neurophysiological approach to calculate the SBF (Kingma et al., 2014b). The skin perfusion in Fiala’s model is a function of the central stimuli for vasodilation and vasoconstriction which in turn are functions of the difference between the actual and set point mean skin temperature (Fiala, 1998; Fiala et al., 1999). The model by Kingma et al. (2014b) formulates SBF regulation as:

$$\beta_i = \beta_{i,bas} \cdot N \cdot Q_{10} \tag{5.1}$$

where $\beta_{i,bas}$ is the basal heat equivalent of SBF of a specific body part i , Q_{10} is the local regulation effect of SBF (Q10-effect) with $Q_{10} = 2^{\frac{(T_i - T_{i,bas})}{10}}$, $T_{i,bas}$ the local tissue temperature under basal conditions and N is the neural regulation signal for SBF. The function for N is:

$$N = \max[0, \gamma_1 - \gamma_2 (H_{warm} - P_{cold}) - \gamma_3 (H_{warm} - P_{warm})] \quad (5.2)$$

where γ_1 is a model constant representing all non-thermal effects on SBF, γ_2 and γ_3 are model parameters for the cold and warm afferent pathway, respectively, H_{warm} is the neuron fire rate of temperature sensitive neurons in the hypothalamus, P_{cold} and P_{warm} are the neural peripheral cold and warm drive, respectively. The values of the models constant γ_1 and parameters γ_2 and γ_3 are given in Table B.1 on page 156. The function for the neural regulation signal is based on the neural concepts described in Mekjavič and Morrison (1985), Boulant (2005) as well as Nakamura and Morrison (2008a,b). H_{warm} , P_{cold} and P_{warm} are calculated as described in Kingma et al. (2014b) using the individual neuronal response characteristics as modeled by Mekjavič and Morrison (1985).

The SBF prediction using the neurophysiological approach was validated using two independent data sets of young male subjects, which were dressed in shorts or light sportswear and were lying in supine position (Kingma et al., 2014b). The results of this validation showed improved SBF prediction as compared to Fiala's model for abdomen, forearm and similar SBF simulation for the hand. However, the model was not validated for higher activities and higher clothing insulation.

Individualized ThermoSEM

In the default setting, ThermoSEM represents an adult male (73.5 kg, body surface area of 1.86 m², body fat percentage of 14 %, and 87.1 W total basal metabolic heat). However, the default geometry of ThermoSEM does not represent the participants of this study. Especially, a large deviation in the fat percentage can be seen in Table 5.1. Van Marken Lichtenbelt et al. (2007) and Severens et al. (2008; 2007) introduced a method to scale the default geometry of ThermoSEM to individual measurement. Firstly, the length of all body parts, except the head, were scaled with a factor λ_1 which is the ratio of the height of the actual person h to the height of the standard person h_0 . The head was scaled with $\sqrt{\lambda_1}$. Secondly, λ_2 and λ_3 were introduced for

scaling the layer thicknesses (i.e. radii) of the body segments. The core and muscle layers were scaled with λ_2 , and the fat layers were scaled with λ_3 . The thickness of the inner and outer skin was not scaled. The factors λ_2 and λ_3 were then calculated using an optimization routine to match the total body mass and fat percentage of the considered subject.

The general scaling method of van Marken Lichtenbelt et al. (2007) and Severens et al. (2008) was adopted for this study. Additionally, differences in fat distribution between males and females were considered. Figure 5.2 shows the distribution of the local body fat for a typical male and a typical female subject as compared to the standard (Fiala/ ThermoSEM) configuration (Wölki, 2017; Wölki and Treack, 2013). The data was obtained from body composition measurements of 190 male and 133 female test persons. To produce similar relations in ThermoSEM additional factors were applied to λ_3 (Table 5.2). The resulting body fat mass distribution of a lean male (1.80 m, 70.1 kg, 16.4 % body fat), the average male and average female human subject of this study are also shown in Figure 5.2. Most male and all female participants of our study had a higher body fat percentage than in Wölki (2017), which results in overall higher body fat mass for all body parts especially on the thorax and abdomen. However, the distribution of body fat mass shows a similar relation. Hence, the additional scaling factors of Table 5.2 are sufficient to account for differences in body fat distribution between males and females in ThermoSEM.

Table 5.2.: Adjusted scaling of the fat layer for male and female subjects

Body part	Scaling factor	
	Male	Female
Face, Neck, Shoulders	λ_3	λ_3
Thorax	λ_3	$\lambda_3 \cdot 1.04$
Abdomen	λ_3	$\lambda_3 \cdot 1.02$
Upper arms	$\lambda_3 \cdot 0.98$	$\lambda_3 \cdot 1.05$
Lower arms	$\lambda_3 \cdot 0.98$	$\lambda_3 \cdot 0.99$
Upper legs	$\lambda_3 \cdot 1.05$	$\lambda_3 \cdot 1.14$
Lower legs	$\lambda_3 \cdot 0.999$	$\lambda_3 \cdot 0.99$
Hands, Feet	λ_3	λ_3

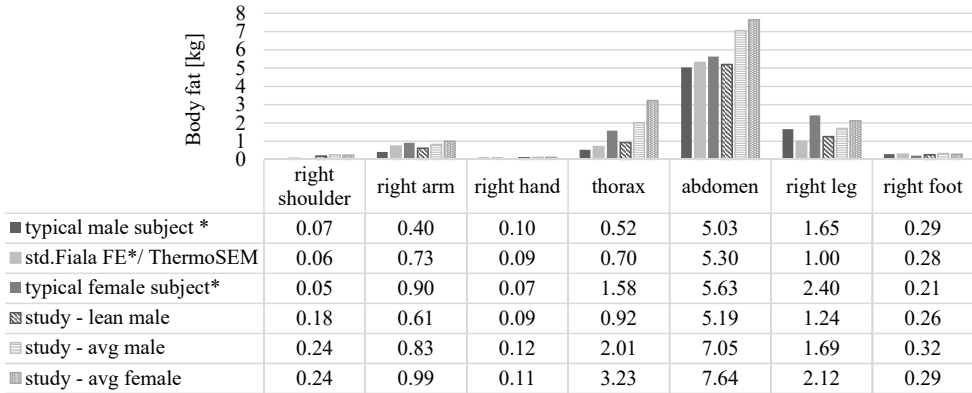


Figure 5.2.: Comparison of body fat mass distribution between the typical male subject, standard Fiala-FE/ ThermoSEM and typical female subject of the study by Wölki (2017) (indicated by *) and the lean and average male and female subjects of this study (Left body parts have the same value as right body parts.)

Activity

If the activity is not constant, ThermoSEM requires an input file for the activity level at each time step t . In the model, the average activity during BMR measurements act_{BMR} is equal to 0.8 met (Fiala et al., 1999). The activity at each time point t (act_t) is then defined as the ratio of the energy expenditure at the time point t (EE_t) and the average metabolic rate during the BMR measurement (EE_{BMR}) times 0.8:

$$act_t = 0.8 \cdot \frac{EE_t}{EE_{BMR}} \quad (5.3)$$

Therefore, the measured data of the energy expenditure is averaged in one minute intervals, and the average of the last 20 minutes during the BMR session is calculated. Because the energy expenditure could not be monitored during breaks, further assumptions had to be applied: 1) for longer breaks, the average metabolic rate of the first sitting session is used, 2) for short breaks during any walking sessions a linear decline to the first value, when the mask is put back on, is implemented.

Clothing

During the experiments, the volunteers wore a light and medium clothing combination. The light clothing ensemble consisted of underwear, shorts, a t-shirt, socks and sneakers. The medium ensemble included underwear, a t-shirt, a sweater, sweatpants, socks and

sneakers. The t-shirt, shorts, sweater and sweatpants were provided for the subjects and were available in different sizes. The participants wore their own underwear and sneakers. The thermal clothing properties of both ensembles were measured at Empa, St. Gallen, Switzerland using the agile sweating thermal manikin SAM under two conditions: 1. the manikin was in stationary (non-moving), upright position and 2. the manikin was attached to the movement simulator and performed a walking motion of 2.5 km h^{-1} . Details on the measurements can be found in Veselá et al. (2018c, 2017c) and Chapter 4 of this thesis. The detailed local clothing area factor, intrinsic dry thermal insulation and clothing moisture permeability are given in Table A.17 on page 141. During BMR measurements, an additional cotton sheet was provided to ensure thermal neutrality. Since the additional clothing insulation provided by the cotton sheet could not be measured and no local values were found in the literature, an additional insulation of $0.07 \text{ m}^2 \text{ K W}^{-1}$ was added based on whole-body covering items found in ISO 9920:2009.

Environmental parameters

The environmental parameters required in ThermoSEM are the air temperature, radiative temperature, relative humidity and relative air speed. The air and radiative temperature as well as the relative humidity at each time step t is the average of the data provided by the four hygrochron iButtons (section 2.1.2). The average air temperature during the experiments was typically $24^\circ\text{C} \pm 0.3^\circ\text{C}$ and the relative humidity $30\% \pm 1\%$. The air speed was measured using a hot-wire thermal anemometer (FVA605TA10U, Ahlborn, Germany) and varied between 0.15 m s^{-1} and 0.20 m s^{-1} . These environmental conditions are prescribed to the model as described by Schellen et al. (2013).

Measured skin blood flow

To analyze the effect on local skin temperature prediction of measured SBF versus simulated SBF, the recorded perfusion response of the LDF measurement needed to be imported in ThermoSEM. However, using LDF for SBF measurements raises two issues: 1) Movement at the site of measurement, as is the case in the two walking modes, results in a Doppler shift associated with movement and not necessarily due to an increase in skin blood perfusion. Since LDF does not discriminate directionality of flow, summation of artifacts can result in large signal (Kirkpatrick et al., 1994), and 2) LDF does not provide absolute measurements of flow.

To estimate the SBF during walking without the movement artifacts, the three minutes of the LDF signal after the participants stopped walking were evaluated. Based on the study by Snell et al. (1987) and the assumption that the reduction in the LDF for the foot is similar to the leg SBF, we assume the mean of the 3 minutes directly after the movement should give a good estimation for SBF during the movement. Furthermore, the moving mean was used to reduce the noise of single peaks that occur during BMR, sitting or in the breaks between walking.

The resulting SBF signal cannot directly be used in ThermoSEM. However, the individual perfusion responses can be imported by normalizing the data based on the average value during BMR measurement. In ThermoSEM, the normalized data is then converted into absolute values by multiplying the data with the averaged, simulated perfusion during the BMR phase. Similar to the EE, the perfusion could not be monitored during longer breaks. Since the subjects were mainly seated during the morning (after BMR) and lunch break, the averaged data of the first two sitting sessions was used to ensure a continuous data set.

Simulation

The simulation in ThermoSEM was done continuously covering the experimental boundary conditions from the beginning of the BMR measurements to the end of the last sitting session in one minute time steps.

5.2.3. Data analysis

To summarize the data of the human subject experiments as well as the simulated results, the data was divided into the BMR measurement and 6 activity sessions: Sitting 1/2, Slow Walk 1/2, Pref Walk 1/2, Sitting 3/4, Slow Walk 3/4, Pref Walk 3/4. The data was averaged for each part of the 6 sessions over the last 5 minutes.

The measured and simulated activity levels and SBF are summarized for each session using Whisker-Box-Plots with outliers. An outlier is defined as a data point lying outside of 1.5 times the interquartile range and are displayed with a '+'. The mean values are marked with an 'x'.

Furthermore, a t-test was applied to the measured activity and SBF to see if there are any significant differences between the male and female subjects and the different

activity levels. Similarly, the foot skin temperature difference was assessed. Beforehand, the data was tested for normality using the Shapiro-Wilk Original Test. For both tests, the significance level was set to $\alpha = 0.05$. The calculations were performed using the program Microsoft Excel.

To display the results on the effect of simulated versus measured local skin temperatures efficiently, the differences between these skin temperatures are shown.

5.3. Results

The averaged energy expenditure and activity level is presented in Figures 5.3 and 5.4, respectively, using Whisker-Box-Plots for the male and female subjects separately. As expected, the energy expenditure and activity level increase with higher level of movement. In fact, the difference between increasing activity steps is significant in all cases for both, the energy expenditure and activity level (Table A.18 on page 142). Between the male and female participants, there are significant differences for the energy expenditure for all activities except the second preferred walking session. In fact, also for the first preferred walking sessions the p-value is close to the significance level $\alpha = 0.05$. This result is most probably due to the large variance of the energy expenditure data for this particular sessions. For the activity level (Figure 5.4), no significant differences between male and female subjects are found.

5.3.1. Comparison of measured and simulated local skin temperatures

The averaged differences between simulated and measured core, mean skin and foot skin temperatures and their standard deviation of the 19 subjects are depicted in Figure 5.5 for all 7 sessions in the order of performance. The results for the other body parts are included in Figure A.10 on page 143. For the average core temperature as well as mean, torso, arm, hand and leg skin temperature, the temperature difference is mostly close to 1°C , which is within the expected measurement error of iButtons of $\pm 1^\circ\text{C}$ (van Marken Lichtenbelt et al., 2006). However, the standard deviations reach values from 0.8 to 1.7°C . The foot skin temperature differences ($\Delta T_{skin,foot}$) and their standard deviations have more extreme values, e.g. up to $6.0 \pm 2.4^\circ\text{C}$ for the second

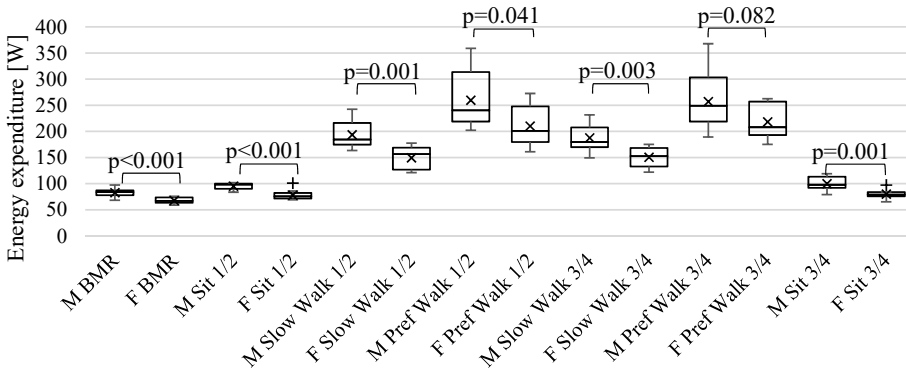


Figure 5.3.: Whisker-Box-Plot for average energy expenditure [W] of ten male (M) and nine female (F) subjects

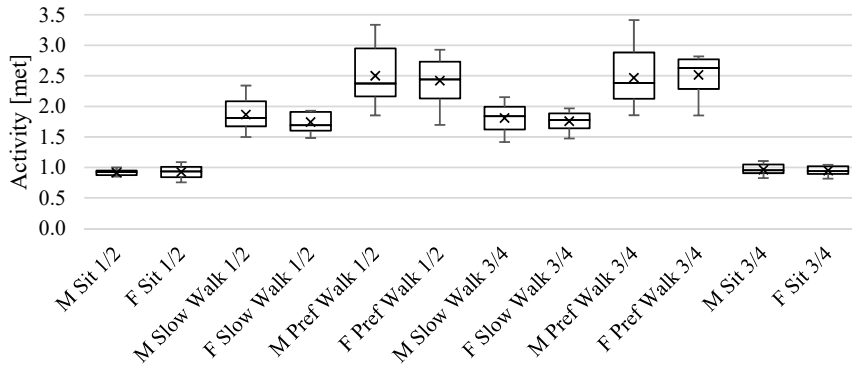


Figure 5.4.: Whisker-Box-Plot for average activity level [met] of ten male (M) and nine female (F) subjects as calculated in equation (5.3)

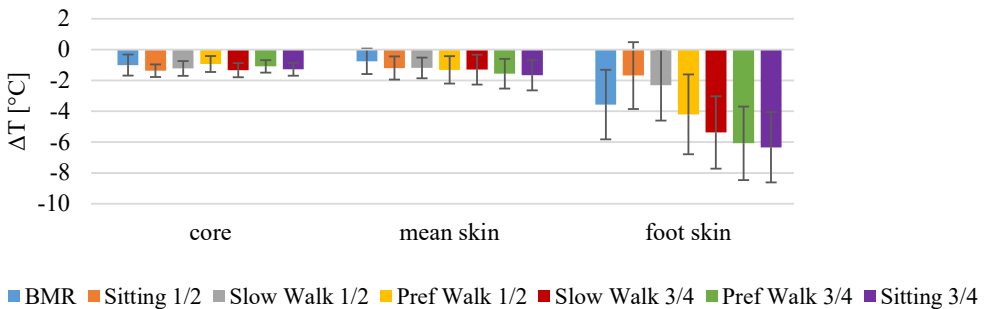


Figure 5.5.: Comparison of ΔT_{core} , $\Delta T_{skin,mean}$ and $\Delta T_{skin,foot}$ of all subjects (simulated - measured) using the standard SBF model (Kingma et al., 2014b) in ThermoSEM

preferred walking session. Even though $\Delta T_{skin,foot}$ is increasing over the day, there is no significant difference between step-wise increasing activity levels (Table A.19 on page 143). However, a significant difference between morning and afternoon sessions can be seen (Table A.19). In the following sections, the influence of SBF on this finding is investigated. Further causes are debated in the discussion.

5.3.2. Measured versus simulated SBF

Figure 5.6 shows examples of an LDF recording at the ankle for one male participant during the last 5 minutes of the subsessions BMR, sitting 2, and the last 5 minutes and subsequent 3 minutes of the subsessions slow walking 1 as well as preferred walking 1 and 3. The graphs of the other subsessions can be found in the supplementary information in Figure A.11 on page 144. The LDF signal is very different for BMR and sitting sessions compared to walking sessions. During BMR and sitting, the signal is at one level with occasionally appearing larger peaks. For all walking sessions, it can be seen that the signal during walking is much higher than in the non-moving case with a high frequency of peaks and lows due to movement artifacts. The LDF signal after motion is stopped is similar to the one of the BMR and sitting session. For further analysis of all subjects, the moving mean of the LDF signal is used to reduce noise by occasional peaks and the values are normalized using the average of the BMR measurement.

The results for the normalized, measured foot SBF are summarized in Figure 5.7. The mean values for the sitting session 1/2 and sitting session 3/4 are 0.7 and 0.9 for males and 1.2 and 1.7 for females, respectively. For both the male and female subjects, the normalized SBF increases for the slow walking session and again for the preferred walking session. This increase in SBF for increased, prescribed activity is significant (p -value < 0.05) for most performance steps (Table A.20 on page 145). However, for slow walking 3/4 to preferred walking 3/4 it is not significant (p -value of 0.09 for male and females), which is probably due to the large variations in between the subjects. In general, for the male subjects, the difference between the periods of slow walking and preferred walking is smaller than for the females. For all sessions, there is a significant difference ($\alpha = 0.05$) between the normalized foot SBF of the male and female participants (Figure 5.7).

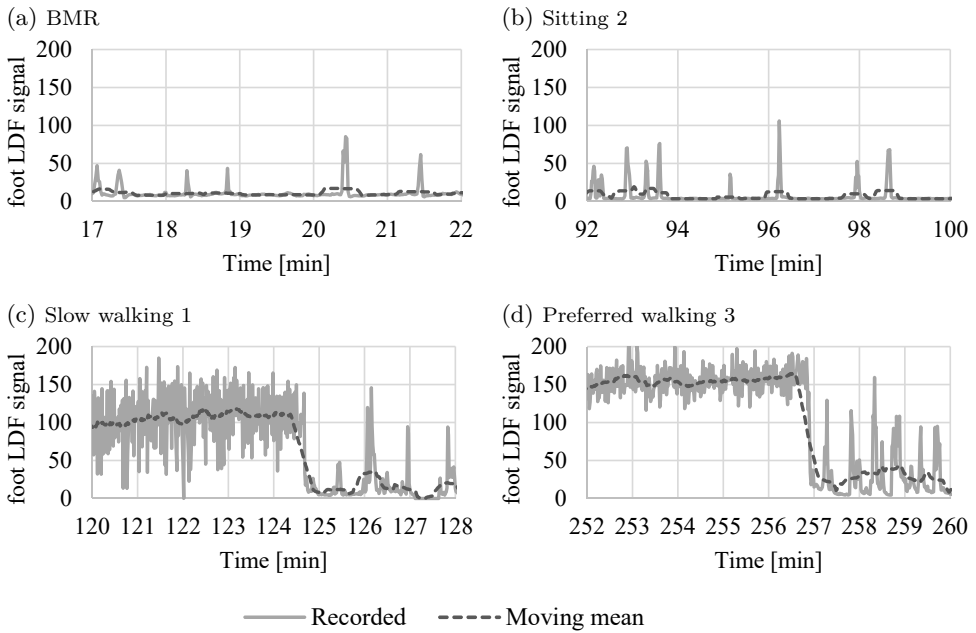


Figure 5.6.: Individual recording of LDF signal at the ankle and its moving mean

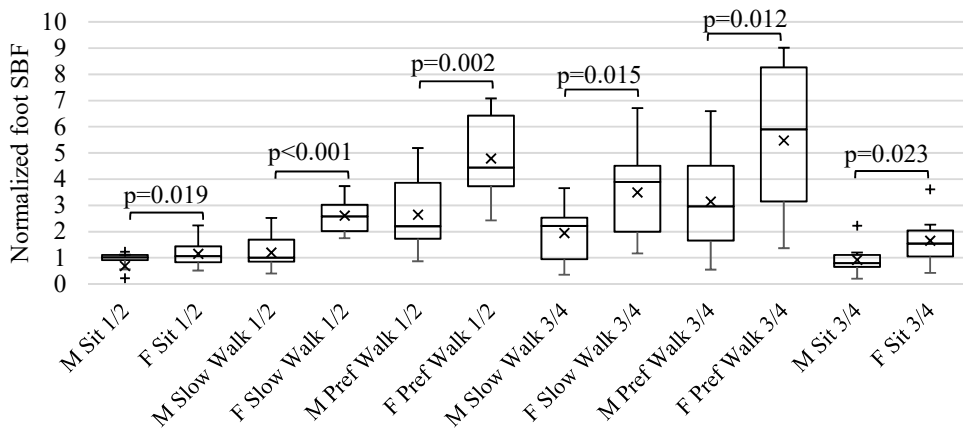


Figure 5.7.: Whisker-Box-Plots for normalized, measured foot SBF for ten male (M) and nine female (F) subjects with outliers (+)

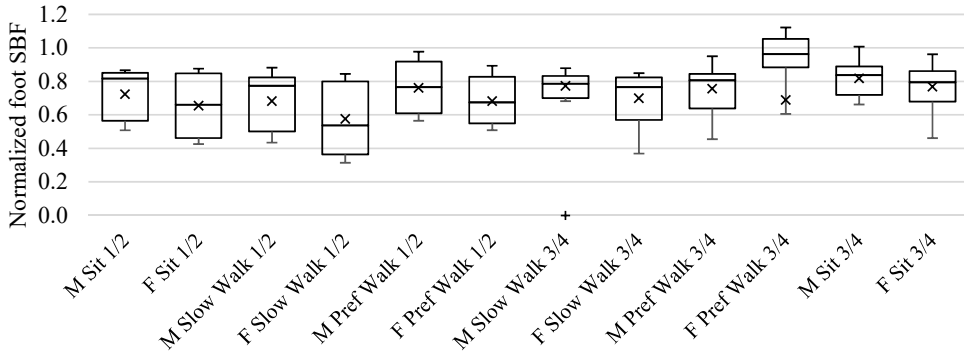


Figure 5.8.: Whisker-Box-Plots for normalized, simulated foot SBF for ten male (M) and nine female (F) subjects with outliers (+)

The normalized, simulated SBF for the default SBF settings (Kingma’s neurophysiological model) and individual geometry in ThermoSEM are depicted in Figure 5.8. The mean normalized, simulated foot SBF hardly differs for the sessions. Also, no differences can be found between male and female subjects. Moreover, the values are all below 1, which means that ThermoSEM predicts less SBF in the sessions with activity as compared to the basal situation.

All in all, the simulated foot SBF generally underestimate the measured foot SBF. The ratios of the mean normalized, measured SBF to the mean normalized, simulated SBF are summarized in Tables 5.3 and 5.4. The magnitude for this underestimation corresponds to the activity level, but is different for male and female subjects. The ratio of the mean foot SBF of the walking sessions reaches values from 1.8 to 4.2 for males and 4.5 to 7.9 for females.

Table 5.3.: Ratios of mean normalized, measured SBF and mean normalized, simulated SBF for the feet - morning sessions

	M Sit 1/2	F Sit 1/2	M Slow Walk 1/2	F Slow Walk 1/2	M Pref Walk 1/2	F Pref Walk 1/2
$\frac{SBF_{norm, meas}}{SBF_{norm, simu}}$	1.0	1.8	1.8	4.5	3.5	7.0

Table 5.4.: Ratios of mean normalized, measured SBF and mean normalized, simulated SBF for the feet - afternoon sessions

	M Slow Walk 3/4	F Slow Walk 3/4	M Pref Walk 3/4	F Pref Walk 3/4	M Sit 3/4	F Sit 3/4
$\frac{SBF_{norm,meas}}{SBF_{norm,sim}}$	2.5	5.0	4.2	7.9	1.1	2.2

5.3.3. Changes in skin temperature prediction for prescribed measured skin blood flow

Figures 5.9 and 5.10 compare simulation results for the difference in simulated and measured core, mean skin and foot skin temperatures ($\Delta T_{skin} = T_{skin,simulated} - T_{skin,measured}$) of the ThermoSEM simulation using a) the SBF for all body parts which is completely determined by the original thermoregulation model ThermoSEM (Kingma’s neurophysiological model), named “original simulated SBF model” and b) the ThermoSEM model with the adjusted foot SBF, named “prescribed measured SBF model”. The model is adjusted in such way that the computed SBF for the foot resembles the measured local SBF (see section 5.2.2 on page 88). The results for the other body parts can be found in Table A.20 on page 145.

Apart from the feet, $\Delta T_{skin,loc}$ is mostly the same for both simulations (Figure 5.9 and Figure A.12 on page 145). The core temperature difference is larger than the expected measurement error of $\pm 0.27^\circ\text{C}$ (Bongers et al., 2018) for the original and adjusted simulation with a mean difference of 1 to 1.3°C and a standard deviation for all subjects of 0.4 to 0.7°C depending on the activity. The individual recording and simulation results as well as the individual residual mean squared deviation are shown in the appendix in Figures A.13 and A.14 on page 146 and on page 147 as well as Table A.21 on page 148. A slight increase (about 0.05°C) can be seen for the simulation with the prescribed measured SBF. However, the difference of simulated minus measured core temperature is almost constant over the course of the simulation. Hence, on average the increase in core temperature due to activity is represented correctly by the simulation, even though the absolute values are not a precise representation of reality.

Running the adjusted ThermoSEM model lowers $\Delta T_{skin,foot}$ by about 1 to 2.7°C (Figures 5.9 and 5.10). The standard deviation is mostly unchanged at 1.5 to 3°C .

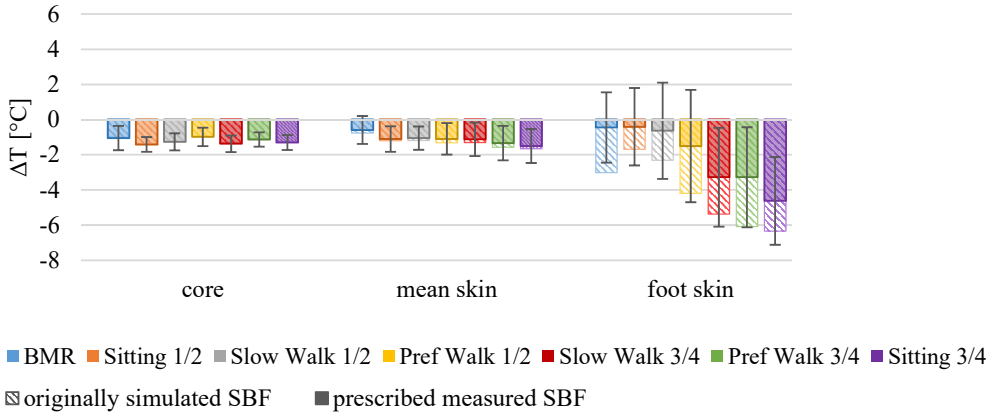


Figure 5.9.: Comparison of ΔT_{core} , $\Delta T_{skin,mean}$ and $\Delta T_{skin,foot}$ of all subjects (simulated - measured) using the standard SBF model (Kingma et al., 2014b) in ThermoSEM

A slight difference can be seen between male and female foot ΔT_{skin} (Figure 5.10). Especially, for female subjects, $\Delta T_{skin,foot}$ is overcompensated in the simulation with the prescribed, measured SBF resulting in positive values, which in absolute measures are sometimes higher than the original $\Delta T_{skin,foot}$. The significant difference between the morning and afternoon sessions for sitting and slow walking can be seen for both genders and in the original and adjusted simulation (Table A.19 on page 143). In fact, the magnitude of $\Delta T_{skin,foot}$ increases during the course of the day. Since this effect is not seen in other body parts, it might be due to the clothing of the foot during the experiments as will be elaborated in the discussion section.

5.3.4. Improvement of the model

The results in the previous sections show that 1) the normalized, simulated SBF is 2 to 8 times lower than the normalized, measured SBF, 2) there is a significant difference in foot SBF between males and females, and 3) the local skin temperature prediction is improved by up to 3°C (new max deviation = 4°C), when the measured foot SBF serves as input data in ThermoSEM. To make the predictive SBF model also suitable for higher activity levels, there is a need to adjust the neurophysiological SBF model (equations (5.1) and (5.2)) by including the increase in activity level compared to BMR (0.8 met), the gender of the simulated person and the interaction of these two parameters in equation (5.2). Hence, an extended neural regulation signal N_{new} is

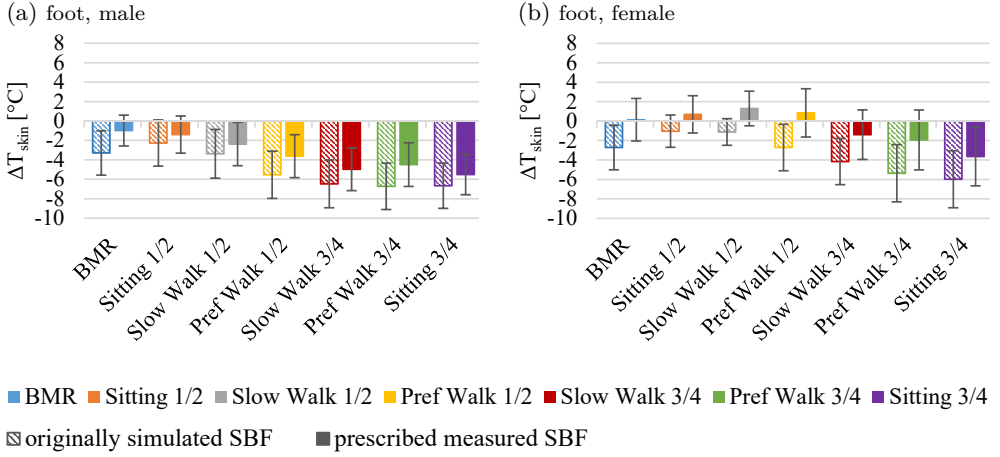


Figure 5.10.: Comparison of $\Delta T_{skin,foot}$ for male and female subjects (simulated - measured) using the originally simulated SBF (shaded area) versus the prescribed measured SBF (filled area) in ThermoSEM

introduced:

$$N_{new} = \max[0, \gamma_1 - \gamma_2 (H_{warm} - P_{cold}) - \gamma_3 (H_{warm} - P_{warm}) + \gamma_4 \cdot (act - 0.8) + \gamma_5 \cdot gen + \gamma_6 \cdot (act - 0.8) \cdot gen] \quad (5.4)$$

where $(act - 0.8)$ is the increase activity level in met, gen represents the gender of the simulated person. For this study, the default gender is chosen to be “male” ($gen = 0$). The value for gender “female” is chosen to be $gen = 1$. The parameters γ_1 to γ_6 of this model have to be determined for each body part.

As an example, the new neural regulation signal equation is determined for the foot using the k-fold cross validation scheme as described by Kingma et al. (2014b). In this method, the coefficients γ_1 to γ_6 are iteratively fitted for $n - 1$ subjects for n iterations, meaning that always one subject is left out at each iteration. Then, the root mean squared residual is calculated for the left-out subject. After all iterations, the n sets of coefficients are averaged. For the regression analysis, the measured, normalized foot SBF of this study had to be transferred to the equivalent absolute values in ThermoSEM (see section 5.3.2 on page 92). Because of missing data points in core or skin temperatures for four subjects, which are needed to calculate H_{warm} , P_{cold} and P_{warm} , 15 subjects were included in the analysis. Moreover, the data was averaged over the last 5 minutes for each subsession (sitting 1, sitting 2, slow walking 1, etc.),

Table 5.5.: Mean, standard error and ratio of mean and standard error of regression coefficients for the feet

coefficient	mean	SE	mean/ SE
γ_1	3.5268	0.2392	14.7432 ^a
γ_2	-0.1414	0.0111	-12.6956 ^a
γ_3	0.3979	0.0323	12.3368 ^a
γ_4	0.2873	0.0124	23.0798 ^a
γ_5	-0.2085	0.0094	-22.1114 ^a
γ_6	0.2573	0.0127	20.3262 ^a

^a = $|mean/SE|$ is above significance level (>2.13)

resulting in 12 data points for each participant. Hence, the regression analysis included 180 data points. Furthermore, the significance of the coefficients is tested using the t-statistics with a confidence level of 95 %. The critical value of the t distribution is 2.13 for our data. Hence, the absolute value of the ratio of the mean of the fitted coefficients and the standard error SE should be larger than 2.13 for the parameters to be significant. In Table 5.5, the mean of the fitted coefficients, their standard error (SE), and the ratio of the coefficients mean and standard error for the feet are shown. All coefficients are significant for the regression equation. Hence, the SBF of the foot is estimated using the following equation for the neural regulation signal:

$$\begin{aligned}
 N_{new} = & \max[0, 3.5268 + 0.1414 (H_{warm} - P_{cold}) \\
 & - 0.3979 (H_{warm} - P_{warm}) + 0.2873 \cdot (act - 0.8) \\
 & - 0.2085 \cdot gen + 0.2573 \cdot (act - 0.8) \cdot gen]
 \end{aligned} \tag{5.5}$$

The simulations of the experiments were re-run using the new neurophysiological equation (5.4) for the foot SBF and the standard neurophysiological model (equation (5.2)) for all other body parts. The resulting $\Delta T_{skin,foot}$ using the new foot SBF equation, as shown in Figure 5.11, has improved clearly for the male subjects. These values are similar to the situation, where the measured foot SBF were explicitly prescribed in ThermoSEM. In fact, for the male participants a slight improvement, i.e. lower $\Delta T_{skin,foot}$, can be seen compared to the result from the measured SBF. For the female subjects, the $T_{skin,foot}$ is now overestimated by 1.5 to 4 °C in the first sitting, slow walking and preferred walking sessions. This observation can already be seen for the results using the prescribed measured SBF, but is now more pronounced, which might be due to the exclusion of subjects and the regression method.

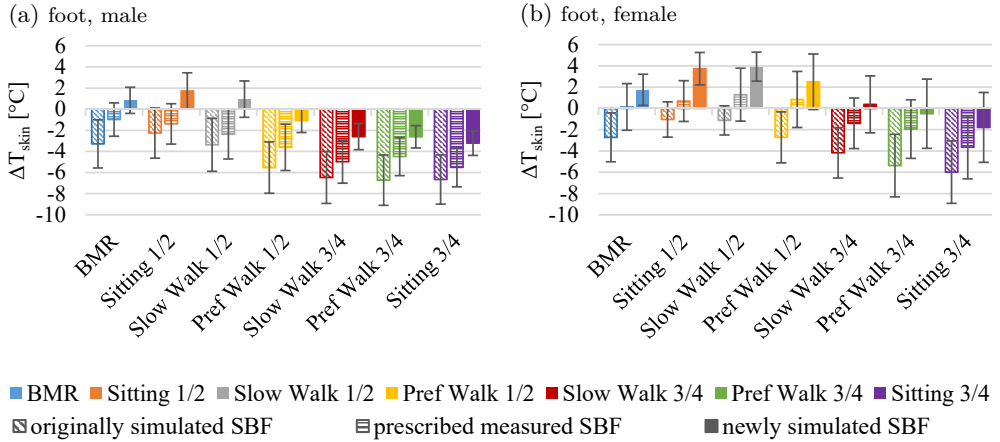


Figure 5.11.: Comparison of $\Delta T_{skin,foot}$ for male and female subjects (simulated - measured) using the originally simulated SBF (eq. (5.2)) versus the newly simulated SBF (eq. (5.5))

5.4. Discussion

The results showed that the prediction of local skin temperatures by a thermophysiological model could be improved for higher activity levels, if the neurophysiological SBF model includes the activity level and gender of the subjects. For the most accurate prediction of SBF, the model might be extended by further factors such as blood pressure, hormonal changes or local muscle activity levels (Kingma et al., 2014b). At the current stage these factors are indirectly included in the constant γ_1 of the neurophysiological model (equations (5.2) and (5.4)). However, it is important to weigh the contribution to accuracy of a variable against the effort it takes and the possibility to obtain it. For example, the whole simulation model would probably benefit from measurements of local muscular heat production due to activity e.g. using EMG. However, even though this value might be measured in the laboratory, users of the simulation model might not be able to access the data. In contrast, the estimation of the whole-body activity level is well-documented in the literature and standards (EN-ISO 8996: 2004; Parsons, 2014). In future research, an indirect method, e.g. measuring local blood perfusion and local skin temperatures, and a detailed heat transfer model might be used to reconstruct the local metabolic rates. An alternative implementation would be that the neurophysiological model is maintained in pure form and then a unique set of weights on the afferent neurophysiological input is required based on the activity pattern (i.e. a table of weights based on *act*).

The skin temperature predictions for the foot showed the largest ΔT_{skin} and standard deviation of all body parts of up to 6.0 ± 2.4 °C. Furthermore, $\Delta T_{skin,foot}$ was up to 4.5 °C different for morning and afternoon sessions of the same activity. Both effects were most dominant in the original simulation, but could still be seen when the simulation was run with the measured SBF or the new neural signal equation for foot SBF. This observation might suggest that the large deviation was not only due to a simulation inaccuracy, but also due to a systematic effect or an error in measurement. In the study by van Marken Lichtenbelt et al. (2007), which validated an earlier version of an individualized ThermoSEM model for male subjects lying in a neutral and mildly cold environment, the mean $\Delta T_{skin,foot}$ and $\Delta T_{skin,hand}$ was reported to be the highest compared to other body parts with $\Delta T_{skin,foot}$ being 2.5 °C or less. Hence, it could be expected that $\Delta T_{skin,foot}$ is slightly higher than for other body parts. However, this reasoning does not explain the change in $\Delta T_{skin,foot}$ between morning and afternoon sessions. For this difference, the effect of circadian rhythm may have played role. Kräuchi et al. (1999; 1994) and van Marken Lichtenbelt et al. (2006) showed that distal skin temperatures can vary between 1 to 5 °C during the course of a 24-hour period. However, in the time period of our experiments, which was from about 8:30 to 14:00 hours, the variations were lower at 0.5 °C at maximum for $\Delta T_{skin,foot}$ (Kräuchi and Wirz-Justice, 1994). Also, the difference in ΔT_{skin} between the morning and afternoon sessions was less than 1 °C for all other body parts. Hence, the effect of circadian rhythm might only have had a minor part of the differences in $\Delta T_{skin,foot}$ of the morning and afternoon session. Another reason could be that the thermal properties of some shoes of the participants did not match the measured (average) thermal properties which were included in the input parameters of the thermo-physiological model. Shoes with higher dry and evaporative resistance values could lead to heat and sweat accumulation in the shoes, causing the temperature to rise over time (Gavin, 2003; Kuklane et al., 1999). Also, the swelling of the feet or legs after longer periods of sitting or wearing footwear might play a role (Kristjuhan, 1995). Due to this tissue swelling, the blood perfusion would be hindered resulting in different skin temperatures between the morning and afternoon sessions. However, this assumption is not supported by the SBF measurements as shown in Figure 5.7, which are similar for the morning and afternoon session. Hence, future studies may consider that participants take off shoes during breaks to reduce heat accumulation. Standardized footwear might also be an option, but could be too costly because of the variety of shoe sizes and may not provide a suitable fit and comfort to the participants.

The foot skin temperature is not only affected by foot SBF, but also by the total blood flow into the foot (warming from the foot core). Thus, plethysmography would have been another method to cover the total blood flow, since it measures the total blood flow in the deep and superficial tissue layers. However, exercise would have to be interrupted for that. The blood flow in the deeper tissue layers is generally related to the metabolic functions of the extremity and has a constant and modest blood flow (Lotens, 1989). In the extremities, most effects are caused by the change in the SBF, which can be measured by LDF. The blood flow in the deeper tissue layers was not directly measured but included in the ThermoSEM model. The effects of (partly) cooling by other body parts on the core temperature of the feet ($T_{c,foot}$) is taken into account by the counter current heat exchange (CCX) coefficients in the ThermoSEM model. The warming from the foot core depends on $T_{c,foot}$ and the thermal insulation of its surrounding tissue, which is affected by the local skin perfusion.

To avoid the artifacts in the LDF signal during walking, the LDF data was evaluated for the three minutes directly after the subjects stopped moving. In Snell et al. (1987), the leg SBF was relatively constant for the recorded 2:20 min after the prescribed exercise with a peak at about one minute after the exercise. Hence, we assumed that the mean of the LDF signal of the three minutes gives a sufficient estimate for the foot SBF. Also, the small breaks during an activity were designed to be about 3-4 minutes, to avoid large changes in energy expenditure and SBF. In some cases, these small breaks were shorter or had error values due to adjustments of the probe. For these occurrences, a shorter period of stable LDF signal was evaluated. For future studies, a second probe on the other foot and more repetitions of the same session, could improve the interpretation of the LDF signal.

In the literature, no direct comparison for the increase in ankle SBF due to walking at moderate speeds was found. In the studies by Hinds et al. (2004), Joyner et al. (2001), Savard et al. (1988) and Snell et al. (1987), the increase in leg SBF was between 20–50-fold compared to a resting scenario. However, the level of exercise was with 80 to 100% of the subjects' leg maximal performance capacity much higher compared to the slow and preferred walking scenario of this study. Hence, a mean 3–5-fold increase in foot SBF seems to be in reasonable relation, especially since Joyner et al. (2001) show a more steep increase in SBF with elevated walking speeds.

In this study, the variances in the measured foot SBF were very large as shown in

Figure 5.7. To some extent, the range of participants' characteristics might have caused these variations. Also, local basal SBF changed due to a circadian and ultradian rhythm of the course of 24 hours (Yosipovitch et al., 2004). Since this effect might be overshadowed by the prescribed activities, it most likely only has had a minor effect of the foot SBF during walking. Three main reasons can be identified that might have caused the high variances and influenced the results. Firstly, the menstrual phase of the female subjects during the experiments were not considered due to organizational reasons. Bartelink et al. (1990) show that the peripheral perfusion changes significantly during the menstrual cycle, which also cause significant skin temperature differences in the same environmental conditions. Hence, this might be one of the reasons for the larger variance in females than males for the measured foot SBF. Secondly, the study by Snell et al. (1987) showed a significant difference in maximal leg SBF for untrained and trained participants. When recruiting the subjects for our study, this aspect was not considered. The stature and background of the subjects (e.g. daily use of bicycle) may suggest slight difference in fitness. Hence, some variation might due to this issue. Thirdly, even though the experimenters paid great attention to the fixation of the probes, it is possible that the LDF probe on the ankle became looser during the walking session, causing measurement artifacts. Because of the walking movement, the probe was exposed to higher forces than for measurements at seated or lying postures. These issues on the high variance in SBF might be reduced in future studies by using a second probe on the other foot or other measured body part, and more repetitions of the same session with adjusting the probe in between.

Another difference between male and female subjects can be seen in the increase of the ratios of mean normalized, measured SBF and mean normalized, simulated SBF of the foot. For males, the values varied from 1.8 to 4.2 and for females from 4.5 to 7.9. This observation raises the question on whether the smaller change in males is due their generally higher foot skin temperature (about 0.8°C for this study) and higher absolute SBF. Local foot temperatures will affect the local thermoregulatory responses and therefore, the SBF (Brenzelmann and Savage, 1997). However, it is not clear if this can explain all these differences or if other effects also play a role.

For all simulations and participants in this study, T_{core} was underestimated by 1.2 to 1.3°C on average (Figure 5.9). There was a slight increase in ΔT_{core} due to the implementation of the measured SBF compared to the simulated SBF of 0.05°C . In general, the values were larger than could be expected from the accuracy of the

CorTemp pill of $\pm 0.27^\circ\text{C}$ (Bongers et al., 2018). One reason for the relatively large ΔT_{core} was found in the individualization of ThermoSEM (subjects' geometry), which accounts for approximately 0.7°C . This effect might be due to the fact that the model was developed for an average male human, and parameters, such as the basal blood perfusion rate, are scaled with the volume of the body parts. Probably, the scaling should not only be based one-to-one on the geometry, but corrected by some unknown factor. Kingma et al. (2014b) also identified CCX as a source for deviations in T_{core} . In their study, increased CCX coefficients led to a higher T_{core} by 0.2°C . Moreover, Kräuchi et al. (1999; 1994) showed that the changes in T_{core} during a 24-hour period (circadian effect). The difference in T_{core} between 8 o'clock and 14 o'clock was about 0.4°C for resting subjects. In contrast, this study considered active participants. The influence of activity on T_{core} might exceed the influence of the circadian effect. Hence, the influence of the circadian effect on the ΔT_{skin} cannot be quantified. In summary, further research on the physiological individualization of ThermoSEM and on CCX is needed to provide further improvement of the core temperature prediction.

The new neurophysiological model of the foot SBF mostly led to improved foot skin temperature prediction. This result is promising for developing an extended set of new neural regulation signal equations that include activity levels above 1 met and gender differences in SBF, especially since the largest deviations in ΔT_{skin} were seen for this body part. In future research, the SBF measurements should be extended to additional body sites, especially at upper and lower extremities, since they are part of the moving process. Additionally, one or two locations at the torso might be included for comparison to the SBF of the neurophysiological model by Kingma et al. (2014b).

In this study, the measurements were performed at a uniform and constant ambient temperature ($T = 24^\circ\text{C}$), at activity levels in the range 1 to 3 met (sitting – walking) and subjects wearing light and medium clothing ensembles including sneakers. In contrast, the original neurophysiological model was developed on a measurement protocol which included temperature changes, but only in supine position and with low clothing insulation and only socks instead of shoes (Kingma et al., 2014b). To have a complete adjusted neurophysiological model, future research could also include a combination of increased activity levels and different ambient temperatures.

Overall, although some issues have been raised, the results showed that by including the walking activity level and gender in the neural signal model for the SBF, local T_{skin}

can be predicted more accurately. Ideally, the improvements implemented through future studies will predict individual local skin temperatures within the error of the skin temperatures measurement (e.g. with iButtons), which would practically be $\pm 1^\circ\text{C}$ (van Marken Lichtenbelt et al., 2006). At the current stage, individual results were deviating from this aim by up to 6°C for the feet and up to 4°C for all other body parts. However, the average was much closer to the ideal value. Hence, the current version including the improved neurophysiological model of the foot would be applicable to a group of people rather than to individuals, which is the case, for example, in the built environment.

Apart from applications in the built environment, an advanced thermo-physiological model including a precise SBF model might also be applied to other research areas of human physiology such as sport science and medical purposes. In sport science, a thermoregulation model might be used to investigate athletes' heat stress of athletes before a training unit or competition (Havenith, 2001; Havenith and Fiala, 2016). The use of precooling or percooling can reduce this heat stress and improve performance (Bongers et al., 2015; Eijsvogels et al., 2014; Luomala et al., 2012). A thermo-physiological model can be used to preselect promising cooling strategies, without the time and monetary investment of human subject experiments. In medicine, the prediction and observation of a patient's temperature can be critical for the success of medical surgeries. The studies by Droog et al. (2012) and Severens et al. (2007) give examples of applying a thermo-physiological model to the human temperature management during kidney dialysis and open-heart surgery, respectively.

5.5. Conclusions

The accuracy of local skin temperature and local thermal sensation prediction using human thermo-physiological models largely depends on the precision of their local heat balances. Local skin blood flow is a major part of these balances. This study reveals that the skin blood flow and local skin temperature prediction using current neurophysiological model can be improved when walking activity levels above 1 met and gender differences are included in the neurophysiological model. A precise thermo-physiological model including accurate skin blood flow prediction can help to optimize the energy consumption and thermal comfort in the built environment. Additionally, it might be applied to other research areas in human physiology such as sport science and patient's temperature management.

CHAPTER 6

Performance improvements of ThermoSEM in realistic environments – case study revisited*

6.1. Introduction

Chapter 2 of this thesis showed that the local skin temperature prediction quality of ThermoSEM needed to be improved to be applied in realistic office environments. In addition with the literature review described in Chapter 3, the two main resulting aspects were the need for more local clothing input data (e.g. local dry and evaporative thermal resistance and local clothing area factor for casual clothing combinations) and a better inclusion of local internal heat gains (e.g. local muscular heat production,

*Contents of this chapter have been published in:

- Veselá, Stephanie; Kingma, Boris R.M., and Frijns, Arjan J.H. (2019a). “Application of an adjusted neurophysiological (foot) skin blood flow model to a real life case study”. In: *The 18th International Conference on Environmental Ergonomics ICEE2019*. Ed. by Gerrett, N.M.; Daanen, Hein A.M., and Teunissen, L.P.J. Amsterdam, p. 139

local skin blood flow (SBF)). The previous chapters of this thesis revised these issues separately: Chapter 4 presents the local clothing properties of a large variety of office clothing ensembles, and Chapter 5 investigates the influence of the local SBF on the resulting local skin temperature for the foot. The analysis of the local metabolic heat production due to muscle activity had to be excluded due to the lack of adequate measuring methods (see Chapter 7).

The aim of this chapter is to revisit the case study and investigate how the gained data and improvements will affect the local skin temperature prediction of the five subjects as discussed in Chapter 2. The case study scenario “walking outdoors” is skipped in this chapter, because no clothing data was collected for winter clothing items.

6.2. Methods

In this chapter, the human subject measurements from the case study of Chapter 2, section 2.2 on page 10 are used and then compared to the results of ThermoSEM implementing:

1. the measured clothing properties of Chapter 4,
2. the individualized body composition (see Chapter 5, section 5.2.2 on page 85),
3. the improved foot SBF model of Chapter 5, section 5.3.4 on page 96
4. and the combination of the three points above.

The scenarios included in this new analysis are “sitting in an office” as well as “walking indoors” with clothing combinations 1 and 2. The scenario “walking indoors” and “walking outdoors” with clothing combination 3 are not included, since no measured data for combination 3 (including a winter jacket) is available. The average differences of the simulated minus the measured local skin temperatures for the last 45 minutes of the experiments are compared.

6.2.1. Adjusted clothing properties

For the two clothing combinations, the measured data of Outfit 1 and Outfit 15 from Chapter 4 are used for clothing combination 1 and 2, respectively. The dry

clothing resistance for clothing ensemble 2, moving case, was not directly measured, but calculated using the average correction factors from Table A.15 on page 139. The resulting clothing properties of both clothing combinations are summarized in Table 6.1.

6.2.2. Individualization

The default ThermoSEM configuration represents a male subject with a weight of 73.5 kg, a body surface area of 1.86 m², a body fat percentage of 14 %, and total basal metabolic heat of 87.1 W. To meet the individual height, body mass and body fat percentage of each subject (Table 6.2), the length and layer thickness of each body part in ThermoSEM was scaled. The same scaling procedure as described in Chapter 5, section 5.2.2 on page 85 was used. The body fat percentage was estimated using the equation by provided by Deurenberg et al. (1998):



$$bodyfat[\%] = 1.294BMI + 0.20age - 11.4gender - 8.0 \quad (6.1)$$

where BMI is the body mass index [kg m⁻²], *age* is the age of the subject in years and *gender* is the gender of the subject with males = 1 and females = 0. Also, since the basal metabolic rates (BMR) of the subjects were not measured, the calculated BMR of ThermoSEM with individual body compositions was used for all subjects (Table 6.2). In the laboratory study of Chapter 5, these calculated values were mostly close to the measured values by plus-minus 5 %. Additionally, the body surface area of the subjects was calculated using the formula by Du Bois and Du Bois (1916).

6.2.3. Improved SBF neurophysiological model

As a result of Chapter 5, section 5.3.4 on page 96, the neurophysiological model for calculating the foot SBF was revised and depends now also on the overall activity level and gender of the subject. In this chapter, the equation is used for the foot SBF and the equations of the (default) neurophysiological model by Kingma et al. (2014b) is used for all other body parts.

Table 6.1.: Details and thermal properties of all two clothing ensemble

	Clothing ensemble 1 (Outfit 1)					Clothing ensemble 2 (Outfit 15)				
										
Clothing	Underwear, t-shirt, jeans, socks shoes					Clothing ensemble 1 + long-sleeved shirt				
Thermal properties	non-moving		moving			non-moving		moving		
	$f_{cl,i}$	$I_{cl,i}$	$i_{cl,i}$	$I_{cl,i}$	$i_{cl,i}$	$f_{cl,i}$	$I_{cl,i}$	$i_{cl,i}$	$I_{cl,i}$	$i_{cl,i}$
	[-]	$\frac{m^2 W}{K}$	[-]	$\frac{m^2 W}{K}$	[-]	[-]	$\frac{m^2 W}{K}$	[-]	$\frac{m^2 W}{K}$	[-]
Upper arm	1.15	0.081	0.45	0.052	1.0 ^b	1.42	0.150	0.37	0.09	0.58
Lower arm	/	/	/	/	/	1.72	0.095	0.71	0.06	0.64
Chest	1.13	0.092	0.46	0.071	0.64	1.16	0.147	0.51	0.09	0.71
Back	1.11	0.172	0.23	0.165	0.56	1.12	0.268	0.33	0.25	0.71
Front hip	1.11	0.129	0.52	0.082	0.66	1.13	0.192	0.64	0.11	0.68
Back hip	1.15	0.153	0.36	0.164	0.97	1.18	0.241	0.45	0.22	0.90
Upper leg	1.01	0.062 (0.175) ^c	0.77	0.039	0.42	1.01	0.071 (0.263) ^c	0.51	0.04	0.47
Lower leg	1.29	0.091 (0.078) ^c	0.40	0.068	1.35	1.29	0.088 (0.087) ^c	0.33	0.06	1.40
Foot	1.40	0.070	0.08	0.05 ^a	0.06	1.40	0.070	0.08	0.05 ^a	0.06

Nomenclature: $f_{cl,i}$: local clothing area factor; $I_{cl,i}$: local intrinsic dry thermal insulation; $i_{cl,i}$: local clothing moisture permeability

^a estimated value

^b moving, 0.2 m s^{-1} air speed

^c estimated insulation value due to chair (Lee et al., 2013)

Table 6.2.: Measured and calculated subject characteristics

	Male 1	Male 2	Male 3	Female 1	Female 2	ThermoSEM
Body mass [kg]	80	90	76	62	63	73.5
Height [m]	1.92	1.82	1.86	1.68	1.70	1.73
BMI [kg m^{-2}]	21.7	27.2	22	22	21.8	/
Age [years]	42	32	32	27	26	24.6
Calc. body fat [%]	17.1	22.2	15.5	25.9	25.4	14.0
Calc. BMR [W]	94.0	97.2	90.66	67.2	68.7	87.1
Calc. body surface area [m^2]	2.09	2.12	2.00	1.70	1.73	1.86

6.3. Results and Discussion

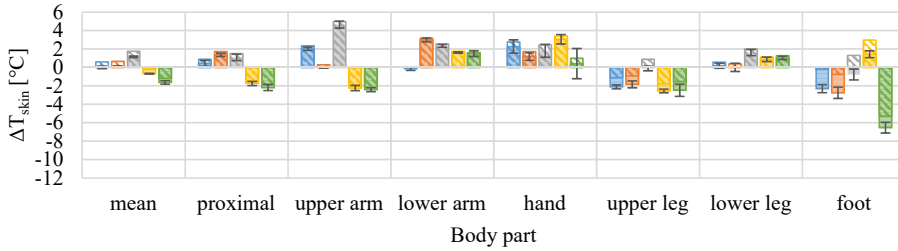
6.3.1. Adjusted clothing properties

The resulting skin temperature differences using the newly measured clothing properties in comparison to the results of Chapter 2 are shown in Figure 6.1 for all five subjects and four scenarios. The detailed data is provided in Table A.22 on page 149. As a general trend for all scenarios, subjects and body parts, the skin temperature difference is lowered by up to 2°C, meaning that more heat is lost through the clothing layers. This result leads to lower predicted skin temperatures, i. e. either less overestimation by the simulation, for example for the hands and lower arms, or larger underestimation, especially for proximal skin sites, upper arms and the lower body. An exception to this trend are the results for the upper leg, lower leg and foot while walking indoors with clothing combination 2. Here, the temperature differences are raised by up to 1.5°C, meaning heat losses are reduced.

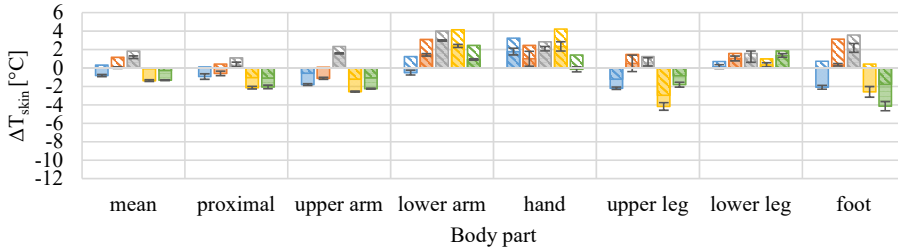
Implementing the measured clothing properties in ThermoSEM generally adds to heat losses at the local heat balances of the model, especially for clothing combination 2. The clothing properties of the clothing combination 1 and 2 by Lee et al. (2013) and Veselá et al. (2018c)/ Chapter 4 are compared in Table 4.6 on page 65 and in Table 6.3, respectively. The comparison reveals that 1) the dry thermal insulation is lower in the study by Veselá et al. (2018c) and 2) the moisture permeability tends to be slightly larger than the assumed value of 0.38. Both findings lead to increased heat losses at local body parts. At the foot, the measured moisture permeability by Veselá et al. (2018c) is much less than 0.38. Hence, it might lead to heat gain (or less heat loss) at this body site. In combination with the larger upper body insulation of clothing combination 2, this finding might explain the increased foot, upper and lower leg skin temperature difference while walking indoors with clothing combination 2. Hence, it also gives an example of the dependence of the one local skin temperature to the others.

In the case study, the subjects wore their own clothing, which may have slightly different clothing properties than the measured ones. Hence, also the newly measured clothing properties only provide an estimation of the real values. This uncertainty can be limited to a certain extent by considering the fit of the garment, i.e. the air gap between the skin and the clothing layer. Section 4.3.2 provides regression equations

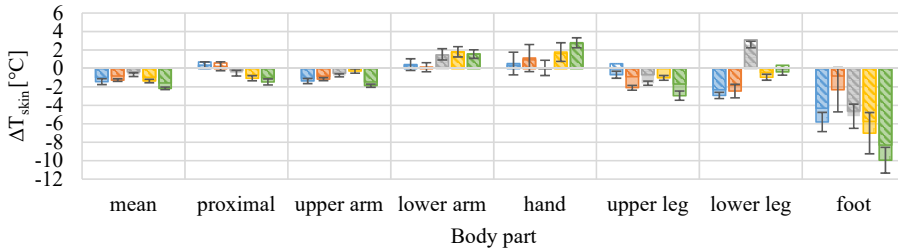
(a) Sitting in office, clothing combination 1



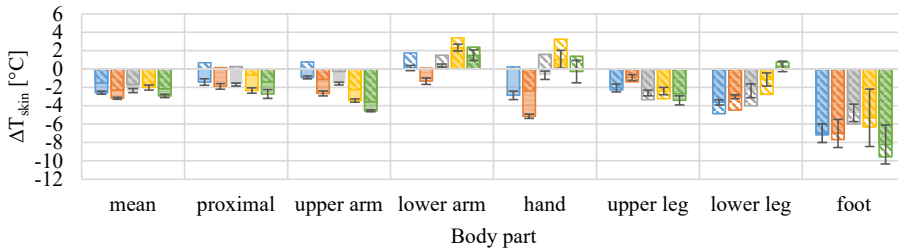
(b) Sitting in office, clothing combination 2



(c) Walking indoors, clothing combination 1



(d) Walking indoors, clothing combination 2



M1 default
 M2 default
 M3 default
 F1 default
 F2 default

M1 new clo
 M2 new clo
 M3 new clo
 F1 new clo
 F2 new clo

Figure 6.1.: Local skin temperature differences (simulated minus measured) and standard deviations for five subject while performing at two activity levels with two clothing combinations: solid fill – results for newly measured clothing properties; shaded fill – results of default simulation as in Chapter 2

Table 6.3.: Comparison of the clothing properties Veselá et al. (2018c) and Lee et al. (2013) of clothing combination 2

Clothing	Veselá et al.			Lee et al.		
	Underwear, short-sleeved t-shirt, jeans, socks, shoes, long-sleeved shirt					
	$f_{cl,i}$	$I_{cl,i}$	$i_{cl,i}$	$f_{cl,i}$	$I_{cl,i}$	$i_{cl,i}$
	[–]	$\frac{\text{m}^2 \text{W}}{\text{K}}$	[–]	[–]	$\frac{\text{m}^2 \text{W}}{\text{K}}$	[–]
Upper arm	1.42	0.15	0.365	1.13	0.293	0.38
Lower arm	1.72	0.095	0.714	1.13	0.219	0.38
Chest	1.16	0.147	0.506	1.13	0.602	0.38
Back	1.12	0.268	0.332	1.13	0.353	0.38
Front hip	1.13	0.192	0.641	1.13	0.602	0.38
Back hip	1.18	0.241	0.450	1.13	0.353	0.38
		(0.263)			(0.375)	
Upper leg	1.01	0.071	0.506	1.09	0.113	0.38
		(0.087)			(0.129)	
Lower leg	1.29	0.088	0.330	1.2	0.090	0.38
Foot	1.40	0.070	0.076	1.03	0.128	0.38

Nomenclature: $f_{cl,i}$: local clothing area factor; $I_{cl,i}$: local intrinsic dry thermal insulation;
 $i_{cl,i}$: local clothing moisture permeability

for the clothing area factor and dry clothing insulation of one layer clothing items depending on the fit of the garments for a specific subject (Veselá et al., 2018c). To apply these equations, the circumferences at different body landmarks would have needed to be measured. During the time of the described case study, this knowledge was not available, and therefore, no body circumferences of the subjects were taken. For future studies, this information would add to the certainty of local clothing properties.

All in all, the newly measured clothing properties do not necessary improve the results, meaning less absolute skin temperature difference between simulated and measured values. However, it adds to the certainty of the skin temperature prediction and other local effect of the local heat balances can be investigated more thoroughly.

6.3.2. Individualization

Figure 6.2 depicts the skin temperature differences using only the individual morphology of the subjects in comparison to the default simulation. The detailed data is given in Table A.23 on page 150. In all cases, the individual geometry causes the skin temperatures difference to shift towards lower values, meaning either the overestimation

of the simulation is reduced or the underestimation is increased. For the two male subjects, M1 and M3, the change in skin temperature difference is relatively low at 0.2 to 0.6 °C compared to the male subject M2 and the two female subjects. For the latter, the skin temperature differences are mostly reduced by 0.4 °C up to 1.5 °C. However, larger deviations can be found for the upper and lower leg for the female subjects while walking indoors, where the differences can be up to 4 °C.

The low changes for males M1 and M2 are most likely because their body composition is closest to the one of default ThermoSEM, whereas M3, F1 and F2 have more different values. When comparing the detailed body composition (Table 6.2), it seems that especially the fat percentage is an important factor. On one hand, the larger fat percentage of M3, F1 and F2 results in an increased radius of the fat layer at all body parts. This would lead to a larger insulation (Baker and Daniels, 1956; Jéquier et al., 1974; Savastano et al., 2009). On the other hand, a higher fat percentage means a higher fat mass and, consequently, a lower muscle mass. Since muscles produce heat while active and have a larger blood perfusion rate, a lower muscle mass would reduce the heat input for each body part. Since the skin temperature differences of the walking scenarios show a larger change towards negative values than the skin temperature differences of the seated scenarios, it seems that the effect by lower muscle mass might be dominant in our cases. Additionally, it has to be considered that the body fat percentage was not measured but estimated based on mass, height, age and gender of the participant. Hence, the accuracy of the results seem to strongly depend on the fat percentage. Thus, it might also be the case that the accuracy of the results depend on the accuracy of the fat percentage determination.

6.3.3. Improved foot SBF neurophysiological model

Implementing the new foot SBF model affects mainly the mean and foot skin temperature difference as depicted in Figure 6.3. The detailed data is provided in Table A.24 on page 151. The change in skin temperature difference for all other body parts is very low at 0.1 to 0.2 °C. For the foot, the skin temperature difference is raised towards positive values. Here, the change in skin temperature difference ranges from 0.4 to 5 °C for the scenarios “sitting in an office” and from 6 to 9 °C for “walking indoors”.

In contrast to the results with the newly measured clothing properties and individual



Figure 6.2.: Local skin temperature differences (simulated minus measured) and standard deviations for five subject while performing at two activity levels with two clothing combinations: solid fill – results for implemented individual geometry; shaded fill – results of default simulation as in Chapter 2

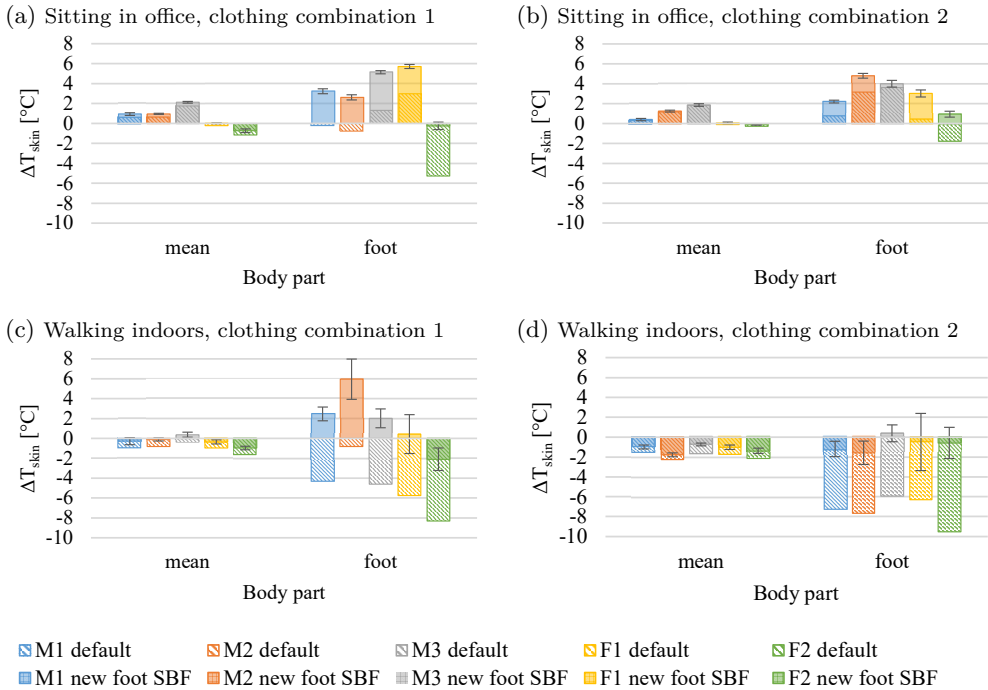


Figure 6.3.: Local skin temperature differences (simulated minus measured) and standard deviations for five subjects while performing at two activity levels with two clothing combinations: solid fill – results for implemented new foot SBF; shaded fill – results of default simulation as in Chapter 2

subject geometry, the new foot SBF model contributes to the heat gain of the local heat balances. In line with the findings of Chapter 5, this effect is larger with increased activity levels. For the foot skin temperature prediction, it leads mostly to a higher overestimation of the measured values by the simulation in case of “sitting in an office”, and lower underestimation for “walking indoors”.

6.3.4. Combined effect

The results for the combined effect of newly measured clothing properties, individual geometry and improved foot SBF are given in Figure 6.4. The detailed data is provided in Table A.25 on page 152. Apart from the foot, the newly simulated skin temperatures are lowered for most body parts of the five subjects in the four scenarios. The decrease in skin temperature difference is hereby slightly higher than for the newly measured

clothing properties and individualization alone. The foot skin temperature difference increases in all cases, but less than for the exclusive implementation of the new foot SBF model.

The combined results of the three implementation options are in line with the single effects. At the foot, the heat losses due to newly measured clothing properties and individualization are balanced by the heat gain due to the improved foot SBF model. This balance mostly leads to improved foot skin temperature prediction for the walking scenarios. As mentioned in Chapter 5, also the skin temperature prediction of other body parts might profit from renewed SBF models. Especially, the skin temperature of the upper arm as well as upper and lower leg is underestimated by the simulation, and increased heat gains via increased SBF could improve the results.

6.4. Conclusions

The newly measured clothing properties, individualization and new foot SBF model can be applied to the case study and lead to the expected changes in the skin temperature differences. The combination of all three options at the foot balances the heat losses due to clothing as well as individualization, and the heat gains due to SBF. Hence, the improvement of the SBF model at all body parts seems to be the most important next step in future work in improving the local skin temperature prediction.

Chapter 6. Case study - revisited

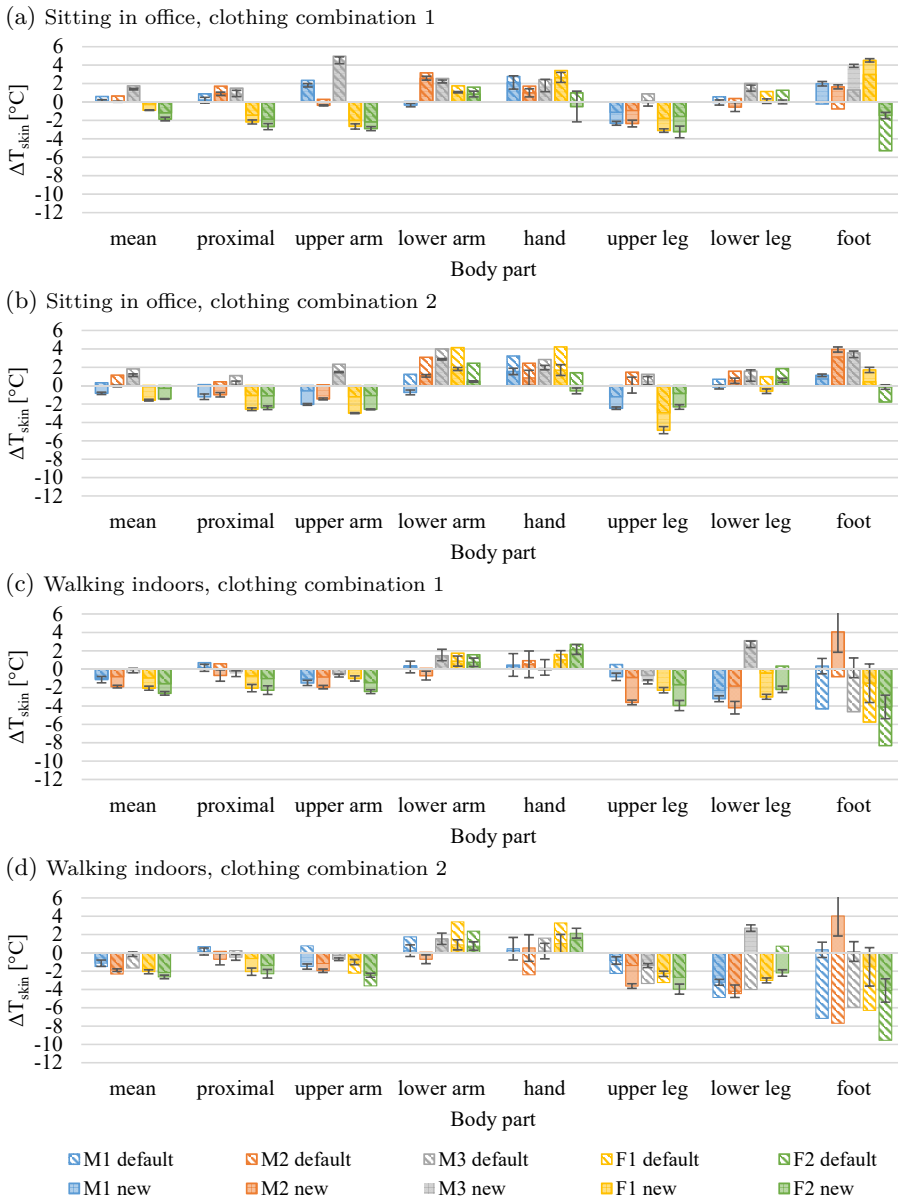


Figure 6.4.: Local skin temperature differences (simulated minus measured) and standard deviations for five subjects while performing at two activity levels with two clothing combinations: solid fill – results for the combination of newly measured clothing properties, individual geometry and new foot SBF model; shaded fill – results of default simulation as in Chapter 2

CHAPTER 7

General conclusions and future work

7.1. Conclusions

The prediction of human local thermal comfort and sensation in office buildings is essential to ensure that energy efficient HVAC designs maintain a thermal environment for an optimal performance of the building occupants. This challenge is increased when personalized heating and cooling solutions are implemented. Here, the consideration of the skin temperature of each body part (local skin temperature) is important to ensure that no local discomfort is apparent. To meet this requisition, this thesis investigated major influences on local heat balances while working in an office environment. For this analysis, we conducted a case study, where 5 participants performed medium level activities in an office environment (Chapter 2), and an extensive literature review that focused on the influence of local clothing properties and local metabolic heat production on skin temperature prediction (Chapter 3). Our detailed analyses showed that variations in input parameters, such as local clothing parameters and local heat generation, can lead to local skin temperature differences ($\Delta T = 0.4\text{ }^{\circ}\text{C} - 4.4\text{ }^{\circ}\text{C}$). These differences can affect the local sensation output, where $\Delta T = 1\text{ }^{\circ}\text{C}$ is approximately one step on a 9-point thermal sensation scale. Thus, two major issues were addressed:

1. no appropriate data sets for local clothing properties of typical office clothing were available in the literature, and 2. local heat gain due to skin blood flow (SBF) and muscular activity, especially on the extremities, was underestimated for low to medium activity levels of 1 to 3 met ($1 \text{ met} \cong 58.2 \text{ W m}^{-2}$). Hence, we hypothesized that the local skin temperature prediction quality of ThermoSEM would be increased by improving these matters. In this thesis, the local properties of clothing ensembles typically worn in an office environment and the influence of local SBF on the local heat balances were investigated experimentally, and then applied to the thermo-physiological modeling. Additionally, the effect of individual body composition as compared to the standard model was considered.

We, in cooperation with Empa, St. Gallen, Switzerland, determined local clothing parameters on a thermal sweating manikin (Chapter 4). For the dry thermal insulation and local area factors, we measured these values for 23 typical office outfits at three air speeds and body movement. The evaporative resistance was determined for two representative outfits at all air speeds and body movement. Additionally, we measured the clothing properties of three typical office shoes. For the dry thermal insulation, we found a correlation to the fit of the clothing (ease allowance) for most body parts of one level clothing outfits. In summary, these data sets increase the certainty of the local clothing properties that are used for modeling. Hence, the skin temperature prediction quality could also be increased.

While planning our human subject experiments at Maastricht University (Chapter 5), we paid special attention capturing influences on the local heat balances. During the experiments, participants performed light to medium activities on a treadmill while skin and core temperature, skin blood perfusion at the foot and their energy expenditure were measured. In this thesis, our focus was directed towards the prediction of SBF at the feet. An enhanced neurophysiological model for SBF at the feet was developed that includes the walking activity levels above 1 met and gender differences. The enhanced SBF model lead to a higher accuracy of skin temperature prediction at the feet.

In Chapter 6, we investigated the influence of using the newly measured clothing properties, the enhanced SBF model for the feet, and an individual body composition in ThermoSEM on the resulting local skin temperatures of the case study from Chapter 2. Overall, our local skin temperature prediction quality increased. The detailed analysis

shows that the largest improvement on local skin temperature prediction is due to the improved foot SBF model.

7.2. Recommendation for future research

7.2.1. Application to personalized heating and cooling

One of the main motivations to advance the thermo-physiological model is to substitute part of the human subject experiments for testing personalized heating and cooling systems. This thesis sets the basis in measuring local clothing properties and improving the local SBF model. However, to apply the model to personalized heating and cooling systems, also the input of the thermal environment needs to be advanced. Currently, the model needs the knowledge of the operative temperature, relative humidity and air speed next to a specific body part. To obtain these values either the data needs to be measured or simulated. In Schellen et al. (2013), the temperature around the human are simulated via CFD simulation. The advantages of this method are that different settings can be implemented accurately and the operative temperatures around the human have a good resolution. However, an additional software is required. Another method would be to prescribe the heat fluxes from the heating or cooling equipment to the body surface. This method could be implemented in ThermoSEM without an additional program. However, the resolution should be checked for larger body parts. In conclusion, it is suggested to implement a heat flux input file for ThermoSEM and validate the results with human subject experiments in a climate chamber.

7.2.2. Muscle Activity level of specific body parts

The local heat gain due to local increase in metabolic rates and local increase in SBF can have a large impact on local skin temperatures (see Chapters 2, 3 and 5). In the future, the aim is to extend the thermo-physiological model ThermoSEM such that it includes localized increase in tissue perfusion as well as local increase in metabolic rates depending on the type of activity. The next step should be on the local increase in metabolic rates. However, that requires an additional set of measurements in which local metabolic rates are obtained. This might be done using electromyography (EMG)

under laboratory conditions. EMG measures the the electrical signal in a muscle, which corresponds to its activity (Mills, 2005; Reaz et al., 2006). To conduct the measurement, invasive (needle) or non-invasive electrodes can be placed on the skin. However, motion artifacts cause electrical noise, which affects the EMG signal (Reaz et al., 2006). Hence, it is difficult to use in human subject experiments, where the participants are moving. Another option is to further advance the indirect method, i.e. measuring all important influences of the local heat balance and then estimate the metabolic heat production due to activity in an optimization routine using a detailed heat transfer model. In the experiments of Chapter 5, a difficulty arose for the sweat rates. Hence, a different method might be applied, e.g. ventilated capsule method or technical absorbent method (Morris et al., 2013), or a sophisticated sweating model could be implemented.

7.2.3. Advancing the SBF model for further body parts

As discussed in Chapter 5, the SBF model of all body parts should be revised for activity levels above 1 met as shown for the foot. In an office environment, this usually means sitting, standing or walking. However, other activities might be also considered depending on the application of ThermoSEM. Hence, human subject experiments similar to the ones of Chapter 5 should be performed. The sensors of the LDF would be ideally attached to all limbs, since there are the most active parts in the moving process. Additionally, there probably should be at least on position on the upper body, to check for changes in SBF due to motion there. In practice, each LDF monitor usually provides two wired sensors. Hence, it might not be feasible to have more than 4 sensors during one measurement, since also the wires might interfere with the motion trajectory. As discussed in section 5.2.2 on page 88, the SBF needs to be evaluated shortly after the motion is stopped to avoid Doppler shift associated with the movement (Kirkpatrick et al., 1994; Snell et al., 1987).

Apart from the measuring technique, also the specific location of the LDF sensors need to be considered carefully. Here, skin sites of non-glabrous (hairy) skin might be preferred. In glabrous (non-hairy) skin also arterio venous anastomoses (AVAs) are present, which can form a direct connection from arterioles to venules when open (Johnson et al., 1986; Roddie, 1983; Walløe, 2016). Hence, SBF and heat transport can be increased significantly by active AVAs (Grahn and Craig Heller, 2004; Roddie,

1983; Sparks, 1978). This effect also depends on the thermal state of the person which is a function of the environmental temperature, clothing and activity among others (Kingma et al., 2014a). According to Bergersen (1993) and Walløe (2016), frequency of SBF fluctuation in the middle of the thermal neutral zone is about 2 to 3 vasoconstrictions per minute, and the AVAs are regarded as fully open at the upper end of the thermal neutral zone.

With the measured and analyzed local SBF, an improved SBF model including the activity level similar to the one in section 5.3.4 on page 96 can be found for all body parts. The models might also depend on the gender of the subjects or other factors such as blood pressure, blood glucose level or hormones (Kingma et al., 2014b; I. B. Mekjavič and Eiken, 2006). However, keeping the purpose of ThermoSEM in mind, they might only be included if they contribute to improving the skin temperature prediction quality or are required for specific uses.

APPENDIX A

Supplementary figures and tables

A.1. Introduction

Table A.1.: Overview of single-segment thermophysiological models

year	model	description	restrictions
1970	Fanger (1970)	<ul style="list-style-type: none">• one node• empirical	<ul style="list-style-type: none">• uniform temperature• whole body• steady state
1971	Givoni (Givoni and Goldman, 1971)	<ul style="list-style-type: none">• one node• empirical	<ul style="list-style-type: none">• hot environment
1971	Pierce two-node model (Gagge et al., 1971)	<ul style="list-style-type: none">• two node: core and skin• control and controlled system• moderate activity levels	<ul style="list-style-type: none">• exposure time <1 h• uniform environment
1977	KSU-model (Azer and Hsu, 1977)	<ul style="list-style-type: none">• like Gagge (1971), but other control equation	
2014	Kingma TNZ/TCZ (Kingma et al., 2014a)	<ul style="list-style-type: none">• two node model• biophysical	<ul style="list-style-type: none">• uniform skin temperature• whole body• steady state

Appendix A. Supplementary figures and tables

Table A.2.: Overview of multi-segment thermophysiological models

year	model	description	restrictions
1966/ 1971	Stolwijk (Stolwijk, 1971; Stolwijk and Hardy, 1966)	<ul style="list-style-type: none"> • 6 segments, 4 layers, 25 nodes 	<ul style="list-style-type: none"> • uniform environments • steady state
1985	Wissler (1985)	<ul style="list-style-type: none"> • 15 segments, 225 nodes • detailed passive system • steady-state and transient bioheat equation 	<ul style="list-style-type: none"> • uniform environments
1991	Smith (Smith, 1991) as cited by (Miimu et al., 2013)	<ul style="list-style-type: none"> • three-dimensional finite element model • 15 cylindrical body parts, 576 body tissue elements, 1500 circulatory system elements 	<ul style="list-style-type: none"> • no clothing model • fat and skin layer considered as one
1992	Lotens (Lotens, 1993; Lotens and Havenith, 1992)	<ul style="list-style-type: none"> • emphasis on clothing model • 13 cylindrical body parts, 5 layers • control equations from Gagge et al. (1986) 	<ul style="list-style-type: none"> • limited physiology and thermo-regulation
1995	Fu (G. Fu, 1995; G. Fu and Jones, 1996)	<ul style="list-style-type: none"> • based on Smith (1991) • improved heat exchange between blood & body • separation of skin and fat layer • clothing model by Jones & Ogawa (1993) 	<ul style="list-style-type: none"> • high demand on computational resources
1999	UTCI-Fiala (Fiala et al., 2012, 1999, 2001)	<ul style="list-style-type: none"> • based on Stolwijk • 19 segments, 4 -5 layers, 3 sectors; 187 nodes • passive and active system; steady-state + transient 	<ul style="list-style-type: none"> • $5\text{ }^{\circ}\text{C} < T_{amb} < 50\text{ }^{\circ}\text{C}$ • 0.8-10 met • regression based
2001	UCB model (Huizenga et al., 2001)	<ul style="list-style-type: none"> • based on Stolwijk and cooperation with Tanabe • arbitrary number of segments • individualized • passive + active system; steady state & transient 	<ul style="list-style-type: none"> • regression based • setpoint based
2002	Tanabe (Tanabe et al., 2002)	<ul style="list-style-type: none"> • based on Stolwijk; cooperation with UC Berkeley • 16 segments, 65 nodes • passive + active system • steady state and transient conditions 	<ul style="list-style-type: none"> • setpoint based
2007	ThermoSEM (Kingma, 2012; Severens, 2008)	<ul style="list-style-type: none"> • based on Fiala (1999) • Individualization possible • active system based on neurophysiology 	<ul style="list-style-type: none"> • validated for mild environmental conditions
2011	Multi-segmental Pierce model (Foda and Sirén, 2011)	<ul style="list-style-type: none"> • Pierce two-node model applied to 20 body parts • local skin setpoints based on neutral conditions 	<ul style="list-style-type: none"> • steady state • measured in neutral conditions

Table A.3.: Overview of thermal sensation models

year	model	description	restrictions
1970	Fanger PMV model (1970)	<ul style="list-style-type: none"> empirical 	<ul style="list-style-type: none"> uniform temperature whole body
1993	de Dear et al. (Dear et al., 1993)	<ul style="list-style-type: none"> Dynamic Thermal Stimulus model: area aver-aged thermal sensation 	<ul style="list-style-type: none"> local skin temperatures; not enough for whole body thermal state
2003	Nilsson (Nilsson, 2007; Nilsson and Holmér, 2003)	<ul style="list-style-type: none"> local thermal sensation based on equivalent temperature clothing independent comfort zones 	<ul style="list-style-type: none"> empirical model steady state for automotive application for thermal neutral zone
2003	Lomas/ Fiala (Lomas et al., 2003)	<ul style="list-style-type: none"> dynamic thermal sensation model mean skin & core temp. & time derivatives transient conditions 	<ul style="list-style-type: none"> whole body thermal sensation, not local regression analysis
2003	Zhang/ UC Berkley (H. Zhang, 2003)	<ul style="list-style-type: none"> uniform and non-uniform environment local/ whole-body thermal sensation & comfort mean skin & core temp. & time derivatives 	<ul style="list-style-type: none"> regression analysis set points for neutral conditions required
2011	ThermoSEM (Kingma, 2012; Schellen et al., 2013)	<ul style="list-style-type: none"> thermal sensation based on neuro-physiology uniform & non-uniform whole-body thermal sensation 	<ul style="list-style-type: none"> validated for mild thermal challenges only

A.2. Case study - Performance of ThermoSEM

Table A.4.: Average difference and standard deviation between simulated and measured mean and local skin temperature [$^{\circ}\text{C}$] (for the last 45 min)

	Mean	Proximal	Upper arm	Lower arm	Hand	Upper leg	Lower leg	Foot
<i>Sitting in office, clothing combination 1</i>								
M1	0.61±0.15	0.87±0.32	2.36±0.19	0.07±0.19	2.77±0.69	-1.12±0.21	0.58±0.27	-0.23±0.42
M2	0.66±0.06	1.74±0.18	0.29±0.06	3.16±0.21	1.72±0.30	-0.91±0.38	0.37±0.46	-0.76±0.55
M3	1.76±0.09	1.49±0.34	4.97±0.37	2.54±0.16	2.44±0.57	0.88±0.25	2.01±0.33	1.31±0.52
F1	-0.23±0.03	-1.43±0.22	-1.97±0.28	1.76±0.08	3.42±0.49	-1.77±0.20	1.14±0.25	2.98±0.34
F2	-1.17±0.19	-1.86±0.33	-2.16±0.22	1.63±0.31	0.99±1.69	-1.58±0.69	1.29±0.18	-5.29±0.63
avg	0.33±0.98	0.16±1.51	0.70±2.70	1.83±1.04	2.27±0.84	-0.90±0.94	1.08±0.58	-0.40±2.77
<i>Sitting in office, clothing combination 2</i>								
M1	0.31±0.11	0.11±0.29	-0.58±0.09	1.22±0.25	3.22±0.33	-1.23±0.13	0.70±0.21	0.72±0.15
M2	1.15±0.09	0.42±0.24	0.07±0.09	3.09±0.15	2.44±0.73	1.45±0.89	1.58±0.27	3.11±0.16
M3	1.83±0.14	1.10±0.24	2.32±0.07	3.99±0.07	2.84±0.22	1.23±0.45	1.57±0.62	3.57±0.42
F1	-0.10±0.09	-1.04±0.15	-1.21±0.07	4.13±0.20	4.20±0.37	-2.97±0.43	0.98±0.24	0.41±0.49
F2	-0.28±0.04	-1.11±0.19	-1.08±0.06	2.45±0.10	1.40±0.26	-0.84±0.28	1.85±0.21	-1.79±0.43
avg	0.58±0.80	-0.10±0.86	-0.10±1.29	2.98±0.92	2.82±0.92	-0.47±1.65	1.33±0.43	1.20±1.95
<i>Walking indoors, clothing combination 1</i>								
M1	-0.98±0.34	0.70±0.35	-1.07±0.28	0.35±0.62	0.33±1.20	0.50±0.47	-2.31±0.32	-4.32±0.77
M2	-0.82±0.15	0.58±0.49	-0.86±0.17	0.07±0.48	0.93±1.44	-0.92±0.25	-1.84±0.71	-0.82±2.11
M3	-0.37±0.23	-0.22±0.31	-0.51±0.16	1.45±0.60	-0.09±0.79	-0.68±0.25	3.09±0.35	-4.62±1.04
F1	-0.98±0.21	-0.75±0.27	0.00±0.24	1.74±0.54	1.59±0.98	0.00±0.36	-0.43±0.33	-5.76±2.01
F2	-1.59±0.16	-1.03±0.33	-1.47±0.17	1.57±0.45	2.68±0.51	-1.69±0.61	0.32±0.39	-8.32±1.19
avg	-0.95±0.39	-0.14±0.69	-0.78±0.50	1.03±0.69	1.09±0.98	-0.56±0.76	-0.23±1.91	-4.77±2.43
<i>Walking indoors, clothing combination 2</i>								
M1	-1.51±0.20	0.69±0.25	0.76±0.16	1.74±0.37	0.25±0.62	-2.27±0.50	-4.86±0.22	-7.16±0.83
M2	-2.30±0.19	0.16±0.25	-1.14±0.38	0.08±0.54	-2.40±0.40	-1.39±0.45	-4.46±0.16	-7.68±1.29
M3	-1.67±0.12	0.27±0.16	-0.27±0.22	1.49±0.25	1.59±0.61	-3.35±0.21	-4.00±0.55	-5.95±0.81
F1	-1.73±0.22	-0.63±0.19	-2.23±0.18	3.38±0.42	3.26±1.21	-3.24±0.35	-2.76±0.66	-6.29±3.05
F2	-2.15±0.25	-1.39±0.40	-3.60±0.11	2.37±0.76	1.40±1.45	-2.69±0.70	0.74±0.60	-9.55±1.86
avg	-1.87±0.30	-0.18±0.74	-1.30±1.52	1.81±1.08	0.82±1.87	-2.58±0.71	-3.07±2.03	-7.33±1.27
<i>Walking indoors, clothing combination 3</i>								
M1	-1.34±0.39	0.61±0.55	-1.15±0.44	1.34±0.24	0.96±0.79	-1.88±0.35	-4.05±0.56	-4.52±1.86
M2	-2.59±0.29	-0.29±0.22	-0.44±0.22	0.40±0.19	-3.04±1.06	-1.62±0.60	-4.34±0.30	-9.06±0.16
M3	-0.59±0.35	0.71±0.24	3.63±0.41	3.28±0.08	0.46±0.85	-2.37±0.43	-1.85±0.80	-3.14±1.27
F1	-3.56±0.18	-2.78±0.09	-3.71±0.07	2.28±0.09	-1.13±1.63	-5.77±0.54	-2.97±0.25	-11.05±1.39
F2	-3.57±0.20	-3.11±0.15	-2.95±0.23	0.32±0.12	-4.89±0.26	-1.01±0.62	-3.25±0.36	-10.82±0.18
avg	-2.33±1.19	-0.97±1.65	-0.93±2.56	1.52±1.13	-1.53±2.19	-2.53±1.68	-3.29±0.88	-7.72±3.28
<i>Walking outdoors, clothing combination 3</i>								
M1	-1.74±0.23	0.36±0.35	-1.43±0.09	-0.11±0.35	3.08±1.83	-3.17±0.72	-4.00±0.31	-10.48±0.75
M2	-1.72±0.60	1.05±0.24	-0.33±0.50	2.45±0.67	3.89±2.48	-3.65±0.54	-4.96±0.68	-8.59±0.19
M3	-0.62±0.22	0.05±0.31	0.35±0.16	0.37±0.13	3.74±1.31	-0.73±0.43	-1.42±0.65	-7.67±0.85
F1	-1.53±0.37	-1.38±0.19	-2.72±0.07	2.86±0.81	3.17±2.34	-1.59±0.81	-1.90±0.35	-12.17±1.64
F2	-2.78±0.32	-3.66±0.25	-3.33±0.13	0.16±0.27	2.34±3.12	-1.31±0.99	-0.96±0.35	-9.04±1.13
avg	-1.68±0.69	-0.72±1.67	-1.49±1.39	1.15±1.25	3.25±0.55	-2.09±1.12	-2.65±1.56	-9.59±1.57

A.2. Case study - Performance of ThermoSEM

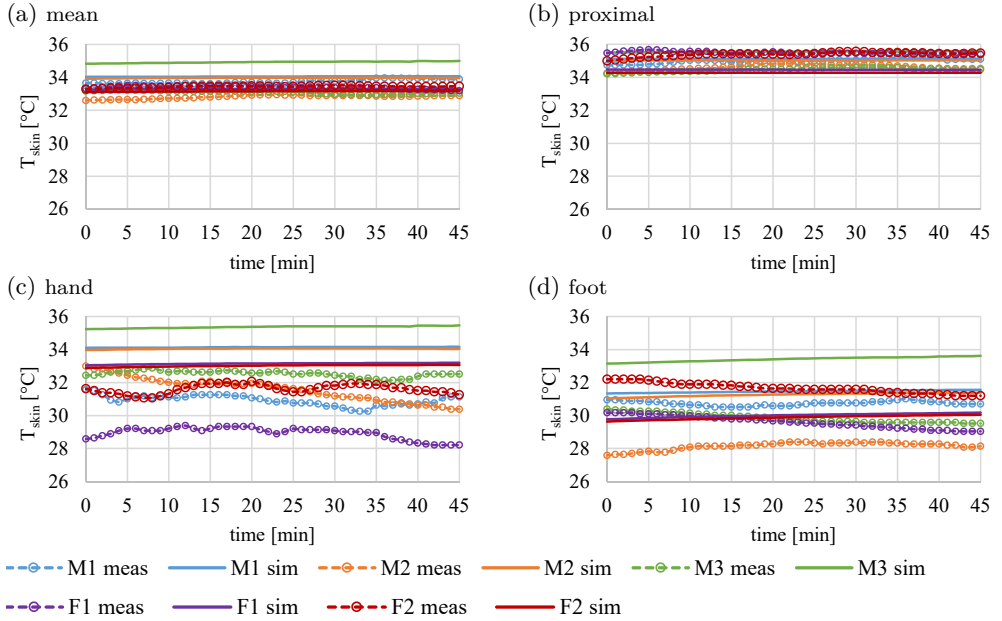


Figure A.1.: Sitting in office, clothing comb. 2: Measured and simulated T_{skin} of last 45 min

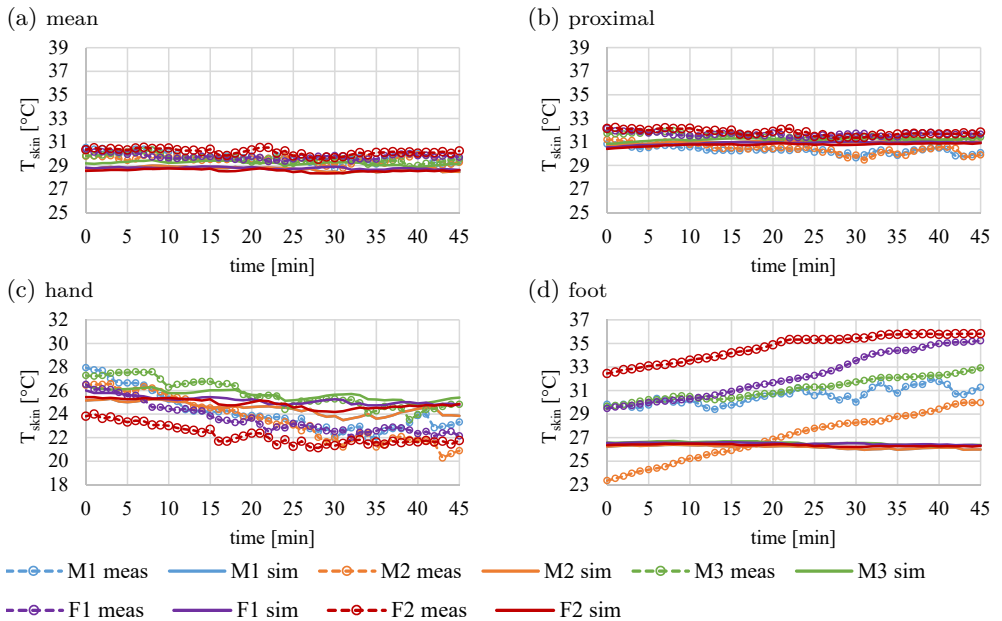


Figure A.2.: Walking indoors, clothing comb. 1: Measured and simulated T_{skin} of last 45 min

Appendix A. Supplementary figures and tables

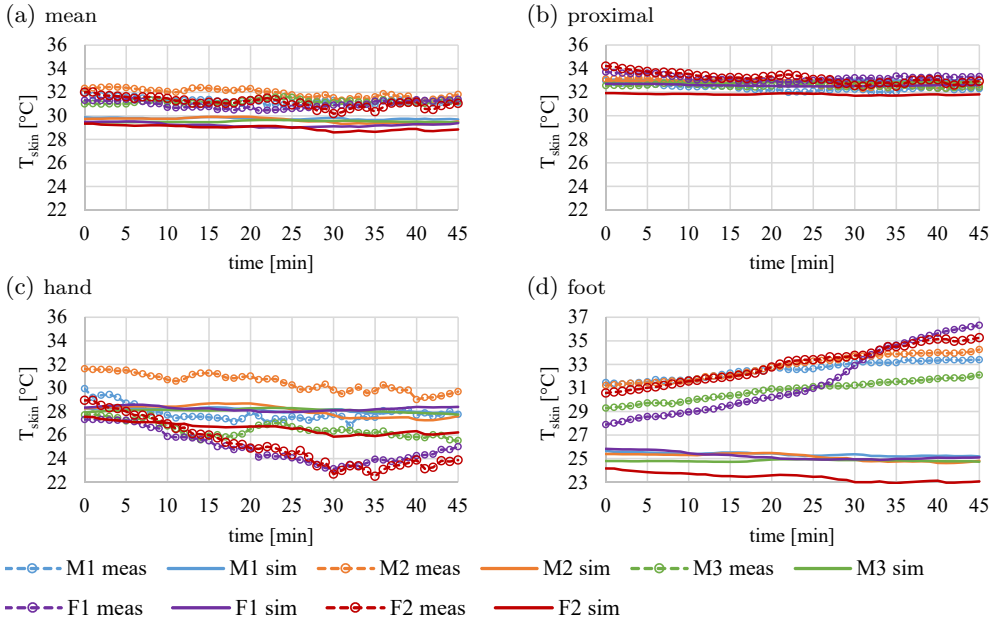


Figure A.3.: Walking indoors, clothing comb. 2: Measured and simulated T_{skin} of last 45 min

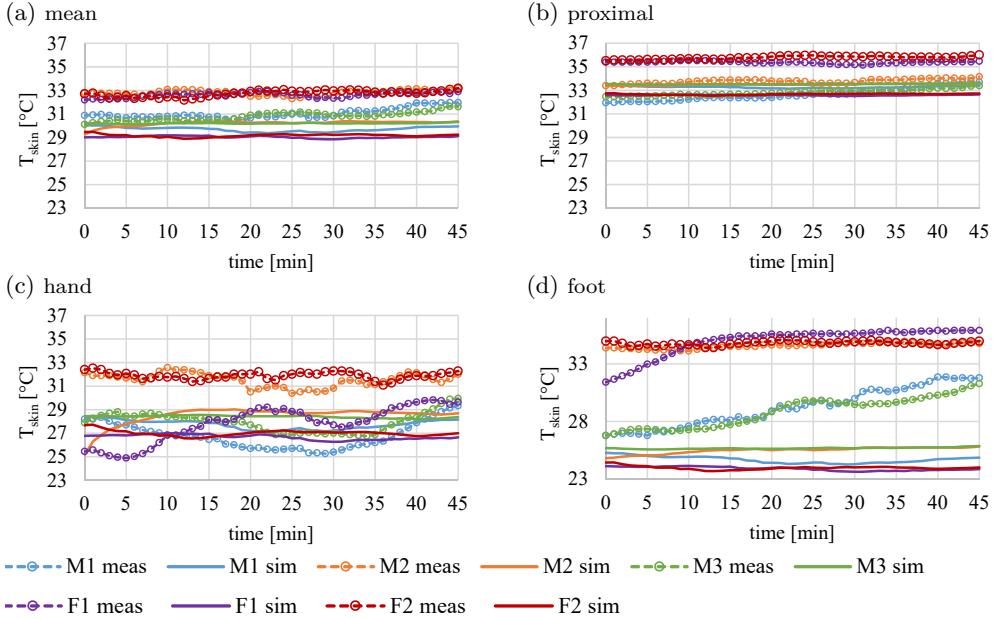


Figure A.4.: Walking indoors, clothing comb. 3: Measured and simulated T_{skin} of last 45 min

A.3. Local thermal sensation modeling – a review

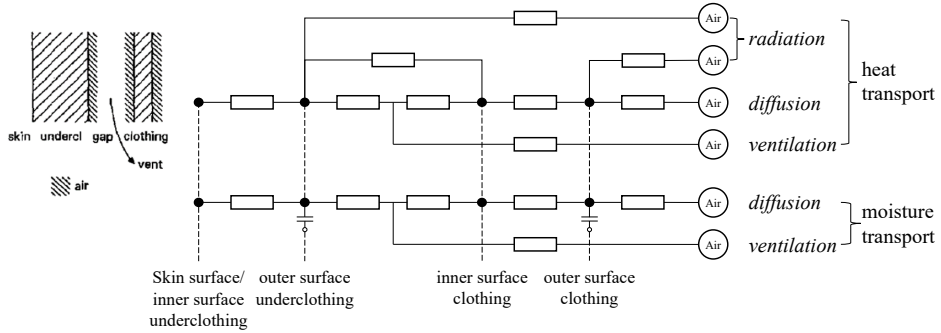


Figure A.5.: Heat and moisture transport resistance model by Lotens & Havenith (1992)

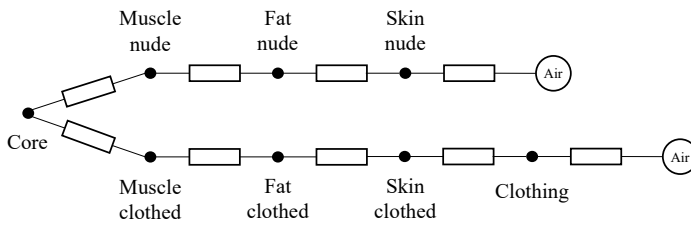


Figure A.6.: Node network model according to Fu et al. (2014)

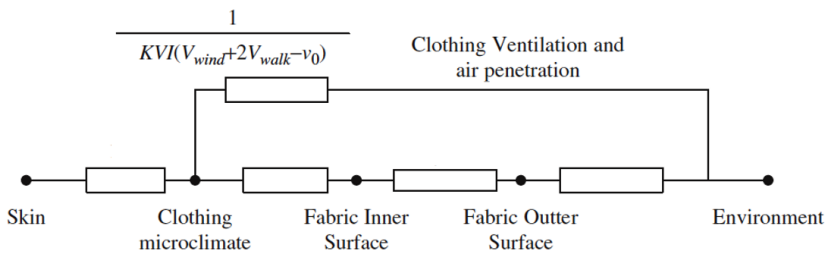


Figure A.7.: Electric circuit analogy for including clothing ventilation and air penetration into a body-clothing-environment system by Wan and Fan (2008)

Table A.5.: Implementation of clothing in multi-segment thermophysiological models - Part 1

Year	Model	Clothing model	Required data input	Methods for obtaining input data
1971	Stolwijk (Stolwijk, 1971; Stolwijk and Hardy, 1966)	<ul style="list-style-type: none"> • none • during validation subjects wore shorts, but clo value not considered 	<ul style="list-style-type: none"> • none 	<ul style="list-style-type: none"> • none
1985	Wissler (1985)	<ul style="list-style-type: none"> • reference to Shitzer and Chato (1985) • heat & mass transfer differential equations for fabric-air-space-skin-body system • set of equations and boundary conditions solved numerically 	<ul style="list-style-type: none"> • air gap widths • diffusion & heat transfer coefficients • conductivity of fabric • local clothing insulation and evaporative resistance of fabric 	<ul style="list-style-type: none"> • through measurements, but no details given in Wissler (1985) or Shitzer and Chato (1985)
1991/1995	Smith/Fu (G. Fu, 1995; G. Fu and Jones, 1996; Smith, 1991)	<ul style="list-style-type: none"> • transient, quasi-two-dimensional model of clothing heat & moisture transfer based on the clothing model by Jones and Ogawa (1992, 1993) • resulting differential equations solved using finite difference • heat transport through air layers by radiation, and conduction • moisture transport through air layers by diffusion • vapor pressure model instead of skin wetness model • describes upper limit of the moisture accumulation: 35 g m^{-2} 	<ul style="list-style-type: none"> • thermal resistance of fabrics • evaporative resistance of fabrics • dry fabric density • thickness of fabric • width between skin and fabric 	<ul style="list-style-type: none"> • No information given
1992	Lotens (Lotens, 1993; Lotens and Havenith, 1992)	<ul style="list-style-type: none"> • four layer model: under clothing, trapped air layer, outer garment, adjacent air • resistance network for dry heat and evaporative transfer systems 	<ul style="list-style-type: none"> • heat transfer coefficients, moisture uptake, weight, radiation properties of clothing items • width of trapped air layer • ventilation and wind speed • clothing area factor 	<ul style="list-style-type: none"> • measurements • data from literature

Table A.6.: Implementation of clothing in multi-segment thermophysiological models - Part 2

Year	Model	Clothing model	Required data input	Methods for obtaining input data
1999	UTCI-Fiala (Fiala et al., 2012; 1999, 2001)	<ul style="list-style-type: none"> • clothing included for each sector of every segment. • local effective heat transfer coefficient U_{cl}^* and a local effective evaporative coefficient $U_{e,cl}^*$ for multi-layered clothing ensemble. • evaporative heat losses through clothing with approach as in Jones and Ogawa (1992) 	<ul style="list-style-type: none"> • local values for clothing insulation • local clothing area factor • local permeability index or evaporative resistance 	<ul style="list-style-type: none"> • recalculation of local values I_{cl}^*, f_{cl}^* and i_{cl}^* based on the values by McCullough et al. (1985, 1989) • procedure & values not published
2001	UCB model (Huizenga et al., 2001)	<ul style="list-style-type: none"> • improved clothing model by Fu et al. (2014) • distinction between clothed and non-clothed pathway from body core to environment • absorption and desorption by clothing included by balancing the specific heat flux around the clothing node 	<ul style="list-style-type: none"> • local values for clothing insulation • local evaporative resistance • local clothing area factors • correction factors for air and body movement 	<ul style="list-style-type: none"> • measurements done by Lee et al. (2013)
2002	Tanabe (Tanabe et al., 2002)	same as UTCI-Fiala	same as UTCI-Fiala	<ul style="list-style-type: none"> • data taken from thermal manikin experiments, but not published
2007	ThermoSEM (Kingma et al., 2014b; Severens, 2008)	same as UTCI-Fiala	same as UTCI-Fiala	<ul style="list-style-type: none"> • from literature
2011	Multi-segmental Pierce model (Foda and Sirén, 2011)	<ul style="list-style-type: none"> • radiative & convective heat losses as functions of clothing temperature • iterative procedure for estimating clothing & temperature T_{cl} as function of radiative & convective heat transfer coefficients • procedure repeated if temperatures T_{cl}^* and T_{cl} deviate more than 0.001 °C 	<ul style="list-style-type: none"> • local values for clothing insulation • local clothing area factor 	<ul style="list-style-type: none"> • local I_{cl} from measured air and total resistances on a thermal manikin clothed in light office clothing consisting of under-shirt, shorts, shirt, denim trousers, calf length socks

A.4. Local clothing properties

Table A.7.: Garments and their properties

Item	Briefs	Undershirt	T-shirt	Long-sleeved shirt	Long-sleeved smart shirt
Fits			Regular/ Loose	Tight/ Regular/ Loose	Tight/ Regular/ Loose
Picture					
Fibre content	100% Cotton	100% Cotton	95% Cotton/ 5% Elastane	98% Cotton / 2% Spandex	100% Cotton
Mass per unit area	145.13 g/m ³	145.13 g/m ³	176 g/m ³	188 g/m ³	137 g/m ³
Thickness	0.454 mm	0.454 mm	0.633 mm	0.87 mm	0.71 mm
Item	Sweater	Jacket	Jeans	Pants	Skirt
Fits			Tight/ Regular/ Loose		
Picture					
Fibre content	100% Cotton	65 % Polyester/ 35% Viskose	100% Cotton	60% Wool/ 38% Polyester/ 2% Elastane	93% Polyester/ 7% Elastane
Mass per unit area	361.58 g/m ³	unknown	179 g/m ³	202.15 g/m ³	unknown
Thickness	1.680 mm	unknown	0.67 mm	0.416 mm	unknown
Item	Athletic sock	Nylon socks	Sneakers	Business shoes	Ballerinas
Picture					
Fibre content	75% Cotton/ 25% Polyamid	100% Polyamid			

Table A.8.: Local area factors measured on manikin James – Part 1

Item	Body part	Local area factor James				
		1	2	3	avg	SD
Tshirt regular	Upper arm	1.23	1.17	1.23	1.21	0.03
	Chest	1.13	1.12	1.14	1.13	0.01
	Front hip	1.22	1.20	1.20	1.21	0.01
	Back	1.13	1.12	1.12	1.12	0.01
	Back hip	1.20	1.21	1.24	1.21	0.02
Tshirt loose	Upper arm	1.38	1.40	1.37	1.39	0.01
	Chest	1.18	1.21	1.21	1.20	0.01
	Front hip	1.23	1.31	1.26	1.27	0.03
	Back	1.19	1.18	1.17	1.18	0.01
	Back hip	1.63	1.54	1.59	1.59	0.04
Shirt tight	Upper arm	1.15	1.16	1.15	1.15	0.00
	Lower arm	1.17	1.16	1.16	1.16	0.00
	Chest	1.02	1.04	1.03	1.03	0.01
	Front hip	1.02	1.03	1.03	1.03	0.00
	Back	1.04	1.03	1.04	1.04	0.00
	Back hip	1.07	1.07	1.07	1.07	0.00
Shirt regular	Upper arm	1.22	1.24	1.23	1.23	0.01
	Lower arm	1.23	1.24	1.24	1.24	0.01
	Chest	1.06	1.07	1.05	1.06	0.01
	Front hip	1.07	1.12	1.07	1.09	0.02
	Back	1.07	1.06	1.07	1.07	0.01
	Back hip	1.15	1.13	1.15	1.14	0.01
Shirt loose	Upper arm	1.27	1.32	1.30	1.30	0.02
	Lower arm	1.27	1.29	1.30	1.29	0.01
	Chest	1.08	1.10	1.12	1.10	0.02
	Front hip	1.21	1.22	1.21	1.21	0.01
	Back	1.12	1.11	1.11	1.11	0.01
	Back hip	1.21	1.21	1.22	1.21	0.01
Smart shirt tight	Upper arm	1.36	1.37	1.38	1.37	0.01
	Lower arm	1.54	1.54	1.54	1.54	0.00
	Chest	1.11	1.10	1.12	1.11	0.01
	Front hip	1.04	1.04	1.05	1.04	0.00
	Back	1.07	1.08	1.07	1.07	0.00
	Back hip	1.09	1.08	1.09	1.08	0.00
Smart shirt regular	Upper arm	1.44	1.45	1.48	1.46	0.02
	Lower arm	1.57	1.57	1.56	1.57	0.00
	Chest	1.17	1.15	1.18	1.17	0.01
	Front hip	1.15	1.16	1.13	1.15	0.01
	Back	1.14	1.12	1.13	1.13	0.01
	Back hip	1.22	1.22	1.24	1.23	0.01
Smart shirt loose	Upper arm	1.54	1.51	1.58	1.54	0.03
	Lower arm	1.73	1.72	1.76	1.74	0.02
	Chest	1.18	1.20	1.20	1.19	0.01
	Front hip	1.33	1.38	1.38	1.36	0.02
	Back	1.19	1.17	1.17	1.17	0.01
	Back hip	1.34	1.27	1.26	1.29	0.04

Appendix A. Supplementary figures and tables

Table A.9.: Local area factors measured on manikin James – Part 2

Item	Body part	Local area factor James				
		1	2	3	avg	SD
Sweater	Upper arm	1.33	1.28	1.29	1.30	0.02
	Lower arm	1.36	1.33	1.33	1.34	0.01
	Chest	1.12	1.22	1.17	1.17	0.04
	Front hip	1.24	1.27	1.39	1.30	0.06
	Back	1.13	1.10	1.12	1.12	0.01
	Back hip	1.44	1.44	1.42	1.43	0.01
Jacket	Upper arm	1.79	1.63	1.61	1.68	0.08
	Lower arm	1.68	1.69	1.68	1.69	0.00
	Chest	1.44	1.31	1.31	1.35	0.06
	Front hip	1.54	1.31	1.37	1.41	0.09
	Back	1.14	1.16	1.12	1.14	0.02
	Back hip	1.19	1.41	1.38	1.33	0.10
Jeans tight	Front hip	1.07	1.06	1.06	1.06	0.00
	Back hip	1.00	1.00	1.00	1.00	0.00
	upper leg total	1.06	1.06	1.06	1.06	0.00
	lower leg total	1.26	1.27	1.28	1.27	0.01
Jeans regular	Front hip	1.07	1.06	1.07	1.07	0.01
	Back hip	1.01	1.00	1.00	1.01	0.00
	upper leg total	1.13	1.13	1.13	1.13	0.00
	lower leg total	1.41	1.41	1.41	1.41	0.00
Jeans loose	Front hip	1.11	1.11	1.11	1.11	0.00
	Back hip	1.02	1.02	1.01	1.02	0.00
	upper leg total	1.21	1.20	1.20	1.20	0.00
	lower leg total	1.56	1.55	1.56	1.56	0.00
Trousers	Front hip	1.07	1.06	1.08	1.07	0.01
	Back hip	1.05	1.04	1.04	1.04	0.00
	upper leg total	1.30	1.27	1.28	1.28	0.01
	lower leg total	1.57	1.56	1.56	1.56	0.00
Skirt	Front hip	1.35	1.30		1.32	0.03
	Back hip	1.22	1.16		1.19	0.03
	upper leg total	2.30	2.29		2.29	0.00

Table A.10.: Results for local clothing dry thermal resistance of all outfits and all test cases in $[m^2 KW^{-1}]$

Outfit	Posture	v_{air} [m/s]	Upper arm	Lower arm	Chest	Back	Front hip	Back hip	Upper leg	Lower leg
	standing	0.2	0.081	n/a	0.092	0.172	0.129	0.153	0.062	0.091
	standing	0.4	0.079	n/a	0.090	0.158	0.137	0.182	0.054	0.090
1	standing	1	0.071	n/a	0.078	0.167	0.094	0.183	0.056	0.092
	moving	0.2	0.061	n/a	0.084	0.212	0.125	0.135	0.043	0.068
	moving	1	0.052	n/a	0.071	0.165	0.082	0.164	0.039	0.068
2	standing.	0.2	0.078	0.069	0.075	0.143	0.153	0.211	0.056	0.089
	standing	0.2	0.122	0.093	0.115	0.192	0.181	0.213	0.065	0.090
	standing	0.4	0.116	0.088	0.105	0.183	0.151	0.198	0.060	0.089
3	standing	1	0.097	0.081	0.079	0.156	0.108	0.209	0.056	0.082
	moving	0.2	0.089	0.076	0.084	0.234	0.132	0.171	0.047	0.070
	moving	1	0.075	0.065	0.063	0.177	0.089	0.182	0.048	0.068
4	standing	0.2	0.119	n/a	0.103	0.178	0.162	0.192	0.055	0.088
5	standing	0.2	0.066	0.062	0.051	0.110	0.122	0.156	0.054	0.087
6	standing	0.2	0.102	0.095	0.072	0.161	0.120	0.157	0.056	0.089
7	standing	0.2	0.112	0.076	0.095	0.164	0.168	0.213	0.062	0.089
8	standing	0.2	0.148	0.095	0.122	0.215	0.186	0.227	0.069	0.090
9	standing	0.2	0.125	0.091	0.117	0.189	0.191	0.213	0.102	0.092
10	standing	0.2	0.124	0.091	0.114	0.196	0.149	0.196	0.052	0.067
11	standing	0.2	0.104	0.091	0.077	0.159	0.107	0.155	0.043	0.067
12	standing	0.2	0.150	0.097	0.128	0.228	0.214	0.228	0.100	0.093
13	standing	0.2	0.131	0.090	0.120	0.212	0.181	0.198	0.156	0.080
	standing	0.2	0.129	0.092	0.120	0.202	0.140	0.142	0.153	0.082
	standing	0.4	0.125	0.093	0.105	0.179	0.135	0.135	0.142	0.081
14	standing	1	0.106	0.088	0.085	0.159	0.108	0.143	0.156	0.087
	moving	0.2	0.079	0.069	0.087	0.212	0.109	0.140	0.072	0.048
	moving	1	0.074	0.066	0.066	0.176	0.079	0.108	0.059	0.045
15	standing	0.2	0.129	0.095	0.147	0.268	0.192	0.241	0.071	0.088

Table A.10.: Results for local clothing dry thermal resistance of all outfits and all test cases in $[m^2 KW^{-1}]$ - continued

Outfit	Posture	v_{air} [m/s]	Upper arm	Lower arm	Chest	Back	Front hip	Back hip	Upper leg	Lower leg
16	standing	0.2	0.184	0.094	0.180	0.316	0.224	0.277	0.074	0.092
17	standing	0.2	0.120	0.084	0.144	0.296	0.174	0.209	0.166	0.087
18	standing	0.2	0.194	0.098	0.177	0.324	0.188	0.196	0.160	0.086
	standing	0.2	0.183	0.099	0.157	0.303	0.246	0.274	0.062	0.087
	standing	0.4	0.164	0.095	0.152	0.311	0.182	0.217	0.061	0.093
19	standing	1	0.159	0.089	0.139	0.309	0.145	0.259	0.055	0.089
	moving	0.2	0.140	0.083	0.148	0.393	0.226	0.290	0.054	0.069
	moving	1	0.124	0.064	0.119	0.282	0.149	0.217	0.048	0.070
20	standing	0.2	0.158	0.122	0.187	0.379	0.232	0.265	0.065	0.089
	standing	0.2	0.287	0.172	0.283	0.505	0.330	0.368	0.206	0.085
	standing	0.4	0.284	0.164	0.279	0.574	0.299	0.416	0.206	0.088
21	standing	1	0.243	0.151	0.205	0.520	0.166	0.347	0.183	0.084
	moving	0.2	0.175	0.094	0.216	0.587	0.213	0.273	0.071	0.046
	moving	1	0.161	0.095	0.177	0.535	0.158	0.299	0.074	0.045
	standing	0.2	0.122	0.094	0.120	0.183	0.143	0.144	0.175	0.010
22	standing	0.4	0.122	0.095	0.108	0.178	0.137	0.142	0.150	0.007
	standing	1	0.098	0.075	0.081	0.159	0.110	0.136	0.127	0.005
	moving	0.2	0.079	0.073	0.083	0.188	0.142	0.157	0.071	0.006
	moving	1	0.076	0.067	0.068	0.177	0.111	0.155	0.074	0.007
23	standing	0.2	0.298	0.166	0.270	0.515	0.296	0.354	0.207	0.006

Table A.11.: Results for local dry and evaporative air layer resistance of all test cases

Outfit	Posture	v_{air} [m/s]	Upper arm	Lower arm	Chest	Back	Front hip	Back hip	Upper leg	Lower leg
Dry air layer resistance [$\text{m}^2 \text{K W}^{-1}$]										
TC 1	standing	0.2	0.09	0.06	0.10	0.15	0.06	0.07	0.08	0.07
TC 2	standing	0.4	0.07	0.05	0.08	0.15	0.05	0.07	0.07	0.06
TC 3	standing	1.0	0.05	0.03	0.05	0.10	0.03	0.05	0.04	0.04
TC 4	moving	0.2	0.09	0.05	0.10	0.18	0.06	0.07	0.07	0.05
TC 5	moving	1.0	0.05	0.03	0.05	0.11	0.04	0.05	0.04	0.04
Evaporative air layer resistance [$\text{m}^2 \text{kPa W}^{-1}$]										
TC 1	standing	0.2	0.02	0.02	0.03	0.05	0.01	0.03	0.01	0.01
TC 2	standing	0.4	0.02	0.02	0.02	0.04	0.01	0.02	0.01	0.01
TC 3	standing	1.0	0.02	0.02	0.01	0.03	0.01	0.01	0.01	0.01
TC 4	moving	0.2	0.02	0.01	0.03	0.06	0.01	0.02	0.01	0.01
TC 5	moving	1.0	0.02	0.01	0.01	0.03	0.01	0.01	0.01	0.01

Appendix A. Supplementary figures and tables

Table A.12.: Results for local clothing evaporative resistance of all outfits and all test cases in $[\text{m}^2 \text{kPa W}^{-1}]$

Outfit	Posture	v_{air} [m/s]	Upper arm	Lower arm	Chest	Back	Front hip	Back hip	Upper leg	Lower leg
1	standing	0.2	0.011	n/a	0.012	0.045	0.015	0.026	0.005	0.013
	standing	0.4	0.014	n/a	0.009	0.030	0.015	0.027	0.006	0.011
	standing	1	0.006	n/a	0.008	0.021	0.010	0.019	0.006	0.008
	moving	0.2	0.009	n/a	0.009	0.038	0.011	0.012	0.008	0.009
2	moving	1	0.001	n/a	0.007	0.018	0.007	0.010	0.006	0.005
	standing	0.2	0.015	0.007	0.008	0.032	0.015	0.062	0.006	0.015
3	standing	0.2	0.020	0.008	0.015	0.065	0.018	0.039	0.005	0.012
4	standing	0.2	0.019	n/a	0.014	0.039	0.016	0.018	0.005	0.014
6	standing	0.2	0.016	0.006	0.006	0.018	0.009	0.003	0.005	0.015
8	standing	0.2	0.026	0.008	0.021	0.079	0.018	0.037	0.006	0.015
9	standing	0.2	0.023	0.007	0.013	0.050	0.018	0.032	0.012	0.015
11	standing	0.2	0.018	0.009	0.009	0.023	0.008	0.007	0.005	0.010
12	standing	0.2	0.026	0.010	0.020	0.073	0.021	0.052	0.010	0.015
13	standing	0.2	0.022	0.013	0.019	0.063	0.021	0.045	0.021	0.016
14	standing	0.2	0.020	0.007	0.017	0.033	0.012	0.016	0.022	0.017
	standing	0.4	0.020	0.008	0.013	0.027	0.013	0.018	0.019	0.014
	standing	1	0.012	0.006	0.011	0.025	0.010	0.019	0.015	0.007
	moving	0.2	0.013	0.012	0.007	0.024	0.008	0.009	0.008	0.007
15	moving	1	0.007	0.006	0.006	0.016	0.008	0.009	0.007	0.002
	standing	0.2	0.021	0.008	0.017	0.048	0.018	0.032	0.008	0.016
16	standing	0.2	0.029	0.009	0.025	0.085	0.023	0.045	0.007	0.016
17	standing	0.2	0.020	0.005	0.015	0.042	0.013	0.020	0.021	0.016
18	standing	0.2	0.031	0.012	0.024	0.051	0.017	0.021	0.021	0.016
19	standing	0.2	0.032	0.007	0.021	0.071	0.021	0.034	0.007	0.013
22	standing	0.2	0.032	0.006	0.015	0.047	0.012	0.017	0.020	0.000

Table A.13.: Correction factors for total insulation of nude $I_{T,0.4\text{ m s}^{-1},st}/I_{T,0.2\text{ m s}^{-1},st}$ and clothing insulation $I_{cl,0.4\text{ m s}^{-1},st}/I_{cl,0.2\text{ m s}^{-1},st}$ of measured outfits

	Upper arm	Lower arm	Chest	Back	Front hip	Back hip	Upper leg	Lower leg
Nude	0.83	0.85	0.79	0.95	0.78	0.91	0.84	0.87
1	0.98	/	0.98	0.92	1.06	1.19	0.86	1.00
3	0.96	0.95	0.91	0.95	0.83	0.92	0.92	0.99
14	0.97	1.01	0.88	0.89	0.97	0.95	0.93	0.98
19	0.90	0.96	0.97	1.03	0.74	0.79	0.98	1.07
21	0.99	0.95	0.99	1.14	0.91	1.13	1.00	1.02
22	1.00	1.01	0.90	0.97	0.96	0.99	0.85	0.67

Table A.14.: Correction factors for total insulation of nude $I_{T,1\text{ m s}^{-1},st}/I_{T,0.2\text{ m s}^{-1},st}$ and clothing insulation $I_{cl,1\text{ m s}^{-1},st}/I_{cl,0.2\text{ m s}^{-1},st}$ of measured outfits

	Upper arm	Lower arm	Chest	Back	Front hip	Back hip	Upper leg	Lower leg
Nude	0.53	0.56	0.52	0.66	0.53	0.68	0.55	0.62
1	0.88	/	0.85	0.97	0.73	1.19	0.91	1.05
3	0.73	0.72	0.68	0.81	0.60	0.99	0.88	0.95
14	0.82	0.96	0.71	0.79	0.78	1.01	1.02	1.06
19	0.87	0.61	0.89	1.02	0.59	0.95	0.90	1.04
21	0.85	0.88	0.72	1.03	0.50	0.94	0.89	0.99
22	0.81	0.80	0.68	0.87	0.77	0.94	0.72	0.48

Table A.15.: Correction factors for total insulation of nude $I_{T,0.2\text{ m s}^{-1},move}/I_{T,0.2\text{ m s}^{-1},stand}$ and clothing insulation $I_{cl,0.2\text{ m s}^{-1},move}/I_{cl,0.2\text{ m s}^{-1},stand}$ of measured outfits

	Upper arm	Lower arm	Chest	Back	Front hip	Back hip	Upper leg	Lower leg
Nude	0.96	0.83	1.00	1.14	0.98	1.02	0.91	0.75
1	0.76		0.92	1.23	0.97	0.88	0.68	0.75
3	0.73	0.82	0.73	1.22	0.73	0.80	0.72	0.77
14	0.61	0.76	0.73	1.05	0.77	0.98	0.47	0.59
19	0.77	0.84	0.94	1.30	0.92	1.06	0.87	0.80
21	0.61	0.55	0.76	1.16	0.65	0.74	0.34	0.53
22	0.66	0.77	0.69	1.03	1.00	1.09	0.52	0.57

Table A.16.: Correction factors for total insulation of nude $I_{T,1\text{ m s}^{-1},move}/I_{T,0.2\text{ m s}^{-1},stand}$ and clothing insulation $I_{cl,1\text{ m s}^{-1},move}/I_{cl,0.2\text{ m s}^{-1},stand}$ of measured outfits

	Upper arm	Lower arm	Chest	Back	Front hip	Back hip	Upper leg	Lower leg
Nude	0.54	0.58	0.52	0.70	0.54	0.65	0.55	0.62
1	0.65		0.77	0.96	0.63	1.07	0.63	0.77
3	0.61	0.69	0.55	0.92	0.49	0.85	0.73	0.76
14	0.57	0.71	0.55	0.87	0.57	0.76	0.39	0.56
19	0.68	0.65	0.76	0.93	0.60	0.79	0.77	0.81
21	0.56	0.55	0.63	1.06	0.48	0.81	0.36	0.53
22	0.62	0.71	0.57	0.97	0.78	1.08	0.49	0.67

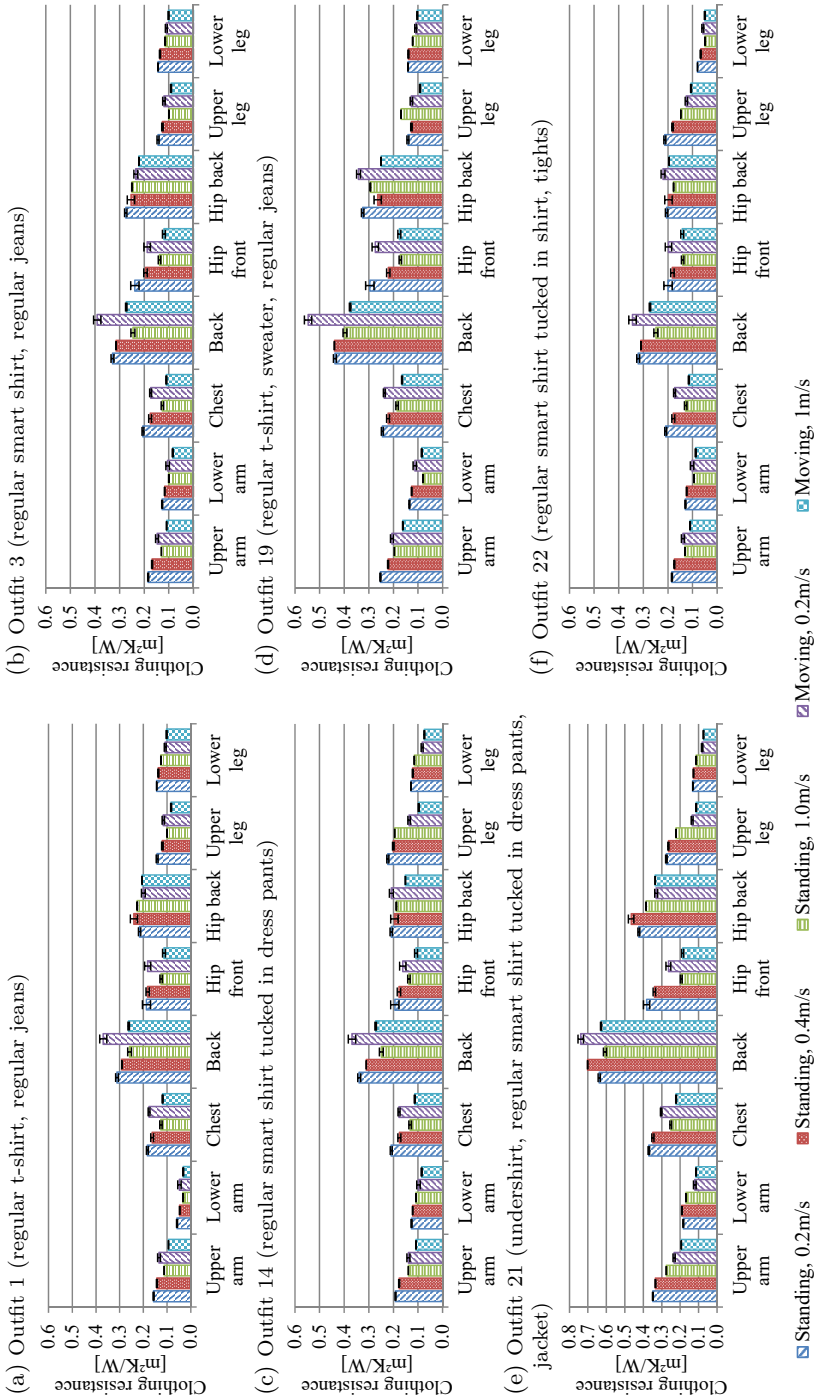




Figure A.8.: Influence of air speed and body movement on local intrinsic clothing insulation

A.5. Effect of local SBF on local skin temperature

Table A.17.: Details and thermal properties of light and medium clothing ensemble

	Light clothing ensemble					Medium clothing ensemble				
										
Clothing	Underwear, t-shirt, shorts					Underwear, t-shirt, sweater, sweatpants				
Thermal properties	$f_{cl,i}$ [-]	non-moving		moving		$f_{cl,i}$ [-]	non-moving		moving	
		$I_{cl,i}$ $\frac{m^2 W}{K}$	$i_{cl,i}$ [-]	$I_{cl,i}$ $\frac{m^2 W}{K}$	$i_{cl,i}$ [-]		$I_{cl,i}$ $\frac{m^2 W}{K}$	$i_{cl,i}$ [-]	$I_{cl,i}$ $\frac{m^2 W}{K}$	$i_{cl,i}$ [-]
Upper arm	1.37	0.074	0.31	0.054	0.25	1.45	0.194	0.34	0.145	0.37
Lower arm	/	/	/	/	/	1.71	0.107	0.60	0.082	0.31
Chest	1.10	0.085	0.50	0.078	0.51	1.37	0.188	0.33	0.167	0.41
Back	1.08	0.166	0.42	0.173	0.25	1.28	0.649	0.33	0.567	0.39
Front hip	1.18	0.135	0.40	0.135	0.46	1.33	0.268	0.41	0.199	0.45
Back hip	1.22	0.163	0.23	0.157	0.41	1.39	0.299	0.28	0.200	0.49
Upper leg	1.35	0.128	0.37	0.058	0.40	1.23	0.172	0.43	0.093	0.40
Lower leg	/	/	/	/	/	1.52	0.098	0.36	0.068	0.41
Foot	1.40	0.05	0.042	0.04	0.045	1.40	0.04	0.042	0.05	0.045

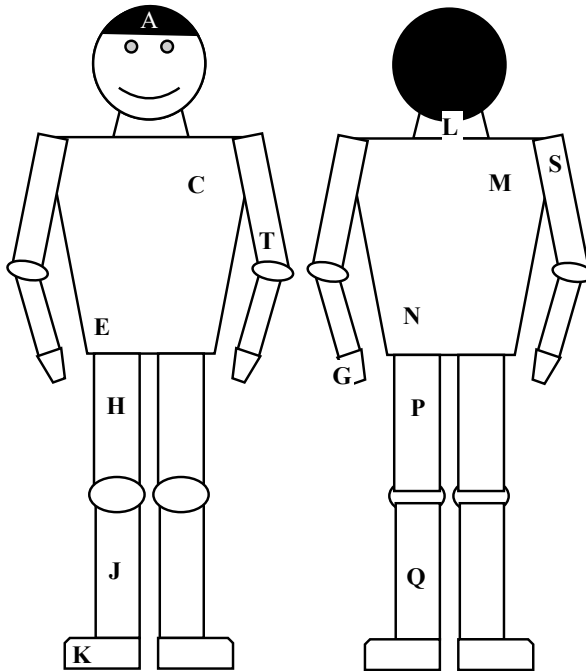


Figure A.9.: Body landmarks for placement of iButtons for skin temperature measurement (modified picture based on Parsons (2014)): A:=Forehead, C:=Left upper chest, E:=Right abdomen, G:=Left hand, H:=Right anterior thigh, J:=Right shin, K:=Right instep, L:=Neck, M:=Right scapular, N:=Left paravertebral, P:=Left posterior thigh, Q:=Left calf, S:=Right upper arm, T:=Left upper elbow

Table A.18.: P-values of t-test analyzing increasing activity steps for energy expenditure and activity level

		p-value	
		Energy expenditure	Activity level
M BMR	vs M Sit 1/2	0.001	<0.001
F BMR	vs F Sit 1/2	0.020	0.007
M Sit 1/2	vs M Slow Walk 1/2	<0.001	<0.001
F Sit 1/2	vs F Slow Walk 1/2	<0.001	<0.001
M Slow Walk 1/2	vs M Pref Walk 1/2	0.005	0.004
F Slow Walk 1/2	vs F Pref Walk 1/2	0.001	0.001
M Sit 3/4	vs M Slow Walk 3/4	<0.001	<0.001
F Sit 3/4	vs F Slow Walk 3/4	<0.001	<0.001
M Slow Walk 3/4	vs M Pref Walk 3/4	0.003	0.002
F Slow Walk 3/4	vs F Pref Walk 3/4	<0.001	<0.001

A.5. Effect of local SBF on local skin temperature

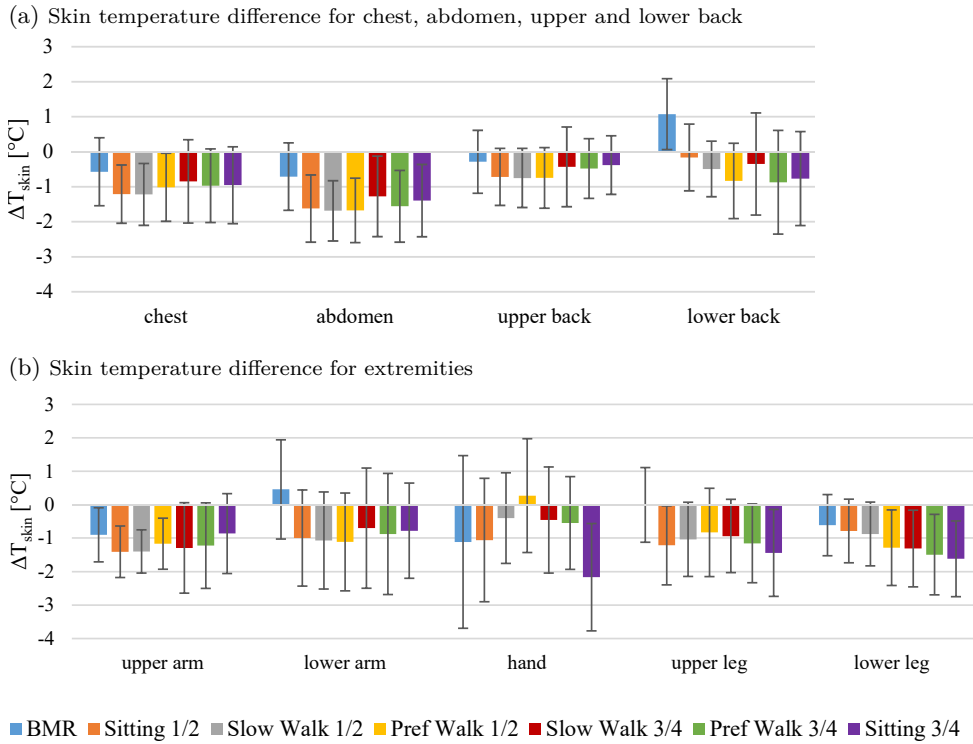


Figure A.10.: Comparison of the local skin temperature differences of all subjects (simulated - measured) using the originally simulated SBF in ThermoSEM

Table A.19.: P-values of t-test analyzing the foot skin temperature difference of the original simulation (Kingma's SBF model) and adjusted simulation (prescribed SBF) with $\alpha = 0.05$

	P-values for foot skin temperature difference					
	all		male		female	
	original	adjusted	original	adjusted	original	adjusted
BMR vs Sit 1/2	0.094	0.916	0.424	0.692	0.113	0.599
Sit 1/2 vs Slow 1/2	0.474	0.755	0.400	0.316	0.913	0.523
Slow 1/2 vs Pref 1/2	0.072	0.475	0.215	0.395	0.117	0.678
Sit 3/4 vs Slow 3/4	0.210	0.123	0.762	0.417	0.190	0.126
Slow 3/4 vs Pref 3/4	0.363	0.968	0.703	0.627	0.378	0.705
Sit 1/2 vs Sit 3/4	<0.001	<0.001	<0.001	<0.001	0.001	0.003
Slow 1/2 vs Slow 3/4	<0.001	0.007	0.006	0.013	0.006	0.025
Pref 1/2 vs Pref 3/4	0.017	0.063	0.110	0.274	0.064	0.062

Appendix A. Supplementary figures and tables

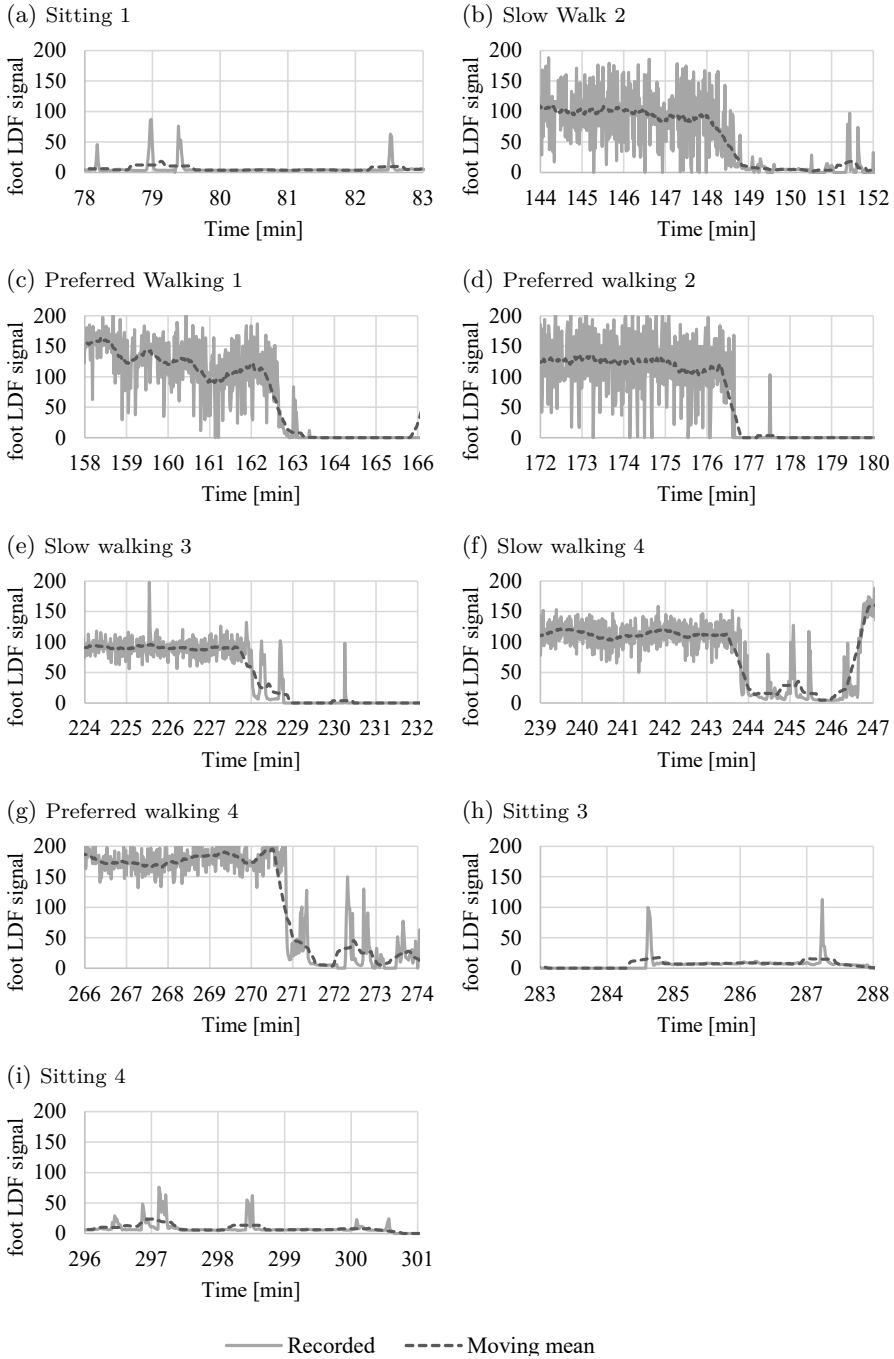


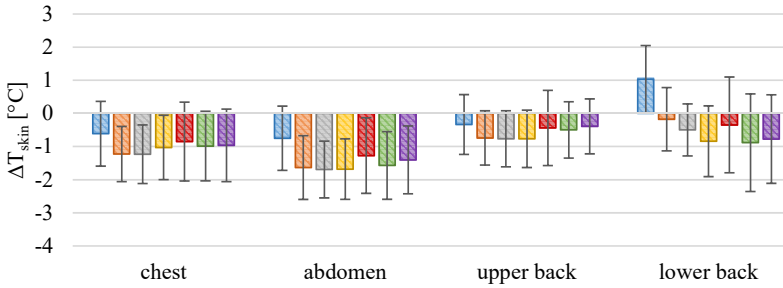
Figure A.11.: Individual recording of LDF signal at the ankle and its moving mean

A.5. Effect of local SBF on local skin temperature

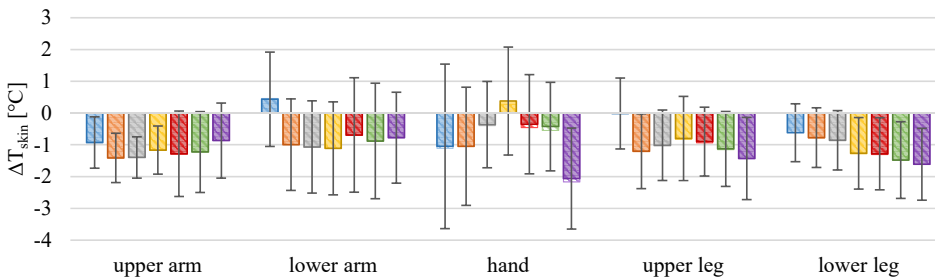
Table A.20.: P-values of t-test analyzing increasing activity steps for measured, normalized SBF

		p-value
M Sit 1/2	vs M Slow Walk 1/2	0.030
F Sit 1/2	vs F Slow Walk 1/2	<0.001
M Slow Walk 1/2	vs M Pref Walk 1/2	0.013
F Slow Walk 1/2	vs F Pref Walk 1/2	0.003
M Sit 3/4	vs M Slow Walk 3/4	0.090
F Sit 3/4	vs F Slow Walk 3/4	0.086
M Slow Walk 3/4	vs M Pref Walk 3/4	0.012
F Slow Walk 3/4	vs F Pref Walk 3/4	0.015

(a) Skin temperature difference for chest, abdomen, upper and lower back



(b) Skin temperature difference for extremities



■ BMR
 ■ Sitting 1/2
 ■ Slow Walk 1/2
 ■ Pref Walk 1/2
 ■ Slow Walk 3/4
 ■ Pref Walk 3/4
 ■ Sitting 3/4
 originally simulated SBF
 prescribed measured SBF

Figure A.12.: Comparison of the local skin temperature differences of all subjects (simulated - measured) using the originally simulated SBF (shaded area) versus the prescribed measured SBF (filled area) in ThermoSEM

Appendix A. Supplementary figures and tables

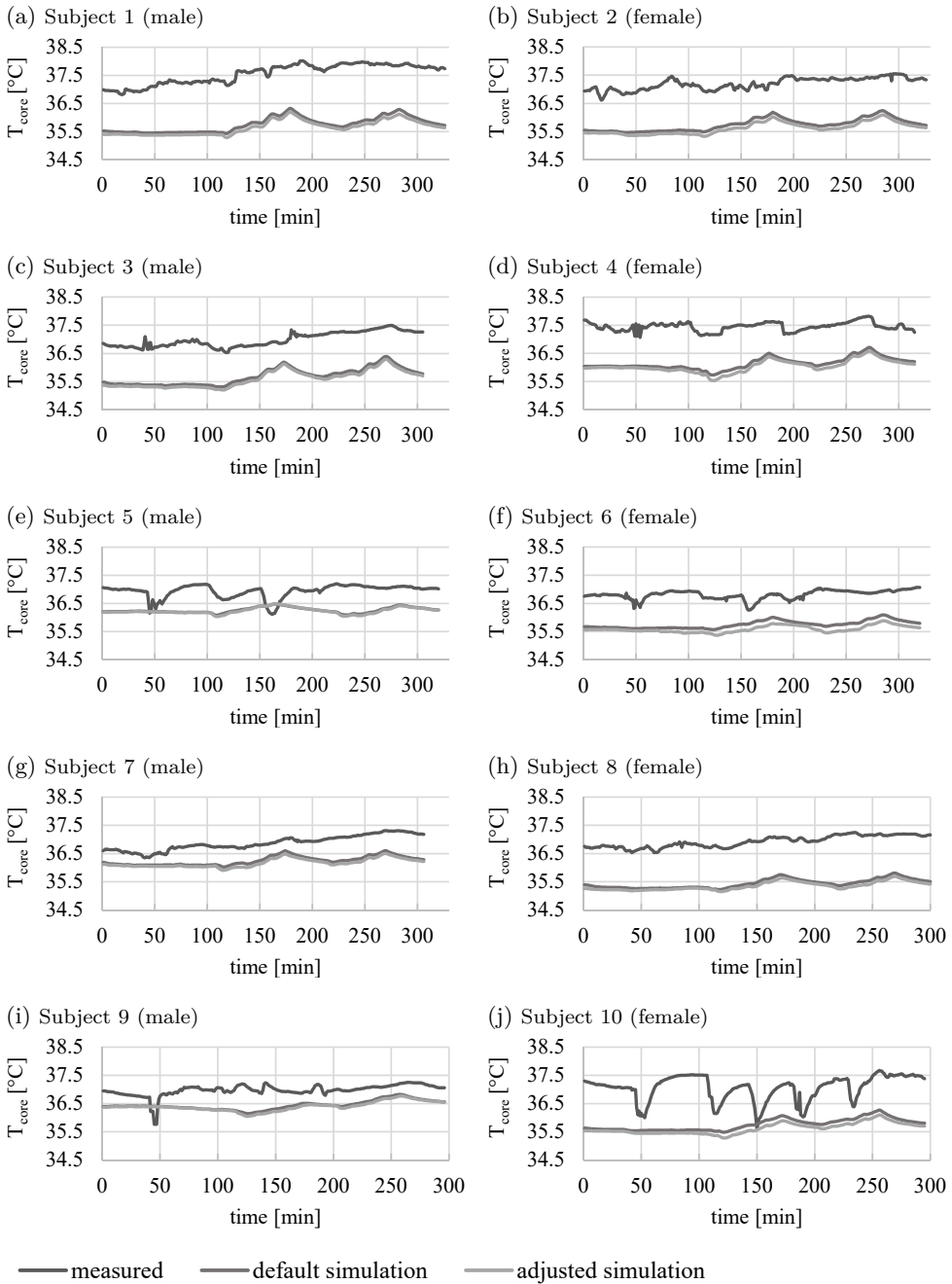


Figure A.13.: Absolute core temperature for subjects 1-10 over the course of the experiment (Start of BMR to end of sitting 4)

A.5. Effect of local SBF on local skin temperature

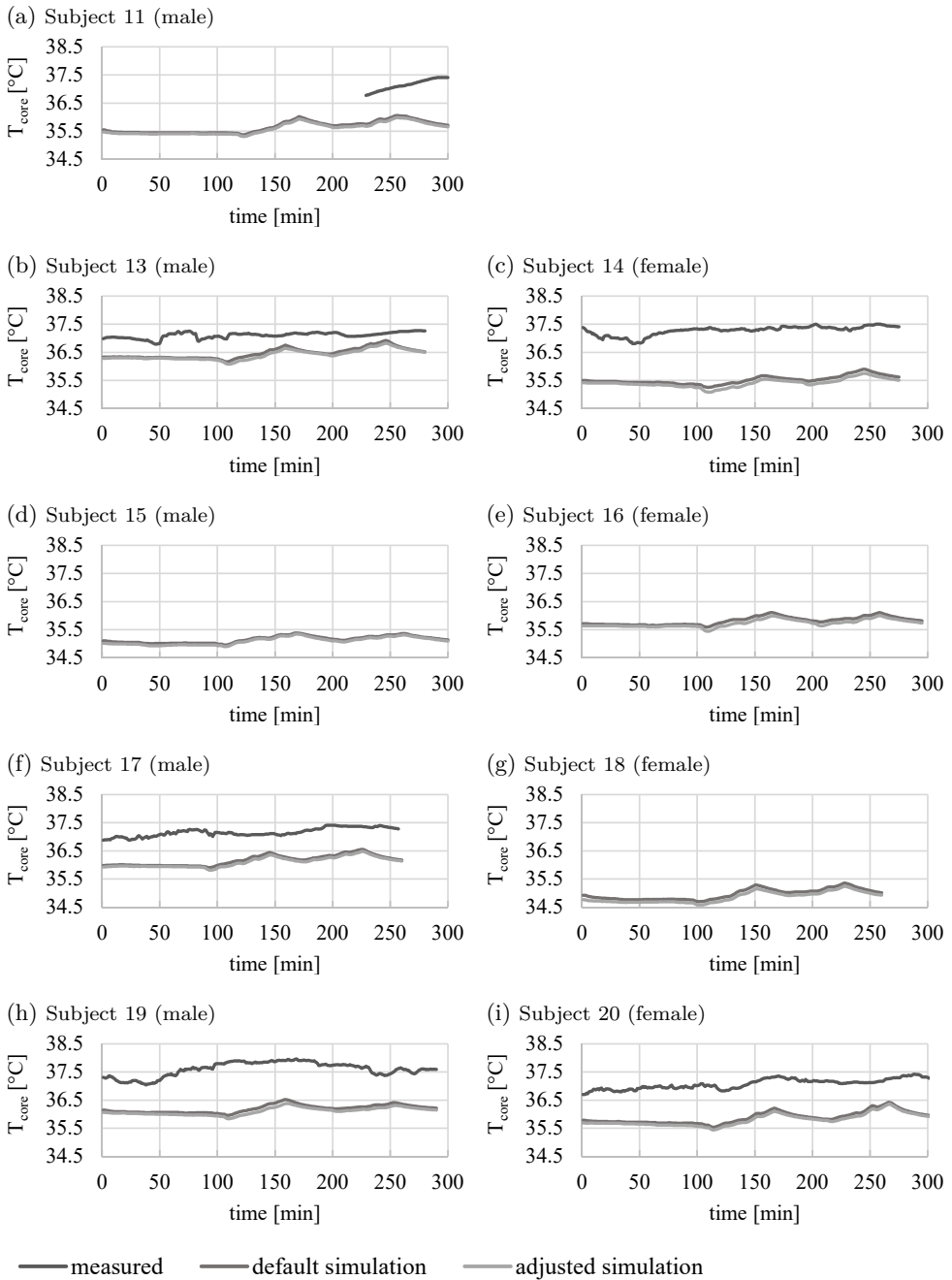


Figure A.14.: Absolute core temperature for subjects 11-20 over the course of the experiment (Start of BMR to end of sitting 4) [Subject 12 was excluded]

Table A.21.: Residual mean squared deviation of the core temperature for the original simulation and the simulation with prescribed SBF

	Residual mean squared deviation [$^{\circ}\text{C}$]	
	Original simulation	Simulation with prescribed SBF
Subject 1	1.96	2.06
Subject 2	2.19	2.26
Subject 3	1.32	1.40
Subject 4	1.32	1.42
Subject 5	0.73	0.75
Subject 6	1.17	1.31
Subject 7	1.33	1.37
Subject 8	1.56	1.64
Subject 9	0.60	0.64
Subject 10	1.52	1.63
Subject 11	NaN	NaN
Subject 13	0.66	0.72
Subject 14	1.76	1.87
Subject 15	NaN	NaN
Subject 16	NaN	NaN
Subject 17	1.01	1.07
Subject 18	NaN	NaN
Subject 19	1.43	1.52
Subject 20	1.20	1.28

A.6. Case study - revisited

Table A.22.: Average difference and standard deviation between simulated and measured mean and local skin temperature [°C] with newly measured clothing properties (last 45 min)

	Mean	Proximal	Upper arm	Lower arm	Hand	Upper leg	Lower leg	Foot
<i>Sitting in office, clothing combination 1</i>								
M1	0.01±0.15	0.46±0.32	2.03±0.18	-0.13±0.19	2.27±0.72	-2.11±0.21	0.19±0.27	-2.30±0.44
M2	0.11±0.06	1.37±0.18	0.00±0.07	2.99±0.22	1.18±0.41	-1.83±0.37	0.01±0.45	-2.75±0.61
M3	1.16±0.09	1.09±0.35	4.65±0.38	2.34±0.15	1.81±0.70	-0.11±0.25	1.62±0.33	-0.76±0.59
F1	-0.67±0.03	-1.75±0.22	-2.23±0.29	1.62±0.07	3.06±0.51	-2.55±0.20	0.88±0.24	1.43±0.37
F2	-1.62±0.19	-2.18±0.33	-2.41±0.22	1.50±0.31	0.42±1.64	-2.47±0.66	1.04±0.19	-6.53±0.58
avg	-0.20±0.92	-0.20±1.47	0.41±2.67	1.66±1.04	1.75±0.90	-1.81±0.89	0.75±0.58	-2.18±2.62
<i>Sitting in office, clothing combination 2</i>								
M1	-0.83±0.11	-0.93±0.30	-1.80±0.10	-0.50±0.26	1.77±0.36	-2.20±0.13	0.14±0.21	-2.10±0.21
M2	0.04±0.09	-0.59±0.24	-1.13±0.11	1.42±0.13	1.00±0.81	0.49±0.89	1.03±0.26	0.34±0.13
M3	1.16±0.14	0.39±0.23	1.58±0.07	2.97±0.08	2.09±0.24	0.66±0.45	1.22±0.61	2.17±0.48
F1	-1.38±0.10	-2.14±0.14	-2.56±0.06	2.39±0.17	2.34±0.50	-4.17±0.41	0.34±0.23	-2.6±0.58
F2	-1.34±0.04	-2.06±0.20	-2.25±0.05	0.92±0.08	-0.15±0.27	-1.82±0.27	1.35±0.20	-4.14±0.5
avg	-0.47±0.96	-1.07±0.95	-1.23±1.49	1.44±1.21	1.41±0.9	-1.41±1.81	0.82±0.49	-1.26±2.24
<i>Walking indoors, clothing combination 1</i>								
M1	-1.44±0.32	0.35±0.35	-1.37±0.28	0.40±0.63	0.53±1.23	-0.68±0.38	-2.94±0.34	-5.81±1.04
M2	-1.27±0.14	0.23±0.48	-1.17±0.16	0.12±0.49	1.12±1.47	-2.11±0.26	-2.46±0.73	-2.31±2.40
M3	-0.68±0.20	-0.52±0.31	-0.76±0.16	1.52±0.61	0.05±0.83	-1.60±0.23	2.58±0.36	-5.19±1.31
F1	-1.37±0.19	-1.07±0.28	-0.29±0.23	1.80±0.56	1.77±1.01	-1.03±0.25	-0.96±0.32	-7.02±2.24
F2	-2.16±0.14	-1.47±0.32	-1.88±0.17	1.55±0.46	2.77±0.54	-2.96±0.50	-0.37±0.37	-9.95±1.39
avg	-1.39±0.47	-0.5±0.71	-1.09±0.54	1.08±0.68	1.25±0.95	-1.68±0.80	-0.83±1.95	-6.06±2.49
<i>Walking indoors, clothing combination 2</i>								
M1	-2.57±0.17	-1.41±0.36	-0.91±0.16	0.11±0.29	-2.87±0.46	-2.06±0.43	-3.63±0.29	-6.99±1.01
M2	-3.18±0.12	-1.89±0.31	-2.66±0.27	-1.33±0.35	-5.14±0.23	-0.92±0.31	-3.02±0.21	-7.02±1.53
M3	-2.34±0.22	-1.69±0.16	-1.59±0.15	0.38±0.17	-0.68±0.45	-2.61±0.31	-2.36±0.75	-4.77±0.95
F1	-2.02±0.27	-2.34±0.29	-3.43±0.18	2.33±0.37	1.06±0.97	-2.40±0.40	-1.14±0.72	-5.31±3.12
F2	-2.93±0.18	-2.71±0.48	-4.54±0.11	1.50±0.57	-0.28±1.22	-3.41±0.50	0.28±0.57	-8.21±2.12
avg	-2.61±0.41	-2.01±0.46	-2.63±1.29	0.60±1.25	-1.58±2.18	-2.28±0.81	-1.97±1.40	-6.46±1.25

Table A.23.: Average difference and standard deviation between simulated and measured mean and local skin temperature [°C] for implemented *individual geometry* (last 45 min)

	Mean	Proximal	Upper arm	Lower arm	Hand	Upper leg	Lower leg	Foot
<i>Sitting in office, clothing combination 1</i>								
M1	0.27±0.15	0.58±0.32	2.10±0.18	-0.19±0.19	2.46±0.71	-1.47±0.21	0.20±0.27	-0.82±0.45
M2	0.15±0.07	1.28±0.18	-0.10±0.07	2.72±0.21	1.31±0.43	-1.53±0.37	-0.30±0.48	-1.56±0.61
M3	1.54±0.09	1.32±0.34	4.81±0.37	2.38±0.16	2.15±0.63	0.66±0.25	1.78±0.33	0.84±0.55
F1	-0.82±0.03	-1.84±0.22	-2.42±0.29	1.18±0.07	2.93±0.54	-2.40±0.20	0.29±0.24	1.43±0.39
F2	-1.89±0.2	-2.28±0.33	-2.63±0.22	0.99±0.31	-0.19±1.70	-2.45±0.65	0.22±0.20	-6.57±0.54
avg	-0.15±1.15	-0.19±1.56	0.35±2.82	1.41±1.04	1.73±1.10	-1.44±1.13	0.44±0.70	-1.34±2.83
<i>Sitting in office, clothing combination 2</i>								
M1	0.13±0.11	-0.06±0.29	-0.72±0.09	1.07±0.25	3.03±0.33	-1.43±0.12	0.46±0.21	0.51±0.15
M2	0.96±0.09	0.21±0.24	-0.10±0.09	2.90±0.15	2.38±0.73	1.17±0.88	1.22±0.28	3.09±0.15
M3	1.73±0.14	0.99±0.24	2.24±0.07	3.91±0.07	2.72±0.23	1.12±0.45	1.45±0.62	3.44±0.42
F1	-0.48±0.10	-1.24±0.15	-1.42±0.06	3.81±0.19	3.9±0.39	-3.43±0.43	0.24±0.25	-0.72±0.53
F2	-0.60±0.04	-1.28±0.19	-1.25±0.06	2.19±0.09	1.17±0.25	-1.23±0.27	1.19±0.22	-2.74±0.47
avg	0.35±0.89	-0.27±0.87	-0.25±1.33	2.78±1.06	2.64±0.89	-0.76±1.73	0.91±0.47	0.72±2.33
<i>Walking indoors, clothing combination 1</i>								
M1	-1.34±0.35	0.40±0.40	-1.30±0.28	0.09±0.62	0.18±1.19	0.07±0.49	-2.81±0.32	-4.43±0.76
M2	-2.24±0.17	-0.46±0.65	-1.80±0.20	-0.88±0.46	0.24±1.40	-2.90±0.24	-3.89±0.66	-1.66±2.10
M3	-0.44±0.23	-0.31±0.33	-0.57±0.16	1.39±0.59	-0.14±0.80	-0.74±0.25	2.98±0.35	-4.61±1.03
F1	-2.86±0.23	-2.94±0.46	-0.86±0.31	0.73±0.54	0.81±0.98	-1.78±0.41	-2.66±0.26	-8.77±2.15
F2	-3.02±0.22	-2.11±0.49	-2.35±0.22	0.55±0.44	1.83±0.50	-3.42±0.63	-1.91±0.37	-9.74±1.15
avg	-1.98±0.97	-1.08±1.24	-1.38±0.64	0.38±0.75	0.58±0.70	-1.75±1.30	-1.66±2.40	-5.84±2.99
<i>Walking indoors, clothing combination 2</i>								
M1	-1.84±0.19	0.49±0.25	0.58±0.16	1.54±0.37	-0.35±0.60	-2.66±0.50	-5.35±0.22	-7.44±0.85
M2	-3.37±0.18	-0.27±0.28	-1.65±0.38	-0.52±0.54	-4.60±0.27	-2.72±0.48	-6.03±0.15	-8.48±1.32
M3	-1.81±0.12	0.15±0.17	-0.37±0.22	1.38±0.25	1.43±0.61	-3.49±0.21	-4.19±0.55	-6.10±0.82
F1	-2.77±0.23	-0.92±0.20	-2.56±0.20	2.80±0.38	-1.95±1.02	-4.06±0.36	-4.52±0.72	-7.15±3.09
F2	-3.79±0.24	-1.79±0.41	-4.10±0.10	1.62±0.71	0.38±1.54	-6.04±0.57	-3.99±0.59	-10.32±1.89
avg	-2.71±0.80	-0.47±0.81	-1.62±1.64	1.36±1.07	-1.02±2.10	-3.79±1.24	-4.82±0.76	-7.90±1.43

Table A.24.: Average difference and standard deviation between simulated and measured mean and local skin temperature [°C] for implemented *new foot skin blood flow model* (last 45 min)

	Mean	Proximal	Upper arm	Lower arm	Hand	Upper leg	Lower leg	Foot
<i>Sitting in office, clothing combination 1</i>								
M1	0.94±0.14	0.92±0.32	2.42±0.19	0.14±0.20	2.9±±0.67	-0.98±0.21	0.71±0.28	3.23±0.25
M2	0.97±0.05	1.76±0.18	0.32±0.06	3.20±0.20	1.88±0.26	-0.82±0.38	0.46±0.47	2.61±0.26
M3	2.12±0.09	1.52±0.33	5.01±0.36	2.59±0.17	2.65±0.50	1.01±0.25	2.13±0.32	5.14±0.16
F1	0.01±0.03	-1.42±0.21	-1.95±0.28	1.78±0.08	3.5±±0.48	-1.70±0.02	1.19±0.25	5.71±0.20
F2	-0.73±0.19	-1.87±0.33	-2.15±0.22	1.64±0.32	1.34±1.69	-1.43±0.70	1.36±0.19	-0.24±0.37
avg	0.66±0.97	0.18±1.52	0.73±2.72	1.87±1.03	2.45±0.76	-0.78±0.95	1.17±0.58	3.29±2.11
<i>Sitting in office, clothing combination 2</i>								
M1	0.40±0.12	0.09±0.29	-0.60±0.09	1.20±0.25	3.21±0.33	-1.24±0.12	0.69±0.21	2.21±0.14
M2	1.25±0.09	0.39±0.24	0.04±0.09	3.06±0.16	2.44±0.73	1.43±0.89	1.56±0.28	4.80±0.24
M3	1.86±0.13	1.09±0.24	2.31±0.07	3.99±0.07	2.83±0.22	1.23±0.45	1.56±0.62	4.00±0.34
F1	0.06±0.09	-1.09±0.15	-1.25±0.08	4.08±0.20	4.21±0.37	-2.98±0.43	0.96±0.25	3.02±0.35
F2	-0.11±0.05	-1.16±0.19	-1.12±0.07	2.40±0.10	1.41±0.26	-0.85±0.28	1.82±0.22	0.94±0.30
avg	0.69±0.75	-0.14±0.87	-0.13±1.30	2.95±1.07	2.82±0.92	-0.48±1.64	1.32±0.43	3.00±1.35
<i>Walking indoors, clothing combination 1</i>								
M1	-0.28±0.36	0.78±0.34	-0.97±0.29	0.42±0.63	0.60±1.27	0.77±0.50	-2.12±0.31	2.46±0.69
M2	-0.11±0.15	0.66±0.48	-0.77±0.18	0.14±0.49	1.19±1.51	-0.65±0.25	-1.64±0.68	5.96±2.03
M3	0.37±0.25	-0.12±0.31	-0.42±0.15	1.53±0.61	0.63±0.88	-0.39±0.26	3.30±0.35	2.02±0.94
F1	-0.35±0.21	-0.67±0.26	0.09±0.24	1.80±0.55	1.64±0.99	0.30±0.39	-0.31±0.31	0.43±1.96
F2	-0.97±0.18	-0.96±0.32	-1.38±0.18	1.63±0.46	2.73±0.52	-1.40±0.64	0.43±0.38	-2.10±1.14
avg	-0.27±0.43	-0.06±0.70	-0.69±0.50	1.11±0.68	1.36±0.79	-0.27±0.76	-0.07±1.91	1.70±2.64
<i>Walking indoors, clothing combination 2</i>								
M1	-1.00±0.20	0.56±0.24	0.66±0.16	1.65±0.37	1.10±0.68	-2.26±0.49	-4.89±0.23	-1.19±0.77
M2	-1.78±0.20	0.03±0.24	-1.24±0.37	-0.01±0.54	-1.56±0.48	-1.39±0.44	-4.49±0.16	-1.58±1.17
M3	-0.74±0.14	0.16±0.16	-0.32±0.22	1.45±0.25	2.57±0.64	-3.22±0.21	-1.51±0.73	0.38±0.85
F1	-1.02±0.22	-0.76±0.19	-2.31±0.17	3.30±0.42	3.74±1.20	-3.22±0.35	-2.81±0.66	-0.50±2.87
F2	-1.37±0.27	-1.48±0.39	-3.62±0.11	2.34±0.76	1.89±1.41	-2.36±0.72	0.87±0.58	-0.58±1.57
avg	-1.18±0.36	-0.30±0.73	-1.37±1.49	1.75±1.09	1.55±1.78	-2.49±0.69	-2.56±2.10	-0.69±0.67

Table A.25.: Average difference and standard deviation between simulated and measured mean and local skin temperature [°C] for the combination of newly measured clothing properties, implemented individual geometry and implemented new foot skin flow model (last 45 min)

	Mean	Proximal	Upper arm	Lower arm	Hand	Upper leg	Lower leg	Foot
<i>Sitting in office, clothing combination 1</i>								
M1	0.12±0.14	0.20±0.32	1.82±0.19	-0.33±0.19	2.12±0.72	-2.31±0.21	-0.05±0.27	1.98±0.24
M2	0.04±0.06	0.90±0.18	-0.36±0.07	2.59±0.21	1.00±0.44	-2.34±0.36	-0.54±0.48	1.65±0.22
M3	1.40±0.09	0.93±0.34	4.52±0.37	2.23±0.16	1.79±0.67	-0.18±0.26	1.51±0.32	3.93±0.17
F1	-0.89±0.03	-2.16±0.22	-2.65±0.29	1.06±0.07	2.67±0.54	-3.09±0.19	0.10±0.25	4.52±0.18
F2	-1.85±0.19	-2.67±0.33	-2.89±0.22	0.87±0.31	-0.48±1.67	-3.24±0.63	0.01±0.21	-1.46±0.34
avg	-0.23±1.08	-0.56±1.54	0.09±2.80	1.28±1.04	1.42±1.10	-2.23±1.09	0.20±0.69	2.12±2.10
<i>Sitting in office, clothing combination 2</i>								
M1	-0.83±0.13	-1.21±0.30	-2.04±0.10	-0.74±0.26	1.54±0.35	-2.45±0.13	-0.15±0.21	1.11±0.14
M2	-0.04±0.09	-0.99±0.24	-1.45±0.10	1.06±0.14	0.84±0.83	0.06±0.87	0.53±0.29	3.93±0.28
M3	1.14±0.14	0.26±0.23	1.47±0.07	2.87±0.08	1.96±0.24	0.54±0.45	1.10±0.62	3.41±0.35
F1	-1.58±0.09	-2.57±0.15	-2.99±0.05	1.81±0.16	1.69±0.59	-4.85±0.39	-0.61±0.25	1.71±0.28
F2	-1.44±0.04	-2.4±0.20	-2.58±0.05	0.45±0.08	-0.57±0.32	-2.32±0.25	0.58±0.21	-0.15±0.24
avg	-0.55±1.00	-1.38±1.03	-1.52±1.58	1.09±1.22	1.09±0.91	-1.80±1.94	0.29±0.60	2.00±1.50
<i>Walking indoors, clothing combination 1</i>								
M1	-1.14±0.35	0.15±0.38	-1.50±0.29	0.23±0.63	0.45±1.23	-0.84±0.40	-3.22±0.32	0.33±0.84
M2	-1.89±0.15	-0.69±0.62	-1.96±0.19	-0.70±0.48	0.53±1.45	-3.62±0.25	-4.19±0.68	4.04±2.20
M3	-0.15±0.24	-0.49±0.32	-0.70±0.15	1.54±0.62	0.19±0.85	-1.39±0.22	2.70±0.35	1.04±1.07
F1	-2.07±0.22	-2.06±0.40	-1.01±0.28	0.88±0.55	1.00±1.01	-2.29±0.29	-3.01±0.27	-1.53±2.10
F2	-2.63±0.20	-2.28±0.47	-2.44±0.21	0.74±0.46	2.14±0.54	-3.96±0.55	-2.20±0.35	-4.11±1.28
avg	-1.57±0.86	-1.07±0.94	-1.52±0.63	0.54±0.75	0.86±0.69	-2.42±1.22	-1.98±2.43	-0.22±2.66
<i>Walking indoors, clothing combination 2</i>								
M1	-1.14±0.35	0.15±0.38	-1.50±0.29	0.23±0.63	0.45±1.23	-0.84±0.40	-3.22±0.32	0.33±0.84
M2	-1.89±0.15	-0.69±0.62	-1.96±0.19	-0.70±0.48	0.53±1.45	-3.62±0.25	-4.19±0.68	4.04±2.20
M3	-0.15±0.24	-0.49±0.32	-0.70±0.15	1.54±0.62	0.19±0.85	-1.39±0.22	2.70±0.35	1.04±1.07
F1	-2.07±0.22	-2.06±0.40	-1.01±0.28	0.88±0.55	1.00±1.01	-2.29±0.29	-3.01±0.27	-1.53±2.10
F2	-2.63±0.20	-2.28±0.47	-2.44±0.21	0.74±0.46	2.14±0.54	-3.96±0.55	-2.20±0.35	-4.11±1.28
avg	-1.57±0.86	-1.07±0.94	-1.52±0.63	0.54±0.75	0.86±0.69	-2.42±1.22	-1.98±2.43	-0.22±2.66

APPENDIX B

The thermo-physiological model ThermoSEM

The ThermoSEM model is a thermo-physiological model, which is based on the thermoregulation model by Fiala (1999, 2001). It was first implemented as ThermoSEM by Severens (2008) for a medical based application in the field of patient's temperature management after cardiac surgeries. Kingma (2012) later introduced the neurophysiological approach for modeling skin blood flow (SBF).

Passive system

In ThermoSEM, the human body is modeled using 18 concentric cylinders and one concentric semi-sphere for the head. All elements are divided into section namely anterior, posterior and inferior sectors, and they consist of several tissue layers with specific attributes as shown in Figure B.1 and described in Tables B.2 and B.3. In this default configuration, these specifications represent an average adult man with a

Appendix B. The thermo-physiological model ThermoSEM

weight of 73.5 kg, a height of 1.73 m, a body surface area of 1.86 m² and a body fat percentage of 14 %. The resulting basal metabolic heat production is 87.1 W.

For modeling the *heat exchange within the body*, nodes are spread along the tissue layers (see Figure B.1). Between the resulting volumetric elements the heat transfer is then calculated using Pennes' bioheat equation (Pennes, 1948):

$$\rho c \frac{\delta T}{\delta t} = k \nabla^2 T + \rho_b c_b \omega_b (T_a - T) + q_m \quad (\text{B.1})$$

where ρ is the density of the tissue, c is the heat capacity of the tissue, $\frac{\delta T}{\delta t}$ is the change in temperature, k is the tissue heat conductivity, T is the tissue temperature, ρ_b is the density of the blood, c_b is the specific heat of the blood, ω_b is the blood perfusion rate, T_a is the arterial blood temperature, and q_m is the metabolic heat production of the tissue. The values of each tissue layer are given in Tables B.2 and B.3. The three terms on the right hand side of the equation represent conduction ($k \nabla^2 T$), convection ($\rho_b c_b \omega_b (T_a - T)$) and heat production within the body (q_m). The heat exchange between the venous and arterial blood occurs in a central blood pool according to Fiala et al. (1999). For large arteries and veins, is also corrected for counter current heat exchange (Kingma, 2012). The factors for the counter current heat exchange are given in Tables B.2 and B.3.

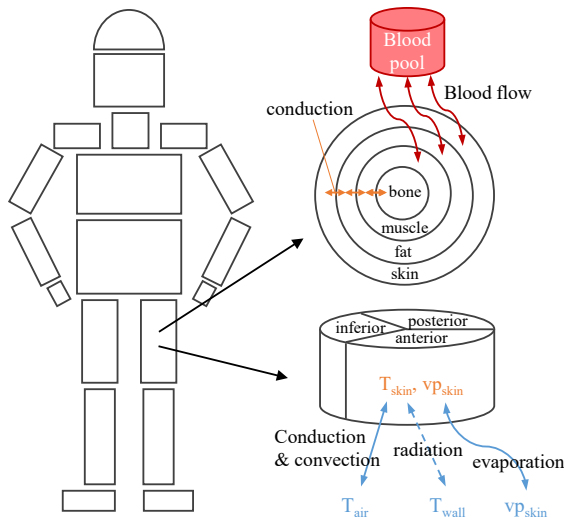


Figure B.1.: Representation of the human body by ThermoSEM based on Kingma (2012)

The *heat exchange between the body and environment* can be divided into the heat exchange between the skin's surface and the environment through convection, conduction and radiation, and the heat exchange through respiration. The detailed description of each heat exchange pathway can be found in Fiala et al. (1999) and Kingma (2012). The details on heat transfer through clothing can also be found in this thesis in section 3.2 on page 24.

Active system

The human thermoregulatory system is represented in the so-called active model of ThermoSEM. This part of the model includes the heat production due to metabolic heat production and shivering, heat transport within the body via a blood flow model, heat loss due to sweating. The calculations are mostly based on Fiala et al. (1999). The detailed descriptions can also be found in Kingma (2012).

The biggest difference between Fiala's model and the current version of ThermoSEM is the implementation of a neurophysiological approach to calculate the SBF (Kingma et al., 2014b). The skin perfusion in Fiala's model is a function of the central stimuli for vasodilation and vasoconstriction which in turn are functions of the difference between the actual and set point mean skin temperature (Fiala, 1998; Fiala et al., 1999). The model by Kingma et al. (2014b) formulates SBF regulation as:

$$\beta_i = \beta_{i,bas} \cdot N \cdot Q_{10} \quad (\text{B.2})$$

where $\beta_{i,bas}$ is the basal heat equivalent of SBF of a specific body part i , Q_{10} is the local regulation effect of SBF (Q10-effect) with $Q_{10} = 2^{\frac{(T_i - T_{i,bas})}{10}}$, $T_{i,bas}$ the local tissue temperature under basal conditions and N is the neural regulation signal for SBF. The function for N is:

$$N = \max[0, \gamma_1 - \gamma_2 (H_{warm} - P_{cold}) - \gamma_3 (H_{warm} - P_{warm})] \quad (\text{B.3})$$

where γ_1 is a model constant representing all non-thermal effects on SBF, γ_2 and γ_3 are model parameters for the cold and warm afferent pathway, respectively, H_{warm} is the neuron fire rate of temperature sensitive neurons in the hypothalamus, P_{cold} and P_{warm} are the neural peripheral cold and warm drive, respectively. The values of the

Appendix B. The thermo-physiological model ThermoSEM

models constant γ_1 and parameters γ_2 and γ_3 are given in Table B.1. The function for the neural regulation signal is based on the neural concepts described in Mekjavič and Morrison (1985), Boulant (2005) as well as Nakamura and Morrison (2008a,b). H_{warm} , P_{cold} and P_{warm} are calculated as described in Kingma et al. (2014b) using the individual neuronal response characteristics as modeled by Mekjavič and Morrison (1985).

Table B.1.: Model constant γ_1 and parameters γ_2 and γ_3 of the neurophysiological SBF model (Kingma, 2012; Kingma et al., 2014b)

Element	γ_1	γ_2	γ_3
1. Head	0.7906	-0.1853	-0.0816
2. Face	0.7906	-0.1853	-0.0816
3. Neck	0.7906	-0.1853	-0.0816
4. Shoulders	0.7906	-0.1853	-0.0816
5. Thorax	0.7906	-0.1853	-0.0816
6. Abdomen	2.4250	-0.1246	0.1658
7. Arms	-0.2301	-0.0231	-0.2126
8. Hands	0.7368	-0.2190	-0.0704
9. Legs	0.7906	-0.1853	-0.0816
10. Feet	0.7368	-0.2190	-0.0704

Table B.2.: Element and respective tissue properties - Part 1

Element	Tissue	n	L 10^{-2} [m]	r 10^{-2} [m]	k [W m ⁻¹ K]	ρ [kg m ⁻³]	c [J kg ⁻¹ K]	ω_b [s ⁻¹ m ³]	q_m [W m ⁻³]	h_x [W K ⁻¹]
1. Head	Brain	3		8.6	0.75	1080	3850	10.132	13400	
	Bone	1		10.05	0.42	1500	1591	0	0	
	Fat	1	*	10.2	0.16	850	2300	0.0036	58	0.0
	Inner skin	1		10.3	0.47	1085	3680	5.48	743.21	
	Outer skin	1		10.4	0.47	1085	3680	0	0	
2. Face	Muscle	1		2.68	0.42	1085	3768	0.538	684	
	Bone	1		5.42	1.16	1500	1591	0	0	
	Muscle	1	9.84	6.8	0.42	1085	3768	0.538	684	0.0
	Fat	2		7.6	0.16	850	2300	0.0036	58	
	Inner skin	1		5.64	0.47	1085	3680	11.17	740.82	
	Outer skin	1		5.67	0.47	1085	3680	0	0	
3. Neck	Bone	1		1.9	0.75	1357	1700	0	0	
	Muscle	2		5.46	0.42	1085	3768	0.538	684	
	Fat	1	8.42	5.56	0.16	850	2300	0.0036	58	0.0
	Inner skin	1		5.64	0.47	1085	3680	6.8	507.36	
	Outer skin	1		5.67	0.47	1085	3680	0	0	
		Bone	1		3.7	0.75	1357	1700	0	0
4. Shoulders	Muscle	1		3.9	0.42	1085	3768	0.538	684	
	Fat	2	16.00	4.4	0.16	850	2300	0.0036	58	0.4
	Inner skin	1		4.5	0.47	1085	3680	1.01	744.28	
	Outer skin	1		4.6	0.47	1085	3680	0	0	
		Lung	1		7.73	0.28	550	3718	4.3	600
5. Thorax	Bone	1		8.91	0.75	1357	1700	0	0	
	Muscle	1	30.60	12.34	0.42	1085	3768	0.538	684	0.0
	Fat	2		12.68	0.16	850	2300	0.0036	58	
	Inner skin	1		12.8	0.47	1085	3680	1.58	677.3	
	Outer skin	1		12.9	0.47	1085	3680	0	0	

Table B.3.: Element and respective tissue properties - Part 2

Element	Tissue	n	L 10^{-2} [m]	r 10^{-2} [m]	k [$\text{W m}^{-1} \text{K}$]	ρ [kg m^{-3}]	c [$\text{J kg}^{-1} \text{K}$]	ω_b [$\text{s}^{-1} \text{m}^3$]	q_m [W m^{-3}]	h_x [W K^{-1}]
6. Abdomen	Guts	1		7.85	0.53	1000	3697	4.3100	4100	
	Bone	1		8.34	0.75	1357	1700	0	0	
	Muscle	1		10.90	0.42	1085	3768	0.5380	684	0.0
	Fat	2	55.20	12.44	0.16	850	2300	0.0036	58	
	Inner skin	1		12.54	0.47	1085	3680	1.4400	590.2	
	Outer skin	1		12.60	0.47	1085	3680	0	0	
7. Arms	Bone	1		1.53	0.75	1357	1700	0	0	
	Muscle	2		3.43	0.42	1085	3768	0.538	684	
	Fat	1		4.01	0.16	850	2300	0.0036	58	1.0325
	Inner skin	1	31.85	4.11	0.47	1085	3680	1.100	631	
	Outer skin	1		4.18	0.47	1085	3680	0	0	
8. Hands	Bone	1		0.70	0.75	1357	1700	0	0	
	Muscle	1		1.74	0.42	1085	3768	0.538	684	
	Fat	1	31.00	2.04	0.16	850	2300	0.0036	58	0.2850
	Inner skin	1		2.16	0.47	1085	3680	4.540	744.43	
	Outer skin	1		2.26	0.47	1085	3680	0	0	
9. Legs	Bone	1		2.20	0.75	1357	1700	0	0	
	Muscle	2		4.80	0.42	1085	3768	0.538	684	
	Fat	2	34.75	5.33	0.16	850	2300	0.0036	58	1.725
	Inner skin	1		5.43	0.47	1085	3680	1.05	742.8	
	Outer skin	1		5.53	0.47	1085	3680	0	0	
10. Feet	Bone	1		2.00	0.75	1357	1700	0	0	
	Muscle	1		2.50	0.42	1085	3768	0.538	684	
	Fat	2	24.00	3.26	0.16	850	2300	0.0036	58	1.700
	Inner skin	1		3.40	0.47	1085	3680	1.500	640.3	
	Outer skin	1		3.50	0.47	1085	3680	0	0	

Bibliography

- Ainsworth, Barbara E.; Haskell, William L.; Herrmann, Stephen D.; Meckes, Nathanael; Bassett, David R., et al. (2011). “2011 compendium of physical activities: A second update of codes and MET values”. In: *Medicine and Science in Sports and Exercise* 43, pp. 1575–1581.
- Anttonen, Hannu and Hiltunen, Esa (2009). “The Effect of Wind on Thermal Insulation of Military Clothing”. In: *RTO Human Factors and Medicine Panel Symposium*, pp. 1–12.
- Arens, Edward; Bauman, Fred; Johnston, L P, and Zhang, Hui (1991). “Testing of Localized Ventilation Systems in a New Controlled Environment Chamber”. In: *Indoor Air* 1.3, pp. 263–281.
- Aschoff, Jürgen and Wever, Rütger (1958). “Kern und Schale im Wärmehaushalt des Menschen”. In: *Die Naturwissenschaften* 45.20, pp. 477–485.
- ASHRAE (2001). *2001 ASHRAE Handbook - Fundamentals*. Atlanta.
- ASHRAE (2004). *Thermal Environmental Conditions for Human Occupancy*. Atlanta GA: American Society of Heating, Refrigeration and Air-Conditioning Engineers (ASHRAE Standard 55-2004), p. 30.
- ASTM F2370-10 (2010). *Standard Test Method for Measuring the Evaporative Resistance of Clothing Using a Sweating Manikin*. ASTM International, West Conshohocken, US.
- Azer, N. Z. and Hsu, S. (1977). “The prediction of thermal sensation from a simple thermoregulatory model”. In: *ASHRAE Transactions* 83, Part 1, pp. 88–102.
- Babic, Mitja; Lenarcic, Jadran; Zlajpah, Leon; Taylor, Nigel A.S., and Mekjavič, Igor (2008). “A Device for Simulating the Thermoregulatory Responses of the Foot:

Bibliography

- Estimation of Footwear Insulation and Evaporative Resistance”. In: *Journal of Mechanical Engineering* 54.9, pp. 628–638.
- Baker, Paul T and Daniels, Farrington (1956). “Relationship Between Skinfold Thickness and Body Cooling for Two Hours at 15°C”. In: *Journal of Applied Physiology* 8.4, pp. 409–416.
- Bartelink, M L; Wollersheim, H; Theeuwes, A; Duren, D van, and Thien, T (1990). “Changes in skin blood flow during the menstrual cycle: the influence of the menstrual cycle on the peripheral circulation in healthy female volunteers.” In: *Clinical science (London, England : 1979)* 78.5, pp. 527–532.
- Bergersen, T K (1993). “A search for arteriovenous anastomoses in human skin using ultrasound Doppler”. In: *Acta Physiologica Scandinavica* 147.2, pp. 195–201.
- Bogerd, Cornelis P.; Brühwiler, Paul A., and Rossi, René M. (2012). “Heat loss and moisture retention variations of boot membranes and sock fabrics: A foot manikin study”. In: *International Journal of Industrial Ergonomics* 42.2, pp. 212–218.
- Bongers, Coen C.W.G.; Daanen, Hein A.M.; Bogerd, Cornelis P.; Hopman, Maria T.E., and Eijvogels, Thijs M.H. (2018). “Validity, Reliability, and Inertia of Four Different Temperature Capsule Systems”. In: *Medicine and Science in Sports and Exercise* 50.1, pp. 169–175.
- Bongers, Coen C.W.G.; Thijssen, Dick H.J.; Veltmeijer, Matthijs T.W.; Hopman, Maria T.E., and Eijvogels, Thijs M.H. (2015). “Precooling and percooling (cooling during exercise) both improve performance in the heat: A meta-analytical review”. In: *British Journal of Sports Medicine* 49.6, pp. 377–384.
- Boulant, J. A. (2005). “Neuronal basis of Hammel’s model for set-point thermoregulation”. In: *Journal of Applied Physiology* 100.4, pp. 1347–1354.
- Brengelmann, George L. and Savage, Margaret V. (1997). “Temperature regulation in the neutral zone”. In: *Annals of the New York Academy of Sciences* 813.1, pp. 39–50.
- Cavalcanti, Silvio and Di Marco, Luigi Yuri (1999). “Numerical Simulation of the Hemodynamic Response to Hemodialysis-Induced Hypovolemia”. In: *Artificial organs* 23.12, pp. 1063–1073.
- Cheng, Yuanda; Niu, Jianlei, and Gao, Naiping (2012). “Thermal comfort models: A review and numerical investigation”. In: *Building and Environment* 47.1, pp. 13–22.
- Curlee, John S. (2004). “An approach for determining localized thermal clothing insulation for use in an element based thermoregulation and human comfort code”. Master thesis. Master thesis, Michigan Technological University.

- Dalewski, Mariusz; Melikov, Arsen K., and Veselý, Michal (2014). “Performance of ductless personalized ventilation in conjunction with displacement ventilation: Physical environment and human response”. In: *Building and Environment* 81, pp. 354–364.
- de Dear, Richard J.; Akimoto, Takashi; Arens, Edward; Brager, Gail Schiller; Candido, Christhina, et al. (2013). “Progress in thermal comfort research over the last twenty years”. In: *Indoor Air* 23.6, pp. 442–461.
- de Dear, Richard J. and Brager, Gail Schiller (1998). “Developing an adaptive model of thermal comfort and preference”. In: *ASHRAE Transactions*. Vol. 104. Pt 1A, pp. 145–167.
- Dear, Richard J. de; Ring, J. W., and Fanger, P. Ole (1993). “Thermal Sensations Resulting From Sudden Ambient Temperature Changes”. In: *Indoor Air* 3.3, pp. 181–192.
- Deurenberg, Paul; Yap, Mabel, and Van Staveren, WA (1998). “Body mass index and percent body fat”. In: *International Journal Obesity* 22, pp. 1164–1171.
- Dröog, Rens P J; Kingma, Boris R. M.; van Marken Lichtenbelt, Wouter D.; Kooman, Jeroen P; Sande, Frank M van der, et al. (2012). “Mathematical modeling of thermal and circulatory effects during hemodialysis.” In: *Artificial organs* 36.9, pp. 797–811.
- Du Bois, D. and Du Bois, E. F. (1916). “A formula to estimate the approximate surface area if height and weight be known”. In: *Archives of Internal Medicine* XVII.6_2, pp. 863–871.
- Eijssvogels, Thijs M.H.; Bongers, Coen C.W.G.; Veltmeijer, Matthijs T.W.; Moen, M. H., and Hopman, Maria T.E. (2014). “Cooling during exercise in temperate conditions: impact on performance and thermoregulation”. In: *International Journal of Sports Medicine* 35.10, pp. 840–846.
- Fabbri, Kristian (2015). “Ergonomics of the Thermal Environment. Human Body and Clothes”. In: *Indoor Thermal Comfort Perception*. Springer International Publishing. Chap. 3, pp. 25–74.
- Fanger, P. Ole (1970). “Thermal comfort”. PhD Thesis. Copenhagen: Danish Technical University.
- Fiala, Dusan (1998). “Dynamic Simulation of Human Heat Transfer and Thermal Comfort”. PhD-Thesis. Dissertation, Leicester: De Montfort University.
- Fiala, Dusan; Havenith, George; Bröde, Peter; Kampmann, Bernhard, and Jendritzky, Gerd (2012). “UTCI-Fiala multi-node model of human heat transfer and temperature regulation”. In: *International Journal of Biometeorology* 56.3, pp. 429–441.

Bibliography

- Fiala, Dusan; Lomas, Kevin J., and Stohrer, Martin (1999). "A computer model of human thermoregulation for a wide range of environmental conditions: the passive system." In: *Journal of applied physiology (Bethesda, Md. : 1985)* 87, pp. 1957–1972.
- Fiala, Dusan; Lomas, Kevin J., and Stohrer, Martin (2001). "Computer prediction of human thermoregulatory and temperature responses to a wide range of environmental conditions". In: *International Journal of Biometeorology* 45, pp. 143–159.
- Fiala, Dusan; Lomas, Kevin J., and Stohrer, Martin (2003). "First principles modeling of thermal sensation responses in steady-state and transient conditions". In: *ASHRAE Transactions* 109.1, pp. 179–186.
- Foda, Ehab and Sirén, Kai (2011). "A new approach using the Pierce two-node model for different body parts". In: *International Journal of Biometeorology* 55.4, pp. 519–532.
- Foda, Ehab and Sirén, Kai (2012). "Design strategy for maximizing the energy-efficiency of a localized floor-heating system using a thermal manikin with human thermoregulatory control". In: *Energy and Buildings* 51, pp. 111–121.
- Fojtlín, Miloš; Psikuta, Agnes; Fišer, Jan; Toma, Róbert; Annaheim, Simon, et al. (2019). "Local clothing properties for thermo-physiological modelling: Comparison of methods and body positions". In: *Building and Environment* 155.3, pp. 376–388.
- Frackiewicz-Kaczmarek, Joanna; Psikuta, Agnes; Bueno, Marie-Ange, and Rossi, René M. (2015). "Effect of garment properties on air gap thickness and the contact area distribution". In: *Textile Research Journal* 85.18, pp. 1907–1918.
- Frijns, Arjan J.H.; Veselá, Stephanie, and Kingma, Boris R.M. (2016). "Individualized thermal sensation models: missing links and solutions". In: *Proceedings of the 14th international conference of Indoor Air Quality and Climate*. Ed. by Laverge, J.; Salthammer, T., and Stranger, M. Ghent, Belgium.
- Fu, G. (1995). "A transient 3D mathematical thermal model for the clothed human". PhD Thesis. Kansas State University, Manhattan, Kansas.
- Fu, G. and Jones, B. W. (1996). "Combined finite element human thermal model and finite difference clothing model". In: *Environmental Ergonomics*. Ed. by Shapiro, Y.; Moran, D.S., and Epstein, Y. Tel Aviv, pp. 166–169.
- Fu, Ming; Yu, Tiefeng; Zhang, Hui; Arens, Edward; Weng, Wenguo, et al. (2014). "A model of heat and moisture transfer through clothing integrated with the UC Berkeley comfort model". In: *Building and Environment* 80, pp. 96–104.

- Gagge, A. P.; Fobelets, A. P., and Berglund, L. G. (1986). "A standard predictive index of human response to the thermal environment". In: *ASHRAE Transactions*. Vol. 92. pt 2B, pp. 709–731.
- Gagge, A. P.; Stolwijk, J. A. J., and Nishi, Y. (1971). "An effective temperature scale based on a simple model of human physiological regulatory response". In: *ASHRAE Transactions* 77, pp. 21–36.
- Gavin, Timothy P (2003). "Clothing and Thermoregulation During Exercise". In: *Sports Medicine* 33.13, p. 941.
- Givoni, Baruch and Goldman, Ralph F (1971). "Predicting metabolic energy cost". In: *Journal of applied physiology (Bethesda, Md. : 1985)* 30.3, pp. 429–433.
- Grahn, H. and Craig Heller, H. (2004). "Heat Transfer in Humans: Lessons from Large Hibernators". In: *Life in the Cold: Evolution, Mechanisms, Adaptation, and Application*. Ed. by Barnes, B. M. and Carey, V. Biological papers of the University of Alaska.
- Guyton, Arthur C. and Hall, John E (2006). *Medical Physiology*. Cambridge: Cambridge University Press.
- Harris, JA A and Benedict, FG G (1918). "A Biometric Study of Human Basal Metabolism". In: *Proceedings of the National Academy of Science of the U S A* 4, pp. 370–373.
- Havenith, George (2001). "Individualized model of human thermoregulation for the simulation of heat stress response". In: *Journal of Applied Physiology* 90.5, pp. 1943–1954.
- Havenith, George and Fiala, Dusan (2016). "Thermal indices and thermophysiological modeling for heat stress". In: *Comprehensive Physiology* 6.1, pp. 255–302.
- Havenith, George; Fiala, Dusan; Błażejczyk, Krzysztof; Richards, Mark; Bröde, Peter, et al. (2012). "The UTCI-clothing model." In: *International Journal of Biometeorology* 56.3, pp. 461–70.
- Havenith, George; Heus, Ronald, and Lotens, Wouter A (1990a). "Clothing ventilation, vapour resistance and permeability index: changes due to posture, movement and wind". In: *Ergonomics* 33.8, pp. 989–1005.
- Havenith, George; Heus, Ronald, and Lotens, Wouter A (1990b). "Resultant clothing insulation: a function of body movement, posture, wind, clothing fit and ensemble thickness". In: *Ergonomics* 33.1, pp. 67–84.

Bibliography

- Havenith, George; Holmér, Ingvar, and Parsons, Ken C. (2002). "Personal factors in thermal comfort assessment: Clothing properties and metabolic heat production". In: *Energy and Buildings* 34.6, pp. 581–591.
- Havenith, George and Nilsson, H. O. (2004). "Correction of clothing insulation for movement and wind effects, a meta-analysis". In: *European Journal of Applied Physiology* 92.6, pp. 636–640.
- Havenith, George; Ouzzahra, Yacine; Kuklane, Kalev; Lundgren, Karin; Fan, Jintu, et al. (2015). "A Database of Static Clothing Thermal Insulation and Vapor Permeability Values of Non-Western Ensembles for Use in ASHRAE Standard 55, ISO 7730, and ISO 9920". In: *ASHRAE Transactions* 121, pp. 197–215.
- Hinds, Tessa; McEwan, Islay; Perkes, Jill; Dawson, Ellen; Ball, Derek, et al. (2004). "Effects of massage on limb and skin blood flow after quadriceps exercise". In: *Medicine and Science in Sports and Exercise* 36.8, pp. 1308–1313.
- Holmér, Ingvar; Nilsson, H. O.; Havenith, George, and Parsons, Ken C. (1999). "Clothing convective heat exchange - proposal for improved prediction in standards and models." In: *The Annals of occupational hygiene* 43.5, pp. 329–37.
- Huizenga, Charlie; Zhang, Hui, and Arens, Edward (2001). "A model of human physiology and comfort for assessing complex thermal environments". In: *Building and Environment* 36.6, pp. 691–699.
- IEA (2013). *Transition to Sustainable Buildings*. Paris, France: International Energy Agency.
- EN-ISO 9886: (2004). *EN-ISO 9886 Ergonomics - evaluation of thermal strain by physiological measurements*.
- ISO 15831: (2004). *Clothing - Physiological effects - Measurement of thermal insulation by means of a thermal manikin*. Geneva.
- ISO 7730: (2005). *EN-ISO 7730. Ergonomics of the thermal environment - Analytical determination and interpretation of thermal comfort using calculation of the PMV and PPD indices and local thermal comfort criteria*.
- ISO 8559: (1989). *Garment construction and anthropometric surveys - Body dimensions*.
- EN-ISO 8996: (2004). *EN-ISO 8996, Ergonomics of the thermal environment - Determination of metabolic heat production*.
- ISO 9920: (2009). *Ergonomics of the thermal environment - Estimation of thermal insulation and water vapour resistance of a clothing ensemble*. Berlin.

- Jéquier, E; Gygax, P H; Pittet, P, and Vannotti, A (June 1974). “Increased thermal body insulation: relationship to the development of obesity.” In: *Journal of Applied Physiology* 36.6, pp. 674–678.
- Johnson, J M; Brengelmann, George L.; Hales, J R; Vanhoutte, P M, and Wenger, C B (Dec. 1986). “Regulation of the cutaneous circulation”. In: *Federation proceedings* 45.13, pp. 2841–2850.
- Jones, B. W. and Ogawa, Y. (1992). “Transient interaction between the human and the thermal environment”. In: *ASHRAE Transactions* 98.1, pp. 189–195.
- Jones, B. W. and Ogawa, Y. (1993). “Transient response of the human-clothing system”. In: *Journal of Thermal Biology* 18.5-6, pp. 413–416.
- Joyner, Michael J; Dietz, Niki M, and Shepherd, John T (2001). “From Belfast to Mayo and beyond: the use and future of plethysmography to study blood flow in human limbs”. In: *Journal of Applied Physiology* 91.6, pp. 2431–2441.
- Kaczmarczyk, J.; Melikov, Arsen K., and Sliva, D. (2010). “Effect of warm air supplied facially on occupants’ comfort”. In: *Building and Environment* 45.4, pp. 848–855.
- Katic, Katarina and Zeiler, Wim (2014). “Thermophysiological models : a first comparison”. In: *Fifth German-Austrian IBPSA Conference (BauSIM 2014)*. Aachen, Germany.
- Kellogg, D L (2006). “In vivo mechanisms of cutaneous vasodilation and vasoconstriction in humans during thermoregulatory challenges”. In: *J Appl Physiol* 100.5, pp. 1709–1718.
- Kingma, Boris R. M. (2012). “Human thermoregulation: a synergy between physiology and mathematical modelling”. PhD thesis. Dissertation, Maastricht University.
- Kingma, Boris R. M.; Frijns, Arjan J. H.; Schellen, L., and van Marken Lichtenbelt, Wouter D. (2014a). “Beyond the classic thermoneutral zone Including thermal comfort”. In: *Temperature* 1.2, pp. 142–149.
- Kingma, Boris R. M.; Vosselman, M. J.; Frijns, Arjan J. H.; Van Steenhoven, Anton a., and van Marken Lichtenbelt, Wouter D. (2014b). “Incorporating neurophysiological concepts in mathematical thermoregulation models”. In: *International Journal of Biometeorology* 58, pp. 87–99.
- Kirkpatrick, Peter J.; Smielewski, Piotr; Czosnyka, Marek, and Pickard, John D. (1994). “Continuous monitoring of cortical perfusion by laser Doppler flowmetry in ventilated patients with head injury”. In: *Journal of Neurology, Neurosurgery and Psychiatry* 57.11, pp. 1382–1388.

Bibliography

- Koelblen, Barbara; Psikuta, Agnes; Bogdan, Anna; Annaheim, Simon, and Rossi, René M. (2017). “Comparison of fabric skins for the simulation of sweating on thermal manikins”. In: *International Journal of Biometeorology* 61.9, pp. 1519–1529.
- Kräuchi, Kurt; Cajochen, Christian; Werth, Esther, and Wirz-Justice, Anna (1999). “Warm feet promote the rapid onset of sleep”. In: *Nature* 401, pp. 36–37.
- Kräuchi, Kurt and Wirz-Justice, Anna (1994). “Circadian rhythm of heat production, heart rate, and skin and core temperature under unmasking conditions in men”. In: *American Journal of Physiology-Regulatory, Integrative and Comparative Physiology* 267.3, R819–R829.
- Kristjuhan, Ülo (1995). “Arm and Leg Girths of Industrial Workers During a Workday”. In: *International Journal of Occupational Safety and Ergonomics* 1.2, pp. 193–198.
- Kuklane, Kalev; Holmer, Ingvar, and Giesbrecht, Gordon G. (1999). “Change of Footwear Insulation at Various Sweating Rates”. In: *APPLIED HUMAN SCIENCE Journal of Physiological Anthropology* 18.5, pp. 161–168.
- Kuklane, Kalev; Holmér, Ingvar; Anttonen, Hannu; Burke, Rick; Doughty, Peter, et al. (2005). “Inter-laboratory tests on thermal foot models”. In: *Elsevier Ergonomics Book Series* 3.C, pp. 449–457.
- Kuklane, Kalev; Ueno, Satoru; Sawada, Shin-ichi, and Holmér, Ingvar (2009). “Testing cold protection according to en ISO 20344: Is there any professional footwear that does not pass?” In: *Annals of Occupational Hygiene* 53.1, pp. 63–68.
- Lee, Juyoun; Zhang, Hui, and Arens, Edward (2013). “Typical Clothing Ensemble Insulation Levels for Sixteen Body Parts”. In: *CLIMA Conference 2013*, pp. 1–9.
- Li, Ruixin; Sekhar, S. C., and Melikov, Arsen K. (2010). “Thermal comfort and IAQ assessment of under-floor air distribution system integrated with personalized ventilation in hot and humid climate”. In: *Building and Environment* 45.9, pp. 1906–1913.
- Lomas, Kevin J.; Fiala, Dusan, and Stohrer, Martin (2003). “First principles modeling of thermal sensation responses in steady-state and transient conditions”. In: *ASHRAE Transactions* 109.1, pp. 179–186.
- Lotens, Wouter A (1989). *A simple model for foot temperature simulation*. Tech. rep. IZF 1989-8, Soesterberg: TNO Institute for Perception.
- Lotens, Wouter A (1993). “Heat transfer from humans wearing clothing”. PhD thesis. Dissertation, Technische Universiteit Delft.

- Lotens, Wouter A and Havenith, George (1992). “A comprehensive clothing ensemble heat and vapour transfer model”. In: *The Fifth Int. Conf. on Environmental Ergonomics*. Maastricht, The Netherlands, pp. 74–75.
- Lu, Yehu; Wang, Faming; Wan, Xianfu; Song, Guowen; Shi, Wen, et al. (2015). “Clothing resultant thermal insulation determined on a movable thermal manikin. Part II: effects of wind and body movement on local insulation”. In: *International Journal of Biometeorology* 59.10, pp. 1–12.
- Luomala, Matti J.; Oksa, Juha; Salmi, Jukka A.; Linnamo, Vesa; Holmér, Ingvar, et al. (2012). “Adding a cooling vest during cycling improves performance in warm and humid conditions”. In: *Journal of Thermal Biology* 37.1, pp. 47–55.
- Martínez, Natividad; Quesada, José Ignacio Priego; Corberán, José Miguel; Anda, Rosa María Cibrián Ortiz de; Kuklane, Kalev, et al. (2016). “Validation of the thermophysiological model by Fiala for prediction of local skin temperatures”. In: *International Journal of Biometeorology* 60.12, pp. 1969–1982.
- McCullough, E.A.; Jones, B. W., and Huck, J. (1985). “A comprehensive data base for estimating clothing insulation”. In: *ASHRAE Transactions* 91.2, pp. 29–47.
- McCullough, E.A.; Jones, B. W., and Tamura, T. (1989). “A Data Base for Determining the Evaporative Resistance of Clothing”. In: *ASHRAE Transactions* 95, pp. 316–328.
- Mekjavič, Igor and Morrison, J. B. (1985). “A Model of Shivering Thermogenesis Based on the Neurophysiology of Thermoreception”. In: *IEEE Transactions on Biomedical Engineering* 32.6, pp. 407–417.
- Mekjavič, Igor B. and Eiken, Ola (2006). “Contribution of thermal and nonthermal factors to the regulation of body temperature in humans”. In: *Journal of Applied Physiology* 100.6, pp. 2065–2072.
- Melikov, Arsen K.; Arakelian, R. S.; Halkjaer, L., and Fanger, P. Ole (1994). “Spot cooling. Part 2: Recommendations for design of spot-cooling systems”. In: *ASHRAE Transactions* 100, pp. 500–510.
- Melikov, Arsen K. and Knudsen, G. L. (2007). “Human Response to an Individually Controlled Microenvironment”. In: *HVAC&R Research* 13.4, pp. 645–660.
- Mert, Emel; Böhnisch, Sonja; Psikuta, Agnes; Bueno, Marie-Ange, and Rossi, René M. (2016). “Contribution of garment fit and style to thermal comfort at the lower body”. In: *International Journal of Biometeorology* 60.12, pp. 1995–2004.
- Mert, Emel; Psikuta, Agnes; Bueno, Marie-Ange, and Rossi, René M. (2017). “The effect of body postures on the distribution of air gap thickness and contact area”. In: *International Journal of Biometeorology* 61.2, pp. 363–375.

Bibliography

- Miimu, Airaksinen; Riikka, Holopainen; Pekka, Tuomaala; Jouko, Piippo; Kalevi, Piira, et al. (2013). "Comparison of human thermal models, measured results and questionnaires". In: *13th Conference of International Building Performance Simulation Association*. Chambéry, France, pp. 1657–1664.
- Mills, K R (2005). "The basics of electromyography". In: *Journal of Neurology, Neurosurgery & Psychiatry* 76.suppl 2, pp. ii32–ii35.
- Morris, Nathan B.; Cramer, Matthew N.; Hodder, Simon G.; Havenith, George, and Jay, Ollie (2013). "A comparison between the technical absorbent and ventilated capsule methods for measuring local sweat rate". In: *Journal of Applied Physiology* 114.6, pp. 816–823.
- Morrissey, S. J. and Liou, Y. H. (1984). "Metabolic cost of load carriage with different container sizes". In: *Ergonomics* 27.8, pp. 847–853.
- Munir, Abdul; Takada, Satoru, and Matsushita, Takayuki (2009). "Re-evaluation of Stolwijk's 25-node human thermal model under thermal-transient conditions: Prediction of skin temperature in low-activity conditions". In: *Building and Environment* 44.9, pp. 1777–1787.
- Nakamura, Kazuhiro and Morrison, Shaun F. (2008a). "A thermosensory pathway that controls body temperature". In: *Nature Neuroscience* 11.1, pp. 62–71.
- Nakamura, Kazuhiro and Morrison, Shaun F. (2008b). "Preoptic mechanism for cold-defensive responses to skin cooling". In: *Journal of Physiology* 586.10, pp. 2611–2620.
- Nelson, D. A.; Curlee, John S.; Curran, A. R.; Ziriaux, J. M., and Mason, P. A. (2005). "Determining localized garment insulation values from manikin studies: Computational method and results". In: *European Journal of Applied Physiology* 95.5-6, pp. 464–473.
- Nicol, J. F. and Humphreys, M. a. (2002). "Adaptive thermal comfort and sustainable thermal standards for buildings". In: *Energy and Buildings* 34.6, pp. 563–572.
- Nielsen, Ruth; Olesen, Bjarne W., and Fanger, P. Ole (1985). "Effect of physical activity and air velocity on the thermal insulation of clothing". In: *Ergonomics* 28.12, pp. 1617–1631.
- Nilsson, H. O. (1997). "Analysis of two methods of calculating the total insulation." In: *Proceedings of a European Seminar on Thermal Manikin Testing (1IMM)*. Ed. by Nilsson, H. O. and Holmér, I. Solna, pp. 17–22.
- Nilsson, H. O. (2007). "Thermal comfort evaluation with virtual manikin methods". In: *Building and Environment* 42.12, pp. 4000–4005.

- Nilsson, H. O.; Anttonen, Hannu, and Holmér, Ingvar (2000). “New algorithms for prediction of wind effects on cold protective clothing”. In: *1st European Conference on Protective Clothing*. Ed. by Kuklane K. and Holmér, I. Stockholm, pp. 17–20.
- Nilsson, H. O. and Holmér, Ingvar (2003). “Comfort climate evaluation with thermal manikin methods and computer simulation models.” In: *Indoor air* 13.1, pp. 28–37.
- Oguro, Masayuki; Arens, Edward; Dear, Richard J. de; Zhang, Hui, and Katamaya, T. (2001). “Evaluation of the effect of air flow on clothing insulation and total heat transfer coefficient for each part of the clothed human body”. In: *Journal of Architecture, Planning and Environmental Engineering, AIJ* 549, pp. 13–21.
- Oguro, Masayuki; Arens, Edward; Dear, Richard J. de; Zhang, Hui, and Katamaya, T. (2002). “Convective heat transfer coefficients and clothing insulations for parts of the clothed human body under airflow conditions”. In: *Journal of Architecture, Planning and Environmental Engineering, AIJ* 561.
- Parkinson, Thomas; Dear, Richard J. de, and Candido, Christhina (2015). “Thermal pleasure in built environments: alliesthesia in different thermoregulatory zones”. In: *Building Research & Information* 3218.10, pp. 1–14.
- Parsons, Ken C. (2014). *Human Thermal Environments: The Effects of Hot, Moderate, and Cold Environments on Human Health, Comfort, and Performance*. Third Edit. CRC Press.
- Parsons, Ken C.; Havenith, George, and Holmér, Ingvar (1999). “The effects of wind and human movement on the heat and vapour transfer properties of clothing”. In: *Annals of Occupational Hygiene* 43.5, pp. 347–352.
- Pennes, Harry H (1948). “Analysis of Tissue and Arterial Blood Temperatures in the Resting Human Forearm”. In: *Journal of Applied Physiology* 1.2, pp. 93–122.
- Psikuta, Agnes; Fiala, Dusan; Laschewski, Gudrun; Jendritzky, Gerd; Richards, Mark, et al. (2012). “Validation of the Fiala multi-node thermophysiological model for UTCI application”. In: *International Journal of Biometeorology* 56.3, pp. 443–460.
- Psikuta, Agnes; Frackiewicz-Kaczmarek, Joanna; Mert, Emel; Bueno, Marie-Ange, and Rossi, René M. (2015). “Validation of a novel 3D scanning method for determination of the air gap in clothing”. In: *Measurement* 67.5, pp. 61–70.
- Qian, Xiaoming (2005). “Prediction of Clothing Thermal Insulation and Moisture Vapor Resistance”. PhD thesis. Hong Kong Polytechnic University.
- Reaz, M. B.I.; Hussain, M. S., and Mohd-Yasin, F. (2006). “Techniques of EMG signal analysis: Detection, processing, classification and applications”. In: *Biological Procedures Online* 8.1, pp. 11–35.

Bibliography

- Richards, Mark and Mattle, Niklaus (2001). “A Sweating Agile Thermal Manikin (SAM) Developed to Test Complete Clothing Systems Under Normal and Extreme Conditions”. In: *Human factors and medicine panel symposium - blowing hot and cold: protecting against climatic extremes*. Vol. 4. Dresden, Germany, pp. 1–7.
- Roddie, Ian C (1983). “Circulation to Skin and Adipose Tissue”. In: *Comprehensive Physiology 2011, Supplement 8: Handbook of Physiology, The Cardiovascular System, Peripheral Circulation and Organ Blood Flow*. American Cancer Society, pp. 285–317.
- Roza, A. M. and Shizgal, H. M. (1984). “The Harris Benedict equation reevaluated: Resting energy requirements and the body cell mass”. In: *American Journal of Clinical Nutrition* 40.1, pp. 168–182.
- Savard, G. K.; Nielsen, B.; Laszczynska, J.; Larsen, B. E., and Saltin, B. (1988). “Muscle blood flow is not reduced in humans during moderate exercise and heat stress”. In: *Journal of Applied Physiology* 64.2, pp. 649–657.
- Savastano, David M.; Gorbach, Alexander M.; Eden, Henry S.; Brady, Sheila M.; Reynolds, James C., et al. (2009). “Adiposity and human regional body temperature”. In: *American Journal of Clinical Nutrition* 90.5, pp. 1124–1131.
- Schellen, L.; Loomans, M.G.L.C.; Kingma, Boris R. M.; Wit, M.H. de; Frijns, Arjan J. H., et al. (2013). “The use of a thermophysiological model in the built environment to predict thermal sensation”. In: *Building and Environment* 59, pp. 10–22.
- Seppänen, O.; Fisk, W. J., and Lei, Q. H. (2006). “Room temperature and productivity in office work”. In: *Healthy Buildings Conference*. Lisbon.
- Severens, Natascha M. W. (2008). “Modelling Hypothermia in Patients Undergoing Surgery”. Dissertation. Dissertation, Eindhoven University of Technology.
- Severens, Natascha M. W.; van Marken Lichtenbelt, Wouter D.; Frijns, Arjan J. H.; Steenhoven, Anton A. van; De Mol, B. A J M, et al. (2007). “A model to predict patient temperature during cardiac surgery”. In: *Physics in Medicine and Biology* 52.17, pp. 5131–5145.
- Shitzer, Avraham and Chato, John C. (1985). “Thermal interaction with garments”. In: *Heat Transfer in Medicine and Biology Vol. 1*. Ed. by Shitzer, A. and Eberhart, R. C. New York: Plenum Press. Chap. 14, pp. 375–394.
- Smith, C. (1991). “A Transient, Three-Dimensional Model of the Human Thermal System”. Doctoral Dissertation. Dissertation, Kansas State University, USA.

- Snell, P. G.; Martin, W. H.; Buckey, J. C., and Blomqvist, C. G. (1987). “Maximal vascular leg conductance in trained and untrained men”. In: *Journal of Applied Physiology* 62.2, pp. 606–610.
- Sparks, H. V. (1978). “Skin and Muscle”. In: *Peripheral Circulation*. Ed. by Johnson, C. P. New York: John Wiley & Sons, Inc.
- Stolwijk, J. A. J. (1971). *A mathematical model of physiological temperature regulation in man*. Tech. rep. August. Washington, DC: National Aeronautics and Space Administration. DOI: NASAcontractorreportNASACR-1855.
- Stolwijk, J. A. J. and Hardy, J. D. (1966). “Partitional calorimetric studies of responses of man to thermal transients.” In: *Journal of Applied Physiology (Bethesda, Md. : 1985)* 21.3, pp. 967–977.
- Tanabe, Shin Ichi; Kobayashi, Kozo; Nakano, Junta; Ozeki, Yoshiichi, and Konishi, Masaaki (2002). “Evaluation of thermal comfort using combined multi-node thermoregulation (65MN) and radiation models and computational fluid dynamics (CFD)”. In: *Energy and Buildings* 34.6, pp. 637–646.
- Urlaub, Susanne; Werth, Lioba; Steidle, Anna; Treeck, Christoph van, and Sedlbauer, Klaus (2013). “Methodik zur Quantifizierung der Auswirkung von moderater Wärmebelastung auf die menschliche Leistungsfähigkeit”. In: *Bauphysik* 35.1, pp. 38–44.
- van Marken Lichtenbelt, Wouter D.; Daanen, Hein a M; Wouters, Loek; Fronczek, Rolf; Raymann, Roy J E M, et al. (July 2006). “Evaluation of wireless determination of skin temperature using iButtons.” In: *Physiology & Behavior* 88.4-5, pp. 489–97.
- van Marken Lichtenbelt, Wouter D.; Frijns, Arjan J. H.; Fiala, Dusan; Janssen, F.E.M.; Van Ooijen, Marieke J., et al. (2004). “Effect of individual characteristics on a mathematical model of human thermoregulation”. In: *Journal of Thermal Biology* 29.7-8, pp. 577–581.
- van Marken Lichtenbelt, Wouter D.; Frijns, Arjan J. H.; Van Ooijen, Marieke J.; Fiala, Dusan; Kester, Arnold M., et al. (2007). “Validation of an individualised model of human thermoregulation for predicting responses to cold air”. In: *International Journal of Biometeorology* 51.3, pp. 169–179.
- Veicsteinas, A; Ferretti, G, and Rennie, D W (1982). “Superficial shell insulation in resting and exercising men in cold water.” In: *Journal of Applied Physiology* 52.6, pp. 1557–1564.
- Verhaart, Jacob; Veselý, Michal, and Zeiler, Wim (2015). “Personal heating: Effectiveness and energy use”. In: *Building Research and Information* 43.3, pp. 346–354.

Bibliography

- Veselá, Stephanie; Frijns, Arjan J.H., and Psikuta, Agnes (2017a). “Analysis of local clothing area factors of typical office clothing items and their correlation to the ease allowance at various body landmarks”. In: *The 17th International Conference on Environmental Ergonomics ICEE 2017*. Ed. by ICEE 2017 Local Organising Committee. Kobe, Japan, p. 70.
- Veselá, Stephanie; Frijns, Arjan J.H., and van Marken Lichtenbelt, Wouter D. (2018a). “Comparison of measured and simulated foot skin blood flow during light and medium activities and the effect on foot skin temperature prediction”. In: *BauSIM2018 - 7. Deutsch-Österreichische IBPSA-Konferenz : 26.-28. September 2018, Karlsruhe, Germany*. Ed. by Both, P.; Wagner, A., and Graf, K. Karlsruhe: KIT, pp. 262–267.
- Veselá, Stephanie; Kingma, Boris R. M., and Frijns, Arjan J. H. (2015a). “Effects of sweating on distal skin temperature prediction during walking”. In: *Extreme Physiology and Medicine* 4.Suppl 1, A31.
- Veselá, Stephanie; Kingma, Boris R. M., and Frijns, Arjan J. H. (2015b). “Taking Thermal Regulation Models From the Lab To the World: Are Current Views Ready for the Challenge?” In: *Healthy Buildings Europe 2015*. Ed. by Loomans, M.G.L.C. and Kulve, Marije te. Vol. 2015-May. Eindhoven.
- Veselá, Stephanie; Kingma, Boris R. M., and Frijns, Arjan J. H. (2017b). “Local thermal sensation modeling - a review on the necessity and availability of local clothing properties and local metabolic heat production”. In: *Indoor Air* 27.2, pp. 216–272.
- Veselá, Stephanie; Kingma, Boris R.M., and Frijns, Arjan J.H. (2016a). “Challenges in modelling local thermal sensation”. In: *Proceedings of the 14th international conference of Indoor Air Quality and Climate*. Ed. by Laverge, J.; Salthammer, T., and Stranger, M. Ghent, Belgium.
- Veselá, Stephanie; Kingma, Boris R.M., and Frijns, Arjan J.H. (2016b). “Impact of local clothing values on local skin temperature simulation”. In: *Making Comfort Relevant : Proceedings of the 9th Windsor Conference, 7-10 April 2016*. Ed. by Nicol, J. F.; Roaf, S.; Brotas, L., and Humphreys, M. Windsor, UK, pp. 432–442.
- Veselá, Stephanie; Kingma, Boris R.M., and Frijns, Arjan J.H. (2019a). “Application of an adjusted neurophysiological (foot) skin blood flow model to a real life case study”. In: *The 18th International Conference on Environmental Ergonomics ICEE2019*. Ed. by Gerrett, N.M.; Daanen, Hein A.M., and Teunissen, L.P.J. Amsterdam, p. 139.
- Veselá, Stephanie; Kingma, Boris R.M.; Frijns, Arjan J.H., and van Marken Lichtenbelt, Wouter D. (2019b). “Effect of local skin blood flow during light and medium activities

- on local skin temperature predictions”. In: *Journal of Thermal Biology* 84, pp. 439–450.
- Veselá, Stephanie; Psikuta, Agnes, and Frijns, Arjan J. H. (2018b). “Determination of the local evaporative resistances of two typical office clothing ensembles and the effect of air speed and body movement”. In: *12th International Manikin and Modelling Meeting 29-31 August 2018, St. Gallen, Switzerland*.
- Veselá, Stephanie; Psikuta, Agnes, and Frijns, Arjan J. H. (2018c). “Local clothing thermal properties of typical office ensembles under realistic static and dynamic conditions”. In: *International Journal of Biometeorology* 62.12, pp. 2215–2229.
- Veselá, Stephanie; Psikuta, Agnes; Kingma, Boris R. M., and Frijns, Arjan J. H. (2017c). “Measurements of local clothing resistances and local area factors under various conditions”. In: *Healthy Buildings 2017 Europe*. Lublin, Poland.
- Veselý, Michal and Zeiler, Wim (2014). “Personalized conditioning and its impact on thermal comfort and energy performance - A review”. In: *Renewable and Sustainable Energy Reviews* 34, pp. 401–408.
- Walløe, Lars (2016). “Arterio-venous anastomoses in the human skin and their role in temperature control”. In: *Temperature* 3.1, pp. 92–103.
- Wan, Xianfu and Fan, Jintu (2008). “A transient thermal model of the human body–clothing–environment system”. In: *Journal of Thermal Biology* 33.2, pp. 87–97.
- Wang, Faming; Ferraro, Simona del; Lin, Li-Yen; Sotto Mayor, Tiago; Molinaro, Vincenzo, et al. (2012). “Localised boundary air layer and clothing evaporative resistances for individual body segments”. In: *Ergonomics* 55.7, pp. 799–812.
- Wang, Faming; Lai, Dandan; Shi, Wen, and Fu, Ming (2017). “Effects of fabric thickness and material on apparent ‘wet’ conductive thermal resistance of knitted fabric ‘skin’ on sweating manikins”. In: *Journal of Thermal Biology* 70.3, pp. 69–76.
- Watanabe, Shinichi; Melikov, Arsen K., and Knudsen, Gitte L. (2010). “Design of an individually controlled system for an optimal thermal microenvironment”. In: *Building and Environment* 45.3, pp. 549–558.
- Werner, Jurgen and Buse, M. (1988). “Temperature profiles with respect to inhomogeneity and geometry of the human body.” In: *Journal of applied physiology (Bethesda, Md. : 1985)* 65.3, pp. 1110–1118.
- Wijers, Sander L.J.; Saris, Wim H.M., and Van Marken Lichtenbelt, Wouter D. (2010). “Cold-Induced Adaptive Thermogenesis in Lean and Obese”. In: *Obesity* 18.6, pp. 1092–1099.

Bibliography

- Wissler, Eugene H. (1985). “Mathematical simulation of human thermal behavior using whole body models”. In: *Heat Transfer in Medicine and Biology Vol. 1*. Ed. by Shitzer, A. and Eberhart, R. C. New York: Plenum Press. Chap. 13, pp. 325–373.
- Wissler, Eugene H. (2008). “A quantitative assessment of skin blood flow in humans”. In: *European Journal of Applied Physiology* 104.2, pp. 145–157.
- Wölki, Daniel (2017). “MORPHEUS : Modelica-based implementation of a numerical human model involving individual human aspects”. Dissertation. RWTH Aachen University, Aachen.
- Wölki, Daniel and Treeck, Christoph van (2013). “Individualization of a Mathematical Manikin Model in Terms of Gender, Age and Morphological Issues for Predicting Thermal Comfort: A Preliminary Study”. In: *BS 2013 : 13th International Conference of the International Building Performance Simulation Association, August 26-28*. Ed. by Wurtz, Etienne. Chambéry, France, pp. 1649–1656.
- Wyistdham, C H; Morrison, J F; Williams, C G; Strydom, N B; Rahden, M J E von, et al. (1966). “Inter- and Intra-Individual Differences in Energy Expenditure and Mechanical Efficiency”. In: *Ergonomics* 9.1, pp. 17–29.
- Yosipovitch, Gil; Sackett-Lundeen, Linda; Goon, Anthony; Huak, Chan Ylong; Goh, Chee Leok, et al. (2004). “Circadian and ultradian (12 h) variations of skin blood flow and barrier function in non-irritated and irritated skin - Effect of topical corticosteroids”. In: *Journal of Investigative Dermatology* 122.3, pp. 824–829.
- Zhang, Hui (2003). “Human Thermal Sensation and Comfort in Transient and Non-Uniform Thermal Environments”. PhD thesis. University of California, Berkeley.
- Zhang, Hui; Arens, Edward; Huizenga, Charlie, and Han, T. (2010a). “Thermal sensation and comfort models for non-uniform and transient environments, part III: Whole-body sensation and comfort”. In: *Building and Environment* 45.2, pp. 399–410.
- Zhang, Hui; Arens, Edward; Kim, Dong Eun; Buchberger, Elena; Bauman, Fred, et al. (2010b). “Comfort, perceived air quality, and work performance in a low-power task-ambient conditioning system”. In: *Building and Environment* 45.1, pp. 29–39.
- Zhang, Hui; Huizenga, Charlie; Arens, Edward, and Yu, Tiefeng (2001). “Considering individual physiological differences in a human thermal model”. In: *Journal of Thermal Biology* 26.4-5, pp. 401–408.
- Zhang, Yu F.; Wyon, David P.; Fang, Lei, and Melikov, Arsen K. (2007). “The influence of heated or cooled seats on the acceptable ambient temperature range”. In: *Ergonomics* 50.4, pp. 586–600.

Summary

Advancing human thermo-physiological modeling - Challenges of predicting the local skin temperature during moderate activities

In a world that faces global climate change, the energy consumption of the building sector needs to be reduced. However, heating, ventilation and air conditioning (HVAC) systems should still provide a healthy and comfortable thermal indoor environment for the occupants of the buildings. Among other solutions, energy-efficient localized heating and cooling systems show a high potential for saving energy in office buildings. For testing these systems, thermo-physiological models need to predict local skin temperatures and local thermal sensation accurately. The present models are generally capable of simulating the required local values. However, most models were validated for the mean skin temperature prediction of an average person under low clothing and low activity conditions. The aim of this PhD thesis is to further develop the thermo-physiological model ThermoSEM such that the effects of localized cooling and heating on thermal comfort under office conditions can be predicted.

To investigate the most critical aspects of local skin temperature prediction for higher activity and clothing levels, we performed a case study in a real office environment. For this test, 5 individuals underwent six trials combining typical office activities and clothing insulation values. We measured the local skin temperatures of the participants as well as the environmental temperature and humidity. Then, we simulated the skin temperatures under the same conditions in ThermoSEM. Our results show that the model lacks accuracy in local skin temperature prediction especially on the extremities when typical office clothing ensembles and activity levels are applied.

In our broad literature review, we identified two reasons, which can explain the results of the case study: 1. the available local clothing data in the literature is insufficient for simulating typical office situations, and 2. the local heat balances of the thermo-physiological model need to be re-evaluated for activity levels above 1 met. In a sensitivity analysis, both aspects contributed highly to the simulation outcome of distal skin temperatures.

We addressed the issue of the missing local clothing data by measuring local clothing parameters on a thermal sweating manikin in cooperation with Empa, St. Gallen, Switzerland. We determined the local dry thermal insulation values and local clothing area factors for 23 typical office outfits at three air speeds and body movement. The evaporative resistance was measured for two representative outfits at all air speeds and body movement. Additionally, clothing properties of three pairs of shoes were determined. For the local dry thermal insulation, we also found a correlation to the fit of the clothing (i.e. ease allowance) for most body parts for one level clothing outfits.

Our human subject experiments at Maastricht University, where participants performed light to medium activities on a treadmill while skin and core temperature, skin blood flow (SBF) at the foot and their energy expenditure were measured, showed that the simulated foot SBF by the thermo-physiological model was lower than the measured values for prescribed activity levels. Moreover, significant differences between male and female subjects were identified. Hence, we refined the foot SBF model by including the activity level and gender of the subject.

At last, we revisited the case study to see if applying the reviewed clothing properties and foot SBF model would improve the skin temperature prediction. Moreover, we considered the individual geometry (height, weight, fat, body mass). Our results show that the new foot SBF model has the largest impact on the local skin temperature outcome. In most cases, the skin temperature prediction is improved in the finalized thermo-physiological model.

All in all, the work of this PhD thesis advances the thermo-physiological model ThermoSEM to be able to predict local skin temperature and therefore, local thermal sensation. Future research would include additional factors that influence the local heat balance such as local muscle activity or sweat rates, local skin blood flow models for further body parts, and an advanced geometry adjustment of the model.

Acknowledgments

The realization of this PhD was a long and sometimes challenging process, but was also intertwined with lovely acquaintances throughout the world and insights in a large variety of projects related to the built environment, human thermal comfort and thermo-physiology. Therefore, I would like to say thank all the people, who enabled me to conduct this PhD.

I would like to thank my promoter and head of Energy Technology group David Smeulders and my daily supervisor Arjan Frijns for providing me with the opportunity to conduct this PhD at TU Eindhoven. Thank you for welcoming me into the group. Arjan, a special thank you for guiding me through this PhD from the beginning to the end. I appreciated all the feedback, discussions and encouragement throughout the project, and that you stayed in touch over the longer distance for the last three years. Alongside Arjan, I'd also like to greatly thank Boris Kingma for sharing your knowledge on human physiology, for the feedback and discussions on the human subject experiments, the results and the written papers, and the general support of my PhD.

I would like to thank all the committee members, prof.dr. L.P.H. de Goeij, prof.dr.ir. D.M.J. Smeulders, dr.ir. A.J.H. Frijns, prof.dr.ir. A. A. van Steenhoven, prof.dr. H.A.M. Daanen, prof.dr.ir. J.L.M. Hensen, prof.dr. W.D. van Marken Lichtenbelt and dr. B.R.M. Kingma, for taking the time to read my thesis, to provide feedback, and to be part of the defence ceremony.

Parts of my PhD were conducted in cooperation with the group of Wouter van Marken Lichtenbelt at Maastricht University. I would like to thank you for providing me with the opportunity to conduct the experiments in your research facility, and for

integrating me into your group during my work. Boris, Hannah, Marije, thank you for always making me feel welcome, and the exchange of knowledge.

A large part of this PhD would not have been able to be realized, if not for Agnes Psikuta from Empa, Switzerland. Thank you for giving me the opportunity to stay for six weeks at Empa, and the use the thermal manikin SAM for conducting the measurements of the local clothing properties. Also, your feedback on the conference and journal papers was always very sound, and much appreciated. Special thanks also to the PhD students, colleagues and technical staff at Empa, for your welcome, knowledge exchange and help with the measurements.

Outside this project, I received great support from the PhD students of the department of the Built Environment, Building Services. The lunch discussions provided a welcome balance to the work and its challenges. So, thanks to Katherina, Rongling, Jakob, and Michal.

Special thanks to my husband Michal, who supported me in pursuing a PhD in Eindhoven. Thank you, for your encouragement, and the discussions and input along the way. In addition, I would like to thank my amazing kids Jonas and Lena for filling our lives with laughter, curiosity, and perspective.

Last but not least, I'd like to thank my parents, who always supported me in pursuing an academic career. Thank you, Papa, for providing me with the ambition and stubbornness to continue and finish my PhD. Thank you, Mama, for nurturing and supporting me, for always only being a phone call away, and all the little and big advises throughout the years. Thank you both, for being the best parents and grandparents, my family and I could wish for.

List of Publications

The work described in this thesis has resulted in the following publications:

Journal publications

Veselá, Stephanie; Kingma, Boris R.M.; Frijns, Arjan J.H., and van Marken Lichtenbelt, Wouter D. (2019b). “Effect of local skin blood flow during light and medium activities on local skin temperature predictions”. In: *Journal of Thermal Biology* 84, pp. 439–450

Veselá, Stephanie; Psikuta, Agnes, and Frijns, Arjan J. H. (2018c). “Local clothing thermal properties of typical office ensembles under realistic static and dynamic conditions”. In: *International Journal of Biometeorology* 62.12, pp. 2215–2229

Veselá, Stephanie; Kingma, Boris R. M., and Frijns, Arjan J. H. (2017b). “Local thermal sensation modeling - a review on the necessity and availability of local clothing properties and local metabolic heat production”. In: *Indoor Air* 27.2, pp. 216–272

Other publications

Veselá, Stephanie; Kingma, Boris R.M., and Frijns, Arjan J.H. (2019a). “Application of an adjusted neurophysiological (foot) skin blood flow model to a real life case study”. In: *The 18th International Conference on Environmental Ergonomics ICEE2019*. Ed. by Gerrett, N.M.; Daanen, Hein A.M., and Teunissen, L.P.J. Amsterdam, p. 139

Veselá, Stephanie; Psikuta, Agnes, and Frijns, Arjan J. H. (2018b). “Determination of the local evaporative resistances of two typical office clothing ensembles and the effect of air speed and body movement”. In: *12th International Manikin and Modelling Meeting 29-31 August 2018, St. Gallen, Switzerland*

- Veselá, Stephanie; Frijns, Arjan J.H., and van Marken Lichtenbelt, Wouter D. (2018a). “Comparison of measured and simulated foot skin blood flow during light and medium activities and the effect on foot skin temperature prediction”. In: *BauSIM2018 - 7. Deutsch-Österreichische IBPSA-Konferenz : 26.-28. September 2018, Karlsruhe, Germany*. Ed. by Both, P.; Wagner, A., and Graf, K. Karlsruhe: KIT, pp. 262–267
- Veselá, Stephanie; Frijns, Arjan J.H., and Psikuta, Agnes (2017a). “Analysis of local clothing area factors of typical office clothing items and their correlation to the ease allowance at various body landmarks”. In: *The 17th International Conference on Environmental Ergonomics ICEE 2017*. Ed. by ICEE 2017 Local Organising Committee. Kobe, Japan, p. 70
- Veselá, Stephanie; Psikuta, Agnes; Kingma, Boris R. M., and Frijns, Arjan J. H. (2017c). “Measurements of local clothing resistances and local area factors under various conditions”. In: *Healthy Buildings 2017 Europe*. Lublin, Poland
- Veselá, Stephanie; Kingma, Boris R.M., and Frijns, Arjan J.H. (2016a). “Challenges in modelling local thermal sensation”. In: *Proceedings of the 14th international conference of Indoor Air Quality and Climate*. Ed. by Laverge, J.; Salthammer, T., and Stranger, M. Ghent, Belgium
- Frijns, Arjan J.H.; Veselá, Stephanie, and Kingma, Boris R.M. (2016). “Individualized thermal sensation models: missing links and solutions”. In: *Proceedings of the 14th international conference of Indoor Air Quality and Climate*. Ed. by Laverge, J.; Salthammer, T., and Stranger, M. Ghent, Belgium
- Veselá, Stephanie; Kingma, Boris R.M., and Frijns, Arjan J.H. (2016b). “Impact of local clothing values on local skin temperature simulation”. In: *Making Comfort Relevant : Proceedings of the 9th Windsor Conference, 7-10 April 2016*. Ed. by Nicol, J. F.; Roaf, S.; Brotas, L., and Humphreys, M. Windsor, UK, pp. 432–442
- Veselá, Stephanie; Kingma, Boris R. M., and Frijns, Arjan J. H. (2015a). “Effects of sweating on distal skin temperature prediction during walking”. In: *Extreme Physiology and Medicine* 4, Suppl 1, A31
- Veselá, Stephanie; Kingma, Boris R. M., and Frijns, Arjan J. H. (2015b). “Taking Thermal Regulation Models From the Lab To the World: Are Current Views Ready for the Challenge?” In: *Healthy Buildings Europe 2015*. Ed. by Loomans, M.G.L.C. and Kulve, Marije te. Vol. 2015-May. Eindhoven

Curriculum Vitae

Stephanie Veselá (née Schwarz) was born on 01-01-1987 in Potsdam, Germany. After finishing “Abitur” (high school diploma) at Herman-von-Helmholtz-Gymnasium in 2006 in Potsdam, Germany, she studied Energy- and Process Engineering at the Technical University of Berlin, Germany. In 2013, she graduated from the department of Energy Engineering with majors in Energy Engineering, Renewable Energies and Building Services. After graduation Stephanie Veselá work at RWTH Aachen University at the Institute of Energy Efficiency and Sustainable Building. Her main tasks included the design, performance, and analysis of human subject experiments investigating energy-efficient heating in electrical vehicles, preparation and supervision of student laboratories related to the build environment, and preparatory work for student lectures on measurement technology and the Building Physics. In August 2014, Stephanie Veselá started a PhD project at Eindhoven University of Technology in The Netherlands, of which the results are presented in this dissertation. Since 2019 she is employed at the German Energy Agency (dena) in the Division of Energy-Efficient Buildings in Berlin, Germany.

